Universidad de Valladolid

FACULTAD DE CIENCIAS

DEPARTAMENTO DE FÍSICA DE LA MATERIA CONDENSADA,
CRISTALOGRAFÍA Y MINERALOGÍA

TESIS DOCTORAL:

FABRICACIÓN DE MATERIALES CELULARES MEJORADOS BASADOS EN POLIOLEFINAS. RELACIÓN PROCESADO-COMPOSICIÓN-ESTRUCTURA-PROPIEDADES

Presentada por Cristina Saiz Arroyo para optar al grado de doctor /ra por la Universidad de Valladolid

Dirigida por:
Miguel Ángel Rodríguez Pérez

Capítulo 1

Introducción.

1.1.- MARCO DE LA TESIS

Esta tesis se enmarca dentro de las líneas de investigación del Laboratorio de Materiales Celulares (CellMat) del Departamento de Física de la Materia Condensada de la Universidad de Valladolid. Este grupo fue fundado en 1999 por los catedráticos Dr. D. José Antonio de Saja y Dr. D. Miguel Ángel Rodríguez Pérez teniendo como objetivo fundamental el estudio de los materiales celulares. El trabajo de este equipo está centrado en el desarrollo de *nuevas rutas de producción de materiales celulares* así como en la *obtención de productos aligerados multifuncionales con propiedades mejoradas*, sin dejar de lado por supuesto, la generación de conocimiento en la relación procesado-estructura-propiedades-aplicaciones.

A la tesis doctoral que en el año 1999 presentó el ahora director del grupo, Dr. Miguel Angel Rodríguez Pérez titulada "*Propiedades Térmicas y Mecánicas de Espumas de Poliolefinas*" le han seguido otras [1-8] así como un gran número de publicaciones [9-54] centradas en la *caracterización* de la *microestructura* y *propiedades físicas* de espumas de poliolefina de baja densidad fabricadas mediante diversas rutas de producción.

Hasta aproximadamente el año 2007, la investigación del grupo se centró casi exclusivamente en la caracterización de materiales producidos de forma industrial. A partir de esa fecha, la conjunción de varios factores hace que las líneas de trabajo se amplíen comenzando a producir materiales celulares a escala de laboratorio tomando como base el conocimiento de la relación estructura-propiedades adquirido durante los años previos.

Por otro lado, en el año 1984 Suh, Martini y Waldman presentan la primera patente relacionada con la producción de espumas microcelulares [55] y en el año 1988 los investigadores de Toyota producen los primeros nanocompuestos basados en nylon 6 y nanoarcillas [56]. Estos dos hechos marcan una nueva tendencia en la investigación desarrollada en el campo de los materiales celulares. El proceso de disolución de gas originariamente desarrollado para la producción de espumas microcelulares se extiende rápidamente a la producción de todo tipo de materiales celulares basados en diversos tipos de matrices poliméricas. Por otro lado, las mejoras inducidas por la presencia de nanopartículas en los polímeros sólidos hacen pensar en las posibilidades que éstas pueden ofrecer en materiales espumados. Así en la primera década del siglo XXI se genera una tendencia muy clara en las líneas generales de trabajo dentro de los materiales celulares: la utilización de nanopartículas como agentes nucleantes y de refuerzo y la producción de materiales celulares mediante disolución de gas.

El equipo del laboratorio CellMat asume estos nuevos retos. Se comienza a desarrollar un proceso de producción alternativo que bajo ciertas condiciones puede producir espumas microcelulares. El proceso está descrito en esta memoria de tesis y se conoce como *"Moldeo por Compresión Mejorado"*. Las primeras publicaciones en relación a la producción de materiales celulares producidos utilizando este sistema datan del año 2009 y describen la producción de materiales celulares con tamaños de celda en el rango micrométrico basados en polietileno de baja densidad [57, 58]. Este proceso ha sido posteriormente aplicado a la producción de otro tipo de materiales celulares, tales como mezclas de polietileno de baja densidad (LDPE) o copolímero de etileno acetato de vinilo (EVA) con altas concentraciones de hidróxidos de aluminio o magnesio [59-62] o mezclas de EVA con almidón [63, 64]. Debido a los prometedores resultados obtenidos para LDPE, se decidió que una de las líneas de trabajo de esta tesis estaría centrada en la *producción de materiales celulares con base polipropileno utilizando el proceso de moldeo por compresión mejorado*.

El moldeo por compresión mejorado puede suponer una alternativa para la producción de espumas microcelulares, sin embargo, el equipo de CellMat también ha enfocado sus esfuerzos a dar respuesta a algunas de las dificultades que presenta el proceso de producción más habitual para este tipo de de materiales, (disolución de gas). Una de las principales desventajas es la falta de geometría definida de los materiales así producidos unido a un pobre control de la densidad de las probetas. Estas razones impulsaron la segunda de las líneas de investigación de este trabajo, *la producción de probetas moldeadas y con control de densidad mediante disolución de gas*. Como matriz polimérica en este caso, se eligió el mismo grado de polipropileno utilizado en el proceso anterior. La parte experimental de este apartado se realizó durante dos estancias de la doctoranda en las instalaciones del Centro Catalán del Plástico de la Universidad Politécnica de Cataluña bajo la supervisión del Profesor José Ignacio Velasco.

La línea de investigación en materiales nanocompuestos comenzó a raiz de un trabajo de colaboración con el grupo del Dr. D. José Ignacio Velasco. Como resultado, se publicaron dos trabajos (uno de los cuales se presenta en esta memoria de tesis) [65, 66] en los que se resumen los efectos de partículas nanométricas de hectorita en materiales celulares basados en poliolefina. A partir de ahí se desarrollaron algunas líneas de trabajo enfocadas a desarrollar materiales celulares mejorados mediante la adición de nanopartículas nanométricas. Una de esas líneas está desarrollada en este trabajo. Consiste en *producir materiales celulares con base polietileno de baja densidad con propiedades mejoradas mediante la adición de nanopartículas de tipo esférico, (sílice).* Para producir dichos materiales se utiliza tanto el moldeo por compresión mejorado como la disolución de gas.

Además del "boom" de la tendencia "nano", otra que está comenzando a ser una línea común de investigación es la utilización de polímeros biodegradables o

procedentes de fuentes reciclables, todo ello por supuesto enfocado a contaminar menos. En este trabajo no se ha utilizado ninguno de esos polímeros, pero sí que se contribuye de alguna manera con esa tendencia. Así la cuarta línea de investigación de este trabajo está enmarcada en la tendencia "verde" generalizada dentro del mundo de los polímeros. Se detectó un problema de gestión de residuos de materiales celulares con base LDPE entrecruzado y debido a la dificultad de reciclado de estos productos *se ha puesto a punto un método de recuperación de materiales celulares con base LDPE entrecruzado.*

El trabajo descrito en esta memoria en torno a estas cuatro líneas de investigación mencionadas previamente ha sido desarrollado y en parte financiado en algunos de los proyectos en los que ha participado el grupo CellMat y que se muestran en la tabla 1.1.

Tabla 1.1: Proyectos de Investigación desarrollados por el Grupo CellMat dentro de los cuales se enmarca esta tesis.

PROYECTOS DE INVESTIGACIÓN EN LOS QUE SE ENMARCA LA TESIS
Título: "Obtención de Materiales Aislantes para Construcción a partir de la Reutilización de Residuos de Espumas Plásticas de Origen Industrial (Fase 1)"
Financiado a Través de la Agencia de Desarrollo Económico de Castilla y León (ADE) Empresa Centro Tecnológico de Miranda de Ebro, (CTME)
Duración: Octubre 2005- Marzo 2007
Investigador Principal: J.A. de Saja
Título: "Obtención de Materiales Aislantes para Construcción a partir de la Reutilización de Residuos de Espumas Plásticas de Origen Industrial (Fase 2)"
Financiado a Través de la Agencia de Desarrollo Económico de Castilla y León (ADE) Empresa Centro Tecnológico de Miranda de Ebro, (CTME)
Duración: Septiembre 2006- Junio 2007
Investigador Principal: J.A. de Saja
Título: "Espumación de Metales bajo Presión Mecánica"
Acción Integrada con la Universidad Técnica de Berlín.
Duración: Enero 2009-Diciembre de 2010.
Investigador Principal: M.A. Rodríguez-Pérez.
Título: "Nuevos Desarrollos en el Campo de los Materiales Poliméricos Microcelulares: Fabricación , Estructura, Propiedades, Modelización y Apliaciones"
Proyecto coordinado en colaboración con el Centro Tecnológico Lortek
Financiado por el Programa Nacional de Materiales
Duración: Diciembre 2009- Diciembre 2012
Investigador Principal: M.A. Rodríguez-Pérez
Título: "Nuevos Procesos de Fabricación de Piezas de Plástico Basados en la Obtención de Materiales Microcelulares Mediante Moldeo por Autoinyección".
Entidad financiadora: FECYT y Grupo ABN Pipe. Proyecto Tipo Innocash.

Duración: Enero 2010- Diciembre 2011.
Responsable Técnico: M.A. Rodríguez-Pérez
Título: "Advanced Foams Under Microgravity"
Entidad financiadora: European Spatial Agency
Duración: Junio 2010-Mayo 2012.
Investigador Responsable en la Universidad de Valladolid: M.A. Rodríguez-Pérez

Se puede decir por tanto, que este trabajo está no sólo enmarcado dentro de las líneas de trabajo del Laboratorio CellMat, sino que está en consonancia con la tendencia actual dentro del campo de los materiales celulares. La necesidad actual de reducción de peso y costes en múltiples sectores tales como la automoción la aeronáutica, las energías renovables, la construcción, la biotecnología o el embalaje, hace que algunos de los materiales producidos y analizados durante el desarrollo de este trabajo presenten una multitud de potenciales aplicaciones.

1.2.- OBJETIVOS

Las cuatro líneas de trabajo definidas los párrafos anteriores definen ya por sí mismas los objetivos principales de este trabajo. Si bien, se puede generalizar diciendo que el objetivo de esta tesis es:

Producir materiales celulares con estructuras celulares y propiedades físicas mejoradas mediante la optimización de la composición química y de los parámetros de proceso.

La caracterización de la microestructura y la respuesta física de los materiales ayudará a establecer de forma clara la relación composición-procesado-estructura-propiedades de los materiales bajo estudio.

Estos objetivos sitúan este trabajo en el plano inferior *del tetraedro de los materiales*.

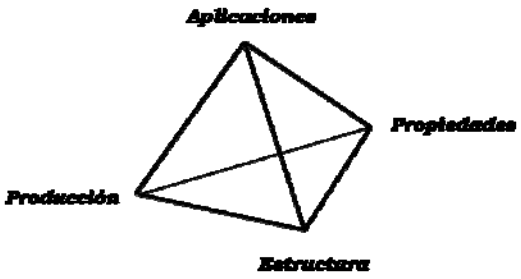

Figura 1.1: *Tetraedro de los materiales*

El objetivo general se puede dividir en sub-objetivos en función de cada una de las líneas de investigación.

Producción de Materiales Celulares con base Polipropileno Mediante Moldeo por Compresión Mejorado

- Optimizar la producción de materiales celulares con base polipropileno mediante el proceso de moldeo por compresión mejorado.
- Producir probetas con diferentes densidades y composiciones químicas con el fin de analizar el efecto de la variación de ambas en la microestructura y respuesta mecánica de dichos materiales celulares.

Producción de Materiales Celulares con base Polipropileno con Geometría Definida y con control de Densidad.

- Diseñar un sistema capaz de producir materiales moldeados mediante disolución de gas y que permita controlar de forma precisa la densidad final del material.
- Optimizar los parámetros de producción de un proceso de disolución de gas para, mediante la utilización del sistema previamente diseñado, producir materiales celulares con base polipropileno con diferentes densidades.
- Analizar los posibles efectos que pueda tener el sistema diseñado tanto en la microestructura como en las propiedades físicas de los materiales diseñados.

Producción de Materiales Celulares con base Polietileno de Baja Densidad con Estructuras y Propiedades Físicas Mejoradas Mediante la Adición de Distintos tipos de Nanopartículas.

- Utilizar nanopartículas de tipo laminar para mejorar las propiedades de materiales celulares producidos mediante un proceso de moldeo por compresión en dos etapas. Analizar la influencia de las nanopartículas en la microestructura y propiedades mecánicas y térmicas de los materiales durante los distintos estadios del proceso de fabricación.
- Fabricar nanocompuestos basados en polietileno de baja densiad y nanopartículas esféricas tipo sílice y espumarlos mediante moldeo por

compresión mejorado para producir materiales celulares con propiedades y estructuras mejoradas. Análisis del grado de mejora inducido por las nanopartículas en los materiales sólidos y aligerados. Análisis de las sinergías nanopartículas-proceso de espumado.

- Fabricar dos tipos de nanocompuestos con basados en polietileno de baja densidad y con composiciones químicas diferentes y espumarlos utilizando el sistema diseñado para producir materiales moldeados y con control de densidad mediante disolución de gas. Determinación del grado de dispersión de las nanopartículas en la matriz polimérica en función de la composición química y análisis de la influencia del grado de dispersión en los efectos producidos por las nanopartículas en la estructura celular y en las propiedades físicas de los materiales.

Puesta a Punto de un Proceso de Recuperación de Materiales Celulares de Baja Densidad con Base Polietileno de Baja Densidad Entrecruzado.

- Diseñar un proceso de recuperación de residuos de espumas de polietileno de baja densidad entrecruzadas capaz de producir un nuevo material celular que pueda ser utilizado en aplicaciones similares a las de los materiales de partida.
- Cuantificar la influencia del proceso de recuperación en la microestructura y propiedades térmicas, mecánicas y acústicas de los materiales recuperados.

1.3.- ESTRUCTURA DE LA TESIS

La presente memoria está estructurada para ser presentada en la modalidad denominada *compendio de publicaciones*. Se presenta un total de 8 artículos, algunos de ellos ya publicados y otros enviados para su publicación en revistas internacionales.

La memoria consta de otros ocho capítulos que incluyen la siguiente información:

- *Capítulo 2*: Se hace una breve revisión de los conceptos relacionados con la microestructura, propiedades y producción de materiales celulares poliméricos.

- *Capítulo 3*: Se enumeran las materias primas utilizadas durante el desarrollo de este trabajo y las técnicas experimentales utilizadas en la caracterización de los materiales bajo estudio. Se incluye además una descripción del proceso de moldeo por compresión y del sistema diseñado para controlar la geometría y la densidad en procesos de disolución de gas.
- *Capítulo 4*: Se muestran dos estudios relacionados con la producción de materiales celulares basados en nanocompuestos de polietileno de baja densidad y nanopartículas esféricas de sílice. En ambos casos se utiliza el proceso de disolución de gas con control de densidad. Se analiza el papel multifuncional que juegan las nanopartículas en los materiales celulares y se explora la presencia de efectos sinérgicos debido al espumado de los nanocompuestos. En el segundo trabajo además se realiza un análisis exhaustivo del grado de dispersión de las nanopartículas en nanocompuestos con dos composiciones químicas diferentes y de los efectos que éste tiene en la microestructura y las propiedades térmicas y mecánicas de las muestras
- *Capítulo 5*: Se analiza el efecto de nanopartículas de tipo laminar en materiales celulares de baja densidad con base LDPE producidos mediante moldeo por compresión en dos etapas. El proceso de producción de los materiales así como los resultados de la caracterización de las propiedades térmicas y mecánicas de los materiales durante los diferentes estadios del proceso de producción se resumen en el trabajo incluido en este capítulo.
- *Capítulo 6*: Se incluyen dos trabajos en los cuales se describe el proceso de producción de materiales celulares con base polipropileno mediante moldeo por compresión mejorado. Se cuantifica el efecto de las condiciones de proceso y de la composición química en la estructura celular y propiedades mecánicas en materiales con distintas geometrías.
- *Capítulo 7*: En este capítulo se incluyen dos trabajos, ambos con un objetivo general que es realizar un estudio comparativo de la microestructura y propiedades de materiales celulares con idénticas matrices poliméricas producidos mediante moldeo por compresión mejorado y disolución de gas. En el primer trabajo incluido el estudio comparativo se refiere a materiales basados en nanocompuestos de polietileno y nanopartículas de sílice y en el segundo a materiales con base polipropileno.
- *Capítulo 8*: El trabajo incluido en este capítulo describe el proceso de producción de materiales celulares recuperados utilizando residuos

procedentes de espumas de baja densidad entrecruzadas. Se estudia la influencia del proceso de recuperado en la estructura celular de los materiales producidos así como en sus propiedades térmicas, mecánicas y acústicas. Para determinar la idoneidad de los materiales recuperados en aplicaciones similares a las de los materiales de partida, se comparan sus propiedades con las de productos comerciales con densidades similares.

- *Capítulo 9*: Se presentan las principales conclusiones de este trabajo así como las futuras líneas de investigación.

En cada capítulo, además de los trabajos enviados o publicados se incluye un resumen de los mismos. En la tabla 1.2 se enumeran las publicaciones incluidas en este trabajo así como el capítulo al que corresponden.

Tabla 1.2: Relación de publicaciones en revistas internacionales presentadas en la memoria de tesis

Publicaciones en Revistas Internacionales	***Capítulo Tesis***
C. Saiz-Arroyo, J. Escudero, M.A. Rodríguez-Perez, J.A. de Saja Improving the Structure and Physical Properties of LDPE Foams using Silica Nanoparticles as an Additive. Cellular Polymers 30: 63-78, (2011)	Capítulo 4
C. Saiz-Arroyo, M.A. Rodríguez-Pérez, J.I. Velasco, J.A. de Saja. LDPE/Silica Nanocomposite Foams. Relationship between Chemical Composition, Particle Dispersion, Cellular Structure and Physical Properties. Journal of Nanoparticle Research, enviado, pendiente de aceptación	Capítulo 4
J.I. Velasco, M. Antunes, O. Ayyad, C. Saiz-Arroyo, M.A. Rodríguez-Pérez, F. Hidalgo, J.A. de Saja. Foams Based on Low Density Polyethylene/Hectorite Nanocomposites: Thermal Stability and Mechanical Properties. Journal of Applied Polymer Science 105: 1658-1667, (2011)	Capítulo 5
C. Saiz-Arroyo, M.A. Rodríguez-Pérez, A. López-Gil, J. Tirado, J.A. de Saja An Alternative Foaming Route to Produce Non-Crosslinked Thermoplastic Foams with Controlled Density and Structure Macromolecular Materials and Engineering, enviado, pendiente de aceptación	Capítulo 6
C. Saiz-Arroyo, M.A. Rodríguez-Pérez, J.A. de Saja Structure-Properties Relationship of Medium Density Polipropylene Foams Polymer International, enviado, pendiente de aceptación.	Capítulo 6
C. Saiz-Arroyo, M.A. Rodríguez-Pérez, J.I. Velasco, J.A. de Saja Influence of Foaming Process on the Structure-Properties Relationship of Foamed LDPE/Silica Nanocomposites Composites Part B, enviado, pendiente de aceptación.	Capítulo 7
C. Saiz-Arroyo, J.A. de Saja, J.I. Velasco, M.A. Rodríguez-Pérez	Capítulo 7

Moulded Polypropylene Foams using Chemical or Physical Blowing Agentes: Structure-Properties Relationship. Journal of Materials Science, DOI 10.1007/s10853-012-6357-7	
C. Saiz-Arroyo, J.A. de Saja, M.A. Rodríguez-Pérez Production and Characterization of Crosslinked Low-Density Polyethylene Foams using Waste of Foams with the Same Composition. Polymer Engineering and Science 52: 751-759, (2012)	Capítulo 8

Los trabajos publicados en esta tesis han generado varias contribuciones a congresos y otras publicaciones. La relación se enumera en la tabla 1.2. Además de las publicaciones incluidas en esta memoria, durante el periodo de tesis se han publicado otros trabajos en revistas internacionales fruto de la colaboración con otros grupos de investigación y no siempre relacionadas con el material bajo estudio en esta memoria. La relación de dichos trabajos se recoge en la tabla 1.3.

Tabla 1.2: Contribuciones a congresos y publicaciones en revistas no indexadas.

Contribuciones a Congresos y Publicaciones en Revistas No Indexadas
M.A. Rodríguez-Pérez, P. García de Acilu Laa, J. Arevalo, C. Saiz-Arroyo, E. Solórzano, J.A. de Saja Foaming of LDPE/Nanosilica Nanocomposites: Improving the Cellular Structure and Mechanical Properties Society of Plastics Engineers Annual Technical Conference 2009, Chicago, Illinois, USA (2009)
M.A. Rodríguez-Pérez, P. García de Acilu Laa, J. Arevalo, C. Saiz-Arroyo, E. Solórzano, J.A. de Saja Microcellular Nanocomposites: A System in which Nanoparticles Play a Multifunctional Role GEP, Valladolid, España. (2009)
C. Saiz-Arroyo, M.A. Rodríguez-Pérez, M. Antunes, J.I. Velasco, J.A. de Saja Foaming of Polypropylene by using both Chemical and Physical Blowing Agents- A Comparative Study of the Structure and Physical Properties" Blowing Agents and Foaming Processes 2010, Colonia, Alemania, (2010)
M.A. Rodríguez-Pérez, C. Saiz-Arroyo, J. Escudero, E. Solórzano, J.A. de Saja, M. Antunes, J.I. Velasco. Gas Dissolution as a Potential Technique to Produce LDPE/Silica Nanocomposite Foams DSL 2010, París, Francia 2010.
C. Saiz-Arroyo, J. Escudero, M.A. Rodríguez-Pérez LDPE/Silica Nanocomposites: A system in which Nanoparticles Play a Multifunctional Role Foams 2011, Seattle, Estados Unidos, (2010)
M.A. Rodríguez-Pérez, C. Saiz-Arroyo, J.A. de Saja Foamed Nanocomposites; A System in which Nanofillers Play a Multifunctional Role European Polymer Congress 2011- XII GEP, Granada, España, (2011)
C. Saiz-Arroyo, M.A. Rodríguez-Pérez, J.A. de Saja Production of Polypropylene Foams from a Conventional PP Grade

SPE Eurotec Conference, Barcelona, España, (2011)
M.A. Rodríguez-Pérez, P. García, J. Arevalo, C. Saiz-Arroyo, E. Solórzano, J.A. de Saja
Using Chemical Blowing Agents to Make Microcellular Nanocomposites
SPE Plastics Research Online DOI 10.2417/1200906.000047 (2009)
C. Saiz-Arroyo, J.A. de Saja, M.A. Rodríguez-Pérez
Recovering Low Density Crosslinked Foams to Produce Foamed Products
SPE Plastics Research Online DOI 10.1002/spepro.003927, (2011)
J. Escudero, C. Saiz-Arroyo, M.A. Rodríguez-Pérez, J.A. de Saja
El Efecto Multifuncional de las Nanopartículas en los Materiales Celulares
Revista de Plásticos Modernos 101 (657) 326-339 (2011)

Tabla 1.3: Otras publicaciones en revistas internacionales realizadas durante el periodo de tesis

Otras Publicaciones en Revistas Internacionales
N.M. Alves, C. Saiz-Arroyo, M.A. Rodríguez-Pérez, R.L. Reis, J.F. Mano
Microhardness of Starch Based Biomaterials in Simulated Physiological Conditions"
Acta Biomaterialia 3: 69-76, (2007)
J.I. Velasco, M. Antunes, O. Ayyad, J.M. López-Cuesta, C. Saiz-Arroyo, M.A. Rodríguez-Pérez, J.A. de Saja.
Foaming Behaviour and Cellular Structure of LDPE/Hectorite Nanocomposites
Polymer 48: 2098-2108, (2007)
C. Saiz-Arroyo, Y. Wang, M.A. Rodríguez-Pérez, N.M. Alves, J.F. Mano.
In Vitro Monitoring the Surface Mechanical Properties of Poly(L-lactic acid) Using Microhardness
Journal of Applied Polymer Science 105: 3860-3864, (2007).
R. Verdejo, C. Saiz-Arroyo, J. Carretero-González, F. Barroso-Bujans, M.A. Rodríguez-Pérez, M.A. López-Manchado
Physical Properties of Silicone Foams filled with Carbon Nanotubes and Functionalized Graphene Sheets
European Polymer Journal 44: 2790-2797, (2008)
A.L. Oliveira, A.J. Pedro, C. Saiz-Arroyo, J.F. Mano, G. Rodríguez, J. San Roman, R.L Reis
Biomimetic Ca-P Coatings Incorporating Bisphosphonates Produced on Starch-Based Degradable Biomaterials
Journal of Biomedical Research Part B: Applied Biomaterials 92B: 55-67, (2010)
J.A. Reglero-Ruiz, C. Saiz-Arroyo, M. Dumon, M.A. Rodríguez-Pérez, L. González
Production, Cellular Structure and Thermal Conductivity of Microcelullar (metil methacryalte)-(butyl acrilate)-(methyl methacrylate) block copolymers
Polymer International 60: 146-157, (2011).
E. Solórzano, M. Antunes, C. Saiz-Arroyo, M.A. Rodríguez-Pérez, J.I. Velasco, J.A. de Saja.
Optical Expandometry: A Technique to Analyze the Expansion Kinetics of Chemically Blown Thermoplastic Foams
Journal of Applied Polymer Science, In press: DOI 10.1002/app.3406

BIBLIOGRAFÍA

[1]. M.A. Rodríguez-Pérez. Propiedades Térmicas y Mecánicas de Espumas de Poliolefinas. Tesis Doctoral, Universidad de Valladolid, (1999).
[2]. O. Almanza. Caracterización y Modelización de las Propiedades Térmicas y Mecánicas en Espumas de Poliolefinas. Tesis Doctoral, Universidad de Valladolid, (2000).
[3]. L.O. Arcos y Rábago. Propiedades Térmicas y Mecánicas de Espumas de Poliolefinas Fabricadas en un Proceso de Moldeo por Compresión. Tesis Doctoral, Universidad de Valladolid, (2002).
[4]. J.L. Ruiz-Herrero. Impacto y Fluencia de Espumas con Base Polietileno. Tesis Doctoral, Universidad de Valladolid, (2004).
[5]. J.I. González-Peña. Efecto de los Tratamientos Térmicos en Bloques de Espuma de Polietileno de Baja Densidad Producidos Mediante Moldeo por Compresión. Tesis Doctoral, Universidad de Valladolid, (2006).
[6]. M. Álvarez-Laínez. Propiedades Térmicas, Mecánicas y Acústicas de Espumas de Poliolefina de Celda Abierta. Tesis Doctoral, Universidad de Valladolid, (2007).
[7]. F. Hidalgo-González. Diseño Optimizado de los Parámetros de Proceso de Fabricación de Espuma de Poliolefina Reticulada mediante Moldeo por Compresión. Tesis Doctoral, Universidad de Valladolid, (2008).
[8]. R. Campo-Arnáiz. Aplicación de Técnicas Espectroscópicas al Estudio de la Morfología Polimérica, Propiedades Térmicas y de Emisión de Espumas de Baja Densidad con Base Poliolefina. Tesis Doctoral, Universidad de Valladolid, (2011).
[9]. M.A. Rodríguez-Pérez, S. Rodríguez-Llorente, J.A. de Saja. Dynamic Mechanical Properties of Polyolefin Foams Studied by DMA. Polymer Engineering and Science 37: 959-965, (1997).
[10]. M.A. Rodríguez-Pérez, O. Alonso, J. Souto, J.A. de Saja. Thermal Conductivity of Crosslinked Closed Cell Polyolefin Foams. Polymer Testing 16: 287-298, (1997).
[11]. M.A. Rodríguez-Pérez, S. Díez-Gutierrez, J.A. de Saja. The Recovery Bheaviour of Crosslinked Closed Cell Polyolefin Foams. Polymer Engineering and Science, 38: 831-838, (1998).
[12]. M.A. Rodríguez-Pérez, A. Duijsens, J.A. de Saja. Effect of the Addition of EVA on the Technical Properties of Extruded Foamed Profiles of Low-Density Polyethylene/EVA Blends. Journal of Applied Polymer Science 36: 2587-2596, (1998).
[13]. J.I. Velasco, A.B. Martínez-Benasat, D. Arencón, M.A. Rodríguez-Pérez, J.A. de Saja. Caracterización Mecánica de Espumas Poliolefinicas mediante Impacto por Caída de Dardo Instrumentado. Anales de Ingeniería Mecánica 2: 639-644, (1998).
[14]. J.I. Velasco, A.B. Martínez-Benasat, M.A. Rodríguez-Pérez, J.A. de Saja. Application of Instrumented Falling Dart Impact to the Mechanical Characterization of Thermoplastic Foams. Journal of Materials Science 34: 431-438, (1999).
[15]. M.A. Rodríguez-Pérez, O. Almanza, J.A. de Saja. Anomalous Thickness Increase in Crosslined Closed Cell Polyolefin Foams During Heat Treatments. Journal of Applied Polymer Science 73: 2825-2835, (1999).
[16]. M.A. Rodríguez-Pérez, J.A. de Saja. The Effect of Blending on the Physical Properties of Crosslinked Closed Cell Polyethylene Foams. Cellular Polymers 18: 1-20, (1999).
[17]. M.A. Rodríguez-Pérez, J.A. de Saja. Diseño de Espumas Poliméricas con Base Poliolefínica (I). Revista de Plásticos Modernos 77: 517-528, (1999).
[18]. M.A. Rodríguez-Pérez, J.A. de Saja. Diseño de Espumas Poliméricas con Base Poliolefínica (II). Revista de Plásticos Modernos 78: 550-558, (1999).
[19]. M.A. Rodríguez-Pérez, J.A. de Saja. Dynamic Mechanical Analysis Applied to the Characterization of Closed Cell Polyolefin Foams. Polymer Testing 19: 831-848, (1999).

[20]. O. Almanza, M.A. Rodríguez-Pérez, J.A. de Saja. The Thermal Conductivity of Polyethylene Foams Manufactured by a Nitrogen Solution Process. Cellular Polymers 18: 385-401, (1999).
[21]. M.A. Rodríguez-Pérez, J.I. Velasco, D. Arencón, O. Almanza, J.A. de Saja. Mechanical Characterization of Closed-Cell Polyolefin Foams. Journal of Applied Polymer Science 75: 156-166, (2000).
[22]. O. Almanza, M.A. Rodríguez-Pérez, J.A. de Saja. Prediction of the Ratiation Term in the Thermal Conductivity of Crosslinked Closed Cell Polyolefin Foams. Journal of Polymer Science. Part B: Polymer Physics 38: 993-1004, (2000).
[23]. J.I. Velasco, A.B. Martínez, D. Arencón, O. Almanza, M.A. Rodríguez-Pérez, J.A. de Saja. Rigidity Characterization of Flexible Foams by Falling Dart Rebound Tests. Cellular Polymers 19: 155-133, (2000).
[24]. M.A. Rodríguez-Pérez, O. Almanza, J.L del Valle, A. González, J.A. de Saja. Improvement of the Measurement Process Used for the Dynamic Mechanical Characterization of Polyolefin Foams. Polymer Testing 20: 253-267, (2001).
[25]. J.A. Martínez-Díez, M.A. Rodríguez-Pérez, J.A. de Saja, L.O. Arcos y Rábago, O. Almanza. The Thermal Conductivity of a Polyethylene Foam Block Produced by a Compression Molding Process. Journal of Cellular Plastics 37: 21-42, (2001).
[26]. O. Almanza, M.A. Rodríguez-Pérez, J.A. de Saja. The Microstructure of Polethylene Foams Produced by a Nitrogen Solution Process. Polymer 42: 7117-7126, (2001).
[27]. O. Almanza, L.O. Arcos y Rábago, M.A. Rodríguez-Pérez, A. González, J.A. de Saja. Structure-Property Relationships in Polyolefin Foams. Journal of Macromolecular Science, Part B: Physics 40: 603-613, (2001).
[28]. N.J. Mills, M.A. Rodríguez-Pérez. Modelling the Gas-Loss Creep Mechanism in EVA Foam from Running Shoes. Cellular Polymers 20: 79-100, (2001).
[29]. M.A. Rodríguez-Pérez, J.A. de Saja. Morphology of Semicrystalline Foams Based on Polyethylene. Journal of Macromolecular Science, Part B: Physics 41: 761-775, (2002).
[30]. M.A. Rodríguez-Pérez, J.I. González-Peña, N. Witten, J.A. de Saja. The Effect of Cell Size on the Physical Properties of Crosslinked Closed Cell Polyethylene Foams Produced by a High Pressure Nitrogen Solution Process. Cellular Polymers 21: 165-194, (2002).
[31]. M.D. Landete-Ruiz, J.A. Martínez-Díez, M.A. Rodríguez-Pérez, J.A. de Saja, J.M. Martín-Martínez. Improved Adhesion of Low-Density Polyethylene/EVA Foams Using Different Surface Treatments. Journal of Adhesion Science and Technology 16: 1073-1101, (2002).
[32]. M.A. Rodríguez-Pérez. The Effect of Density, Chemical Composition and Cellular Structure on the Dynamic Mechanical Response of Foams. Cellular Polymers 21: 117-136 (2002).
[33]. S. Díez-Gutierrez, M.A. Rodríguez-Pérez, M. Machimbarrena, J. González, J.A. de Saja. Technical Note. Impact Sound Reduction of Crosslinked and Non-Crosslinked Polyethylene Foams as Suspended Floors of Concrete Structures. Journal of Building and Acoustics 10: 261-271, (2003).
[34]. O. Almanza, M.A. Rodríguez-Pérez, J.A. de Saja. Applicability of the Transient Plane Source Method to Measure the Thermal Conductivity of Low Density Polyethylene Foams. Journal of Polymer Science, Part B: Polymer Physics 42: 1226-1234, (2004).
[35]. O. Almanza, Y. Masso-Moreau, N.J. Mills, M.A. Rodríguez-Pérez. Thermal Expansion Coefficient and Bulk Modulus of Polyethylene Closed-Cell Foams. Journal of Polymer Science, Part B: Polymer Physics 42: 3741-3749, (2004).
[36]. O. Almanza, M.A. Rodríguez-Pérez, J.A. de Saja. The Measurement of the Thermal Diffusivity and Heat Capacity of Polyehtylene Foams Using the Transient Plane Source Technique. Polymer International, 53: 2038-2044, (2004).
[37]. J.L. Ruiz-Herrero, M.A. Rodríguez-Pérez, J.A. de Saja. Characterization of Polyethylene Foams under Compressive Impact Loading. Materials Science Forum 480-481: 513-518, (2005).

[38]. O. Almanza, M.A. Rodríguez-Pérez, B. Chernev, J.A. de Saja, P. Zipper. Comparative Study on the Lamellar Structure of Polyethylene Foams. European Polymer Journal 41: 599-609, (2005).
[39]. M.A. Rodríguez-Pérez. Crosslinked Closed Cell Polyolefin Foams: Production, Structure, Properties and Applications. Advances in Polymer Science 184: 87-126, (2005).
[40]. J.L. Ruiz-Herrero, M.A. Rodríguez-Pérez, J.A. de Saja. Effective Diffusion Coefficient for the Gas Contained in Closed Cell Polyethylene-Based Foams Subjected to Compressive Creep Tests. Polymer 46: 3105-3110, (2005).
[41]. R.A. Campo-Arnáiz, M.A. Rodríguez-Pérez, B. Calvo, J.A. de Saja. Extinction Coefficient of Polyolefin Foams. Journal of Polymer Science, Part B: Polymer Physics 43: 1608-1617, (2005).
[42]. J.L. Ruiz-Herrero, M.A. Rodríguez-Pérez, J.A. de Saja. Design and Construction of an Instrumented Falling Weight Impact Tester to Characterize Polymer-Based Foams. Polymer Testing 24: 641-647, (2005).
[43]. J.L. Ruiz-Herrero, M.A. Rodríguez-Pérez, J.A. de Saja. Effect of Sample Size on the Effective Diffusion Coefficients for Gas Contained in Closed Cell Polyethylene-Based Foams Subjected to Compressive Creep Tests. Journal of Applied Polymer Science 99: 2204-2210, (2005).
[44]. J.L. Ruiz-Herrero, M.A. Rodríguez-Pérez, J.A. de Saja. Prediction of Cushion Curves for Closed Cell Polyethylene-Based Foams. Part I: Modelling. Cellular Polymers 24: 329-346, (2005).
[45]. M.A. Rodríguez-Pérez, R.A. Campo-Arnáiz, R. Aroca, J.A. de Saja. Characterization of the Matrix Polymer Morphology of Polyolefin Foams by Raman Spectroscopy. Polymer 46: 12093-12102, (2005).
[46]. M.A. Álvarez-Laínez, M.A. Rodríguez-Pérez, G. Antolín, J. González, J.A. de Saja. Absorción Acústica de Espumas de Poliolefina de Celda Abierta y Cerrada. Revista de Acústica 36: 1-8, (2005).
[47]. J.L. Ruiz-Herrero, M.A. Rodríguez-Pérez, J.A. de Saja. Prediction of Cushion Curves for Closed Cell Polyethylene-Based Foams. Part II: Experimental. Cellular Polymers 25: 156-175, (2006)
[48]. M.A. Rodríguez-Pérez, J.L. Ruiz-Herrero, E. Solórzano, J.A. de Saja. Gas Diffusion in Polyolefin Foams During Creep Tests. Effect on Impact Behaviour and Recovery after Creep. Cellular Polymers 25: 221-236, (2006).
[49]. M.A. Rodríguez-Pérez, J.I. González-Peña, J.A. de Saja. Anisotropic and Heterogenous Thermal Expansion of Polyethylene Foam Blocks: Effect of Thermal Treatments. European Polymer Journal 43: 4474-4485, (2007).
[50]. M. Álvarez-Laínez, M.A. Rodríguez-Pérez, J.A. de Saja. Thermal Conductivity of Open Cell Polyolefin Foams. Advanced Engineering Materials 10: 373-377, (2008).
[51]. M.A. Rodríguez-Pérez, O. Almanza, J.L. Ruiz-Herrero, J.A. de Saja. The Effect of Processing on the Structure and Properties of Crosslinked Closed Cell Polyethylene Foams. Cellular Polymers 27: 179-200, (2008).
[52]. M.A. Rodríguez-Pérez, M. Álvarez-Laínez, J.A. de Saja. Microestructure and Physical Properties of Open Cell Polyolefin Foams. Journal of Applied Polymer Science 114: 1176-1186, (2009).
[53]. M.A. Rodríguez-Pérez, F. Hidalgo, E. Solórzano, J.A. de Saja. Measuring the Time Evolution of the Gas Pressure in Closed Cell Polyolefin Foams Produced by Compression Moulding. Polymer Testing 28: 188-195, (2009).
[54]. M.A. Rodríguez-Pérez, J.I. González-Peña, J.A. de Saja. Modifying the Structure and Properties of Polyethylene Foams using Thermal Treatments. Polymer International 58, 620-629, (2009).
[55]. J. Martini-Vvedensky, N.P. Suh, F.A. Waldman. US Patent nº 4.473.665, (1984).
[56]. A. Okada, A. Usuki. Chemistry of Polymer-Clay Hybrids. Materials Science and Engineering 3: 109-115, (1995)
[57]. M.A. Rodríguez-Pérez, J. Lobos, C.A. Pérez-Muñoz, J.A. de Saja, L. González, B.M.A. del Carpio. Mechanical Behaviour at Low Strains of LDPE Foams with Cell Sizes in the Microcellular Range: Advantages of using these materials in structural elements. Cellular Polymers 27: 347-362, (2010).

[58]. M.A. Rodríguez-Pérez, J. Lobos, C.A. Pérez-Muñoz, J.A. de Saja. Mechanical Response of Polyolefin Foams with High Densities and Cell Sizes in the Microcellular Range. Journal of Cellular Plastics 45: 389-403, (2009).

[59]. S. Román Lorza. Formulación y Caracterización de Materiales Celulares Retardantes de Llama Libres de Halógenos basados en Poliolefinas. Tesis Doctoral, Universidad de Valladolid, (2010).

[60]. S. Román-Lorza, M.A. Rodríguez-Pérez, J.A. de Saja. Cellular Structure of Halogen-Free Flame Retardant Foams based on LDPE. Cellular Polymers 28: 249-268, (2009).

[61]. S. Román-Lorza, J. Sabadell, J.J. García-Ruiz, M.A. Rodríguez-Pérez, J.A. de Saja. Fabrication and Characterization of Halogen Free Flame Retardant Polyolefin Foams. Materials Science Forum 636/637: 98-205, (2010)

[62]. S. Román-Lorza, M.A. Rodríguez-Pérez, J.A. de Saja. Cellular Structure of EVA/ATH Halogen-Free Flame Retardant Foams. Journal of Cellular Plastics 10: 1-21, (2010).

[63]. M.A. Rodríguez-Pérez, R.D. Simoes, C.J.L. Constantino. J.A. de Saja. Structure and Physical Properties of EVA/Starch Precursor Materials for Foaming Applications. Journal of Applied Polymer Science 212: 2324-2330, (2011).

[64]. M.A. Rodríguez-Pérez, R.D. Simoes, S. Román-Lorza, M. Álvarez-Laínez, C. Montoya-Mesa. C.J.L. Constantino, J.A. de Saja. Foaming of EVA/Starch Blends: Characterization of the Structure, Physical Properties and Biodegradability. Polymer Engineering and Science 52: 62-70, (2012).

Capítulo 2

Revisión de Conceptos

La versatilidad de los materiales celulares y la amplia variedad de campos en los que son utilizados hace que la cantidad de información relacionada con ellos sea muy extensa. En este capítulo se pretenden introducir aquellos conceptos básicos relacionados con los materiales celulares poliméricos necesarios para la compresión del estudio que se ha realizado. Dado que el principal objetivo de esta investigación es obtener materiales celulares con base poliolefina con propiedades mejoradas, en este capítulo además, se describen brevemente las estrategias más comunes seguidas en la actualidad para obtener materiales celulares más eficientes para cada aplicación.

Además se resumen algunas de las investigaciones precedentes a la presentada en esta memoria, si bien, una descripción detallada del estado del arte de cada tema analizado en esta investigación se muestra en cada uno de los capítulos de resultados.

2.1.- CONCEPTOS BÁSICOS RELACIONADOS CON LOS MATERIALES CELULARES POLIMÉRICOS

Un material celular polimérico es una estructura de dos fases en la cual una fase gaseosa procedente de un agente espumante, bien sea físico o químico, se ha dispersado a lo largo de una matriz polimérica sólida [1].

Aunque en algunas ocasiones se haga referencia a los materiales celulares como espumas, es necesario aclarar que una espuma es un tipo específico de material celular que se ha generado por expansión de un material en estado líquido. Los materiales bajo estudio de esta tesis están enfocados hacia aplicaciones estructurales por lo que en la mayoría de los casos se les denominará materiales celulares en lugar de espumas

Los materiales celulares poliméricos se pueden clasificar en base a varios criterios. El primero de ellos hace referencia al tipo de estructura celular. Así, es posible encontrar materiales celulares de *Celda Abierta* donde el gas puede circular libremente entre las celdillas ya que estas están interconectadas, o materiales de *Celda Cerrada*, en los cuales el gas está ocluido en el interior de las celdas [1].

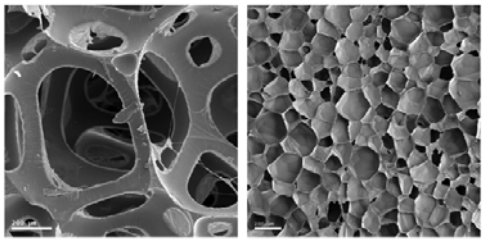

Figura 2.1. Espuma de poliuretano de celda abierta (izquierda) y espuma de polietileno de baja densidad de celda cerrada, (derecha).

Otra característica importante en base a la cual se puedan clasificar los materiales celulares es su densidad, ya que ésta determina tanto sus propiedades como su campo de aplicación [1, 2].

Cuando se habla de la densidad de un material espumado es común hacerlo refiriéndose a su *Densidad Relativa*, que es la relación entre la densidad de la espuma, (ρ_{espuma}) y la del correspondiente material sólido, ($\rho_{sólido}$) [1, 2]

$$\rho_{\text{Relativa}} = \frac{\rho_{espuma}}{\rho_{solido}} \qquad \text{Ec. 2.1}$$

En algunos casos a lo largo de esta tesis también se hablará del *Grado de Expansión (ER)*, que es el inverso de la densidad relativa y que tal y como su nombre indica, cuantifica el número de veces que se ha invertido el volumen del material sólido para formar el material celular.

$$ER = \frac{1}{\rho_{\text{Relativa}}} = \frac{\rho_{sólido}}{\rho_{espuma}} \qquad \text{Ec. 2.2}$$

Los materiales celulares se pueden clasificar en tres categorías dependiendo de su densidad relativa. Cuando ésta es menor de 0.3 se consideran *Materiales Celulares de Baja Densidad*, cuando es mayor de 0.6 se les considera *Materiales Celulares de Alta Densidad* y cuando su densidad relativa alcanza valores intermedios entre estos dos, se las denomina *Materiales Celulares de Densidad Media* [2]

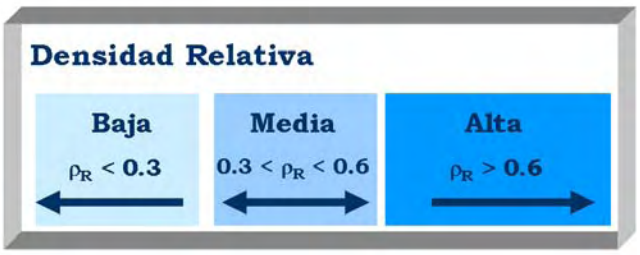

Figura 2.2. Clasificación de los materiales celulares poliméricos en función de su densidad relativa.

La dependencia de las propiedades de un material celular con la densidad es tal, que cualquier propiedad de una espuma se puede estimar en primera aproximación utilizando las conocidas como *Relaciones de Escala* [1, 3]. Estas ecuaciones empíricas (Ec 2.3) simples afirman que el valor de una cierta propiedad P_{espuma} de un material celular, es función de la misma propiedad pero del material 100% sólido, (P_{solido}), de su densidad relativa y de dos parámetros (C y n) que pueden ser determinados de forma experimental.

$$P_{espuma} = C \cdot P_{sólido} \cdot \left(\frac{\rho_{espuma}}{\rho_{sólido}} \right)^{n} \qquad \text{Ec 2.3}$$

C generalmente toma valores cercanos a la unidad (especialmente para altas densidades relativas) y para la mayoría de los materiales celulares y propiedades físicas), *n* suele alcanzar valores comprendidos entre *n=1* y *n=2* [1, 3, 4].

Se definen las Propiedades Relativas de un material celular como la relación entre una determinada propiedad de dicho material y la misma pero del correspondiente material sólido, esto es, $P_{relativa} = \frac{P_{espuma}}{P_{sólido}}$. La relación entre las propiedades relativas y la densidad relativa viene dada por la gráfica siguiente.

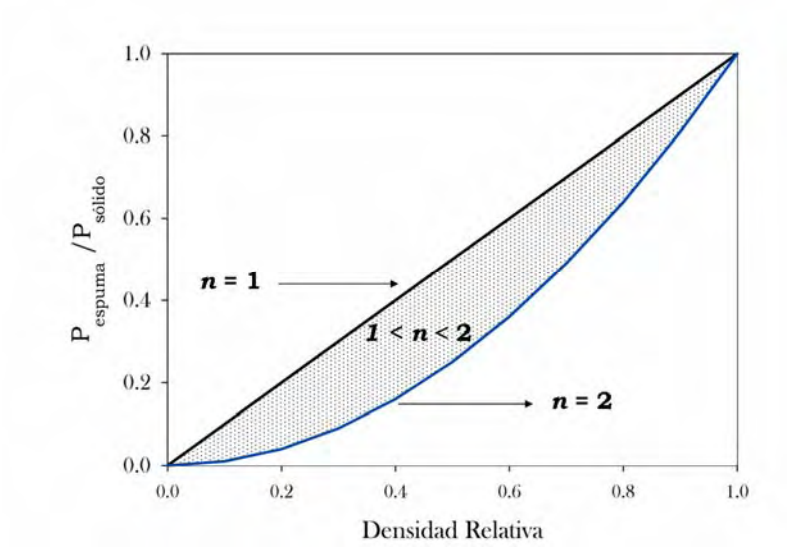

Figura 2.3: Relación entre las propiedades relativas de un material celular y su densidad relativa

Tal y como se puede apreciar en la figura 2.3, cuando *n* = 1, la relación entre la reducción de densidad y la reducción en propiedades es lineal, sin embargo, a medida que *n* aumenta, la disminución de las propiedades es mayor que la reducción de densidad. Como ya se ha mencionado la mayoría de los materiales celulares y para muchas de las propiedades físicas más importantes, presentan un valor de *n* comprendido entre 1 y 2, (zona sombreada) de modo que la relación entre las propiedades relativas y la densidad relativa no es lineal. Si lo que se desea es que la reducción de propiedades sea lo menor posible, (por ejemplo para aplicaciones estructurales y propiedades como el módulo de elasticidad) entonces se debe buscar generar materiales celulares con estructuras que den lugar a valores de *n* cercanos a 1. En el caso de propiedades mecánicas como el módulo de elasticidad o el esfuerzo de colapso en compresión se admite que generalmente estos bajos valores de *n* está

asociado a lograr estructuras celulares de celda cerrada y con gran homogeneidad de tamaños (distribución de tamaños celulares estrechos) [1, 3, 4]. En el caso de propiedades como la resistencia al impacto, tenacidad, comportamiento a fatiga, existen trabajos que indican que para alcanzar bajos valores de n se requieren estructuras de tipo microcelular, (con tamaños de celda menores de aproximadamente 10 μm) [4-6].

Desde el comienzo de su comercialización en los años 50, y debido al gran interés generado por este tipo de materiales, se ha dedicado una cantidad considerable de esfuerzo a obtener materiales con propiedades adaptadas a cada tipo de aplicación. Así, hoy en día, se habla de "*diseño de materiales a la carta*", de modo que se intenta conseguir materiales celulares lo más eficientes posibles en función de los requerimientos que éste deba cumplir.

Las propiedades de un material celular dependen en gran medida de su densidad, pero también de su estructura celular y de las propiedades de la matriz que forma las paredes y las aristas de las celdillas [1, 2, 4, 7, 8]. De ahí, que el diseño de materiales celulares a la carta, pase por la optimización de los materiales a todos esos niveles.

La obtención de materiales altamente eficientes para una determinada aplicación o un determinado sector de mercado, a nivel tecnológico, está basado en la actuación a dos niveles [2], en primer lugar la *modificación de la composición química* de la matriz que forma el material celular y en segundo lugar el *control de los parámetros involucrados en el proceso de espumado* elegido, (figura 2.4).

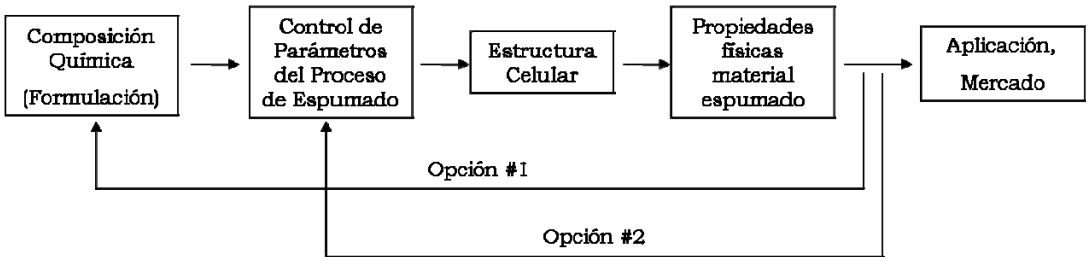

Figura 2.4: Estrategia seguida a nivel tecnológico para optimizar materiales celulares poliméricos.

El proceso de formación de un material celular implica varias etapas. La mayor parte de los procesos de basa en cuatro etapas la primera de ellas consiste en la *formación de una disolución polímero/gas* sobresaturada bajo unas ciertas condiciones de presión y temperatura. El segundo paso es la *nucleación de las celdillas* y el tercero y el cuarto son respectivamente el *crecimiento* y *estabilización* de la estructura celular [2, 4].

Cualquiera de los dos primeros pasos del diagrama anterior, bien sea la modificación de la estructura y/o composición química del polímero base o el control de los parámetros involucrados en el proceso de espumado, están orientados a actuar en las diferentes etapas del proceso de formación del material celular. Esto implica que es necesario conocer en primer lugar como influyen las características de la estructura celular en la respuesta de un material celular, (relación estructura-propiedades) pero también es necesario conocer, sobre qué etapas del proceso pueden actuar las modificaciones llevadas a cabo en la matriz polimérica y/o en los parámetros de proceso.

Este esquema es el mismo que se ha seguido a lo largo del desarrollo de esta tesis. Tomando como base unos determinados polímeros, se ha actuado tanto en la composición química como en los parámetros de proceso con el fin de conseguir materiales poliméricos celulares con distintos tipos de estructuras que además puedan servir para diversas aplicaciones.

2.2.- RELACIÓN ESTRUCTURA-PROPIEDADES EN LOS MATERIALES CELULARES POLIMÉRICOS

Variar la composición o la estructura química de un determinado polímero y modificar los parámetros de proceso permiten obtener distintos tipos de estructuras celulares. Generalizar sobre la influencia de la estructura celular de un material celular en las propiedades físicas del mismo es muy complicado dada la amplia variedad de matrices poliméricas que se pueden espumar utilizando distintos tipos de procesos de fabricación. Sin embargo, en este apartado se han tratado de resumir algunos conceptos generales (para los que puede haber ciertas excepciones) relacionados con la influencia de las propiedades de la estructura celular en las propiedades de un material celular

- *Tamaño medio de celda (ϕ)*

Tal y como su nombre indica hace referencia al diámetro medio de las celdillas que componen un material celular. El modo más común de determinarlo es siguiendo el procedimiento descrito por el estándar ASTM D3576, basado en el Método de las Intersecciones [9]. Para la medida de los tamaños de celda de las espumas analizadas en esta tesis se ha utilizado un software desarrollado en el Laboratorio Cellmat basado en un programa de análisis de imagen, (Image J) [10]. Este software permite determinar

además del tamaño de celda, parámetros tales como la *densidad celular*, (i.e. el número de celdillas por unidad de volumen), o el *Ratio de Anisotropía* (*R*).

En algunos casos, por ejemplo cuando se utilizan agentes espumantes de tipo químico, la relación entre el tamaño de celda y la densidad se puede describir mediante una función hiperbólica (figura 2.5) [2], de modo que el tamaño de celda aumenta de forma considerable a medida que la densidad del material celular disminuye.

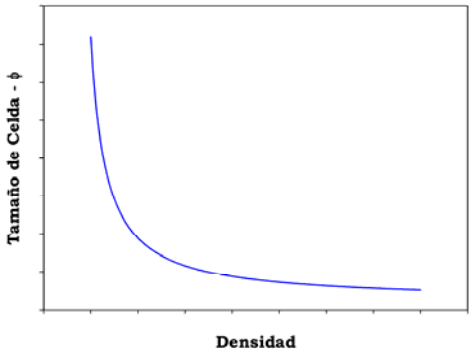

Figura 2.5: Relación entre el tamaño de celda y la densidad de materiales celulares fabricados utilizando agentes espumantes químicos.

La influencia del tamaño de celda en las propiedades térmicas es conocida y ha sido estudiada en trabajos previos del grupo, [11-14] concluyéndose que al disminuir el tamaño de celda, la conductividad térmica de materiales celulares de celda cerrada con densidades relativas menores que 0.15 se reduce ya que decrece el término de radiación. Sin embargo, para elevadas densidades relativas, el tamaño de celda no tiene una influencia significativa en la conductividad térmica*.

Sin embargo, la influencia del tamaño de celda en las propiedades mecánicas a bajas deformaciones no es tan clara. El análisis de espumas con similares densidades pero distintos tamaños de celda, ha permitido concluir que éste no tiene influencia en el comportamiento mecánico de los materiales celulares (a igualdad de densidad) [15-17].

- *Distribución de Tamaños Celulares*

Aunque no se pueda generalizar sobre la influencia del tamaño celular en las propiedades físicas de los materiales espumados, la influencia de la distribución de los tamaños celulares es conocida. Una distribución no uniforme de tamaños de celda a lo largo del material afecta de forma negativa a las propiedades del mismo, [2, 4, 6, 18]. Por ejemplo, las propiedades mecánicas de un material con una distribución de tamaños de celda inhomogénea son inferiores a las de un material con una distribución

*Estas afirmaciones son válidas para materiales de celda cerrada siempre que el tamaño de la celda sea tal que no permita el mecanismo de convección. Estos tamaños son inferiores a los 3mm [11-14].

de tamaños de celda homogénea. En el primero de los casos, la fracción de masa sólida no estaría distribuida de forma homogénea, lo que implicaría que los esfuerzos a los que pueda estar sometido el material no se propaguen de la misma forma a lo largo de todo el volumen del mismo, o que la propagación de grietas y "cracks" se vea favorecida en zonas con menor fracción de material sólido [1].

En la figura 2.6 aparecen dos ejemplos de histogramas típicos de materiales celulares. El de la izquierda corresponde a una muestra con una distribución de tamaños de celda muy inhomogénea y que se desvía mucho de ser una distribución normal. El histograma de la derecha, por el contrario, corresponde a una muestra con una distribución de tamaños de celda muy homogénea más similar a una distribución normal. Lo ideal desde punto de vista macroscópico, es producir espumas cuyo histograma de distribución de tamaños celulares se corresponda con una distribución normal y no multi-modal.

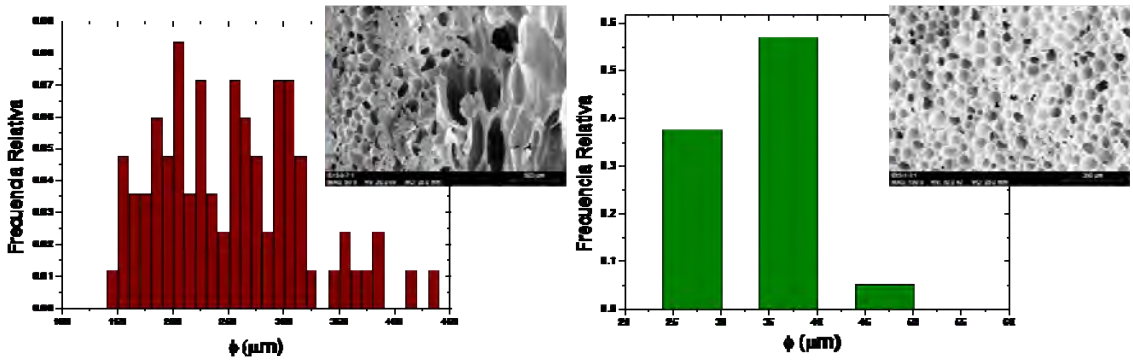

Figura 2.6: Ejemplos de histogramas de distribución de tamaños celulares de espumas poliméricas.

Cuando se desea comparar la distribución de tamaños de celda de una gran cantidad de muestras comparar los histogramas uno a uno suele resultar complicado. Esta tarea se facilita cuando esa comparación se hace en base a la desviación estándar de los tamaños celulares de cada muestra. Ese parámetro, (*SD*) da cuenta de la *anchura de la distribución* y se calcula conforme a la ecuación 2.4, [19, 20].

$$SD = \sqrt{\sum_{i=1}^{n} \frac{(\phi_i - \phi)^2}{n}} \qquad \text{(Ec 2.4)}$$

donde n es el número total de celdas, ϕ_i es el diámetro de la celdilla i, y ϕ es el tamaño promedio de las celdas. Cuanto más pequeño sea el valor de *SD*, más homogénea será la distribución de tamaños de celdilla en esa muestra.

- *Contenido de Celdas Abiertas (C)*

En relación a su morfología celular, las espumas poliméricas pueden presentar estructuras como las mostradas en la figura 2.1 (celda completamente abierta o cerrada), o algo intermedio entre esas dos situaciones. El contenido de celdas abiertas de un material celular se define de la siguiente manera [18]:

$$C = \frac{\text{Volumen de Celdas Interconectadas}}{\text{Volumen de Gas Total}} \qquad \text{(Ec 2.5)}$$

Se puede determinar utilizando un picnómetro de gas o de aire siguiendo el procedimiento descrito en el estándar ASTM D6226-10 [21].

La presencia de celdas abiertas en un material celular es positiva para aplicaciones tales como la absorción o atenuación de ondas sonoras, en bandejas destinadas a contener alimentos, donde es necesario un cierto número de celdas abiertas que controlen la capilaridad del sistema y sean capaces de absorber los líquidos procedentes del alimento en cuestión, en sistemas donde se requiere una gran capacidad de recuperación del material tras un esfuerzo compresivo, (asientos, colchones) o para el uso en filtros. Sin embargo, un cierto grado de interconexión entre las celdillas es perjudicial para la estabilidad dimensional, para la respuesta mecánica de un material celular y para su capacidad como aislante térmico [18].

El contenido de celda abierta, para polímeros termoplásticos, normalmente depende del grado de expansión; a medida que éste aumenta el número de celdas interconectadas también lo hace [2, 18]. Al disminuir la densidad, la matriz polimérica está sometida a mayores fuerzas elongacionales durante el proceso de expansión, por tanto, las paredes de las celdillas son más finas y en consecuencia más débiles y con mayor tendencia a romperse [6, 18].

Los parámetros de proceso y la reología de la matriz polimérica son fundamentales en el control del contenido de celdas abiertas de un material celular [18].

- *Anisotropía*

Algunos materiales celulares, debido al proceso de producción pueden presentar un cierto grado de anisotropía, tanto en la orientación de las celdillas como en sus propiedades [4]. Para materiales con una dirección principal de crecimiento, en los que la celda está preferencialmente orientada en esa dirección y es igual en las otras dos direcciones, se puede caracterizar la anisotropía mediante el *Ratio de Anisotropía* (*R*), definido como el cociente entre el diámetro promedio de la celdilla medido en la dirección de crecimiento y el diámetro medido en la dirección transversal, [1].

El que las celdillas estén orientadas en una cierta dirección preferencial hace que las propiedades medidas en esa dirección sean diferentes que aquellas medidas en la dirección transversal, [1, 4]. En ciertas aplicaciones estructurales, la generación de estructuras altamente anisotrópicas puede ser beneficioso. Cuando la solicitación mecánica a la que esté sometido el material se produzca coincidiendo con la dirección de orientación preferencial de las celdillas, la respuesta de ese material, será superior a la de un material isótropo, ($R = 1$) [1]. Sin embargo, este efecto es perjudicial para el aislamiento térmico en materiales de baja densidad relativa, en los que la conductividad térmica es mayor en la dirección en la que las celdas están orientadas, [22, 23].

2.3.- MODIFICACIÓN DE LA MATRIZ POLIMÉRICA

Según el diagrama mostrado en la figura 2.4, el primer paso para conseguir materiales celulares poliméricos más efectivos para cada aplicación parte de la optimización de las propiedades del polímero base. La estrategia para optimizar las propiedades de la matriz polimérica se basa en dos puntos, la *modificación de la arquitectura molecular del polímero base* y la *adición de diversos tipos de cargas bien orgánicas o inorgánicas* [2, 4, 6, 18, 24]. La utilización de una u otra o de la combinación de ambas ya que su uso no es excluyente, depende tanto de la naturaleza de la matriz polimérica como de las restricciones que puedan ser impuestas por la normativa relacionada con la aplicación final del material. Además, hay que tener en cuenta el factor económico; la modificación de la arquitectura molecular de un polímero en ocasiones es un proceso complejo que puede acarrear aumentos en los costes del material. En relación a la adición de cargas, es necesario valorar, en función del porcentaje en el que deban ser añadidas, si la relación entre el efecto en la estructura y/o propiedades y el aumento de precio generado en el coste del material es viable desde un punto de vista económico.

En cualquier caso, cualquiera que sea la estrategia elegida se puede decir que todas buscan un objetivo común que es obtener un material celular optimizado para una aplicación determinada y para ello actúan a los siguientes niveles [2, 4, 6]:

- Optimización de la *reología* del polímero base.
- Mejora del proceso de *nucleación* de las celdillas.

- Modificación de la *morfología de la matriz polimérica* en el material celular.
- Modificación de las *propiedades físicas* (térmicas o mecánicas) de la matriz polimérica.

No en todos los casos es necesario actuar a cada nivel, sino que las necesidades propias de cada material harán que los esfuerzos se enfoquen en una dirección u otra. Por tanto, es necesario conocer cómo se puede modificar la arquitectura molecular de un polímero o cuales son las cargas más adecuadas de modo que la matriz polimérica tenga una respuesta adecuada a cada uno de esos niveles.

2.3.1.- Modificación de la Arquitectura Molecular de la Matriz Polimérica

En la actualidad es posible encontrar una cantidad de polímeros espumados (tanto termoplásticos como termoestables) muy extensa [2]. Por este motivo, esta revisión se ha centrado en los materiales termoplásticos y más concretamente en las poliolefinas, ya que son los polímeros elegidos como matriz polimérica en el desarrollo de esta tesis.

Las poliolefinas (principalmente polietileno, polipropileno y sus copolímeros) constituyen el grupo más importante de polímeros termoplásticos de gran consumo. Combinan una serie de propiedades como son baja densidad, estabilidad química y resistencia mecánica con una facilidad de procesado que les hace idóneos en multitud de aplicaciones tanto para piezas sólidas como para piezas aligeradas [25].

Para este tipo de polímeros, la modificación de su arquitectura molecular está enfocada a la obtención de materiales con una respuesta reológica más adecuada para un proceso de espumado. Las estrategias más comúnmente utilizadas para conseguir esto son, en primer lugar la *producción de polímeros altamente ramificados* (que generalmente dan lugar a materiales "*alta resistencia en fundido*") o el *entrecruzamiento* de las cadenas poliméricas.

2.3.1.1.- Polímeros Altamente Ramificados y que Presentan "Alta Resistencia en Fundido"

Durante el proceso de espumado, una vez que las celdillas nuclean, el gas en su interior comienza a expandirse haciendo que el polímero que forma las paredes celulares se vea sometido a fuerzas elongacionales similares a las que sufriría en un proceso de moldeo por soplado o de soplado de film [6, 8].

Cuando el polímero no es capaz de soportar el estiramiento al que es sometido durante la expansión, las paredes de las celdillas se rompen, favoreciendo la coalescencia y la degeneración de la estructura celular en general, (mayor contenido de celda abierta, mayores tamaños de celda, menor densidad celular y distribución de tamaños celulares más inhomogénea). Además se obtienen menores grados de expansión de los esperados ya que el gas puede escapar fácilmente a través de las celdas abiertas [6].

En un polímero la resistencia que éste presenta a ser estirado es proporcional a la velocidad a la que se produce dicho estiramiento. La *viscosidad extensional* (o *elongacional*, η_E) da cuenta de esa proporcionalidad. A bajas velocidades de deformación la viscosidad aumenta con el tiempo hasta que se hace independiente del mismo. En algunos polímeros se produce un fenómeno conocido como "*strain hardening*" que está asociado con un rápido aumento de la viscosidad elongacional a altas deformaciones, (figura 2.7) [6, 18]. Este comportamiento sugiere que cuando las moléculas se orientan bajo el efecto de la tensión unidireccional, las ramificaciones del polímero actúan como "ganchos" impidiendo que unas moléculas deslicen sobre otras dificultando de esta manera el flujo. Por el contratrario en polímeros de altamente lineales, unas cadenas moleculares se deslizan más fácilmente sobre otras y como consecuencia el flujo elongational tiende a disminuir a altas deformaciones [26].

El fenómeno "*strain hardening*" se asocia con polímeros altamente ramificados como es el caso del polietileno de baja densidad, (LDPE). Tal y como se aprecia en la figura 2.7 [24], a partir de un cierto valor de deformación, la respuesta del material se desvía de la tendencia lineal propia del comportamiento viscoelástico [6].

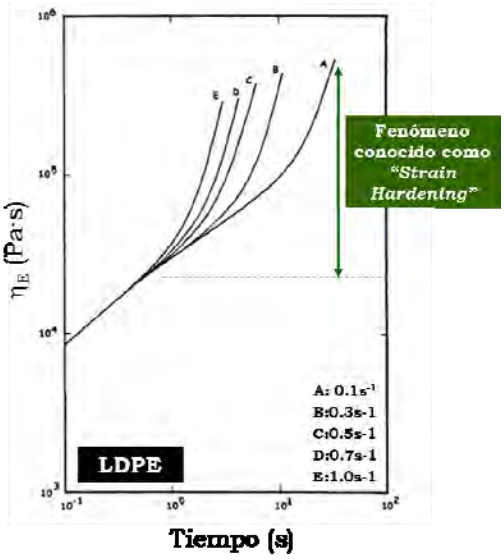

Figura 2.7: Medida de la viscosidad elongacional del LDPE. Se observa la presencia del *strain hardening* a todas las velocidades de deformación ensayadas.

A nivel práctico este fenómeno se traduce en que el polímero puede ser sometido a mayores ratios de estirado ya que a altas velocidades de deformación extensional se comportará como un sólido elástico perfecto favoreciendo la estabilización de las celdillas durante el proceso de crecimiento [2].

En los polímeros de cadena altamente lineal tales como el polipropileno (PP) o el polietileno de alta densidad, (HDPE), las moléculas no presentan tanto grado de empaquetamiento y por tanto el fenómeno "*strain hardening*" no es detectado. Esta es la de que no sean tan aptos para producir espumas como aquellos con alto grado de ramificación [2, 4, 6].

A comienzos de los años 90, Basell comercializó un grado de PP de alta resistencia en fundido (*HMS: high melt strength*). Este tipo de resinas son capaces de exhibir "*strain-hardening*" debido al alto grado de ramificación inducido al ser sometidas a irradiación con electrones en una atmósfera pobre en oxígeno [2]. En la figura 2.8 se pueden apreciar las diferencias en el comportamiento de la viscosidad elongacional entre un grado de polipropileno lineal, (izquierda) y un grado de polipropileno de alta resistencia en fundido (derecha) [6].

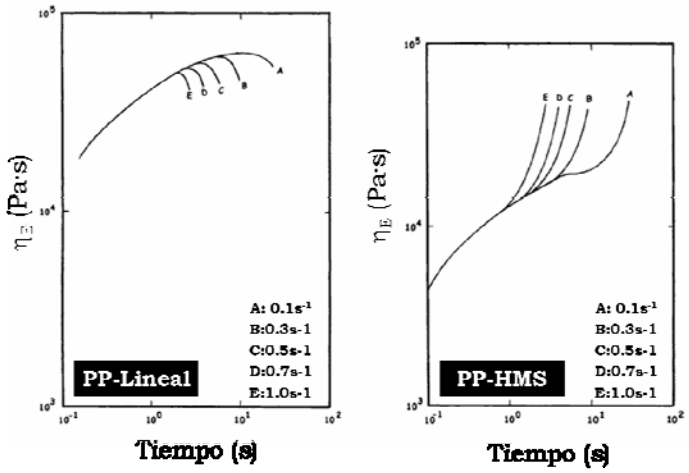

Figura 2.8: Diferencias en el comportamiento reológico de un PP lineal y un PP altamente ramificado, (HMS).

Hasta la comercialización de grados de PP-HMS, la presencia en el mercado de piezas de PP espumado de baja densidad era más bien escasa debido a la baja calidad de los productos fabricados con PP lineal. En 1994, Dow comercializó la primera plancha fabricada con grado de PP altamente ramificado [27] y desde entonces el uso de polipropilenos de alta resistencia en fundido o de mezclas de PP lineal con PP-HMS para la producción de materiales espumados se ha generalizado. Varios autores han probado que la utilización estos polímeros de alta resistencia en fundido lleva a la producción de espumas con base PP de mejor calidad. Se consiguen mayores reducciones de peso y mayores densidades celulares debido a una menor coalescencia y menor porcentaje de celdas abiertas o distribuciones de celda más homogéneas que cuando se utilizan polipropilenos lineales [28-32].

Parece ser por tanto que el uso de grados de PP altamente ramificados es la solución más utilizada hoy en día para producir espumas de alta calidad, ya que además son reciclables. Sin embargo, estos materiales tienen un importante inconveniente y es que su precio en la actualidad es aproximadamente el doble del que tiene un grado convencional de PP lineal.

2.3.1.2.- Polímeros Entrecruzados

El uso de polímeros altamente ramificados no es suficiente en algunos casos para estabilizar las celdillas durante el proceso de expansión. Normalmente, en procesos de

espumado donde el proceso de expansión del polímero se produce a alta temperatura es necesario *entrecruzar* el polímero para poder estabilizar las celdillas durante el crecimiento [2]. Ese es el caso por ejemplo del polietileno de baja densidad, (LDPE), aunque su estructura molecular presenta un alto grado de ramificación, éste, no es suficiente para poder producir materiales espumados de baja densidad en procesos que implican temperaturas elevadas, (típicamente basados en agentes espumantes químicos). La figura 2.9 permite explicar este hecho de forma más gráfica.

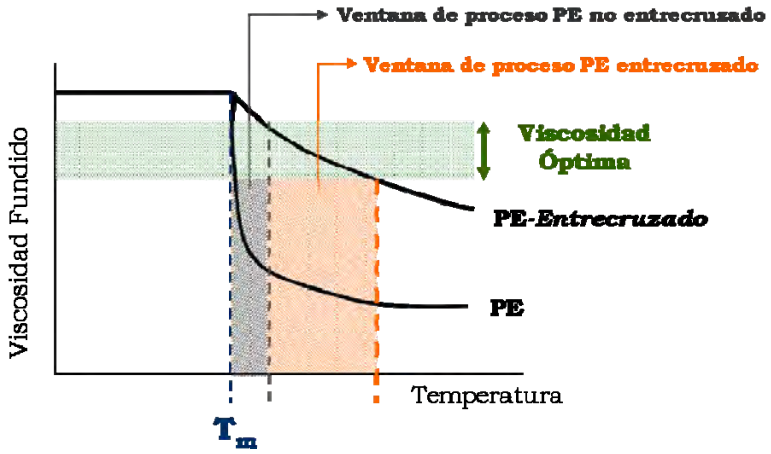

Figura 2.9: Rango de viscosidades óptimas para producir espumas de PE y efecto de la reticulación en la viscosdiad.

El entrecruzamiento del polímero permite estabilizar las celdillas durante el proceso de expansión ya que aumenta la viscosidad extensional del polímero tal y como se puede observar en la figura anterior [2], la ventana de proceso de amplía considerablemente al entrecruzarse el polímero base. Otra de las ventajas añadidas de entrecruzar el polímero es que mejora la estabilidad dimensional del producto final, lo que es beneficioso por ejemplo cuando el material espumado debe ser posteriormente termoconformado [2, 4, 13, 33].

El entrecruzamiento de un polímero implica la formación de estructuras tridimensionales que son los responsables del cambio en las propiedades del polímero. Existen diversos métodos para entrecruzar poliolefinas, aunque se pueden dividir en dos tipos, *químico* o por *irradiación* [2]. Todos ellos están basados en la formación de radicales libres en la molécula de la poliolefina que posteriormente se recombinan dando lugar a enlaces covalentes entre cadenas [25].

El entrecruzamiento por irradiación utiliza una radiación de alta energía, (rayos β, γ, X, o neutrones) para producir los radicales libres. Hay que tener en cuenta en este

proceso que el grado de recombinación debe ser mayor que el de producción de radicales tal y como suele ocurrir para el PE. Por el contrario el PP es más propenso a la rotura de cadenas vía formación de radicales por lo que es difícil de entrecruzar, [2, 4].

El entrecruzamiento químico es más habitual ya que requiere una menor inversión que el entrecruzamiento por irradiación. Los procesos más habituales son la adición de *peróxidos* o la *funcionalización de la poliolefina con silanos*. En el primer caso es necesario elegir el tipo de peróxido teniendo en cuenta la temperatura de fusión del polímero a entrecruzar. En el caso del LDPE el agente reticulante más utilizado es el peróxido de dicumilo. El polipropileno sin embargo, no se puede entrecruzar mediante la adición de peróxidos ya que hacen que el material pierda peso molecular (vía escisión de las cadenas) [2, 4, 25]. En el segundo proceso, la molécula de la poliolefina se funcionaliza con un organosilano polifuncional. El polímero funcionalizado puede ser procesado como cualquier otro termoplástico y sólo se reticula en un proceso secundario al añadir agua. Este proceso es válido para entrecruzar tanto PE como PP [2].

El *grado de entrecruzamiento* del material se define como la fracción de material no soluble en xileno en ebullición [34]. El control del grado de entrecruzamiento es fundamental para obtener un material óptimo, de modo que pueda alcanzar el grado máximo de expansión requerido. Un entrecruzamiento deficiente o excesivo, conllevan ruptura de celdas o ratios de expansión menores de los deseados. En el proceso de irradiación el grado de entrecruzamiento se controla mediante la dosis de radiación a la que el material es expuesto y en el entrecruzamiento químico mediante el porcentaje de peróxido añadido y la temperatura y tiempos aplicados durante el proceso [2].

En la actualidad es posible encontrar en el mercado una cantidad considerable de materiales espumados entrecruzados. Mediante el entrecruzamiento del polímero es posible producir materiales espumados en un rango de densidades mayor, sin embargo, el entrecruzamiento presenta una gran desventaja, ya que los polímeros reticulados no pueden ser reciclados por métodos convencionales [2, 4]. Normalmente, cualquier material termoplástico puede ser triturado y procesado de nuevo, sin embargo, al entrecruzar un polímero éste se convierte en termoestable y no es posible reprocesarlos por técnicas convencionales tales como extrusión o inyección. Por tanto, aunque desde el punto de vista reológico, el entrecruzamiento es beneficioso, desde un punto de vista medioambiental, es una estrategia inadecuada [35].

2.3.2.- Espumado de Polímeros Cargados

La adición de cargas a polímeros es una práctica habitual en la industria del plástico. Puede estar destinada a simplemente abaratar costes, por ejemplo añadiendo cargas de bajo coste como talco o carbonato cálcico o a producir materiales compuestos altamente funcionales. Algunos ejemplos son la adición de hidróxido de magnesio o aluminio a polímeros etilénicos, (LDPE o EVA) para producir compuestos no halogenados de alta resistencia al fuego [36]. Estos materiales se utilizan como "core" o relleno de paneles sándwich destinados al sector de la construcción o como recubrimiento de cables eléctricos. Otro típico ejemplo son los materiales poliméricos cargados con fibras de vidrio o de carbono. La alta resistencia y rigidez de las fibras (50 y 20-150 veces mayor que la matriz polimérica respectivamente) hace que dichos composites combinen unas excelentes propiedades mecánicas, (elevada resistencia y módulo) con una baja densidad [25].

2.3.2.1.- Nanocompuestos Poliméricos

En los últimos años, la tendencia respecto a las cargas añadidas a materiales poliméricos ha pasado por reducir la dimensión de los refuerzos, desde el rango micrométrico, donde se engloban materiales como el talco o las fibras, al rango nanométrico. Así a esta nueva generación de materiales compuestos se les ha denominado como *Nanocompuestos Poliméricos*. El gran impacto que han tenido estos materiales tanto a nivel científico como a nivel industrial se ve reflejado en la gran cantidad de literatura científica, tanto libros como artículos, y patentes publicados en relación a ellos [37-50].

Las nanocargas, se caracterizan por tener al menos una de sus dimensiones en el rango nanométrico y pueden ser de tres tipos, *laminares* (nanoarcillas), *tubulares* (nanofibras o nanotubos de carbono) o *esféricas* (partículas de sílica o de óxido de titano) [43]. La alta superficie específica de las nanopartículas es el factor clave que hace que al dispersarlas en una matriz polimérica, ésta presente una mejora ostensible en las propiedades [48]. La combinación de polímeros con pequeños porcentajes de nanopartículas puede llevar a obtener materiales con morfologías poliméricas modificadas (aumento de la cristalinidad) o con diferente comportamiento reológico además de producir mejoras en las propiedades mecánicas, en la estabilidad tanto dimensional como térmica, o en las propiedades barrera [38-41, 44, 48]. Sin embargo, todas esas mejoras están condicionadas a lograr un grado de dispersión adecuado de

las nanopartículas en la matriz polimérica además de un buen grado de compatibilización entre la nanocarga y el polímero. Un alto grado de aglomeración o una mala compatibilización pueden provocar que las propiedades de los nanocompuestos sean incluso inferiores que las del polímero puro [48]. Hay que tener en cuenta además, que tanto el grado de dispersión como el de compatibilización dependen tanto del tipo de matriz polimérica como del tipo de nanopartícula [44]. Por ejemplo, en el caso de las cargas de tipo arcillas, la dispersión óptima (o *exfoliación*) se consigue cuando laminillas que forman la nanopartícula se separan, lo que permite que el polímero rellene los huecos que quedan entre ellas. En el caso de partículas de tipo esférico, lo ideal sería conseguir que éstas dejen de formar agregados y que estén dispersas en el material de una en una en el mejor de los casos o sino formando los agregados más pequeños posibles [43, 49].

Cómo se realiza la mezcla de las nanocargas con el polímero tiene una gran influencia en el grado de dispersión que se logrará posteriormente. Para polímeros termoplásticos, sin duda alguna, el método de producción de nanocomposites más popular es el *mezclado en fundido* (*melt intercalation*). En este proceso, las cargas se mezclan con el polímero fundido bien en una extrusora de doble husillo o en un mezclador interno. Las altas fuerzas de cizalla que se generan durante el proceso pueden ayudar a separar las laminillas en el caso de las nanopartículas laminares o a romper los agregados en el caso de las nanopartículas esféricas [43, 49]. Además, y con el fin de mejorar la compatibilidad entre la carga y el polímero, suelen utilizarse dos estrategias, bien por separado o bien combinadas, que son la funcionalización de la superficie de las nanopartículas y la adición de polímeros compatibilizantes a la matriz polimérica [43].

2.3.2.2.- Nanocompuestos Poliméricos Celulares

Al igual que para piezas sólidas el uso de cargas en piezas aligeradas es también una práctica habitual, si bien los efectos que producen éstas en un material espumado son mucho más complejos que los que producen en el polímero sólido [48]. El interés despertado por los nanocompuestos poliméricos en los últimos años se ha extendido a los productores e investigadores del campo de las espumas poliméricas.

La combinación de tecnologías de espumado y polímeros que contienen cargas nanométricas da lugar a una nueva clase de materiales celulares: *nanocompuestos poliméricos celulares* [51, 52]. Estos materiales además de "heredar" todas las mejoras que se consiguen en los nanocomposites poliméricos sólidos, presentan estructuras celulares mejoradas ya que las nanocargas también son capaces de actuar en el

proceso de nucleación y crecimiento de las celdillas [51]. Se puede afirmar por tanto que las nanopartículas tienen un papel *multifuncional* cuando se añaden a un material celular polimérico. En algunos casos, la presencia de las nanopartículas hace que en el nanocompuesto espumado se detecte un mayor incremento de algunas propiedades que en el correspondiente material sólido, confirmando así la presencia de *efectos sinérgicos* producidos por la combinación entre materiales celular poliméricos y nanocargas [51, 52].

Tal y como se comentó en el apartado 2.1, obtener un material celular optimizado, pasa por actuar a dos niveles, por un lado mejorando la estructura celular y por otro optimizando las propiedades del polímero base. Las nanopartículas juegan un papel *multifuncional* en los nanocomposites espumados porque son capaces de actuar a esos dos niveles, por un lado consiguiendo *estructuras celulares mejoradas* y por otro, *incrementando las propiedades del polímero base* que forma las paredes celulares. El esquema siguiente pretende reflejar estas ideas, (figura 2.10).

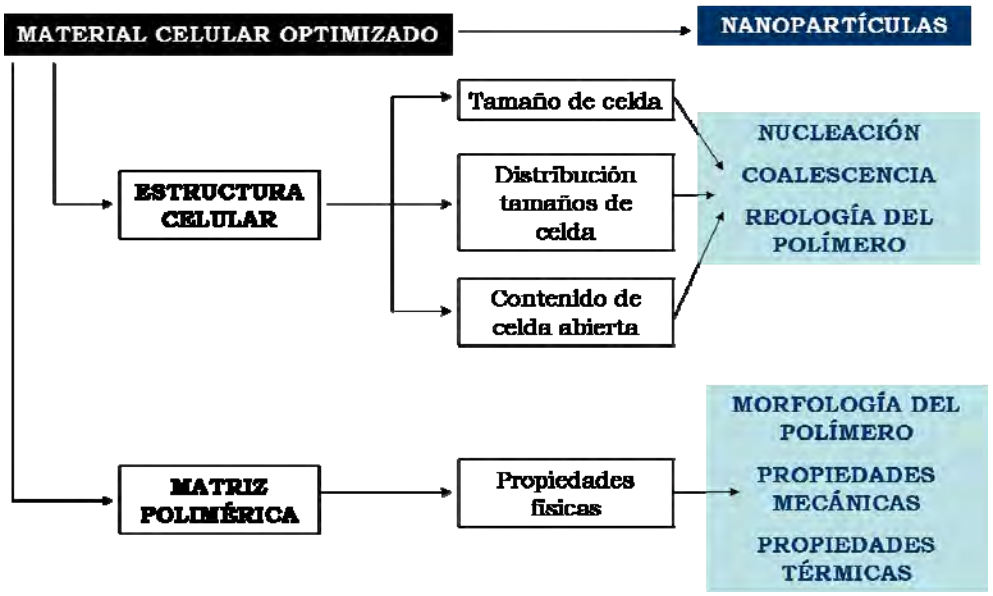

Figura 2.10: Papel multifuncional de las nanopartículas en los nanocompuestos celulares.

Según se puede apreciar en el gráfico anterior, la adición de nanopartículas a un polímero celular se traduce en una mejora de las propiedades debido a la obtención de una estructura celular mejorada y a que las propiedades del polímero base también pueden verse incrementadas debido a la presencia de las nanopartículas.

Las mejoras que producen las nanopartículas tanto a nivel microscópico como macroscópico se deben a un compendio relativamente complejo de actuaciones. La efectividad de las nanopartículas para mejorar un polímero celular depende entre otros

del tipo de nanopartícula, del grado de dispersión de las mismas, del grado de compatibilización polímero-partícula o del tratamiento superficial de la partícula.

A continuación se describen los efectos de las nanopartículas tanto en la estructura celular como en la matriz polimérica y las implicaciones que esos efectos tienen en las propiedades finales del material. De nuevo no es sencillo establecer generalidades en este complejo campo, por lo que puede haber excepciones a lo expresado en los siguientes parrafos.

- *Efecto de las Nanopartículas en la Estructura Celular*

El proceso de formación de un material celular incluye cuatro etapas, la formación de una disolución homogénea polímero/gas, la nucleación de las celdillas y su posterior crecimiento y estabilización [2, 4]. Las nanopartículas son capaces de mejorar la estructura celular de un material celular ya que actúan en varias de estas etapas.

En primer lugar, actúan como *agentes nucleantes* disminuyendo la energía que una celda necesita para nuclear y formarse durante el proceso de espumado [53]. El proceso de nucleación en un material celular puede ser homogéneo o heterogéneo. Se dice que es homogéneo cuando la nucleación se produce únicamente debido a fluctuaciones en la disolución polímero/gas y heterogéneo cuando hay fases secundarias en dicha disolución responsables del proceso de nucleación [52, 53]. El análisis de ambos procesos utilizando la teoría clásica de la nucleación concluye que la velocidad de nucleación en un proceso de tipo heterogéneo, es más elevada debido a la reducción de la energía de activación del proceso cuando éste se produce en la interfase polímero-partícula que cuando se produce en la interfase polímero-gas (nucleación homogénea) [53].

Las cargas inorgánicas distribuidas de forma uniforme a lo largo del polímero, proporcionan puntos de nucleación preferenciales homogéneamente distribuidos lo que conlleva la obtención de polímeros espumados con estructuras celulares más uniformes. Al igual que ocurre con los compuestos poliméricos, en los últimos años, la tendencia general ha sido la de reducir el tamaño de las cargas de micrométrico a nanométrico. La razón es sencilla, utilizando el mismo porcentaje nominal de nanopartículas, si éstas están bien distribuidas, el número de potenciales puntos de nucleación por unidad de volumen del que se dispone es considerablemente más alto que cuando se utilizan cargas de mayor tamaño [52].

Otra de las ventajas de las nanopartículas es su elevada área superficial, lo que favorece la generación de una gran interfase polímero-partícula. La presencia de dicha interfase reduce la energía de activación necesaria en el proceso de nucleación de una celdilla y como consecuencia se produce un aumento en la velocidad de nucleación [53].

El efecto nucleante de las nanopartículas no es el único responsable en la obtención de polímeros espumados con mejores estructuras celulares. Hay que añadir que la presencia de las nanopartículas puede contribuir a reducir tanto la coalescencia como el porcentaje de celdas abiertas en el material [51, 52]. La adición de nanopartículas a un polímero lleva asociado un aumento de la viscosidad elongacional; en algunos casos, cuando las cargas se orientan en la dirección de estiramiento es posible incluso observar *strain hardening* del polímero [54, 55]. Tal y como se comentó en el apartado 2.3.1.1, la presencia de *strain hardening* en la matriz polimérica favorece la estabilización la estructura celular, además de mejorar la capacidad del polímero para retener el gas durante el proceso de expansión del material. En general, todo eso se traduce en materiales con *menores tamaños de celda* y *distribuciones de tamaños de celda más homogeneos* (debido a la suma del efecto nucleante y estabilizante de las partículas) y *mayores densidades celulares,* (menor coalescencia y mayor velocidad de nucleación) [52].

Sin embargo, la obtención de estos efectos depende de múltiples factores entre los que caben destacar, la forma de la nanopartícula (laminar, tubular o esférica), el porcentaje de ellas que se ha añadido al polímero, el tipo de tratamiento superficial de las cargas, el grado de dispersión de las partículas a lo largo de la matriz polimérica y la compatiblización polímero-carga [56, 57].

De entre todos los factores anteriores quizá uno de los más importantes es el *grado de dispersión* de las nanopartículas. Numerosos estudios han analizado la influencia del grado de dispersión en la estructura celular de diversos sistemas polímero/nanopartícula. (En el capítulo 4 se puede encontrar una revisión de esos trabajos y de las principales conclusiones que se infieren de los mismos). En general, se puede decir que cuanto mejor dispersadas están las partículas, más pronunciados son los efectos que estas producen en la estructura celular [57].

Por otro lado, el grado de compatibilización polímero-partícula también juega un papel importante. En términos generales se puede decir que a mayor compatibilidad, menor interfase polímero-partícula y menor efecto nucleante [53]. Por otro lado una mala compatibilidad polímero-carga va en detrimento del resto

de propiedades físicas del sistema, lo que implica que es necesario llegar a un compromiso entre ambas situaciones.

- *Efecto de las Nanopartículas en la Matriz Polimérica*

En un nanocompuesto polimérico espumado, el material que forma las paredes y aristas hereda directamente los efectos que producen las partículas en la matriz polimérica sólida. Por regla general el tamaño de las paredes y aristas de las celdillas de un material celular está en el orden de los micrómetros, por tanto, introducir cargas de tamaño nanométrico puede resultar extremadamente beneficios e interesante [52].

Algunas de los efectos más significativos que se pueden obtener al introducir nanopartículas en la matriz polimérica son entre otros la *modificación de la morfología del polímero* y mejoras en *propiedades térmicas, mecánicas, barrera o de resistencia a la llama* [50, 52].

El elevado área y energía superficial de las nanopartículas las hace especialmente adecuadas para actuar como agentes nucleantes durante el proceso de cristalización de la matriz polimérica. En algunos sistemas polímero/partícula es posible detectar *incrementos en el grado de cristalinidad* del polímero base, lo que por ejemplo se puede traducir en un incremento de las propiedades térmicas y mecánicas [58-60].

La mejora en las propiedades térmicas, barrera y de resistencia a la llama debido a la adición de nanopartículas están íntimamente relacionadas entre si. Las nanopartículas actúan como barrera contra el calor, lo que mejora la estabilidad térmica del sistema aumentando la temperatura de degradación del polímero base. Por otro lado, la capa de ceniza generada mediante la carbonización de la nanopartícula actúa como aislante favoreciendo el comportamiento retardante de llama [43, 61, 62]. Las nanopartículas, actúan en un polímero como barrera de paso a los gases que intentan atravesarlo, (*laberinto de volátiles*). En el caso de las propiedades térmicas y de resistencia a la llama, las nanopartículas actúan en dos direcciones, por un lado impidiendo que el oxígeno penetre en el interior del material (y de este modo reduciendo el poder de combustión) y por otro lado, limitando la salida de productos volátiles generados durante la descomposición del polímero [61, 62].

Mejorar el comportamiento mecánico de los polímeros ha sido quizá una de las principales razones por la que la adición de nanocargas ha centrado tanto interés. Las mejoras que se pueden lograr añadiendo pequeñas porcentajes son muy elevadas, sin embargo están condicionadas a lograr un grado de dispersión adecuado de las partículas y lo que es más importante una buena compatibilización polímero-partícula [63].

2.4.- PROCESOS DE PRODUCCIÓN DE MATERIALES CELULARES POLIMÉRICOS

El interés generado por los materiales celulares debido a su gran versatilidad ha hecho que los procesos de producción de los mismos hayan sido objeto de estudio tanto de la comunidad científica como de la comunidad industrial. La primera patente que describe la producción de un polímero espumado data de 1935 y fue presentada por Munters y Tandberg [64]. Desde entonces, el avance en las tecnologías de espumado de polímeros ha sido constante.

La elección de un proceso de espumado determinado viene condicionada principalmente por dos factores, el primero el tipo de matriz polimérica que se desea espumar y el segundo, la aplicación final del material (forma, densidad, propiedades, etc). Por supuesto, el segundo factor lleva implícito el valor de la densidad del material espumado [2].

En la actualidad existe una amplia variedad de procesos de obtención de materiales celulares poliméricos. Entre los más utilizados cabe destacar el espumado reactivo, típico de materiales termoestables tales como el poliuretano, bien sea rígido o flexible, el moldeo por compresión, el espumado por lotes, espumado mediante moldeo por inyección, extrusión, rotomoldeo, etc. De hecho muchas de las técnicas habituales de transformación de plásticos se pueden utilizar también para producir materiales espumados si bien, llevando a cabo algunas transformaciones de la maquinaria y añadiendo claro está un agente espumante [2, 4].

A continuación se presenta una breve descripción de los tipos de agentes espumantes utilizados hoy en día para producir materiales celulares poliméricos así como una breve revisión de los procesos de producción de materiales termoplásticos espumados más utilizados en la actualidad, extrusión, moldeo por inyección, moldeo por compresión y espumado por lotes basado en disolución de gas.

2.4.1.- Agentes Espumantes

A la hora de fabricar un material celular polimérico, hay que tener en cuenta que la elección del proceso lleva implícita la elección de un tipo de agente espumante. Un agente espumante se puede definir como aquella sustancia que genera una estructura celular en el material [4]. Los agentes espumantes juegan un papel muy importante tanto en el proceso de fabricación como en el comportamiento de una espuma polimérica, ya que son el factor dominante en el control de la densidad del material, y no solo eso, sino que además también afectan tanto a la estructura celular como a la morfología del material, lo que en último térmico define sus propiedades y aplicaciones [4].

La clasificación más común de los tipos de agentes espumantes se hace en base al mecanismo mediante el cual liberan el gas, así se pueden clasificar en *agentes espumantes químicos* o *agentes espumantes físicos* [2]:

- *Agentes espumantes químicos* (CBA)

  Son compuestos o mezclas de compuestos que liberan gas como resultado de una reacción química [2]. En general, los CBA se descomponen dando lugar a uno o varios gases que sirven para expandir el polímero. Como resultado de esa descomposición, además, se genera una cierta cantidad de residuos que permanecen después en el material [4].

  El uso de agentes espumantes químicos presenta dos grandes ventajas, por un lado, son fáciles de introducir en el material que se va a espumar y por otro lado son fácilmente procesables utilizando equipamiento convencional de procesado de plásticos [2].

  Los agentes espumantes químicos se pueden clasificar a su vez en *endotérmicos* o *exotérmicos* en función de si absorben o liberan calor durante su descomposición [2, 4].

  Los CBA *endotérmicos* absorben calor durante su descomposición, de ahí que se utilicen en procesos donde es necesario restar calor al polímero fundido. El ejemplo más común es el *bicarbonato de sodio* que se descompone liberando CO_2 y vapor de agua. La principal desventaja de estos materiales es que el rango de temperaturas en el que descomponen es muy amplio (en el caso del bicarbonato entre 100 y 140ºC) y por tanto definir un intervalo de temperaturas de procesado es complicado [24]. Se puede estrechar dicho intervalo de temperaturas mediante la adición de otro tipo de compuestos químicos; en el caso del bicarbonato ésto se

consigue añadiendo un cierto porcentaje de ácido cítrico o ácido tartárico [2, 4, 24]. Otra desventaja de los CBA endotérmicos frente a los exotérmicos es que la cantidad de gas que liberan es mucho menor, (aproximadamente la mitad), por lo que para conseguir idénticas expansiones es necesario utilizar un porcentaje mayor de espumante [4, 24]. Hay que tener en cuenta además que muchos de ellos liberan agua (vapor de agua) en su descomposición por lo que su uso con polímeros sensibles a la humedad tales como el PET o el PLA, está limitado. Por otro lado, estos compuestos presentan una gran ventaja y es que tanto los gases que liberan como los residuos generados durante su descomposición no suelen ser tóxicos, lo que les hace adecuados para espumar piezas que deban estar en contacto con alimentos [6].

Los agentes espumantes *exotérmicos* liberan calor durante su descomposición, siendo además dicha reacción autocatalítica; ésto hace que se descompongan muy rápido y en un rango de temperaturas muy estrecho [4].

El agente espumante exotérmico más utilizado en el mundo es la Azodicarbonamida, (ADC) [2, 6]. Es un polvo de color amarillento que descompone entre 200 y 220ºC produciendo una gran cantidad de gas (entre 240 y 270 cm^3/g). Al descomponerse, la ADC genera principalmente N_2 (alrededor de un 65%) y cantidades menores de CO, CO_2 o NH_3 [2, 6, 33]. El punto de descomposición se puede reducir hasta temperaturas alrededor de los 150-160ºC mediante la adición de activadores. Compuestos de metales de transición, (zinc, plomo o cadmio), polioles, urea, alcoholaminas o algunos ácidos orgánicos pueden ser utilizados como catalizadores de la reacción de descomposición de la ADC. Se puede modificar o ajustar su velocidad de descomposición variando su tamaño de partícula [6, 33].

- *Agentes Espumantes Físicos* (PBA)

Los agentes espumantes físicos generan el gas necesario para expandir el polímero al sufrir un cambio de estado, o al producirse un cambio en la solubilidad del sistema gas/polímero. Generalmente son líquidos de bajo punto de ebullición o gases. Los más comunes son los hidrocarburos, los hidrocarburos halogenados o algunos gases inertes tales como el CO_2 o el N_2 [4].

Uno de los principales criterios a tener en cuenta a la hora de elegir un agente espumante físico es que debe tener una solubilidad óptima en el polímero [2, 4, 6]. Otros criterios de elección a tener en cuenta son las consideraciones ambientales y de manejo. Los clorofluorocarbonos (CFCs) fueron ampliamente utilizados para espumar poliuretano o poliestireno debido a su alta solubilidad en

los polímeros y a su baja conductividad térmica. Sin embargo, aunque presentan múltiples ventajas, dañan la capa de ozono y fueron prohibidos por el protocolo de Montreal en 1987 [2]. Algunas de las alternativas son los HFC, (hidrofluorocarbonos) o los hidrocarburos tales como el butano, el pentano o el hexano, aunque éstos últimos presentan una alta combustibilidad lo que hace ciertamente peligroso su manejo [4].

Los gases inertes tales como el CO_2 o el N_2 presentan algunas ventajas respecto a los anteriores. Son baratos, abundantes y de lejos los más amigables con el medio ambiente [2]. Una de las razones de que ambos gases sean ampliamente utilizados es su relativamente bajo *punto crítico* (por ejemplo para el CO_2 su punto crítico está en 31ºC y 7.38 MPa). Un fluido está en *estado supercrítico* cuando se mantiene por encima de su punto crítico. En esas condiciones, un gas se vuelve denso como un líquido pero manteniendo su habilidad para fluir sin apenas visocidad o tensión superficial. En estas condiciones, su solubilidad en un polímero aumenta de forma considerable haciendo además disminuir su temperatura de transición vítrea, (T_g) [2, 65].

Cuando un polímero se satura con un gas en estado supercrítico y es despresurizado rápidamente, queda supersaturado, de forma que las celdillas nuclean y crecen hasta que el polímero se vitrifica o solidifica de nuevo [2, 65]. Este fenómeno se utiliza para fabricar *espumas microcelulares* que se caracterizan por tener tamaños de celda menores de 10 μm y densidades celulares muy altas [62].

En la actualidad el CO_2 es con diferencia el agente espumante físico más utilizado para hacer espumas poliméricas. El N_2 se utiliza en menor medida para hacer tanto espumas convencionales como microcelulares aunque su solubilidad en los polímeros más comunes es menor que la del CO_2, lo que requiere mayores presiones de trabajo para conseguir los mismos grados de expansión [2, 65].

2.4.2.- Procesos de Producción de Espumas con base Poliolefina

La evolución de los procesos de producción de polímeros espumados ha ido paralela al desarrollo de nuevos tipos de polímeros y a las nuevas posibles aplicaciones y/o necesidades que han ido surgiendo. Tal y como se ha comentado, la elección del tipo de proceso viene determinada principalmente por el tipo de polímero, la densidad

final del material espumado (y por ende la aplicación final del mismo) y por el tipo de estructura celular que éste debe presentar [2, 4].

En general, cualquier proceso de espumado, se centra en la generación de una disolución polímero/gas lo más homogénea posible. El control de parámetros tales como la presión, el tiempo o la temperatura es fundamental en la mayoría de procesos de producción de materiales celulares. Los procesos de producción de materiales celulares son en muchos casos similares a aquellos utilizados para la transformación de polímeros sólidos, aunque la introducción de una fase gaseosa hace que el control de los parámetros involucrados en el proceso sea ligeramente más compleja [2, 4, 18].

Esta tesis, como se comentó en apartados anteriores, está centrada en un tipo concreto de polímeros denominados poliolefinas. Algunos de los procesos de producción de espumas con base poliolefina más habituales son *extrusión*, *moldeo por inyección*, *moldeo por compresión* y *espumado por lotes basado en disolución de gas* [2, 18]. A continuación se hace una breve descripción de los fundamentos en los que se basan, las ventajas y desventajas que implican cada uno de ellos y el rango de densidades que se puede cubrir con cada uno de ellos.

2.4.2.1. *Proceso de Espumado por Extrusión*

La producción de materiales espumados por extrusión es bastante similar a la transformación de polímeros mediante el mismo proceso. La principal diferencia radica en que es necesario controlar de forma más precisa la temperatura y la presión del fundido debido a la introducción del agente espumante, que puede ser bien de tipo químico o bien de tipo físico [6, 24].

Este proceso consta de las siguientes etapas, (están esquematizadas en la figura 2.11 [6].

1. *Plastificación del polímero*. En caso de utilizar un agente espumante químico, (CBA), éste se añade a la vez que el polímero base con el fin de descomponerse y generar el gas necesario para el proceso.
2. *Dispersión y disolución del agente espumante en el polímero*. Si se utiliza un agente espumante de tipo físico, (PBA) es introducido en este punto. Las fuerzas de cizalla generadas por la rotación de los husillos facilitan el proceso de disolución del líquido o gas en el polímero y la obtención de una disolución polímero/agente espumante homogénea.

3. *Enfriamiento de la mezcla polímero/gas*. El enfriamiento de la disolución polímero/agente espumante es necesario para poder estabilizar la estructura celular posteriormente. Si el polímero fundido expande a una temperatura demasiado elevada, puede hacer que colapse la estructura o que se genere un material con un gran porcentaje de celdas abiertas.

4. *Moldeo del fundido en la boquilla*. Una vez que la mezcla se ha enfriado lo suficiente, se le hace pasar a través de una boquilla con la forma deseada. La caída de presión que se produce en ese punto hace que las celdillas nucleen en la mezcla polímero/gas sobresaturada. Cuanto mayor sea dicha caída de presión, mayor será la cantidad de celdillas nucleadas y menor el tamaño de celda del producto final.

5. *Expansión del fundido*. Una vez nucleadas las celdillas, estas crecen a expensas del gas generado por el agente espumante.

6. *Enfriamiento y estabilización de la estructura*. Es necesario enfriar el material espumado para que éste sea dimensionalmente estable.

Figura 2.11: Etapas del proceso de espumado por extrusión.

Una de las principales ventajas de este proceso, es la alta productividad ya que es un *proceso en continuo*, además es adecuado para espumar todo tipo de poliolefinas. Cuando la densidad final del material espumado debe ser muy baja es preferible utilizar resinas altamente ramificadas y agentes espumantes físicos con el fin de obtener productos con una calidad microestructural adecuada [2]. Si la densidad del producto que se desea fabricar es elevada, entonces, es menos crítica la selección del polímero y se pueden generar productos con adecuadas estructuras celulares utilizando polímeros linales; en estos casos se suelen utilizar agentes espumantes químicos. Quizá la principal desventaja de este proceso, es que solamente permite producir materiales espumados con *geometrías sencillas*, (planchas, perfiles, tubos...). Se pueden obtener materiales con geometrías más complicadas mediante termoconformado, aunque la inclusión de un proceso secundario de transformación siempre tiende a aumentar el coste final del producto [2, 4]. En la imagen siguiente (figura 2.12) se muestran algunos ejemplos de materiales espumados basados en poliolefinas fabricados por extrusión.

Figura 2.12: Ejemplos de productos espumados fabricados por extrusión.

Mediante este proceso lo más común es producir espumas de baja densidad, ($\rho_{relativa}$ < 0.3), cuyas aplicaciones principales están relacionadas con el aislamiento térmico, con la absorción de energía (embalajes) o la disipación de vibraciones [2, 6].

Si bien es más común producir espumas de baja densidad por extrusión, es posible encontrar también algunos ejemplos de materiales celulares de alta densidad fabricados con el mismo proceso. En general, la producción de espumas de alta densidad por extrusión está más enfocada a la fabricación de espumas microcelulares. La empresa Trexel patentó a mediados de los años 90 una tecnología para producir materiales microcelulares conocida como proceso Mucell, aunque el más conocido es el proceso de inyección, también comercializan sistemas de espumado por extrusión [65]. Las reducciones de peso que se obtienen cuando se utilizan poliolefinas como polímero base rondan el 20%, lo que en la mayoría de los casos no justifica la inversión en la maquinaria necesaria [65]. Park y su equipo han publicado numerosos trabajos describiendo la obtención de espumas microcelulares por extrusión. Producen materiales en un rango de densidad bastante amplio utilizando poliolefinas altamente ramificadas y diversos tipos de agentes nucleantes. Sin embargo, la caracterización de dichos materiales está centrada casi exclusivamente en el análisis de la estructura celular. Debido a la elevada caída de presión necesaria para producir espumas con tamaños de celda en el rango microcelular, solamente son capaces de producir filamentos con un diámetro extremadamente pequeño, (0.5 mm) en los que determinar las propiedades físicas es inviable [54, 66-71].

2.4.2.2. *Espumado mediante Moldeo por Inyección*

El moldeo por inyección es junto con la extrusión una de las técnicas de procesado de plásticos más populares. Su principal ventaja es sin duda que permite producir con un alto grado de precisión piezas con formas complejas [72].

Haciendo una serie de modificaciones mínimas a una máquina convencional de inyección es posible utilizarla para producir piezas aligeradas. Existen diversas versiones del proceso de espumado por moldeo por inyección. Las más habituales en la producción de piezas con base poliolefina son el *moldeo por inyección a baja presión* y el *moldeo por inyección a alta presión*. Ambos procesos son similares, y la diferencia entre ellos radica en el modo en el que el material expande en el interior del molde [69]. En cualquiera de los dos casos, las etapas que comprende el proceso son las especificadas en el siguiente esquema (figura 2.13).

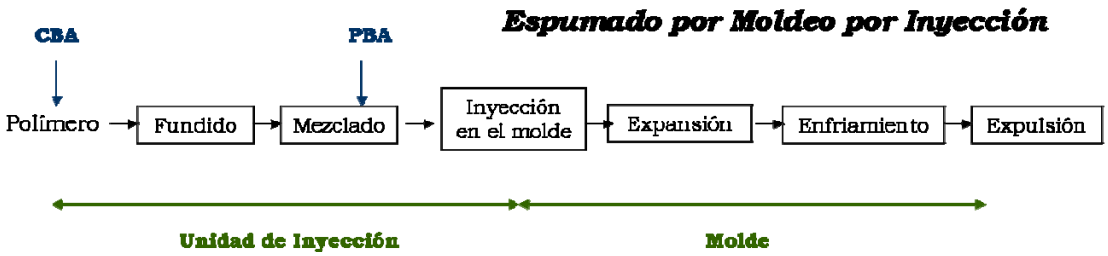

Figura 2.13: Etapas del proceso de moldeo por inyección a baja presión

La primera parte del proceso es similar a lo que ocurre en extrusión. El agente espumante que puede ser de tipo físico o químico se mezcla con el polímero plastificado en el barril de la extrusora de la unidad de inyección. La rotación del husillo favorece la generación de elevadas fuerzas de cizalla que ayudan a disolver el agente espumante en el polímero formando una disolución polímero/agente espumante la cual es posteriormente inyectada en el molde. En el proceso de *baja presión*, la cantidad de material que se inyecta en el molde es un cierto porcentaje menor que la que se inyectaría para la correspondiente pieza sólida. La caída de presión generada en la entrada del molde, hace que las celdillas nucleen y crezcan hasta que el material rellena por completo el molde. Por el contrario en el proceso de *alta presión*, el molde se llena por completo con la disolución polímero/agente espumante, y una vez que está lleno, un lado del molde se desplaza permitiendo la expansión del material. El primer proceso es considerablemente más sencillo y requiere menor inversión ya que se pueden utilizar los mismos moldes que en el procesado de piezas sólidas [6, 72].

Debido al proceso de llenado del molde, mediante moldeo por inyección se generan un tipo de espumas conocidas como *espumas estructurales*, que se caracterizan por presentar una piel exterior sólida y un core espumado. Al entrar en el molde, el polímero que entra en contacto con el molde solidifica más rápido (aunque el molde esté atemperado, siempre está a una temperatura menor que el punto de fusión

del polímero), que el interior de la pieza que continúa caliente permitiendo que las celdillas crezcan hasta rellenar completamente la cavidad del molde. Este tipo de estructuras presentan una relación rigidez-peso superior a la de las espumas convencionales [72-74].

En los últimos años, los esfuerzos se han enfocado a la producción de espumas microcelulares mediante moldeo por inyección. La empresa Trexel comercializa sistemas que utilizan agentes espumantes físicos para producir espumas microcelulares mediante moldeo por inyección. El proceso Mucell permite fabricar piezas con reducciones de peso limitadas a un 25%, con calidad superficial limitada y generalmente no es muy adecuado para producir piezas de elevado tamaño [65].

El proceso de espumado mediante moldeo por inyección está limitado a la producción de espumas de alta densidad, ($\rho_{relativa}$ > 0.6). En general los materiales fabricados por este proceso están destinados a aplicaciones de tipo estructural. Uno de los campos donde más se aplica este proceso es en automoción, donde es beneficioso sustituir piezas sólidas por piezas aligeradas ya que un descenso en el peso total del vehículo puede suponer un ahorro de combustible y en último término de emisiones de CO_2. También es fácil encontrar contenedores o "palets" aligerados fabricados mediante moldeo por inyección [2, 4, 65, 72-74].

Figura 2.14: Ejemplos de piezas aligeradas producidas mediante moldeo por inyección.

La principal ventaja de este proceso reside en la posibilidad de producir piezas con diversos tipos de geometrías. Sin embargo, las reducciones de peso que se pueden conseguir no son muy altas, ya que no suelen superar el 40%. Las espumas estructurales presentan distribuciones de tamaños de celda muy inhomogeneas además de gradientes de densidad debido al propio proceso de producción. Otra de las desventajas del proceso de baja presión es la baja calidad superficial que presentan las

piezas aligeradas; en algunos casos es incluso necesario un tratamiento posterior o un repintado para que la pieza sea apta para su comercialización [73, 74].

2.4.2.3. *Moldeo por Compresión*

El moldeo por compresión, es quizá la técnica más sencilla para producir materiales celulares poliméricos. La expansión del material se puede realizar en uno o en dos pasos, dando lugar a dos procesos diferentes conocidos como *moldeo por compresión en una etapa* y *moldeo por compresión en dos etapas*. En cualquiera de los dos casos, se utilizan polímeros entrecruzados para facilitar la estabilización de las celdillas en la fase de expansión y agentes espumantes químicos [2].

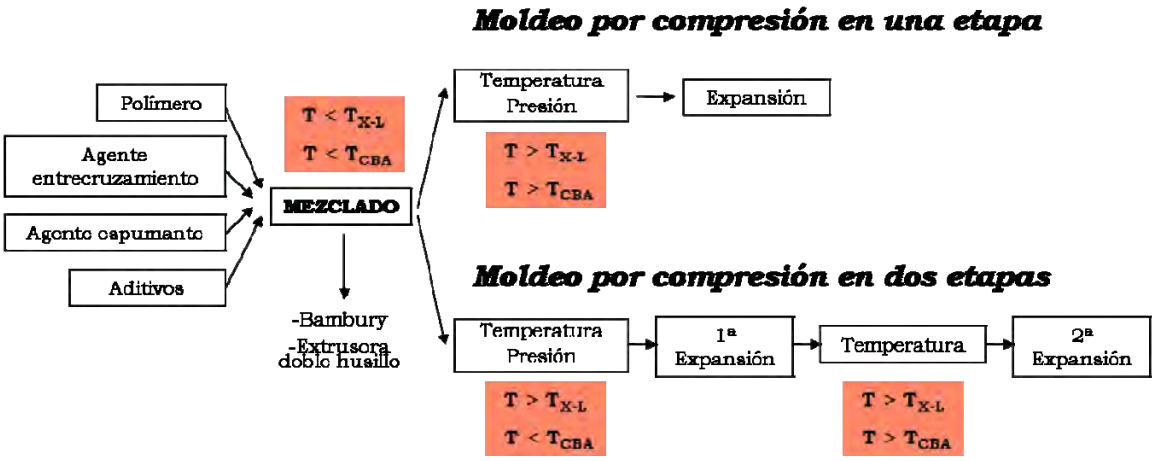

Figura 2.15: Variantes del proceso de moldeo por compresión, (T, temperatura del proceso, $T_{X\text{-}L}$, temperatura de descomposición del agente de entrecruzamiento, T_{CBA}, temperatura de descomposición del agente espumante químico).

Tal y como se puede apreciar en la figura 2.16, la primera fase es común a los dos tipos de procesos. El polímero y todos los aditivos necesarios se procesan bien en un mezclador tipo Bambury o en una extrusora de doble husillo a una temperatura menor que la de descomposición de los agentes espumante y de entrecruzamiento. En el proceso en una etapa, el *compound* así obtenido se introduce en un molde sobre el que se aplica presión mientras se calienta el material hasta una temperatura por encima del punto de descomposición tanto del agente de entrecruzamiento como del agente espumante. Tras un determinado tiempo, se libera la presión y el material expande. El grado de expansión máximo que se puede obtener con el proceso en una etapa es de

unas 15 veces. Cuando se desea disminuir más la densidad es necesario utilizar el proceso en dos etapas [2, 4].

En el proceso en dos etapas, la mezcla del polímero y todos los aditivos se introduce en un molde sobre el cual se aplica presión y temperatura. El material se calienta hasta una temperatura mayor que el punto de descomposición del agente de entrecruzamiento pero menor que el de descomposición del agente espumante, induciendo así el proceso de reticulación del polímero. Cuando se ha conseguido el grado de entrecruzamiento adecuado, la presión se libera permitiendo al material que pre-expanda un número limitado de veces (típicamente entre 3 y 8). El material pre-espumado se coloca en otro molde con las dimensiones finales del bloque a fabricar y se calienta por encima del punto de descomposición del agente espumante, permitiendo la expansión completa del material, (que en este caso sucede a presión atmosférica). Utilizando el proceso en dos etapas es posible expandir el polímero hasta unas 40 veces [2, 4, 33].

El moldeo por compresión permite cubrir aproximadamente el rango completo de densidades relativas, aunque a bajas densidades es necesario entrecruzar el polímero lo que hace que los materiales no sean reciclables por métodos convencionales [2]. Las aplicaciones de las espumas con base poliolefina fabricadas mediante moldeo por compresión son muchas y muy variadas. Se pueden utilizar tanto como aislantes térmicos, absorbedores de energía, (embalajes) o como disipadores de vibraciones, pero también se utilizan en sectores como la juguetería o el calzado [2, 33].

Figura 2.16: Ejemplos de espumas con base poliolefina producidas mediante moldeo por compresión.

La principal ventaja de este proceso es su sencillez, tanto en términos de procesado como en términos de inversión de maquinaria. Sin embargo presenta serias desventajas. La principal es que las espumas reticuladas no son reciclables por métodos convencionales (molido y refundido), lo que conlleva la generación de una gran cantidad de residuos que en la mayoría de los casos acaban en vertederos [35]. Otra de las desventajas es que el control de la densidad final del producto en el proceso en una

etapa no es muy preciso. La densidad de la espuma se controla mediante la cantidad de agente espumante que se añade; la densidad del material es (aproximadamente) inversamente proporcional a la cantidad de agente espumante utilizado. La eficiencia de un agente espumante depende significativamente de los parámetros de proceso, por tanto la densidad del material también se ve seriamente afectada por la elección de dichos parámetros [2]. Además, al igual que ocurría en extrusión, es necesario termoconformar la espuma cuando se desean obtener piezas con geometrías complejas.

2.4.2.4. *Proceso de Espumado por Lotes basado en la Disolución de Gas*

Este proceso, al igual que el anterior y a diferencia del de extrusión es un proceso discontinuo que está basado en la utilización de agentes espumantes físicos.

El proceso de espumado por lotes de espumas con base poliolefina más conocido es el empleado por la empresa *Zotefoams*. El proceso consta de las siguientes etapas, (figura 2.17) [2, 4, 18].

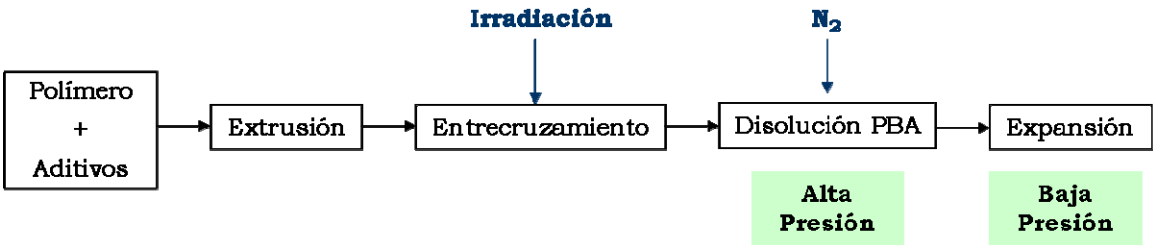

Figura 2.17: Proceso de fabricación de espumas de poliolefina reticulada utilizado por la empresa Zotefoams.

El primer paso consiste en producir mediante extrusión láminas de polímero que posteriormente son sometidas a un proceso de entrecruzamiento por irradiación o usando peróxido. Las planchas reticuladas, se introducen en un autoclave donde el gas (nitrógeno) se disuelve a alta presión, (alrededor de 70MPa). El proceso de difusión del gas en el polímero dura entre 6 y 8 horas y depende de parámetros tales como la temperatura, la presión o el espesor de las planchas. Las planchas saturadas con el gas se introducen posteriormente en otro autoclave esta vez de baja presión (aproximadamente 1.5MPa), donde el polímero se calienta hasta temperaturas ligeramente superiores a su punto de fusión, (*softening point*). El aumento de la

temperatura conlleva una disminución de la solubilidad del gas en el polímero que va unido a la nucleación y posterior crecimiento de las celdillas una vez que se libera la presión de este segundo autoclave [2, 4, 18].

Este proceso permite producir espumas de densidades extremadamente bajas (10-15 kg/m^3) con tamaños de celda uniformes y pequeños. La utilización de agentes espumantes físicos combinados con la reticulación por irradiación produce materiales libres de residuos, pero que siguen sin ser reciclables. El proceso es costoso tanto en términos de maquinaria como en términos de producción. La solubilidad del N_2 en los polímeros es bastante reducida y el coeficiente de difusión es bajo, por lo que el espesor de las láminas está limitado ya que de otra forma, los tiempos necesarios para disolver el gas en el polímero serían extremadamente altos [4]. Habitualmente este proceso está limitado a fabricar bloques de 30 mm de espesor.

Existe otra versión simplificada de este proceso conocido como "*pressure quench method*". El control de la nucleación y crecimiento del material se realiza mediante una caída de presión en lugar de mediante un incremento de la temperatura. Así el proceso funciona siguiendo el siguiente diagrama (figura 2.18):

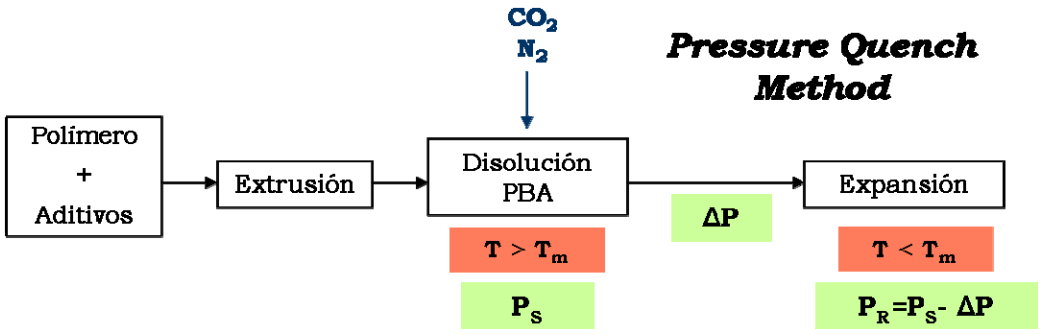

Figura 2.18: *Pressure Quench Method*

En este proceso, el polímero se procesa con los aditivos necesarios mediante extrusión y una plancha de material es introducida en un autoclave donde es saturada con un agente espumante físico. Puede utilizarse N_2, aunque es preferible utilizar CO_2 ya que su solubilidad en el polímero es considerablemente mayor [6]. Además con el fin de favorecer dicho proceso de disolución, esta etapa se puede llevar a cabo a temperaturas ligeramente mayores que la temperatura de fusión de la matriz polimérica, (T_m) y a presiones elevadas (P_s). Una vez que el polímero está sobresaturado con el gas, se despresuriza rápidamente el sistema. La caída de presión (ΔP), hace que la solubilidad del gas en el polímero se reduzca drásticamente, provocando la nucleación y posterior crecimiento de las celdas [75, 76].

Este proceso, no se utiliza actualmente a nivel industrial. Hasta la fecha se ha utilizado exclusivamente con fines académicos. El rango de densidad de los materiales producidos depende enormemente del tipo de matriz polimérica. Presenta sin embargo dos desventajas; en primer lugar los materiales producidos por este método generalmente no tienen una forma definida, lo que dificulta la caracterización de las propiedades físicas de las espumas así producidas y en segundo lugar el control de la densidad final de la pieza es complicado.

Tal y como se ha visto, existen diversos procesos de producción de espumas con base poliolefina. Cada uno de ellos presenta una serie de ventajas que pueden estar relacionadas con la sencillez y coste del proceso o con la calidad final de los materiales y claro está una serie de inconvenientes. Quizá el mayor inconveniente de muchos de estos procesos es la necesitad de entrecruzar el material, ya que posteriormente no se puede reciclar por métodos tradicionales. En la figuras siguiente, (figuras 2.19, 2.20 y 2.21) se presentan uno esquemas que resumen tres características de los procesos de espumado mencionados como son, los rangos de densidades relativas que se pueden cubrir con cada uno de ellos, en cuales de los procesos es necesario reticular la matriz polimérica y por último aquellos que permiten o no controlar de forma exacta la densidad de la pieza final.

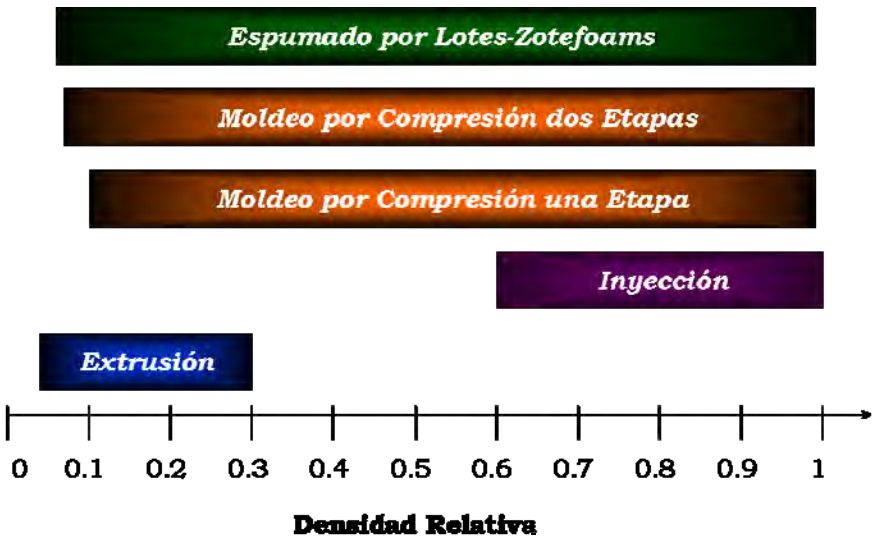

Figura 2.19: Proceso de espumado versus densidad relativa.

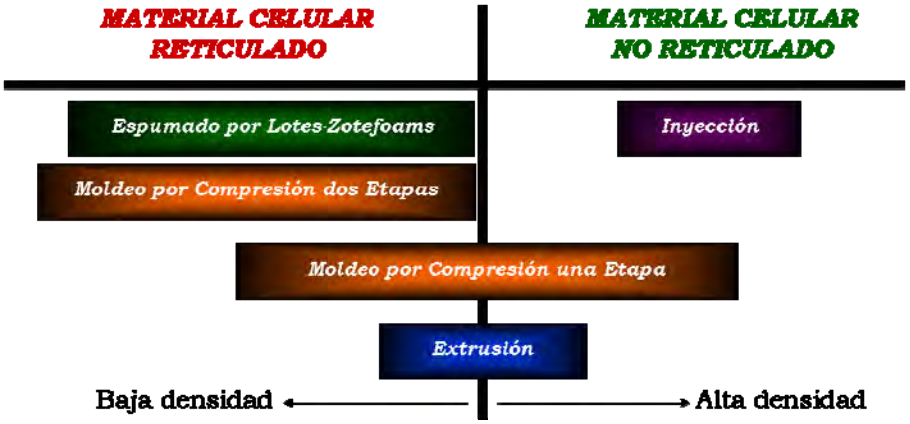

Figura 2.20: Procesos de espumado versus necesidad de reticular

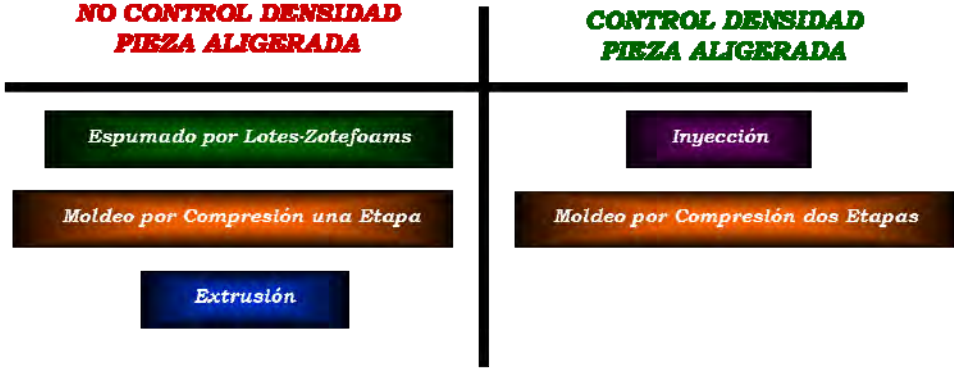

Figura 2.21: Procesos de espumado versus control de densidad

BIBLIOGRAFÍA

[1]. L.J. Gibson, M.F. Ashby. Cellular Solids: Structure and Properties. 2nd Edition, Cambridge University Press, United Kingdom, (1997).

[2]. D. Klempner, V. Sendijarevic. Handbook of Polymeric Foams and Foam Technology. 2nd Edition. Hanser Publishers, Munich, (2004)

[3]. E. Solórzano. Espumas de Aluminio: Proceso de Espumado, Estructura Celular y Propiedades. Tesis Doctoral, Universidad de Valladolid, (2008).

[4]. D. Eaves. Handbook of Polymer Foams. Rapra Technology, United Kingdom, (2004).

[5]. V. Kumar. Microcellular Polymers: Novel Materials for 21st Century. Progress in Rubber and Plastics Technology 9: 54-70, (1993).

[6]. S.T. Lee. Foam Extrusion: Principles and Practice. Technomic Publishing Company. Lancaster-Pennsylvania, (2000).

[7]. M.A. Rodríguez-Pérez. Propiedades Térmicas y Mecánicas de Espumas de Poliolefinas. Tesis Doctoral, Universidad de Valladolid, (1998)

[8]. R. Gendron (Ed). Thermoplastic Foam Processing. Principles and Development. CRC Press, Boca Raton-Florida, (2005).

[9]. ASTM D3576-04. Standard test method for cell size of rigid cellular plastics. Annual Book of ASTM Standards, Vol 8.02, (2011).

[10]. J. Pinto, M.A. Rodríguez-Pérez, J.A. de Saja. Development of an Image J Macro to Characterize the Cellular Structure of Polymeric Foams, XI Reunión del Grupo Especializado de Polímeros, (GEP), 10-24 Septiembre, Valladolid-España, (2009).

[11]. O. Almanza. Caracterización y Modelización de las Propiedades Térmicas y Mecánicas en Espumas de Poliolefina. Tesis Doctoral, Universidad de Valladolid, (2000).

[12]. L.O. Arcos y Rábago. Propiedades Térmicas y Mecánicas de Espumas de Poliolefina Fabricadas en un Proceso de Moldeo por Compresión. Tesis Doctoral, Universidad de Valladolid, (2002).

[13]. J.I. González-Peña. Efecto de los Tratamientos Térmicos en Bloques de Espuma de Polietileno de Baja Densidad Fabricados mediante Moldeo por Compresión. Tesis Doctoral, Universidad de Valladolid, (2006).

[14]. M. Álvarez-Laínez. Propiedades Térmicas, Mecánicas y Acústicas de Espumas de Poliolefina de Celda Abierta. Tesis Doctoral, Universidad de Valladolid, (2007).

[15]. M.A. Rodríguez-Pérez, J. Lobos, C.A. Pérez-Muñoz, J.A. de Saja. Mechanical Behaviour at Low Strains of LDPE Foams with Cell Sizes in the Microcellular Range: Advantages of Using these Materials in Structural Elements. Cellular Polymers 27: 347-362, (2008).

[16]. M.A. Rodríguez-Pérez, J. Lobos, C.A. Pérez-Muñoz, J.A. de Saja. Mechanical Response of Polyethylene Foams with High Densities and Cell Sizes in the Microcellular Range. Journal of Cellular Plastics 45:389-403, (2009).

[17]. J.E. Weller, V. Kumar. Solid State Microcellular Polycarbonate Foams. II. The Effect of Cell Size on Tensile Properties. Polymer Engineering and Science 50: 2170-2175, (2010).

[18]. S. T. Lee, C. B. Park, N. S. Ramesh. Polymeric Foams. Science and Technology. CRC Press, Boca Raton-Florida, (2007).

[19]. M.A. Rodríguez-Pérez, O. Alonso, A. Duijsens, J.A. de Saja. Thermal Expansion of Crosslinked Closed-Cell Polyethylene Foams. Journal of Applied Polymer Science 36: 2587-2596, (1998).

[20]. W. Gong, J. Gao, M. Jiang, L. He, J. Yu, J. Zhu. Influence of Cell Structure Parameters on the Mechanical Properties of Microcellular Polypropylene Materials. Journal of Applied Polymer Science 122: 2907-2914, (2011).

[21]. ASTM D6226-10. Standard Test Method for Open Cell Content of Rigid Cellular Plastics. Annual Book of ASTM Standards, Vol 8.03, (2011).

[22]. M. Antunes, J.I. Velasco, V. Realinho, A.B. Martínez, M.A. Rodríguez-Pérez, J.A. de Saja. Heat Transfer in Polypropylene-Based Foams Produced using Different Foaming Processes. Advanced Engineering Materials 11: 811-817, (2009).
[23]. L.R. Glicksman, Heat Transfer in Foams in N.C. Hilyard, A. Cunningham (Eds). Low Density Cellular Plastics-Physics of Basics of Behaviour. Chapman and Hall, London, pp 107-111, (1994).
[24]. J. L. Throne. Thermoplastic Foam Extrusion. An Introduction. Hanser Publishers, Munich, (2004).
[25]. L. Garrido, L. Ibarra, C. Marco. Ciencia y Tecnología de Materiales Poliméricos. Volumen II. Instituto de Ciencia y Tecnología de Polímeros-CSIC, Madrid, (2004).
[26]. L. Garrido, L. Ibarra, C. Marco. Ciencia y Tecnología de Materiales Poliméricos. Volumen I. Instituto de Ciencia y Tecnología de Polímeros-CSIC, Madrid, (2004).
[27]. K.W. Suh, C.P. Park, M.J. Maurer, M.H. Tusim, R. Genova, R. Broos, D.P. Sophiea. Lightweight Cellular Plastics. Advanced Materials 12: 1779-1789, (2000).
[28]. J. Stange, H. Münstedt. Effect of Long-Chain Branching on the Foaming of Polypropylene with Azodicarbonamide. Journal of Cellular Plastics 42: 445-467, (2006).
[29]. H.E. Naguib, C.B. Park. Strategies for Achieving Ultra Low-Density Polypropylene Foams. Polymer Engineering and Science 42:1481-1492, (2002).
[30]. C.B. Park, L.K. Cheung. A Study of Cell Nucleation in the Extrusion of Polypropylene Foams. Polymer Engineering and Science 37:1-10, (1997).
[31]. C. Liu, D. Wei, A. Zheng, Y. Li, H. Xiao. Improving Foamability of Polypropylene by Grafting Modification. Journal of Applied Polymer Science 101: 4114-4123, (2006).
[32]. G.J. Nam, J.H. Yoo, J.W. Lee. Effect of Long-Chain Branches of Polypropylene on Rheological Properties and Foam-Extrusion Performances. Journal of Applied Polymer Science 96: 1793-1800, (2005).
[33]. F. Hidalgo. Diseño Optimizado de los Parámetros de Proceso en la Fabricación de Espumas de Poliolefina Reticulada mediante Moldeo por Compresión. Tesis Doctoral, Universidad de Valladolid, (2008).
[34]. ASTM D2465-11, Standard test methods for determination of gel content and swell ratio of crosslinked ethylene plastics. Annual Book of ASTM Standards, Vol 8.01, (2011).
[35]. C. Saiz-Arroyo, J.A. de Saja, M.A. Rodríguez-Pérez. Production and characterizacion of crosslinked low-density polyethylene foams using waste of foams with the same composition. Polymer Engineering and Science *In press*-DOI 10.1002/pen.22138, (2012).
[36]. S. Roman Lorza. Formulación y Caracterización de Materiales Celulares Retardantes de Llama Libres de Halógenos basados en Poliolefinas. Tesis Doctoral, Universidad de Valladolid, (2010).
[37]. V. Viswanathan, T. Lahe, K. Baloni, A. Agarwal, S. Seal. Challenges and advances in nanocomposite processing techniques. Materials Science & Engineering R54: 121-285, (2006)
[38]. Y. Du, S.Z. Shen, K. Cai, P.S. Casey. Research progress on polymer-inorganic thermoelectric nanocomposite materials. Progress in Polymer Science, *In press*-DOI 10.1016/j.progpolymsci.2011.11.003, (2011)
[39]. C. Choudalani, A.D. Gotsis. Permeability of polymer/clay nanocomposites. A review. European Polymer Journal 45: 2793-2810, (2010).
[40]. R.F. Gibson. A review of recent research on mechanics of multifunctional composite materials and structures. Composite Materials & Structures 92: 2793-2810, (2010).
[41]. J. Jancar, J.F. Douglas, F.W. Starr, S.K. Kumar, P. Cassagnau, A.J. Lesser, S.S. Sternstein, M.J: Buehler. Current issues in research on structure-property relationship in polymeric nanocomposites. Polymer 51: 3321-3343, (2010).
[42]. S. Pavlidou, C.D. Papaspyrides. A review on polymer layered silicate nanocomposites. Progress in Polymer Science 33: 1119-1198, (2008).
[43]. S.S. Ray, M. Okamoto. Polymer/layered silicate nanocomposites: A review, from preparation to processing. Progress in Polymer Science 28: 1539-1641, (2003).

[44]. S.S. Ray, M. Bousmina. Biodegradable polymers and their layered silicate nanocomposites: In greening the 21st century materials world. Progress in Polymer Science 50: 962-1079, (2005).
[45]. P. Bordes, E. Pollet, L. Avérous. Nano-biocomoposites. Biodegradable polyester/nanoclay systems. Progress in Polymer Science 34: 125-155, (2009).
[46]. T. Kuilla, S. Bhadra, D. Yao, N.H. Kim, S. Bose, J.H. Lee. Recent advances in graphene based polymer composites. Progress in Polymer Science 35: 1350-1375, (2010).
[47]. F. Hussain, M. Hojjati, M. Okamoto, R.E. Gorga. Polymer-matrix nanocomposites, processing, manufacturing and application: An overview. Journal of Composite Materials 40: 1511-1575, (2006).
[48]. Z. Spitalsky, D. Tasis, K. Papagelis, C. Galiotis. Carbon nanotube-polymer composites: Chemistry, processing, mechanical & electrical properties. Progress in Polymer Science 35: 357-401, (2010).
[49]. H. Zou, S. Wu, J. Shen. Polymer/silica nanocomposites: Preparation, characterization, properties and applications. Chemical Reviews 108: 3893-3957, (2008).
[50]. T.J. Pinnavia, G.W. Beall. Polymer-Clay Nanocomposites. John Wiley & Sons, Chichester-England, (2000).
[51]. C.C. Ibeh, M. Bubacz. Current trends in nanocomposite foams. Journal of Cellular Plastics 44: 493-515, (2008).
[52]. L.J. Lee, C. Zeng, X. Cao, X. Han, J. Shen, G. Xu. Polymer nanocomposite foams. Composites Science and Technology 65: 2344-2636, (2005).
[53]. J.S. Colton, N.P. Suh. Nucleation of microcellular foam: Theory and practice. Polymer Engineering and Science 27: 500-503, (1987).
[54]. W. Zhai, C.B. Park, M. Kontopoulou. Nanosilica addition dramatically improves the cell morphology and expansion ratio of polypropylene heterophasic copolymer foams blown in continuous extrusion. Industral & Engineering Chemistry Research 50: 7282-7289, (2011).
[55]. M. Okamoto, P.H. Nam, P. Maiti, T. Kotaka, T. Nakayama, M. Takada, M. Ohshima, A. Usuki, N. Hasegawa, H. Okamoto. Biaxial flow-induced alignment of silicate layers in polypropylene/clay nanocomposite foam. Nano Letters 1: 503-505, (2001).
[56]. C. Saiz-Arroyo, J. Escudero, M.A. Rodríguez-Pérez, J.A. de Saja. Improving the structure and physical properties of LDPE foams using silica nanoparticles as an additive. Cellular Polymers 30: 63-78, (2011).
[57]. C. Saiz-Arroyo, M.A. Rodríguez-Pérez, J.I. Velasco, J.A. de Saja. LDPE/Silica nanocomposite foams. Relationship between chemical composition, particle dispersión, cellular structure and physical properties. Journal of Nanoparticle Research, *Submitted.*
[58]. D.N. Bikiaris, G.Z. Papageorgiou, E. Pavlidou, N. Vouroutzis, P. Palatzoglou, G. P. Karayannidis. Preparation by melt mixing and characterization of isotactiv polypropylene/SiO_2 nanocomposites containing untreated and surface-treated nanoparticles. Journal of Applied Polymer Science 100: 2684-2696, (2006).
[59]. S. Jacob, K.K. Suma, J.M. Mendez, K.E. George. Reinforcing effect of nanosilica on polypropylene-nylon fibre composite. Materials Science and Engineering B 168: 245-249, (2010).
[60]. S.M. Lai, C.Y. Huang, S.C. Li, Y.H. Chen, H.C. Hsu, Y.F. Yu, Y.F. Hsiou. Preparation and properties of melt-mixed metallocene polyethylene/silica nanocomposites. Polymer Engineering and Science 51: 434-444, (2010).
[61]. P. Kiliaris, C.D. Papaspyrides. Polymer/layered silicate (clay) nanocomposites: An overview of flame retardancy. Progress in Polymer Science 35: 902-958, (2010).
[62]. F. Yang, G.L. Nelson. Combination effect of nanoparticles with flame retardants on the flammability of nanocomposites. Polymer Degradation and Stability 96: 270-276, (2011).
[63]. S.C. Tjong. Structural and mechanical properties of polymer nanocomposites. Materials Science and Engineering R 53: 73-197, (2006).
[64]. G. Munters, J.G. Tandberg. U. S. Patent nº 2,023,204, (1935).

[65]. K.T. Okamoto. Microcellular Processing. Hanser Publishers, Munich, (2003).
[66]. S. Doroudiani, C.B. Park, M.T. Kortschot. Effect of crystallinity and morphology on the microcellular foam structure of semicrystalline polymers. Polymer Engineering and Science 36: 2645-2662, (1996).
[67]. C.B. Park, L.K. Cheung. A study of cell nucleation in the extrusion of PP foams. Polymer Engineering and Science 37: 1-10, (1997).
[68]. C.B. Park, A.H. Behravesh. Low density microcellular foam processing in extrusion using CO_2. Polymer Engineering and Science 38: 1812-1823, (1998).
[69]. H.E. Naguib, C.B. Park, U. Panzer, N. Reichelt. Strategies for achieving ultra low density polypropylene foams. Polymer Engineering and Science 42: 1481-1492, (2002).
[70]. H.E. Naguib, C.B. Park, N. Reichelt. Fundamental foaming mechanisms governing the volume expansion of extruded polypropylene foams. Journal of Applied Polymer Science 91: 2661-2668, (2004).
[71]. W.G. Zheng, Y.H. Lee, C.B. Park. Use of nanoparticles for improving the foaming behaviour of linear polypropylene. Journal of Applied Polymer Science 117: 2972-2979, (2010).
[72]. T.A. Osswald, L.S. Turng, P.J. Gramann. Injection Molding Handbook. Hanser Publishers, Munich, (2002).
[73]. P.R. Hornsby. Thermoplastics structural foams. Part 1 Technology of production. Materials in Engineering 3: 354-362, (1982).
[74]. P.R. Hornsby. Thermoplastics structural foams. Part 2 Properties and applications. Materials in Engineering 3: 443-455, (1982).
[75]. L. Singh, V. Kumar, B.D. Ratner. Generation of porous microcellular 85/15 poly (DL-lactide-co-glycolide) foams for biomedical applications. Biomaterials 25: 2611-2617, (2004).
[76]. M. Antunes, V. Realinho, J.I. Velasco. Study of the influence of the pressure drop rateo on the foaming behaviour and dynamic-mechanical properties of CO_2 dissolution microcellular polypropylene. Journal of Cellular Plastics 46: 551-571, (2010)

Capítulo 3

Procesos de Espumado, Materias Primas y Técnicas Experimentales

En este capítulo se resumen los aspectos experimentales relacionados con el desarrollo del trabajo presentado en esta memoria de tesis. En el primer apartado se describen dos de los procesos de producción de materiales celulares utilizados, (el tercero es el moldeo por compresión mejorado y fue descrito en el capítulo anterior). En los siguientes apartados se presentan de forma muy concisa las características de todas las materias primas que se han utilizado durante todo el estudio realizado y en el último apartado se enumera la relación de técnicas experimentales utilizadas para caracterizar los materiales celulares producidos.

3.1.- PROCESOS DE ESPUMADO

Una parte importante de esta tesis se ha centrado en intentar solucionar algunos de los problemas que presentan procesos de fabricación convencionales. Se han elegido dos de los procesos de producción de espumas con base poliolefina descritos en el capítulo anterior, *moldeo por compresión* y *pressure quench method.* Tomando como base las principales deficiencias que ambos presentan se han intentado solventar algunas de ellas utilizando distintos tipos de estrategias. En este capítulo, se describen las mejoras introducidas en cada uno de esos dos procesos.

3.1.1.- Pressure Quench Method. Disolución de CO_2

Este proceso de fabricación de materiales celulares supone una alternativa al proceso utilizado en la empresa *Zotefoams*, y que a diferencia de este último, no ha sido industrializado. Aunque es un proceso sencillo y mediante el cual se pueden obtener materiales con estructuras celulares óptimas, presenta dos serias desventajas que son, probablemente, la causa de su no implantación a nivel industrial.

La primera de las desventajas, es que las piezas aligeradas producidas mediante este método presentan una *forma altamente irregular*, ya que no conservan la geometría del precursor de partida. Esto dificulta enormemente la caracterización de las propiedades físicas de los materiales. Son perfectamente válidas para el análisis de la estructura celular pero para poder caracterizar sus propiedades mecánicas por ejemplo, es necesario pulirlas o cortarlas hasta conseguir una geometría regular. En la mayoría de los casos esto supone que sólo se puede utilizar un porcentaje muy pequeño de la muestra inicial por lo que es complicado tener muestras con tamaños adecuados para analizar sus propiedades. Por supuesto esto, supone un serio problema a nivel industrial, ya que la adecuación de las piezas para su posterior comercialización

supondría unos costes muy elevados, tanto en tiempo de transformación como en pérdidas de material.

La segunda de las desventajas, es la *dificultad en el control de la densidad final* de los materiales. Aunque puede llevarse a cabo controlando la presión de saturación, la temperatura de saturación, la caída de presión y la presión remanente en el autoclave, el grado de precisión obtenido es bastante bajo, lo que hace que la comparación y/o reproducibilidad de los resultados sea complicada.

Partiendo de este punto, se intentó buscar una solución factible para ambos problemas, es decir, que permitiera obtener materiales con densidad controlada y con una geometría determinada. Para ello, se diseñó un molde que permite controlar ambos aspectos. En la figura se puede apreciar una representación esquemática del mismo, (figura 3.1).

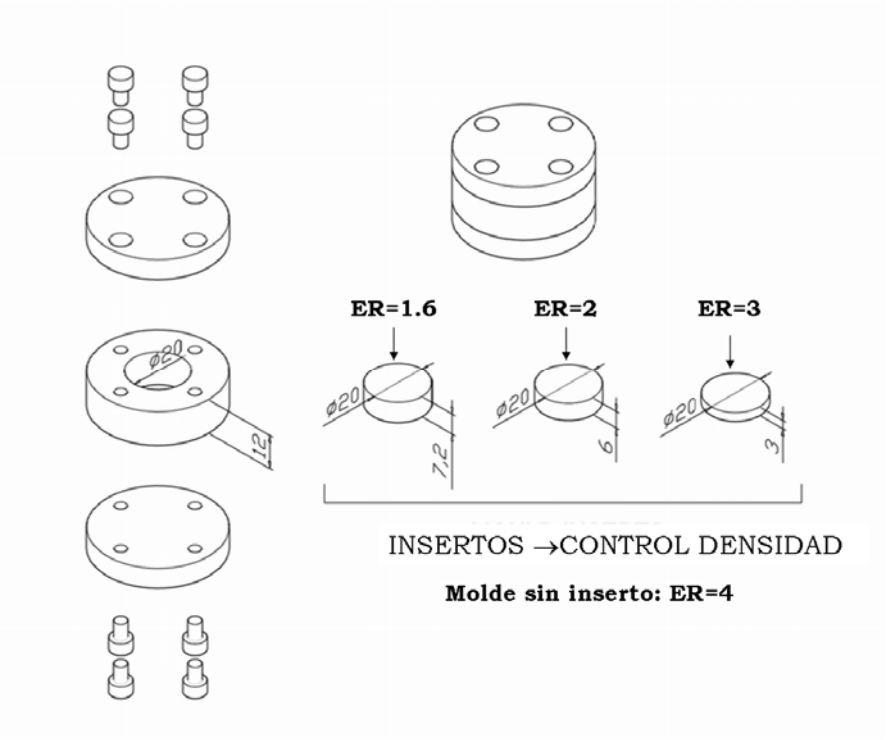

Figura 3.1: Molde utilizado para producir materiales celulares de geometría y densidad controladas utilizando el *pressure quench method.*

El molde está hecho de acero inoxidable y como se puede apreciar en la figura permite obtener muestras cilíndricas, (aunque sería posible fabricar cualquier otro tipo de geometría).

El control de la densidad en este molde se basa en mantener constante el volumen del material precursor, e ir variando el volumen de la cavidad del molde, de modo que el polímero expande hasta distintas alturas.

Los precursores en este caso, son siempre discos, con un diámetro d_0 (20mm) y una altura, h_0, (3mm) constantes. El volumen de la cavidad se controla mediante los insertos mostrados en la figura; todos ellos tienen el mismo diámetro que el precursor, pero distintas alturas, h_i. El molde tiene una altura h_m (12mm), de modo que la altura final de la pieza espumada es, $h_e = h_m - h_i$. En la figura 3.2 se puede ver una representación esquemática del sistema de control de densidad utilizado.

El diseño del molde permite la entrada y salida de gases, siendo estanco al polímero fundido.

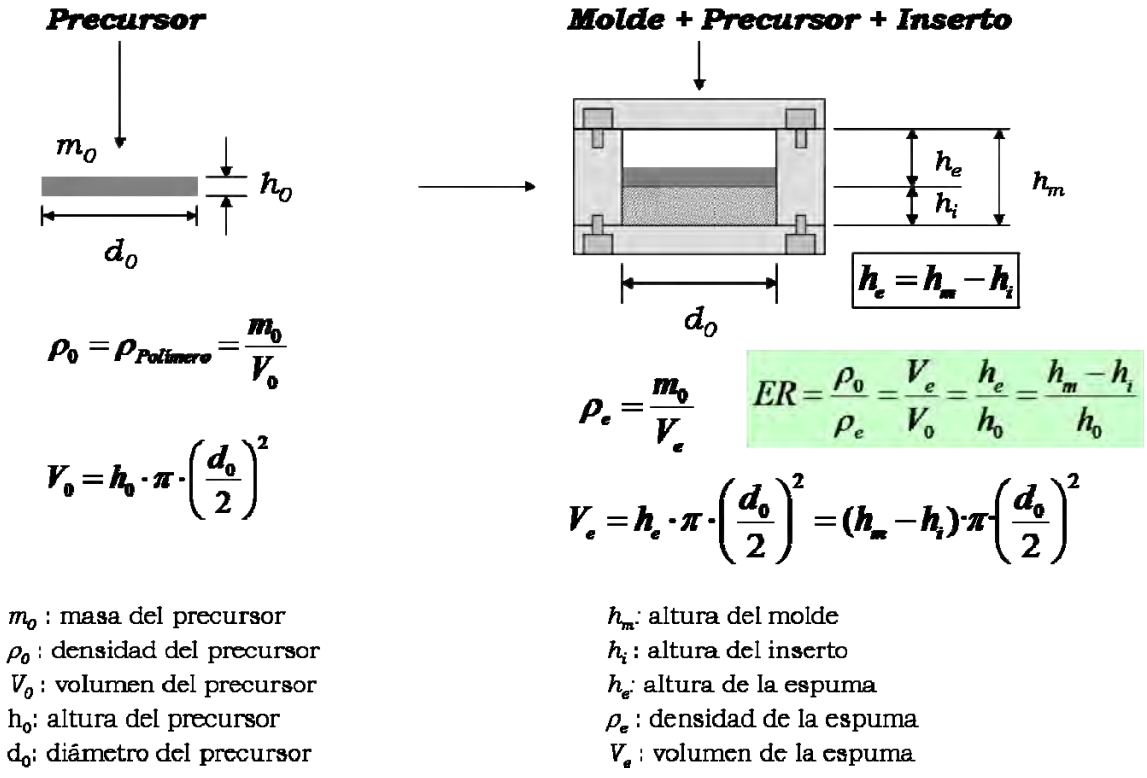

Figura 3.2: Representación esquemática del sistema de control de densidad utilizado con el proceso *pressure quench method.*

La masa de la espuma es la misma que la del precursor y lo que varía respecto a éste último es el volumen, tal y como se puede apreciar en la figura anterior. Según este sistema, el grado de expansión final del material, (*ER*) viene definido por la altura del precursor (h_0), la altura del inserto, (h_i) y la altura del molde, (h_m). Los insertos están diseñados para permitir producir piezas con distintos grados de expansión. En la tabla

siguiente se especifican las alturas de los insertos y los grados de expansión, (*ER*) a los que corresponden, (suponiendo un precursor de altura constante h_0 = 3mm).

Tabla 3.1: Altura de los insertos (h_i) y grados de expansión correspondientes (*ER*).

h_i (mm)	*ER*
7.2	1.6
6	2
3	3
0, (sin inserto)	4

Sin embargo, este sistema, no es por si mismo suficiente para controlar la densidad de las probetas espumadas. Es necesario también lograr un control adecuado de los parámetros involucrados en el proceso.

Figura 3.3: Equipamiento utilizado para producir muestras mediante disolución de CO_2. (Centro Catalán del Plástico)

Los experimentos de espumado mediante el *pressure quench method* fueron realizados en el Centro Catalán del Plástico, (CCP). Se utilizó un reactor autoclave fabricado por la empresa Büchi AG, (modelo Büschiglassuster Stirrer Vessel Type 3), con un volumen interno de 2.1 litros. Puede alcanzar una presión y temperatura máximas de 350 bares y 350ºC respectivamente. La camisa que rodea el vaso está equipada con una resistencia calefactora y un sistema de recirculación de agua que

permite enfriar. Como agentes espumantes físicos se pueden utilizar N_2 o CO_2, aunque se eligió este último debido a su mayor solubilidad en los polímeros, [1]. El gas se inyecta en el vaso mediante un sistema de bombeo (*booster*) que permite aumentar la presión del gas, (respecto de la que tiene en la botella). En la figura 3.3 se muestran tanto el autoclave como el sistema de inyección de gas utilizados.

El proceso consta de una primera etapa de procesado del polímero y los aditivos necesarios en una extrusora o en un mezclador interno y de una segunda etapa de fabricación de los precursores mediante moldeo por compresión.

Una vez fabricados los precursores, éstos son introducidos en el molde descrito previamente, que a su vez es introducido en el autoclave. El sistema se calienta hasta una temperatura inicial, (T_0), a la cual es introducido el gas en el sistema hasta alcanzar una presión determinada, (P_0). El autoclave se programa para que alcance la temperatura de saturación, (T_S) en un tiempo determinado, (t_C), de modo que la presión en el interior del vaso se eleva desde P_0 hasta el valor de saturación P_S. Una vez alcanzadas las condiciones óptimas de saturación, (T_S y P_S), éstas se mantienen durante un tiempo aproximado t_S. A continuación el sistema se lleva a la temperatura de espumación (T_F), que es generalmente inferior a la de saturación y cercana al punto de fusión del polímero. El sistema tarda en alcanzar dicha temperatura un cierto tiempo, t_F. Al disminuir la temperatura, también lo hace la presión, hasta un valor denominado presión de espumado, (P_F). Una vez alcanzadas las condiciones de espumado, el sistema se despresuriza liberando una cantidad de presión determinada, ΔP. En función del grado de expansión deseado dicho valor es mayor o menor, además, se deja una presión remanente en el sistema, (P_R) que facilita el control de la densidad del material. Posteriormente el sistema se enfría hasta temperatura ambiente con el fin de estabilizar la estructura celular y poder extraer la pieza fabricada.

Las condiciones de trabajo dependen del polímero base utilizado en cada caso, si bien se pueden hacer algunas consideraciones generales.

- La temperatura de saturación, (T_S) debe ser ligeramente superior al punto de fusión de la matriz polimérica, (T_m) para así favorecer el proceso de disolución del gas.
- La caída de presión, (ΔP) debe ser mayor a medida que aumenta el grado de expansión del material. Esto implica que la presión de saturación (P_S) debe aumentar a medida que ER lo hace. Sin embargo, la presión remanente (P_R) en el autoclave debe disminuir a medida que ER aumenta con el fin de favorecer la expansión del material.

- La temperatura de espumado (T_F) debe ser ligeramente inferior al punto de fusión de la matriz polimérica y por tanto menor que la temperatura de saturación, para incrementar la viscosidad extensional del material y favorecer la estabilización de la estructura celular.
- A medida que el grado de expansión aumenta, es necesario disminuir la temperatura de espumado (T_F). Cuando el polímero expande es necesario aumentar su viscosidad y el modo más sencillo de hacerlo en este caso es disminuyendo la temperatura. Además, hay que tener en cuenta que el CO_2 disuelto plastifica el polímero [4] haciendo que su viscosidad disminuya gradualmente a medida que aumenta la presión de saturación, (P_S).

En la gráfica siguiente (figura3.4) se resumen las condiciones elegidas para producir espumas con base polipropileno mediante disolución de CO_2 con todos los grados de expansión que permite el molde, (1.6, 2, 3 y 4).

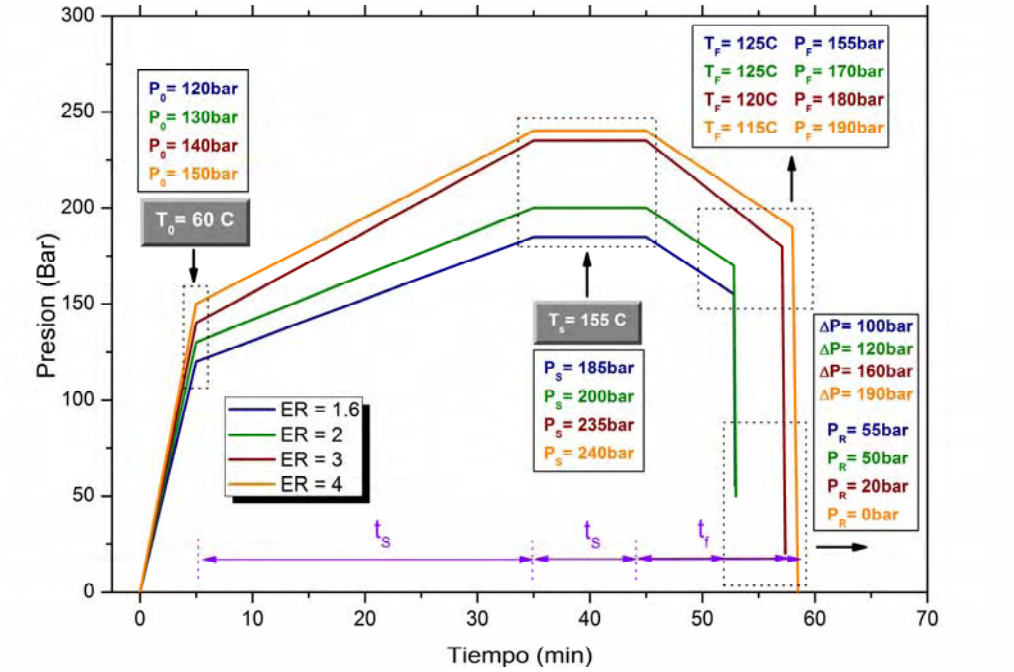

Figura 3.4: Evolución de la presión durante la fabricación de espumas de PP mediante disolución de gas

La temperatura de saturación en este caso es aproximadamente cinco grados mayor que el punto de fusión del polímero, (T_S = 155ºC, T_m =150.4ºC medido por DSC). La temperatura de espumado varía entre 125ºC y 115ºC dependiendo del grado de

expansión. Como se puede apreciar en la figura a medida que ER aumenta, P_S e ΔP aumentan mientras que T_F y P_R disminuyen. Para el mayor grado de expansión, (ER=4), no se aplica una presión de mantenimiento (P_R) sobre el material para así asegurar la completa expansión del mismo y además para favorecer aún más dicha expansión el autoclave permanece abierto después de la despresurización. En el capítulo 7 aparece una descripción más detallada del proceso de producción de dichos materiales así como de los parámetros elegidos.

Este proceso también se ha utilizado para producir espumas de nanocompuestos basados en mezclas de polietileno de baja densidad con nanopartículas de sílice. En la figura 3.5 se representan las condiciones elegidas para la fabricación de dichos materiales.

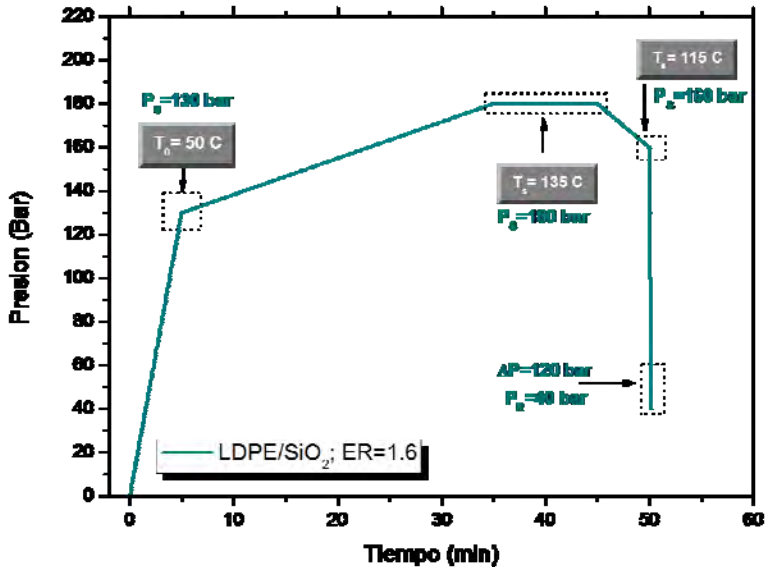

Figura 3.5: Evolución de la presión en el interior del autoclave durante la producción de materiales celulares basados en nanocompuestos de LDPE/sílica.

El punto de fusión del polietileno de baja densidad utilizado es 113.4ºC, (medido por DSC) y la temperatura de saturación y espumado elegidas en este caso son 135 y 115ºC respectivamente. Dado que el grado de expansión es 1.6, se ha elegido un ΔP similar al utilizado para polipropileno para dicho grado de expansión, (ΔP=120bar). En los capítulos 4 y 7 de esta memoria aparecen más detalles sobre el proceso de fabricación de estos materiales así como los resultados obtenidos en su posterior caracterización.

Este método ha resultado ser efectivo para producir materiales celulares con base poliolefina con una geometría definida y buena precisión en el control de la densidad de las probetas. En la figura 3.6 se puede apreciar la diferencia que existe entre utilizar un molde y no utilizarlo cuando se utiliza un proceso de disolución de gas.

Figura 3.6: Ejemplos de muestras producidas mediante disolución de CO_2 con y sin molde.

Respecto al control de la densidad, en la tabla siguiente, (tabla 3.2) se muestran los valores de la densidad real y nominal de muestras de polipropileno fabricadas siguiendo el procedimiento descrito. También se muestran el grado de expansión real y el teórico. El error en ambos casos se ha calculado como la desviación estándar del valor de la densidad o el grado de expansión de unas 10 muestras diferentes de cada tipo y da cuenta de la reproducibilidad del procedimiento. También se ha calculado un parámetro, *%D* (Ecuación 3.1) que contabiliza la desviación que existe entre el valor real y nominal de la densidad de las muestras.

$$\%D = \frac{\rho_{REAL} - \rho_{NOMINAL}}{\rho_{NOMINAL}} \cdot 100 \qquad \text{(Ecuación 3.1)}$$

Tabla 3.2: Valores teóricos y reales de densidad y grado de expansión de muestras de polipropileno producidas mediante disolución de CO_2.

ER_{NOM}	ER_{REAL}	ρ_{REAL} (kg/m³)	ρ_{NOM} (kg/m³)	*%D*
1.6	1.69 ± 0.09	534.8 ± 33.5	562.5	-4.91
2	2.01 ± 0.07	447.9 ± 17.5	450	-0.44
3	3.10 ± 0.05	290.4 ± 5.4	300	-3.33
4	4.12 ± 0.05	218.5 ± 2.8	225	-2.87

Los valores de las desviaciones estándar indican que el proceso la reproducibilidad del proceso es bastante buena. Como se puede apreciar los valores de %D son negativos en todos los casos, lo que indica que la densidad real es siempre menor que la nominal. Esto puede deberse a contracciones del polímero durante el

proceso de enfriamiento en el interior del autoclave. De cualquier modo, ninguno de esos valores excede un 5% de desviación entre la densidad real y la nominal, lo que indica un alto grado de precisión en el control de la densidad de las probetas producidas.

3.1.2.- Moldeo por Compresión Mejorado

El moldeo por compresión bien en una o en dos etapas, permite obtener materiales celulares con base poliolefina de un modo sencillo y bastante económico, además, el rango de densidades que es posible cubrir es considerablemente amplio. Sin embargo, tal y como se comentó en el capítulo anterior el moldeo por compresión, (en una o en dos etapas) presentan dos serias desventajas, la primera y principal es la necesidad de entrecruzar la matriz polimérica para poder producir piezas de densidades muy bajas y la segunda de ellas el control poco preciso de la densidad de los bloques o piezas fabricadas en el proceso de una sola etapa.

La densidad en este proceso se controla ajustando tres parámetros, la tempertura, la presión y la cantidad de agente espumante. En el proceso en una etapa, la precisión en el control de la densidad final es bastante pobre, ya que depende en alta medida de la eficiencia del agente espumante, (que a su vez depende de las condiciones de procesado). En el proceso en dos etapas, la reproducibilidad es mayor, sin embargo las piezas presentan grandes inhomogeneidades en términos de densidad y estructura celular [3, 5, 6]. Por otro lado, y como ya se mencionó en el capítulo anterior, el entrecruzamiento de la matriz polimérica dificulta su reciclaje por métodos convencionales, (molido y re-extrusión) [7].

El *moldeo por compresión mejorado* (*Improved Compression Moulding-ICM*) ha sido desarrollado en el laboratorio CellMat y se presenta como una alternativa al proceso convencional. Permite producir piezas moldeadas y no entrecruzadas en un amplio rango de densidades y está basado en el uso de agentes espumantes de tipo químico además de en un estricto control de la composición química, la presión y la temperatura de procesado. La diferencia fundamental con el moldeo por compresión convencional radica en la *presión aplicada al material durante la fase de expansión*. Esa diferencia se traduce en algunas ventajas respecto a los procesos convencionales:

- *Control preciso de la densidad final de la pieza.*

  En el ICM la densidad del material celular se controla mediante la utilización de unos moldes diseñados especialmente para este

proceso denominados *moldes auto-expandibles*. Dichos moldes son capaces de aplicar y retener la presión tanto durante el proceso de disolución del gas como durante los proceso de expansión y estabilización de la estructura celular. Su diseño hace que permitan controlar el grado de expansión final del material de forma muy precisa. Hasta ahora, este proceso ha permitido producir materiales celulares en un rango de densidades relativas entre 0.1 y 0.9, si bien los analizados en este trabajo están centrados en el rango de densidades relativas medias entre 0.3 y 0.6.

- *Posibilidad de modificar la microestructura del material celular, (diferentes tamaños de celda, tipos de celda o morfología celular).*

  Quizá esta es la mayor ventaja del proceso ICM; permite controlar la estructura celular del material *independientemente* de la densidad del mismo. Mediante el control de la composición química, (cantidad de agente espumante), la presión y la temperatura se pueden obtener muestras con densidades similares, pero diferentes tipos de estructuras celulares, (distintos tamaños de celda, diferentes formas o contenidos de celdas abiertas). Este hecho permite ampliar el rango de aplicaciones de los materiales, así un material con idéntica densidad y un contenido aproximadamente nulo de celdas abiertas podrá ser utilizado para aplicaciones estructurales, mientras que otro con un alto grado de interconexión entre las celdillas podrá ser utilizado como absorbedor acústico.

- *Obtención de piezas moldeadas no entrecruzadas.*

  Los moldes en los que se fabrican las piezas, además de permitir un control preciso de la densidad de la pieza, pueden adoptar diferentes geometrías de modo que se pueden obtener piezas moldeadas de diferentes tamaños y densidades. En principio, cualquier polímero termoplástico o bien materiales compuestos o nanocompuestos con matrices poliméricas de tipo termoplástico se puede espumar utilizando la ruta ICM sin necesidad de entrecruzar la matriz polimérica.

Diversos polímeros puros tales como polietileno de baja densidad (LDPE) o copolímeros de etileno-vinil acetato (EVA), materiales compuestos, tales como mezclas de LDPE o EVA con altas cantidades de hidróxidos de aluminio y/o magnesio, o mezclas de EVA con almidón se han espumado utilizando la ruta ICM [8-16].

El proceso ICM se ha utilizado a lo largo de esta tesis para producir espumas con base polipropileno (PP) y nanocompuestos basados polietileno de baja densidad (LDPE) y nanopartículas de sílica. En los capítulos 6 y 7 de esta memoria se presenta una descripción más detallada del proceso de fabricación y de la posterior caracterización de dichos materiales.

Independientemente del tipo de matriz polimérica utilizada, el proceso consta de las siguientes fases, (figura 3.7)

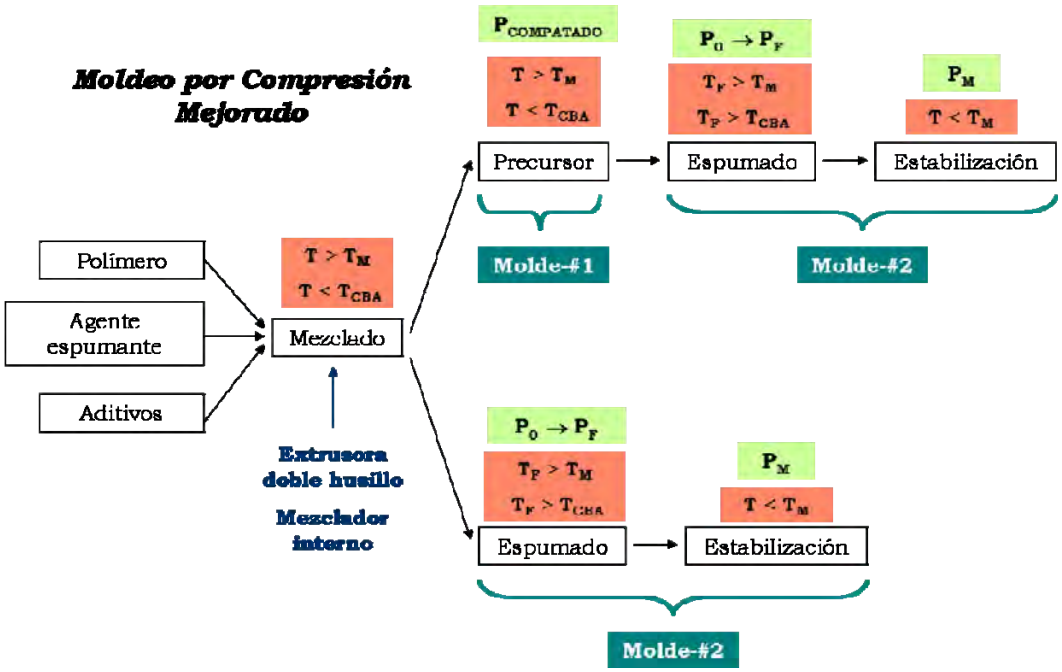

Figura 3.7: Fases del proceso de moldeo por compresión mejorado

Como se puede ver en el esquema anterior la primera etapa del proceso consiste en mezclar todas las materias primas, (polímero, agente espumante y los aditivos necesarios) bien en un mezclador interno o bien en una extrusora de doble husillo. La mezcla así obtenida puede seguir dos rutas diferentes.

El material procesado se puede utilizar para fabricar piezas sólidas que posteriormente serán espumadas, conocidas como *precursores*. Para ello se utiliza un molde con la misma geometría que la de la pieza final espumada, (molde #1). El material extraído de la extrusora o del mezclador se introduce en dicho molde, que a su vez es colocado en una prensa de platos calientes. El material se calienta por encima del punto de fusión del polímero, (T_m) pero por debajo de la temperatura de descomposición del agente espumante, (T_{CBA}) y se aplica una presión suficiente como para lograr una compactación adecuada del material, ($P_{COMPACTADO}$).

Una vez fabricado el precursor, este se introduce en el molde donde será espumado, (*molde autoexpandible,* molde #2). El molde se coloca en una prensa de platos calientes donde se le aplica una presión inicial P_0 además de calentarlo hasta una temperatura T_F, mayor que el punto de fusión del polímero y que el de descomposición del agente espumante. A medida que aumenta la tempertura, el agente espumante comienza a descomponerse haciendo que la presión en el interior del molde aumente hasta un cierto valor P_F. Después de un tiempo, (t_F), cuando el agente espumante se ha descompuesto por completo y P_F se ha estabilizado, (deja de aumentar), se libera la presión de la prensa permitiendo que el polímero expanda hasta el ratio deseado. El molde, capaz de retener la presión que hay en el interior (P_M), es introducido en un tanque de agua fría con el fin de estabilizar la estructura celular lo más rápido posible.

En la segunda ruta, el material directamente extraído del mezclador o de la extrusora es directamente introducido en un molde tipo #2 y espumado siguiendo el procedimiento descrito previamente; es decir, en esta ruta no se fabrica un material precursor.

En este caso se ha seguido la primera ruta, ya que se han caracterizado también los materiales precursores con el fin de poder compararlos con los correspondientes materiales espumados.

En la figura 3.8 se puede ver cómo es la evolución de la etapa de expansión del material y cómo funciona un molde *auto-expandible.* Dichos moldes están fabricados en acero inoxidable y constan de un cuerpo, un pistón y una pieza que controla el grado de expansión, (ER). Además, se dispone de otra pieza, que suele estar fabricada en aluminio, que facilita la conducción entre la superficie caliente de la prensa y el precursor. El gas procedente de la descomposición del agente espumante y hace que la presión del sistema aumente, (P_{CBA}). La resultante entre la presión inicial y dicha la producida por el agente espumante es lo que registra la prensa y a lo que se ha denominado como P_F. Transcurrido el tiempo necesario, la presión se libera haciendo que el pistón pueda desplazarse permitiendo la expansión del polímero. La distancia que recorre el pistón, (d) está regulada por una pieza de retención (ver figura) y determina el grado de expansión final del material. Así haciendo que el pistón recorra diferentes distancias se pueden conseguir materiales con distintos grados de expansión.

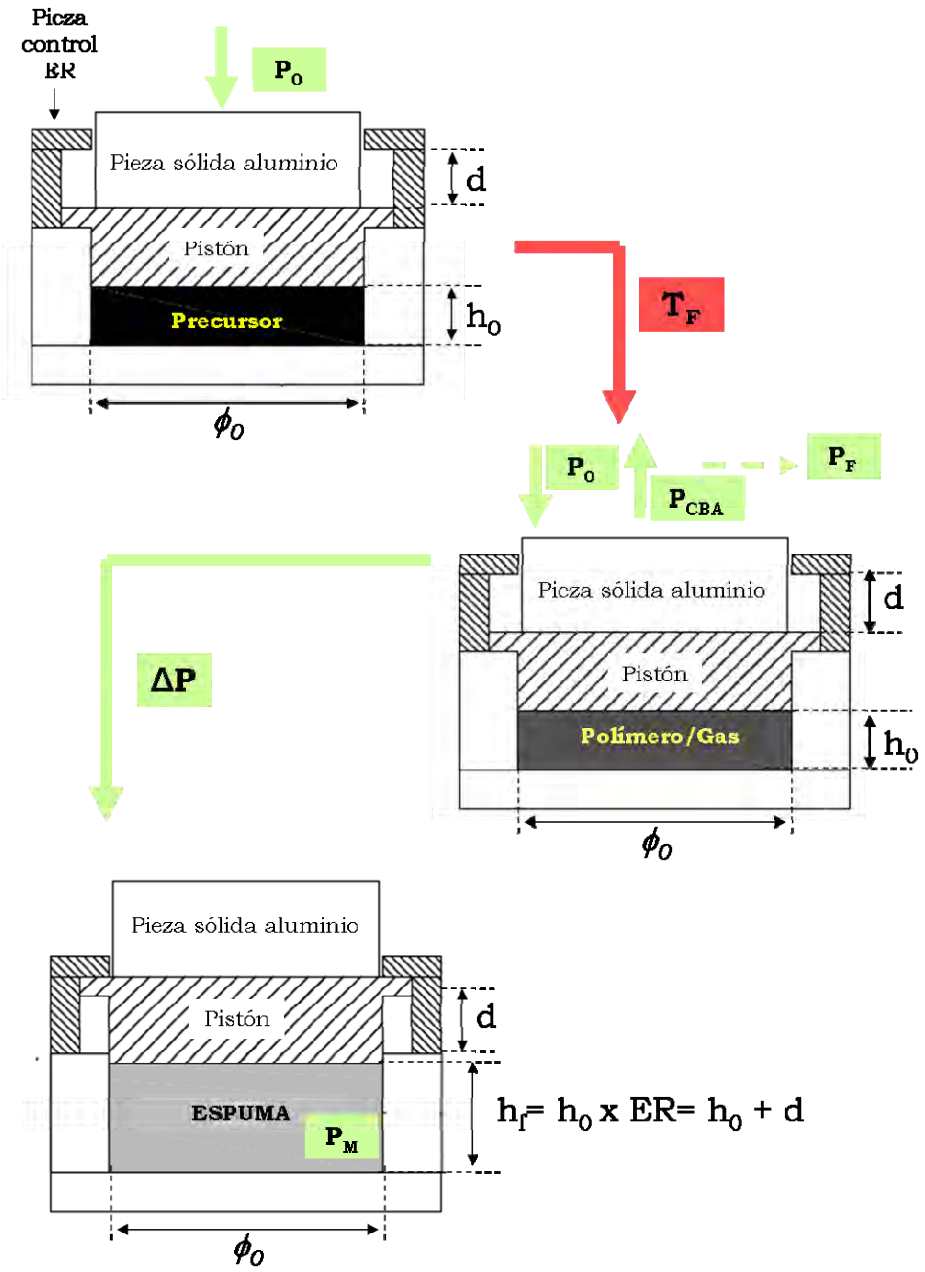

Figura 3.8: Evolución de la etapa de expansión en la ruta ICM

Los parámetros de proceso (tiempo, temperatura y presión inicial y final) dependen tanto del polímero o sistema que se desee espumar como de la cantidad de agente espumante utilizado.

En la imagen siguiente se puede apreciar las muestras fabricadas mediante este proceso tienen una geometría perfectamente definida. Para este estudio se han fabricado probetas con grados de expansión similares a los producidos mediante disolución de CO_2, de modo que ha sido posible realizar un estudio comparativo entre ambos tipos de procesos, (Capítulo 7).

Figura 3.9: Probetas producidas utilizando el proceso de moldeo por compresión mejorado

Al igual que se hizo para el proceso de disolución de gas, se ha analizado la precisión que es posible alcanzar utilizando este proceso en el control de la densidad de discos y cilindros producidos utilizando la ruta ICM y distintos porcentajes (1, 5, 10 y 15 % en peso) de un agente espumante químico, (azodicarbonamida, ADC).

Al igual que se hizo para el proceso de disolución de gas, se presentan los datos de densidad nominal y real así como el grado de expansión real y teórico. Utilizando la ecuación 3.1 se ha calculado %D con el fin de analizar la desviación entre la densidad real y la nominal. En la tabla 3.3 están resumidos los datos correspondientes a muestras cilíndricas y en la tabla 3.4 los de las muestras con forma de disco.

Tabla 3.4: Valores nominales y reales de densidad y grado de expansión de muestras *cilíndricas* producidas por la ruta ICM utilizando diferentes porcentajes de azodicarbonamida

% ADC	ER_{NOM}	ER_{REAL}	ρ_{REAL} (kg/m³)	ρ_{NOM} (kg/m³)	*%D*
1 % ADC	1.6	2.1 ± 0.1	525.2 ± 24.5	562.5	-6.61
	2	2.35 ± 0.09	423.8 ± 5.1	450	-3.81
	3	3.26 ± 0.06	294.0 ± 7.5	300	-1.97
5 % ADC	1.6	1.8 ± 0.1	530.0 ± 20.7	562.5	-5.77
	2	2.1 ± 0.1	461.3 ± 38.9	450	2.52
	3	3.2 ± 0.1	284.0 ± 7.4	300	-5.31
10 % ADC	1.6	1.69 ± 0.08	502.2 ± 34.1	562.5	-10.70
	2	2.0 ± 0.1	424.5 ± 24.1	450	-5.66
	3	3.14 ± 0.06	288.3 ± 4.3	300	-5.55
15 % ADC	1.6	1.68 ± 0.09	450.8 ± 30.3	562.5	-19.84
	2	2.05 ± 0.04	387.9 ± 36.8	450	-13.78
	3	2.95 ± 0.09	287.9 ± 3.6	300	-7.00

Tabla 3.5: Tabla 3.4: Valores nominales y reales de densidad y grado de expansión de *discos* producidos por la ruta ICM utilizando diferentes porcentajes de azodicarbonamida

% ADC	ER_{NOM}	ER_{REAL}	ρ_{REAL} (kg/m³)	ρ_{NOM} (kg/m³)	*%D*
1 % ADC	1.6	1.81 ± 0.09	606.2 ± 15.0	562.5	7.78
	2	2.29± 0.05	459.9 ± 19.9	450	2.20
	3	3.00 ± 0.06	308.2 ± 3.0	300	2.67
5 % ADC	1.6	1.6 ± 0.1	541.7 ± 11.9	562.5	-3.68
	2	2.18 ± 0.04	426.6 ± 11.1	450	-5.17
	3	2.9 ± 0.2	317.3 ± 2.6	300	5.79
10 % ADC	1.6	1.59 ± 0.05	539.8 ± 12.2	562.5	-4.01
	2	2.1 ± 0.1	416.1 ± 9.1	450	-7.51
	3	2.6 ± 0.1	303.8 ± 12.4	300	1.29
15 % ADC	1.6	1.37 ± 0.03	482.8 ± 32.1	562.5	-14.15
	2	1.84 ± 0.09	382.4 ± 2.2	450	-15.00
	3	2.9 ± 0.1	299.5 ± 15.5	300	-0.15

Tal y como se puede apreciar en las tablas anteriores el grado de exactitud logrado en el control de la densidad depende tanto de la geometría de la muestra como de la cantidad de agente espumante utilizado para producirla. Para las muestras cilíndricas se observa que el grado de precisión aumenta a medida que disminuye la cantidad de agente espumante. Cuando se utilizan concentraciones de ADC elevadas, (10, 15 %) se producen ligeros escapes de material, lo que conlleva reducciones indeseadas de la densidad de la pieza. En los cilindros el grado de precisión alcanzado es ligeramente superior debido a la utilización de una presión inicial inferior, (100 MPa para los cilindros y 4 MPa para los discos).

3.2.- MATERIAS PRIMAS

Se enumeran a continuación los nombres comerciales y principales características de todas las materias primas que han sido utilizadas durante el desarrollo de este trabajo.

3.2.1.- *Matrices Poliméricas*

Como indica su título, este trabajo está basado en la fabricación de materiales celulares con base poliolefina, y de entre ellas, se han elegido el polietileno de baja densidad y el polipropileno. Tal y como se puede apreciar, el grado de polipropileno elegido no es en principio adecuado para producir materiales celulares, si bien se eligió dicho grado con el propósito de realizar un análisis más realista de la influencia de los parámetros de proceso en la estructura celular del material.

POLIETILENO DE BAJA DENSIDAD-LDPE	
Nombre Comercial	***Características***
LDPE 2404 Sabic	▪ MFI=3.95 g/10 min, (190 ºC, 2.16 kg) ▪ T_m = 113.4 ºC ▪ χ_C = 49.3 % ▪ ρ = 920 kg/m^3

POLIPROPILENO-PP	
Nombre Comercial	***Características***
200 CA10 Inneos	▪ Copolímero *random* etileno-propileno ▪ MFI=10 g/10 min, (230 ºC, 2.16 kg) ▪ T_m = 150.4 ºC ▪ χ_C = 44.4 % ▪ ρ = 900 kg/m^3

3.2.2.- *Nanopartículas*

Una de las vías utilizadas para mejorar la estructura celular de los materiales fue la adición de nanopartículas. Se han utilizado dos tipos diferentes, una con geometría laminar, (hectorita) y otra con forma esférica, (nanopartículas de sílice).

SILICATO LAMINAR-HECTORITA	
Nombre Comercial	***Características***
Bentone 108 Elementis Specialties	▪ Nanoarcilla organomodificada con 2M2HT, (Dimethyl dehydrogenated tallow ammonium chloride) ▪ Superficie específica = 700 m^2 /g ▪ Distancia basal (d_{001}) = 2.5 nm

NANOPARTÍCULA ESFÉRICA-SILICE (SiO_2)	
Nombre Comercial	***Características***
Aerosil R974 Evonik	▪ Sílice pirogénica hidrofóbica ▪ Tamaño de partícula =12nm ▪ Area específica = 200 m^2 /g ▪ Superficie modificada con dimetildiclorosilano

3.2.3.- *Compatibilizantes*

Con el fin de mejorar el grado de adhesión polímero/partículas, se han utilizado polímeros compatibilizantes basados en poliolefinas funcionalizadas con anhídrido maleico. En las mezclas de LDPE/SiO_2 se ha utilizado uno basado en polietileno lineal de baja densidad, (LLDPE-g-MA) y en las mezclas LDPE/Hectorita otro basado en polietileno de alta densidad, (HDPE-g-MA).

COMPATIBILIZANTE BASADO EN LLDPE-g-MA	
Nombre Comercial	***Características***
Fusabond MB-226DE DuPont	▪ Compatibilizante basado en LDPE-g-MA ▪ MFI= 1.5 g/10 min, (190 ºC, 2.16 kg) ▪ T_m = 115 ºC ▪ ρ = 930 kg/m^3

COMPATIBILIZANTE BASADO EN HDPE-g-MA	
Nombre Comercial	***Características***
Fusabond E MB100D DuPont	▪ Compatibilizante basado en HDPE-g-MA ▪ MFI=2 g/10 min, (190 ºC, 2.16 kg) ▪ T_m = 134 ºC ▪ ρ = 960 kg/m^3

3.2.4.- *Agentes Espumantes*

Durante este estudio se han utilizado ambos tipos de agentes espumantes, físicos y químicos. Como agente espumante físico se ha utilizado un gas inerte, (CO_2) y como agente espumante químico, azodicarbonamida.

AGENTE ESPUMANTE FÍSICO-CO_2	
Nombre Comercial	***Características***
CO_2 Air Liquide	▪ CO_2 líquido ▪ Presión (botella)= 40 bar ▪ Pureza: 99.95 %

AGENTE ESPUMANTE QUÍMICO-AZODICARBONAMIDA (ADC)	
Nombre Comercial	***Características***
Porofor ADC/M-C1 Lanxess	▪ Agente espumante químico exotérmico ▪ Temperatura descomposición : 210 ºC ▪ Gas liberado (210ºC) : 228 ml/g ▪ ρ = 1650 kg/m^3

3.2.5.- *Otros Aditivos*

Además de las materias primas descritas hasta ahora, se han añadido otra serie de aditivos, generalmente en menor concentración, pero que son necesarios para que los materiales presenten unas características y propiedades óptimas.

OTROS ADITIVOS	
Nombre Comercial	***Características***
Ácido Esteárico 301 Renichem	▪ Ayudante de proceso. Utilizado en todas las formulaciones.
Irganox 1010 Ciba	▪ Antioxidante. Utilizado en todas las formulaciones que contienen LDPE/SiO_2.
Irganox B561 Ciba	▪ Antioxidante. Utilizado en todos los materiales con base PP.
Silox Active Grade Silox	▪ Óxido de Zinc, (ZnO) ▪ Utilizado como activador de la reacción de descomposición de la azodicarbonamida.
Luperox DC40P Arkema	▪ Agente reticulante basado en peróxido de dicumilo, (DCP). ▪ Mezcla que contiene un 40 % de DCP, un 55% de carbonato de calcio y un 5% de sílica gel.

3.4.- TÉCNICAS EXPERIMENTALES

Aunque en la mayoría de los artículos incluidos en esta memoria se hace una descripción de las técnicas experimentales utilizadas para caracterizar los materiales fabricados, en este apartado se presenta un resumen conjunto de todas ellas, así como de los procedimientos o normas utilizados, y de los equipos utilizados en cada caso.

Tabla 3.5: Técnicas utilizadas para caracterizar los materiales celulares con base poliolefina producidos a lo largo de este trabajo

Técnicas Experimentales	***Capítulo (s)***
Determinación de la densidad. Método de Arquímedes Norma UNE-EN 1183/1 Balanza Mettler Toledo AT261	4, 5, 7 y 8
Determinación de la densidad. Método Volumétrico. ASTM Standard D1622-08 Balanza Mettler Toledo AT261	6, 7 y 8
Microscopía Electrónica de Barrido, (SEM) Microscopio electrónico Jeol JSM-820	4, 5, 6, 7 y 8
Microscopía Electrónica de Barrido de Alta Resolución, (ESEM) ESEM Quanta 200FEG	4 y 7
Microscopía Electrónica de Transmisión, (TEM) Microscopio elctrónico de transmisión Hitachi H800	5 y 7
Calorimetría Diferencial de Barrido, (DSC) Mettler DSC 822^{e}	4, 5 y 8
Análisis Termogravimétrico, (TGA) Mettler TGA/SDTA 851^{e}	4, 5 y 7
Análisis Térmico-Dinámico-Mecánico, (DMTA) DMA 7, Perkin Elmer	5
Análisis Termomecánico, (TMA) DMA 7, Perkin Elmer	5
Reología Extensional Reómetro ARES, TA Instruments	4
Difracción de Rayos X a Ángulos Altos, (WAXS) Difractómetro Bruker D8	5
Picnometría de Aire ASTM Standard D6226-10 Picnómetro Eijkelkamp 08.06	6, 7 y 8
Máquina Universal de Ensayos, (compresión, tracción, flexión) Norma ISO 604-2002- Compresión Norma ISO 527- Tracción Norma ISO 178- Flexión Máquina Universal Instron Modelo 5500R625	4, 6, 7 y 8
Impacto Charpy Norma UNE EN ISO 179-1/1eA Péndulo Charpy Tester Frank Modelo 53.566	6
Determinación de la Conductividad Térmica utilizando un Sistema basado en Régimen Transitorio Equipo Hot Disk TPS Thermal Constant Analyzer	8
Tubo de Impedancias Tubo de Impedancias Tipo 4206, Brüel & Kjaer Norma ISO 10534-2	8

BIBLIOGRAFÍA

[1]. K.T. Okamoto. Microcellular Processing. Hanser Publishers, Munich, (2003).
[2]. L.J. Gibson, M.F. Ashby. Cellular Solids: Structure and Properties. 2nd Edition, Cambridge University Press, United Kingdom, (1997).
[3]. D. Klempner, V. Sendijarevic. Handbook of Polymeric Foams and Foam Technology. 2nd Edition. Hanser Publishers, Munich, (2004).
[4]. S.T. Lee. Foam Extrusion: Principles and Practice. Tecnomic Publishing Company, Lancaster-Pennsylvania, (2000).
[5]. J.I. González-Peña. Efecto de los Tratamientos Térmicos en Bloques de Espuma de Polietileno de Baja Densidad fabricados mediante Molde por Compresión. Tesis Doctoral, Universidad de Valladolid, (2006).
[6]. F. Hidalgo. Diseño Optimizado de los Parámetros de Proceso en la Fabricación de Espumas de Poliolefina Reticulada mediante Moldeo por Compresión. Tesis Doctoral, Universidad de Valladolid, (2008).
[7]. C. Saiz-Arroyo, J.A. de Saja, M.A. Rodríguez-Pérez. Production and characterization of crosslinked low-density polyethylene foams using waste of foams with the same composition. Polymer Engineering and Science, *In press*-DOI 10.1002/pen.22138, (2012).
[8]. M.A. Rodríguez-Pérez, J. Lobos, C.A. Pérez-Muñoz, J.A. de Saja, L. González, B.M.A. del Carpio. Mechanical behaviour at low strains of LDPE foams with cell sizes in the microcellular range: Advantages of using these materials in structural elements. Cellular Polymers 27: 347-362, (2008).
[9]. M.A. Rodríguez-Pérez, J. Lobos, C.A. Pérez-Muñoz, J.A. de Saja. Mechanical response of polyolefin foams with high densities and cell sizes in the microcellular range. Journal of Cellular Plastics 45: 389-403, (2009).
[10]. S. Román-Lorza. Formulación y Caracterización de Materiales Celulares Retardantes de Llama libres de Halógenos basados en Poliolefinas. Tesis Doctoral, Universidad de Valladolid, (2010).
[11]. S. Román-Lorza, M.A. Rodríguez-Pérez, J.A. de Saja. Cellular structure of halogen-free flame retardant foams base don LDPE. Cellular Polymers 28: 249-268, (2009).
[12]. S. Román-Lorza, M.A. Rodríguez-Pérez, J.A. de Saja, J. Zurro. Cellular structure of EVA/ATH halogen-free flame retardant foams. Journal of Cellular Plastics 10: 1-21, (2010).
[13]. S. Román-Lorza, J. Sabadell, J.J. García-Ruiz, M.A. Rodríguez-Pérez, J.A. de Saja. Fabrication and characterization of halogen free flame retardant polyolefin foams. Materials Science Forum 636/637: 98-205, (2010).
[14]. M.A. Rodríguez-Pérez, R.D. Simoes, C.J.L. Constantino, J.A. de Saja. Structure and physical properties of EVA/Storch precursor materials for foaming applications. Journal of Applied Polymer Science 212: 2324-2330, (2011).
[15]. M.A. Rodríguez-Pérez, R.D. Simoes, S. Román-Lorza, M. Álvarez-Laínez, C. Montoya-Mesa, C.J.L. Constantino, J.A. de Saja. Foaming of EVA/starch blends: Characterization of the structure, physical properties and biodegradability. Polymer Engineering and Science 52: 62-70, (2012).

Capítulo 4

Obtención de Materiales Celulares con base LDPE Mediante Disolución de CO_2. Adición de Nanopartículas de Sílica

En este capítulo se presentan dos trabajos relacionados con la obtención de materiales celulares con base polietileno de baja densidad, (LDPE). Todos los materiales a los que hacen referencia ambos trabajos están fabricados mediante disolución de CO_2 (*pressure quench method*) utilizando el molde y las condiciones descritas en el capítulo 3. En este caso, la obtención de materiales celulares con propiedades mejoradas se ha centrado en la adición de nanopartículas a la matriz polimérica. La utilización de nanopartículas de sílice en la fabricación de nanocompuestos sólidos está bastante extendida, sin embargo su utilización en nanocompuestos espumados es mucho menos común y está casi exclusivamente limitada a matrices poliméricas amorfas.

Por estas razones, estos dos trabajos presentan un primer aspecto bastante novedoso que es la combinación de una matriz polimérica semicristalina no polar con partículas nanométricas de sílice para producir tanto nanocompuestos sólidos como espumados. En ambos artículos se decidió centrar el estudio en los efectos que producen distintos porcentajes de nanopartículas, (1, 3, 6 y 9 % en peso) y se fijó el grado de expansión de todos los materiales espumados en un valor de 1.6. Al utilizar un molde durante el proceso de fabricación la precisión obtenida en el control de la expansión de todos los tipos de nanocompuestos espumados es bastante alta. Dado que además todas las muestras tienen una forma regular (cilíndrica) es posible caracterizar tanto su microestructura como sus propiedades físicas (térmicas y mecánicas).

El primer trabajo incluido en este capítulo titulado *"Improving the Structure and Physical Properties of LDPE Foams using Silica Nanoparticles as an Additive"* está publicado en la revista **Cellular Polymers**. El principal objetivo de este trabajo es evaluar si las nanopartículas de sílice juegan un papel *multifuncional* en materiales celulares con base LDPE, es decir, si son capaces de actuar mejorando por un lado la estructura celular y por otro las propiedades del polímero base. Para ello, se ha analizado la microestructura de los nanocompuestos espumados así como la morfología y las propiedades reológicas de los materiales con diferentes porcentajes de partículas de SiO_2. También se ha analizado si la presencia de las nanopartículas tiene algún efecto en las propiedades térmicas y mecánicas de los nanocompuestos sólidos y espumados. El análisis comparativo de las propiedades de los nanocompuestos sólidos y espumados es también un aspecto novedoso que se presenta en este trabajo y que además permite dilucidar si los efectos que produce la inclusión de una fase nanométrica son mayores en los materiales sólidos o en los aligerados. Cuando la presencia de dicha fase nanométrica lleva a un grado de mejora más elevado en el material celular que en el correspondiente material sólido se puede hablar de la presencia de *efectos sinérgicos* debidos a la combinación de nanopartículas y del proceso de espumado.

La caracterización de los materiales permite concluir que las partículas de SiO_2 actúan como *agentes nucleantes* durante el proceso de espumado de los materiales ya que la adición de un porcentaje muy bajo de dichas partículas (1%) conlleva una reducción del tamaño de celda y un aumento de la densidad celular. Se ha detectado además un aumento en la cristalinidad del polímero base debido a la presencia de las partículas de sílice, siendo dicho aumento además proporcional al aumento en la concentración de partículas. El análisis de las propiedades reológicas de los materiales indica que existe un aumento de la viscosidad extensional de los materiales a medida que aumenta el porcentaje de partículas. En cualquier caso se puede concluir que este aumento no afecta significativamente al proceso de espumado ya que en la zona de bajas deformaciones (que son las importantes a materiales celulares de bajo grado de expansión) el efecto de las partículas es indetectable. El análisis de la estabilidad dimensional mediante TGA permite concluir que la estabilidad térmica de los nanocompuestos es superior a la del polímero puro. Las propiedades mecánicas de ambos tipos de nanocompuestos, (sólidos y espumados) se determinaron mediante ensayos de compresión. Las nanopartículas producen un aumento general de la respuesta mecánica tanto en los materiales aligerados como en los sólidos obteniéndose además un mayor porcentaje de mejora en los primeros, lo que indica la presencia de efectos sinérgicos debido al espumado de nanocompuestos basados en LDPE/sílice mediante disolución de CO_2. Los resultados obtenidos de la caracterización de los materiales a nivel tanto nivel microscópico como macroscópico permiten concluir que efectivamente las nanopartículas de sílice juegan un papel multifuncional en nanocomposites espumados con base LDPE ya que actúan mejorando las propiedades de los materiales a todos los niveles previamente descritos.

El segundo de los trabajos incluidos en este capítulo ha sido enviado al **Journal of Nanoparticle Research** y se titula "*LDPE/Silica Nanocomposite Foams. Relationship between Chemical Composition, Cellular Structure and Physical Properties*". Una vez probado que las nanopartículas de sílice juegan un papel multifuncional en materiales celulares con base LDPE, el objetivo principal de este segundo artículo es dilucidar la relación que existe entre la *composición química* de dos tipos de nanocompuestos (sólidos y aligerados) basados en LDPE/SiO_2, la *dispersión* de la fase nanométrica y la *microestructura* y *propiedades físicas* de dichos materiales.

Las mejoras que se pueden lograr a nivel microestructural o a nivel macroscópico debido a la adición de nanopartículas están condicionadas a conseguir un balance adecuado entre el grado de dispersión de las nanopartículas y el grado de adhesión partícula/polímero. Se ha analizado el comportamiento de dos sistemas basados en LDPE/SiO_2 pero con composiciones químicas diferentes. Así, el primero de ellos

contiene el polímero y partículas de sílice sometidas a un tratamiento superficial con silanos y el segundo, además del polímero y el mismo tipo de nanopartículas, contiene un compatibilizante basado en polietileno lineal de baja densidad funcionalizado con anhídrido maleico, (LLDPE-g-MA). El uso de tratamientos superficiales de la fase nanométrica así como la utilización de compatibilizantes son dos aproximaciones utilizadas con frecuencia con el fin de mejorar la dispersión de las nanopartículas a lo largo de la matriz polimérica.

La principal novedad de este trabajo reside en el tipo de análisis que se ha realizado. Utilizando microscopía electrónica de alta resolución se ha podido cuantificar el grado de dispersión de las partículas en ambos sistemas. Con la ayuda de varios parámetros, se ha podido extender este análisis a los efectos que el grado de dispersión de las nanopartículas tiene en la efectividad de las mismas como agentes nucleantes durante el proceso de espumado. Además el análisis de las propiedades físicas (térmicas y mecánicas) de los materiales permite establecer la relación entre la composición química y el grado de dispersión y los efectos que éstos producen tanto a nivel microestructural como a nivel macroscópico. La mayoría de trabajos publicados hasta ahora quedan limitados al análisis de dicha relación a nivel microestructural pero en nuestro caso, la obtención de muestras moldeadas permite ampliar dicho análisis hasta el nivel macroscópico.

Los resultados obtenidos indican que en ambos sistemas las nanopartículas no se encuentran dispersas de forma individual sino formando agregados de entre unos 100 y 200 nm. Utilizando microscopía electrónica de alta resolución se ha contabilizado el número de agregados por unidad de volumen presentes en los nanocompuestos sólidos. Comparando dichos valores con estimaciones teóricas se puede concluir que la presencia del compatibilizante no mejora el grado de dispersión y que el tratamiento superficial de las nanocargas es suficiente para obtener un grado de dispersión óptimo. En cualquiera de ambos sistemas las partículas de sílice actúan como agentes nucleantes ya que su presencia lleva asociada una reducción del tamaño de celda y un aumento de la densidad celular. Sin embargo el efecto como nucleantes de las partículas de SiO_2 es más acusado en los materiales que no contienen compatibilizante, (LLDPE-g-MA). La interfase en los materiales que sólo contienen las nanopartículas organomodificadas es mayor que en aquellos que contienen compatibilizante (mayor grado de adhesión polímero/partícula) de modo que la nucleación en los primeros se ve favorecida respecto a los segundos. Este mismo efecto se observa en los valores de cristalinidad del polímero base, en ambos tipos de materiales la cristalinidad aumenta debido a la presencia de la fase nanométrica siendo mayor el aumento en aquellos que no contienen compatibilizante.

Por otro lado, el compatibilizante no parece afectar a las propiedades térmicas de los materiales. La estabilidad dimensional de los nanocompuestos tanto sólidos como aligerados mejora sin observarse ninguna tendencia en relación a la diferencia de composición química. Las propiedades mecánicas medidas en compresión de todos los tipos de materiales, tanto sólidos como espumados y con compatibilizante o no mejoran debido a la presencia de las nanopartículas aunque el porcentaje de mejora es mayor en los materiales con compatibilizante debido al mayor grado de adhesión polímero/partícula. La resistencia de los materiales se ve más favorecida que la rigidez de los mismos ya que los porcentajes de mejora obtenidos son superiores en el primer caso. Al igual que ocurría en el trabajo amnterior, también es posible detectar efectos sinérgicos debidos a la presencia de las partículas de sílice.

Improving the Structure and Physical Properties of LDPE Foams using Silica Nanoparticles as an Additive

C. Saiz-Arroyo[1,2], J. Escudero[1], M.A. Rodríguez-Pérez[1], and J.A. de Saja[1]*

[1] *Cellular Materials Laboratory (CellMat), Condensed Matter Physics Department, University of Valladolid, 47011, Valladolid, Spain*

[2] *Technological Centre of Miranda de Ebro (CTME), Miranda de Ebro, Spain*

Received: 17 December 2011, Accepted: 14 February 2011

SUMMARY

Low density polyethylene/silica nanocomposites have been produced by melt blending and foamed in a high pressure autoclave by gas (CO_2) dissolution. Different amounts of nanosilica, (from 1 wt% to 9 wt%) were used in order to analyze the influence of silica content on thermal and mechanical properties of both foamed and un-foamed composites.

It has been proved that the presence of silica nanoparticles modifies the structure and properties of both foamed and un-foamed materials. An increase in the crystallinity of the polymeric matrix as well as a decrease in cell size (for low contents of silica) have been observed. In addition it was found a significant increment of melt strength, thermal stability and mechanical properties for both solids and foams. From the obtained results, it has been concluded that silica particles play a multifunctional role in this system, and in addition to this, it has been demonstrated that the use of nanoparticles can produce synergetic effects, increasing foam mechanical properties in a greater extend than that of the solids.

Keywords: Silica, LDPE, foams, nanocomposites

INTRODUCTION

Polymer nanocomposites have attracted a great interest both in industrial and academic areas since these materials possess a high potential to achieve excellent

*E-mail: csaiz@fmc.uva.es

improvements in physical properties using smaller amounts of inorganic particles in the polymeric matrices [1]. These improvements include high dimensional stability, high heat deflection temperatures, reduced gas permeability, improved flame retardation and enhanced mechanical properties [1-3].

Polymeric foams are two-phase materials in which a gas is dispersed in a continuous macromolecular phase [4]. With the inclusion of voids into polymer matrix, foams usually exhibit lower mechanical stiffness and strength and lower dimensional stability than the solid (non porous) material. Foams can be classified depending on their density. Low density foams, (with density values between 30 and 300 kg/m^3) are mainly used for thermal insulation applications or as damping elements in packaging while high density foams, (with density values higher than 500 kg/m^3) are used in structural applications, (pipes, parts for automotive industry, etc).

The combination of polymeric nanocomposites and foaming technologies has lead to a new class of materials, polymeric nanocomposite foams, which are lightweight, high strength and multifunctional. Small amounts of well dispersed nanoparticles in polymer matrices serve as nucleation sites to facilitate the bubble nucleation process. Moreover, the nano-scaled particles are suitable for microscaled reinforcement, and can lead to the achievement of macroscopic mechanical enhancement [1, 5].

In the literature, it is possible to find several examples of foamed nanocomposites that exhibit smaller cell sizes, higher cell densities as well as more uniform cells size distribution and better mechanical properties than the neat foams [1]. More common fillers are nanoclays, carbon nanotubes or carbon nanofibers [1, 5] and they have been added to a wide variety of polymeric matrices, (polyethylene [6, 7, 8], polypropylene [9], polystyrene [10, 11], polyurethane [12] ethylene vinyl acetate [13], etc).

Silica nanoparticles due to its great natural abundance, low cost, high thermal resistance and surface functionalizability have been widely used to prepare solid nanocomposites by combining them with different polymers such as polyethylene [14, 15, 16], poly-lactic acid [17, 18], polypropylene [19, 20, 21, 22], etc [23]. From these papers, it can be inferred that the addition of small amounts (between 1 and 5 wt%) of well dispersed silica nanoparticles into polymer matrices enhance thermal stability as well as mechanical properties. It has been also reported that silica nanoparticles act as nucleating agents for polymers increasing crystallinity; in addition its presence increase viscosity of melted polymers. It can be also deduced from aforementioned papers that when silica content is higher than 5 wt% instead of achieving a well dispersion of the nanoparticles, aggregates of nanosilica start to appear. The presence of aggregates into polymer matrix has a negative impact in thermal stability

and mechanical properties leading to values sometimes lower than those of to the neat polymer.

Regarding the obtention of foamed silica/polymer foams, it is possible to find some papers analyzing the effect of silica nanoparticles in foams. Zhai and co-workers [24], investigated microcellular polycarbonate/silica nanocomposites using supercritical CO_2 as blowing agent. They obtained a good dispersion of the nanoparticles which allowed a quite narrow distribution of cell sizes, reducing it until 0.3-0.5 μm in size and increasing cell density from 10^{11} to 10^{13} cells/cm^3. Sirirapu et al. [25, 26] investigated the nucleation effect of silica nanoparticles in poly(methyl methacrylate), (PMMA) foamed under different conditions. They concluded that cell size decreased as well as cellular density increased with the addition of nanoparticles until an optimum loading, (8 wt%). For higher silica contents, (up to 12 wt%) the formation of aggregates inhibited the nucleation effect of nanoparticles. Yeh and co-workers [27] also produced foamed PMMA/silica nanocomposites concluding that silica served as heterogeneous nucleating agent in polymer matrix reducing cell size and increasing cell density leading to the formation of foams with enhanced physical properties. They also observed that when particles are well dispersed foams showed much stronger thermal stability than that of aggregated silica particle clusters. Other example of polymer/silica foamed system can be found in the work of Nikje and Tehrani [28] who used silica particles as filler in rigid polyurethane foams. Apart from the expected nucleating effect of the silica particles, they found a great improvement (89%) in elastic modulus value for PU/silica foams with the addition of 1 wt% of nanosilica.

All these papers deal with amorphous polymers, (PC; PMMA and PU). As far as we know silica nanoparticles have not been used in semicrystalline foamed products such as polyethylene. Another aspect in which there is a lack of information is the analysis of the differences between the improvements caused by the particles in the foams and those promoted in solids of the same compositions. These analysis could provide interesting and valuable information on the suitability of a given polymer/nanoparticle combination for foaming.

In this work, the effect of addition of silica nanoparticles to low density polyethylene will be analyzed. Solid LDPE/silica nanocomposites will be prepared by melt blending and after that high density foams for structural applications will be produced by the pressure quench method using CO_2 as blowing agent. By analyzing the structure, thermal, rheological and mechanical properties of both solid and foamed nanocomposites it will be determined if silica plays a multifunctional role in this system. In addition, it will be analyzed if the use of nanoparticles in the formulation, combined with foaming could produce synergetic effects in the mechanical properties of the foams, (i.e.

the properties of the foams increase in a greater extent than that of the corresponding solid materials due to the addition of the particles).

EXPERIMENTAL

Materials

Low density polyethylene supplied by Sabic, (LDPE 2404) with a melt flow index of 3.95 g/10 min (measured at 190ºC and 2.16 kg), a density of 0.92 g/cm^3 and a melting point of 113.4ºC was used. Nanosilica (Aerosil R-974) was supplied by Evonik, (Germany). The silica particles presented a primary particle size of 12 nm, a specific surface area of 200 m^2/g and particles surface was modified with dimethyldichlorosilane.

A coupling agent, (Fusabond MB-226DE from DuPont) was added in order to improve the interfacial adhesion between the nanoparticles and the polymeric matrix. A small amount of stearic acid (Stearic Acid 301 from Renichem S.L.) was also used as processing aid. In order to avoid polymer degradation, an antioxidant (Irganox 1010 from Ciba) was also added.

Carbon dioxide with a high purity, (99.95%) was used as physical blowing agent.

Preparation of Solid LDPE/Silica Nanocomposites

In a first stage, solid nanocomposites have been prepared by melt blending of the polymer and the nanoparticles.

First of all, a masterbatch with a high silica content (27 wt%) and 4 wt% of coupling agent was fabricated. This initial composite was then diluted by melt blending in order to obtain several mixtures with different silica contents, (0, 1, 3, 6 and 9 wt%) that will be called hereafter as NC0, NC1, NC3, NC6 and NC9 respectively. The chemical composition of the nanocomposites is shown in detail in **Table 1**.

Table 1. Composition of LDPE/silica nanocomposites, (%wt)

	NC0	NC1	NC3	NC6	NC9
LDPE	99.75	98.62	96.36	92.96	89.6
Silica	0	1	3	6	9
Stearic Acid	0.15	0.15	0.15	0.15	0.15
Coupling Agent	0	0.13	0.39	0.79	1.15
Antioxidant	0.1	0.1	0.1	0.1	0.1

All mixing operations were carried out in a batch mixer, (Rheodrive 5000 from Haake Fisions) at 130ºC and a screw speed of 50 rpm for 6 minutes.

Foaming of LDPE/Silica Nanocomposites

In a first step, precursors were compression moulded in a two hot plates press at 150ºC and 4 MPa. Discs with 20 mm in diameter and 3 mm in thickness were prepared for each formulation. These materials were used both for foaming experiments and for characterization of the solid materials.

After that, in a second step, precursors were placed in a high pressure autoclave and foamed using the pressure quench method. The materials were saturated with CO_2 at 18 MPa for 40 minutes at a constant temperature of 135ºC. After saturation time, samples were cooled down until foaming temperature, (115ºC) and foamed by a rapid pressure drop.

In order to focus our study on the effect of nanoparticles content, nominal expansion ratio was fixed at 1.6 for all the materials. The average experimental expansion ratio value for foamed nanocomposites is shown in **Table 2**.

Table 2. Density of solid and foamed nanocomposites; experimental expansion ratio values for foamed samples

Sample	ρ_{solid} (kg/m^3)	Sample	ρ_{foam} (kg/m^3)	Expansion Ratio
NC0	917.1 ± 3.2	**F-NC0**	586.7 ± 31.2	1.56 ± 0.08
NC1	924.8 ± 4.5	**F-NC1**	624.7 ± 32.7	1.48 ± 0.07
NC3	937.2 ± 0.2	**F-NC3**	582.9 ± 31.7	1.61 ± 0.08
NC6	945.5 ± 2.5	**F-NC6**	561.6 ± 7.2	1.68 ± 0.02
NC9	971.5 ± 15.5	**F-NC9**	563.6 ± 19.1	1.72 ± 0.05

Characterization of Foamed and Solid LDPE/Silica Nanocomposites

Density measurements of solid and foamed composites were performed by Archimedes principle using the density determination kit for the AT261 Mettler-Toledo balance.

In order to analyze the effect of the presence of silica particles in polymeric matrix, characteristic thermal properties of the materials were studied by means of a Mettler DSC822^e differential scanning calorimeter previously calibrated with Indium and Zinc. Weight of the samples was around 5mg. Samples were heated from -40ºC to 200ºC at a heating rate of 10ºC/min in

a nitrogen atmosphere. The melting point was taken at the minimum of the heat flow-temperature curve. Crystallinity degree was calculated from the area of the DSC peak, by dividing the heat of fusion by the heat of fusion of a 100% crystalline material, (288 J/g for a 100% crystalline polyethylene [29]). A correction was introduced in the calculation of the crystallinity degree in order to account for the real polymer content in each material.

To study nanosilica dispersion in both solid and foamed samples their morphology was analyzed using a high resolution scanning electron microscopy, (ESEM Quanta 200FEG).

Cellular structure of foamed nanocomposites was analyzed by SEM using a Jeol JSM-820 scanning electron microscope. Samples were freeze-fractured in liquid nitrogen and the fractured surface was sputter-coated with gold. Cell size and cell density were determined using an image processing tool based on the software ImageJ.

Thermal stability of samples was measured in order to study the possible improvement due to the addition of the silica phase. Thermogravimetric tests were carried out in a Mettler TGA/SDTA 851ᵉ. Samples were subjected to a heating program from 50 to 850ºC at a heating rate of 20ºC/min under nitrogen atmosphere. Samples mass was approximately 10 mg. The thermal stability was characterized using the peak in the derivative curve of the thermogram.

The extensional viscosity behaviour of the solid nanocomposites was characterized by means of an ARES rheometer from TA instruments. For this purpose, plates of 18 x 10 mm and 0.8 mm in thickness were compression moulded at 190ºC and 20 MPa for 15 minutes. The measurements were performed at 180ºC and a constant elongational rate of 0.1 s^{-1}. A minimum of 5 different measurements were performed for each material.

Elastic modulus of foamed and solid nanocomposites was determined from compression tests which were performed in a universal testing machine Instron 5500R6025 following the standard ISO 604-2002 at a strain rate of 1 mm/min.

RESULTS

Density

Table 2 summarizes the densities of both solid and foamed nanocomposites as well as the experimental average value of expansion ratio reached for foamed samples. Expansion ratio can be defined as the ratio between the density of the solid precursor and the density of the corresponding foamed sample.

As it could be expected, density of solid nanocomposites increased as nanosilica content did. Nominal expansion ratio was fixed at a constant value of 1.6 and as it can be seen in **Table 2**, experimental data reached values very close to the nominal one. This indicates a proper control of foams density during foaming experiments.

Polymer Morphology

The effect of the presence of silica particles in LDPE was analyzed by DSC. Values of melting point and crystallinity degree of LDPE/silica nanocomposites appear in **Table 3**. As it can be observed, the addition of silica does not affect melting temperature. On the other hand, crystallinity degree increases as nanosilica content does which indicates that silica nanoparticles have some activity on the crystallization process of the polymeric matrix. This effect can be quantified by calculating the increment of crystallinity for nanocomposites with respect to the neat polymer, (NC0 sample); results are also summarized in **Table 3**. As it can be observed, by adding nanosilicas crystallinity of low density polyethylene can be increased up to a 6%, (for 9 wt% of filler).

Table 3. Melting point, crystallinity degree and percentage of crystallinity increase for analyzed LDPE composites measured by DSC. Thermal stability of the samples measured by TGA

Sample	T_M (°C)	X_C (%)	ΔX_C (%)	Thermal Stability (°C)
NC0	112.25	44.55	-	479.13
NC1	112.37	45.39	1.89	477.05
NC3	113.03	46.21	3.72	489.12
NC6	110.76	46.89	5.25	490.61
NC9	112.55	47.28	6.13	493.30

Nanoparticles Dispersion

The dispersion of particles in foamed and un-foamed LDPE/silica composites was analyzed using high resolution scanning electron microscopy. **Figure 1** shows several micrographs of foamed and solid nanocomposites with different silica contents, (1, 3 and 9 wt%).

As it can be inferred well-dispersed aggregates of 100 to 200 nm can be observed in both foamed and solid nanocomposites for a given silica content. There were not found significant differences between foams and solids in

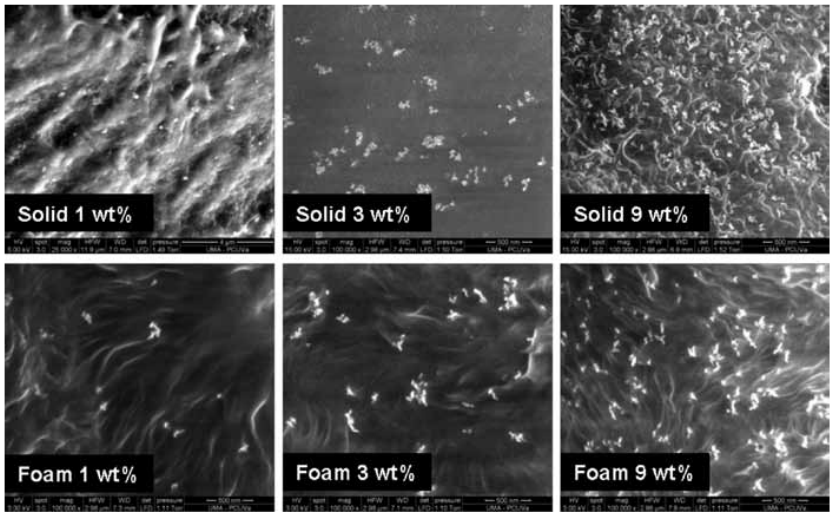

***Figure 1**. High resolution micrographs showing silica particles dispersion in foamed and un-foamed LDPE/composites with different silica contents*

terms of nanosilica dispersion. Therefore, formulations and used processing parameters were suitable to provide well-scattered silica aggregates, although they were ineffective to disperse silica particles individually.

As it was expected, a better dispersion of the aggregates was reached for samples with lower silica contents.

Cellular Structure of Nanocomposite Foams

Results corresponding to observation and characterization of cellular structure of LDPE/silica foams are summarized in **Figures 2** and **3**. **Figure 2** corresponds to micrographs showing cellular structure of LDPE/silica nanocomposites for all silica contents and **Figure 3** shows values of the average cell size and cell density of foamed nanocomposites as a function of silica content.

As it can be observed in **Figure 2**, foamed nanocomposites exhibit an homogeneous, isotropic and closed cell structure for all filler contents. A significant reduction in cell size can be achieved when a small amount of nanoparticles are added to low density polyethylene. In fact, by adding 1 wt% of silica, cell size was reduced from 65 to 45 μm approximately.

For higher silica contents, (higher than 1 wt%), cell size is similar to that of the foam of neat LDPE except for the foams with 9 wt% where cell size

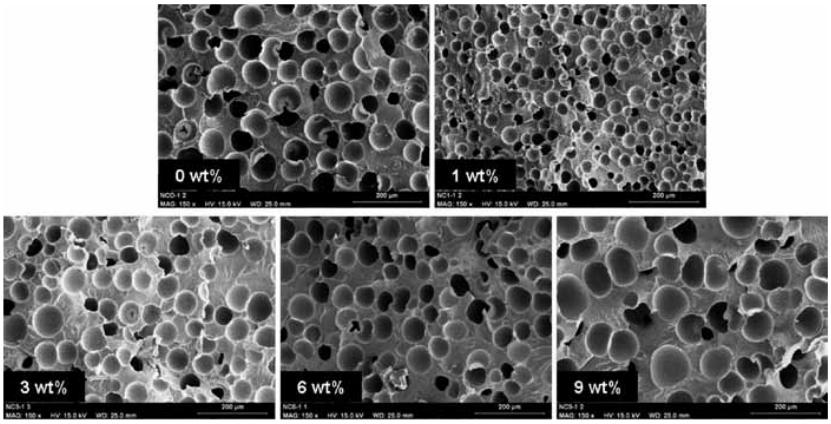

***Figure 2**. Micrographs showing cellular structure of foamed LDPE/silica composites with different silica contents*

is significantly higher than for the rest of the samples. Therefore, it can be concluded that low amounts of silica nanoparticles play a role during foaming reducing cell size, which could be due to a nucleating effect as it will be further discuss in the next section. Moreover the nucleating effect is stronger for low filler contents where particles are better dispersed than for higher particles contents where the dispersion of the particles was poorer. This result is in concordance with previous findings [25, 26]. In these papers, it was reported that for high silica contents where aggregates are bigger and dispersion is lower, nucleating effect of silica particles mitigates.

Melt Strength

It is known [17, 30] that the presence of nanofillers in a polymeric matrix tend to increase its melt strength. In order to analyze if this effect appear in the produced LDPE/silica nanocomposites measurements of elongational viscosity were performed. In addition, the reproducibility in elongational viscosity measurements can give us an idea of the filler dispersion. **Figure 4** shows an example of different elongational viscosity measurements in specimens of samples NC3 and NC9.

As it can be observed, the reproducibility in the measurements for samples containing low filler contents, (3 wt% in this example) is higher than for samples with high filler contents, (9 wt%). This indicates that silica nanoparticles are

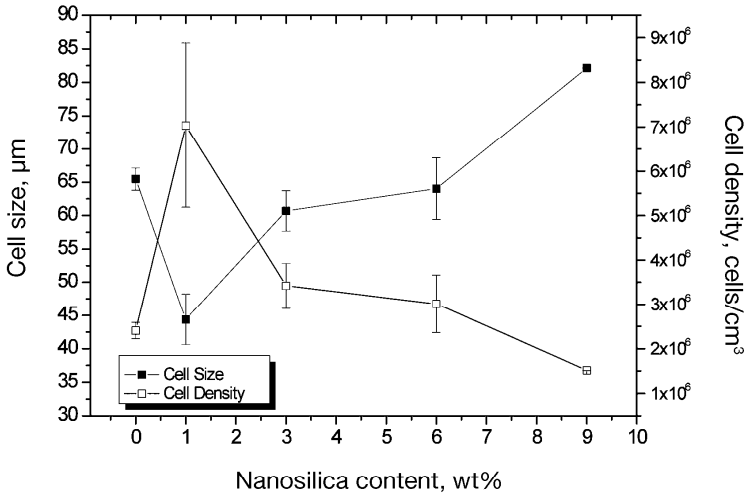

***Figure 3**. Cell size and cell density for foamed nanocomposites as a function of silica content. Error bars in cell size are a measurement of the cell size homogeneity*

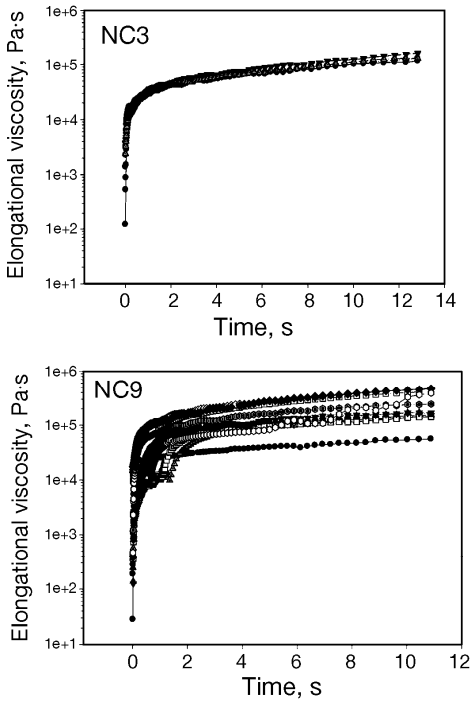

***Figure 4**. Elongational viscosity for different specimens for samples NC3 and NC9*

better dispersed in samples with a low filler content which is in agreement with SEM observations.

Moreover, a mean value of elongational viscosity for each material was calculated. Results are shown in **Figure 5**. As it can be inferred from these results, melt strength of the material does not increase in a significant extent until silica contents higher than 3 wt%. Besides, for low strains (initial seconds of the measurements), melt strength of samples with different silica contents is very similar.

From these measurements, it is possible to conclude that for low expansion ratios and low silica contents nanoparticles do not have an influence on the foaming behaviour in terms of melt strength increase. Therefore, the reduction in cell size observed in **Figure 3** is mainly due to a nucleating effect of silica particles.

Thermal Stability

One of the main aims of adding nanosilica particles to polymers is to improve thermal stability. Thus, the effect of the presence of silica particles in the thermal degradation of LDPE was analyzed by TGA measurements.

Results are summarized in **Table 3**. As it was expected, thermal stability of neat LDPE increased with the addition of silica nanoparticles. An increase

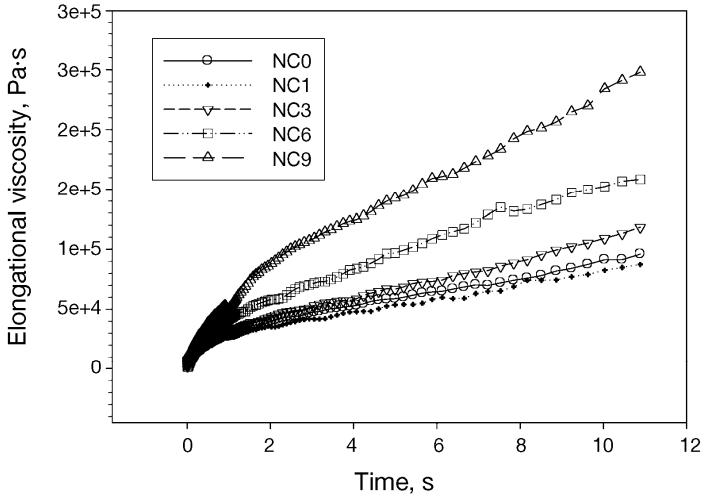

***Figure 5**. Elongational viscosity as a function of time for all the analyzed nanocomposites*

of 20ºC in thermal decomposition temperature can be reached by adding 9 wt% of silica nanoparticles to LDPE.

Mechanical Properties

Compression tests were performed for both solid and foamed nanocomposites. Results of elastic modulus for both types of materials are presented in **Figure 6**. As it can be observed, mechanical properties of both materials are improved by adding silica nanoparticles.

For solid samples the highest value of elastic modulus is obtained for a silica content of 6 wt%. An improvement of 17% with respect to neat LDPE is achieved by adding this amount of nanoparticles. On the other hand, for foamed samples the highest elastic modulus value is obtained for samples with a silica content of 3 wt%. In this case, an improvement of 51% with respect to pristine LDPE foam was achieved. Therefore, as it can be observed, the improvement in compressive elastic modulus is much higher in the foamed nanocomposites than in the solid ones. Moreover, a lower amount of filler is needed to obtain the optimum foamed sample.

This behaviour indicates that the addition of silica nanoparticles combined with foaming the material produces synergetic effects. The explanations to this effect lays in the fact that silica particles are, on the one hand, improving the

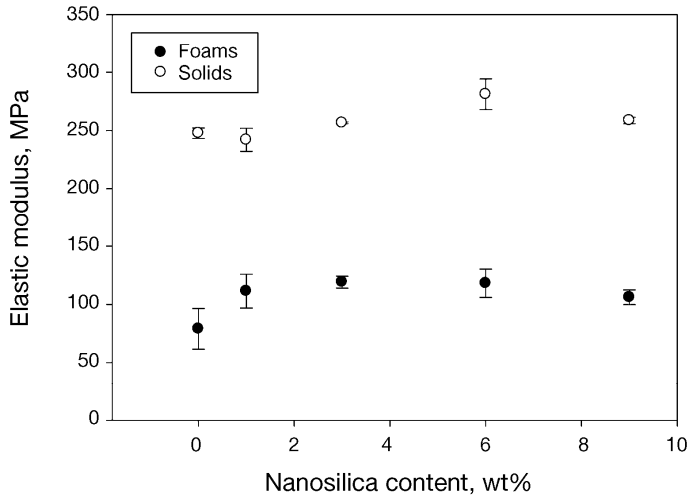

***Figure 6**. Elastic modulus of solid and foamed nanocomposites represented as a function of nanosilica content*

stiffness of the polymer, (silica acts as stiff filler and it increases crystallinity of the polymer) and, on the other hand, allow producing a stiffer cellular structure.

In order to analyze the relationship between the mechanical response of the foamed nanocomposites and the cellular structure, the relative elastic modulus of foamed LDPE/silica samples was calculated. Relative elastic modulus of foams is defined as the ratio between Young's modulus of foams and solids. By calculating this parameter the effect of cellular structure on mechanical properties of the samples can be analyzed. Results are presented in **Figure 7**.

As it can be seen, the highest value of relative elastic modulus is obtained for foams with 1 wt% of silica nanoparticles. This result indicates that the optimum cellular structure to improve stiffness is obtained for this silica content. This result is in agreement with the results of the cellular structure, the smallest cell size was obtained for samples with the same silica content.

Aforementioned results can be supported by the results obtained for other two magnitudes such as collapse stress and density of absorbed energy. **Figure 8** shows both of them as a function of silica content. As it can be inferred from the results, the optimum mechanical behaviour in terms of strength and energy absorption is obtained for samples with 1 wt% of silica particles.

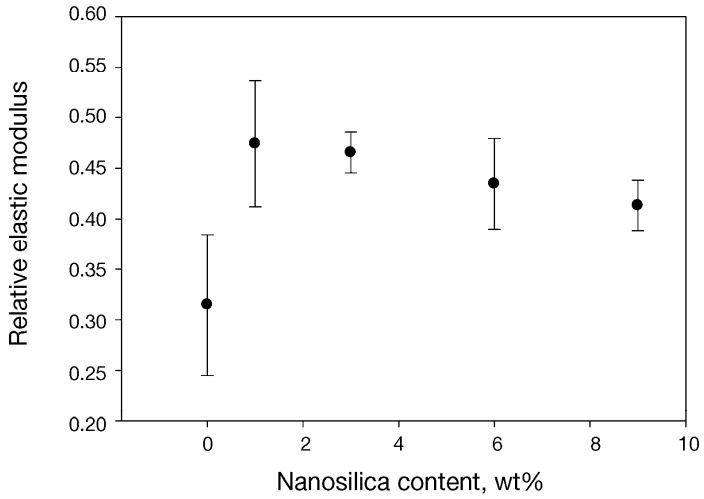

***Figure 7**. Relative elastic modulus of foamed LDPE/silica nanocomposites represented as a function of filler content*

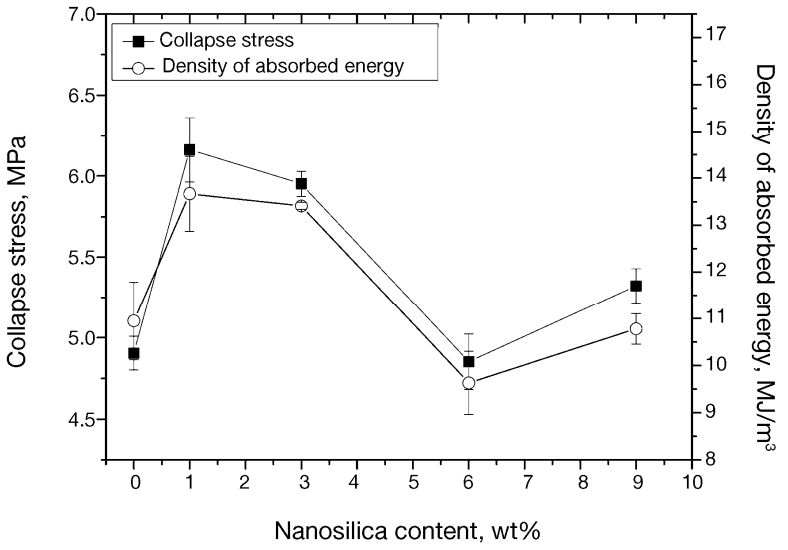

***Figure 8**. Collapse stress and density of absorbed energy of foamed samples represented as a function of nanosilica content*

CONCLUSIONS

LDPE/silica nanocomposites have been produced by melt blending and high density foams have been obtained using the pressure quench method using CO_2 as blowing agent.

The incorporation of silica particles to LDPE matrix produces several effects. First of all, the addition of silica particles allows modifying the polymer morphology. In fact, an increase in polymer crystallinity degree was detected. Second, a reduction in cell size and an increase in cell density were achieved by adding a small amount (1 wt%) of silica nanoparticles due to its nucleating effect. Third, extensional viscosity measurements showed an increase in extensional viscosity when increasing amounts of fillers are added. Besides, thermal stability of nanocomposites was improved with the addition of silica. Finally, the stiffness was improved in both foamed and un-foamed nanocomposites. Consequently due to all these effects, the first main conclusion of this work is that silica nanoparticles play a multifunctional role for LDPE/silica nanocomposite foams.

The second main conclusion of this paper lays in the fact that the improvement in mechanical properties was much higher for foams than for solid

nanocomposites. The synergetic effect achieved by combining the use of nanoparticles and foaming the materials using gas dissolution is due to the multifunctional role played by nanoparticles, which act both in the polymeric matrix morphology and in the cellular structure of the foams.

Results are very interesting for structural (high density) foams because with very low silica contents a significant improvement of the mechanical properties is obtained. Moreover, an interesting topic for the future would be the analysis of silica addition in foams with lower relative density values, (between 0.03 and 0.3).

ACKNOWLEDGEMENTS

Financial assistance from the local government, (Junta of Castile and Leon, Excellence Group GR39); Spanish Ministry of Science and Education, (Predoctoral grant FPU ref. 2009-14001) and Feder Program (MAT 2009-14001 CO2-01) as well as Innocash Project (INC-0193) are gratefully acknowledged.

REFERENCES

1. L.J. Lee, C.Z.X. Cao, X. Han, J. Shen, G. Xu, *Composites Science and Technology*, **65**, (2005), 2344-2363.
2. S.S. Ray and M. Okamoto, *Progress in Polymer Science*, **28**, (2003), 1539
3. R.A. Vaia and E.P. Giannelis, *MRS Bulletin*, **26**, (2001), 394.
4. M.A. Rodríguez-Pérez, *Advances in Polymer Science*, **184**, (2005), 97-126
5. C.C. Ibeh and M. Bubacz, *Journal of Cellular Plastics*, **44**, (2008), 493-515.
6. J.I. Velasco, M. Antunes, O. Ayyad, C. Saiz-Arroyo, M.A. Rodríguez-Pérez, F. Hidalgo, and J.A. de Saja, *Journal of Applied Polymer Science*, **195** (2007), 1658.
7. J.I. Velasco, M. Antunes, O. Ayyad, J.M. Lopez-Cuesta, P. Gaudon, C. Saiz-Arroyo, M.A. Rodríguez-Pérez, and J.A. de Saja, *Polymer*, **48**, (2007), 2098.
8. C. Jo and H.E. Naguib, *Polymer*, **48**, (2007), 3349.
9. W.G. Zheng, Y.H. Lee, and C.B. Park, *Journal of Applied Polymer Science*, **117**, (2010), 2972.
10. B. Zhu, W. Zha, J. Yang, C. Zhang, and L.J. Lee, Polymer, **51**, (2010) 2177.

11. J. Shen, C. Zen, and L.J. Lee, *Polymer*, **46**, (2005), 5218.

12. M.C. Saha, Md.E. Kabir, and S. Jeelani, *Materials Science and Engineering A*, **479**, (2008), 213.

13. Z.R. Xu, H.Y.Park, H.Y.Kim, and K.H. Seo, *Macromolecular Symposia*, **264**, (2008), 18.

14. S. Barus, M. Zanetti, M. Lazzari, and L. Costa, *Polymer*, **50** (2009), 2595.

15. N. García, M. Hoyos, J. Guzmán, and P. Tiemblo, *Polymer Degradation and Stability*, **94**, (2009) 39.

16. M. Pöllänen, U. Pelz, M. Suvanto, and T.T. Pakkanen, *Journal of Applied Polymer Science*, **116**, (2010) 1218.

17. X. Wen, K. Zhang, Y. Wang, L. Han, C. Han, H. Zhang, S. Chen, and L. Dong, *Polymer International*, (2010) DOI 10.1002/pi.2927.

18. A. Zhu, H. Diao, Q. Rong, and A. Cai, *Journal of Applied Polymer Science*, **116**, (2010), 2866.

19. V. Vladimirov, C. Betchev, A. Vassiliou, G. Papageorgiou, and D. Bikiaris, *Composites Science and Technology*, **66**, (2006) 2935.

20. J.H. Chen, M.Z. Rong, W. H. Ruan, Y.L. Mai, and M.Q. Zhang, *Macromolecules Chemistry and Physics, 209*, (2008) 1826.

21. M. Bailly and M. Kontopolou, *Polymer,* **50**, (2008) 2472.

22. J.H.Chen, M.Z. Rong, W.H. Ruan, and M.Q, Zhang, *Composites Science and Technology,* **69**, (2009) 252.

23. H. Zou, S. Wu, and J. Shen, *Chemical Reviews*, **108**, (2008) 3893.

24. W. Zhai, J. Yu, L. Wu, W. Ma, and J. He, *Polymer* **47**, (2006), 7580.

25. S. Siripurapu, J. M. DeSimone, S. A. Khan, and R.J. Spontak, Macromolecules, **38**, (2005), 2271.

26. S. Siripurapu, J.M. DeSimone, S.A. Khan, and R.J. Spontak, *Advanced Materials*, **16**, (2004) 989.

27. J.M. Yeh, K.C. Chang, C.W. Peng, B.G. Chand, S.C. Chiou, H.H. Huang, C.Y. Lin, J.C. Yang, H.R. Lin, and C.L. Chen, *Polymer Composites*, **30** (2009) 715.

28. M.M.A. Nikje and Z.M. Tehrani, *Polymer Engineering and Science*, **50**, (2010) 468.

29. B. Wunderlich, in "Macromolecular Physics", Vol. 2. Academic Press, New York, 1973-1976.

30. Y. Song and Q. Zheng, *Polymer*, **51** (2010) 3262.

LDPE/Silica Nanocomposite Foams. Relationship between Chemical Composition, Particle Dispersion, Cellular Structure and Physical Properties.

C. Saiz-Arroyo[1,2], M.A. Rodríguez-Pérez[1], J.I. Velasco[3], J.A. de Saja[1]

[1] Cellular Materials Laboratory, (CellMat), Condensed Matter Physics Department, University of Valladolid, 47011, Spain. E-mail: csaiz@fmc.uva.es, marrod@fmc.uva.es

[2] Technological Centre of Miranda de Ebro, (CTME), Miranda de Ebro, 09200, Spain.

[3] Centre Català del Plástic. Universitat Politècnica de Catalunya. C/Colom 114. E-08222, Terrassa, Barcelona, Spain.

Abstract

This paper presents the production and characterization of polymeric nanocomposite foams based on low density polyethylene, (LDPE) and silica nanoparticles. Achieving all the potential improvements that can be reached by adding nanoparticles is conditioned to accomplish a good dispersion of the filler into the polymeric matrix. Due to this reason, nanocomposites of LDPE and surface treated silica nanoparticles with and without the addition of a linear low density polyethylene grafted with maleic anhydride (LLDPE-g-MA) were melt compounded to study the compositions leading to a higher dispersion level of the nanofiller. A modified version of the pressure quench method was used to produce foamed samples, because it allows obtaining net-shaped foams adequate for analyzing both their microstructure and mechanical properties. Results showed that surface-modification of silica particles with a silane coupling agent is enough to promote a proper dispersion of the nanofiller as well as an effective nucleating effect of the silica aggregates. For this particular system, the incorporation of the LLDPE-g-MA polymer does not promote a better dispersion and/or a better

nucleation efficiency. Silica particles also act modifying polymer morphology by slightly increasing crystallinity. From a macroscopic point of view, the presence of surface treated SiO_2 leads to a slight increase in thermal stability of the LDPE matrix and to an overall improvement of the mechanical properties.

Key-words

Nanocomposites, silica nanoparticles, low density polyethylene, foams, coupling agent, nanofiller dispersion, synergetic effects.

Introduction

During the last years, polymer nanocomposites foams have focused the attention of both the scientific and industrial communities. The combination of foaming technologies and polymeric nanocomposites can lead to a new class of multifunctional materials (Ibeh and Bubacz 2008).

The multifunctional role played by nanoparticles in polymeric foams lies in an improvement of the overall properties of the foam by acting at two levels, on the one hand by optimizing the cellular structure due to its nucleating effect and on the other hand by improving morphology and properties of the polymeric matrix comprising the cell walls (Ibeh and Bubacz 2008; Lee et al 2005).

Foams with reduced cell sizes and more uniform and narrower cell sizes distributions usually exhibit enhanced physical properties, (Gibson and Ashby 1997; Eaves 2004; Klempner and Sendijarevic 2004). Nanoparticles, on one hand can contribute to obtain such improved cellular structures due to their nucleating effect (Ibeh and Bubacz 2008; Lee et al 2005, Zhai et al 2011; Zhai et al 2010) and on the other hand they can modify

polymer rheology increasing melt strength or even inducing strain hardening of the polymeric matrix and thus favouring gas retention during foaming step (Zhai et al 2011; Zhai et al 2010)

Considering that cell walls of foams are in the micron and sub-micron regime, reinforcing them with nanoparticles can be especially beneficial due to their nanometer dimension (Ibeh and Bubacz 2008). The presence of nanoparticles can induce some very well known effects on the polymer matrix such as polymer morphology modification, (increased crystallinity in semicrystalline polymers), improved thermal stability or enhanced mechanical response among others, (Fu et al 2008; Tjong 2006; Zou et al 2008; Ray and Okamoto 2003; Pavlidou and Papaspyrides 2008).

However, reaching all these potential improvements is conditioned to achieve a proper dispersion of the nanofillers (Ibeh and Bubacz 2008; Lee et al 2005). Several authors, by analyzing different nanoparticle/polymer foamed systems, have concluded that only when nanofillers are adequately dispersed an effective nucleating effect accompanied by an improvement in physical properties are accomplished. For example, Zhen and co-workers (2003), demonstrated the high impact of filler delamination level on polymer foamability as well as on the final foam properties. They observed a higher cell nucleation efficiency for the exfoliated nanoclays compared to the intercalated ones in both polystyrene and poly(methyl-methacrylate). Urbanczyk et al (2010) dealt with the foaming of SAN/clay nanocomposites using supercritical CO_2. They concluded that while for intercalated nanocomposites nucleating effect of nanofillers was negligible, for completely exfoliated ones, cell density reached values two orders of magnitude higher than for the neat polymeric foam. Lee and co-workers (2007) and Seraji and his collaborators (2011) performed similar studies using LDPE as polymeric matrix and montmorillonite (MMT) as filler. They both concluded that the addition of a

compatibilizer led to clay exfoliation and only in this case the nucleation effect induced by the montmorillonite was effective. Other interesting study was carried out by Shen, Zeng and Lee, (2005); they produced nanocomposite foams based on polystyrene filled with carbon nanofibers (CNFs), single-walled carbon nanotubes (SWCNTs) and clays. After analyzing the dispersion degree of each filler, they calculated the nucleation efficiency of each nanomaterial finding that (in percentages) it was 1.97 for CNFs, 9.06 x 10^{-5} and 7.37 x 10^{-4} for SWCNTs and nanoclays respectively. Those results were in agreement with the dispersion degree reached by each type of filler; carbon nanotubes were forming aggregates and carbon nanofibers well dispersed.

In addition, it is possible to find in scientific literature several examples correlating the effective nucleation of well dispersed nanoparticles with an improvement in the physical (thermal and mechanical) properties of nanocomposite foamed systems. Saha and co-workers (2008) measured the thermal and mechanical properties of polyurethane foams infused with several types of nanoparticles, (namely TiO_2, CNFs and MMT). They found that although all were acting as nucleating agents, (by reducing cell size and increasing cell density) the greatest improvement in both thermal and mechanical properties was reached by CNFs filled foams. Other example is provided by Chen et al (2011); they measured the compressive response of PMMA filled with multi-walled carbon nanotubes, (MWCNTs). A significant increase in elastic modulus was detected with the addition of 1wt% of MWCNTs due to an improvement of the cellular structure of such foams.

As it has been highlighted with the previous examples, it is possible to find a substantial amount of papers analyzing the role played by nanoclays, CNTs or CNFs as nucleating and reinforcing elements in different polymeric foamed systems. On the other hand, as

far as we know, the number of scientific studies concerning the production and/or characterization of polymeric foams filled with silica nanoparticles is more limited.

Fumed silica is a fine, white, amorphous powder, which is odourless and tasteless. It exhibits an extremely large surface area and smooth nonporous surface which could promote strong physical contact between the filler and the polymeric matrix, (Zou et al 2008; Vladimirov et al 2006). In addition, fumed silica tends to form aggregates and particle-particle interactions due to the presence of silanol groups (Si-OH) on their surface, (due to their manufacturing process) and also because of their very high surface energy (caused by their large surface area) (Zou et al 2008).

Due to this strong tendency of silica particles to form aggregates is often difficult to achieve a good dispersion with the existing compounding techniques. This is specially difficult for non-polar polymers such as polyethylene. The most commonly used approaches to overcome this problem are, first of all surface modification of silica nanoparticles, (typically with silane coupling agents), and second the use of functionalized polymers, (polymers grafted with maleic anyhride) as compatibilizers between the filler and the polymeric matrix, (Ibeh and Bubacz 2008; Lee et al 2005; Zou et al 2008; Vladimirov et al 2006).

Silica/polymer foamed systems described in the literature uses any of those two approaches to ensure a correct dispersion of the nanofiller. Zhai and co-workers (2006) add surface modified SiO_2 particles to polycarbonate. They obtain a good dispersion of the filler which leads to an effective reduction of cell size and to an increase of two orders of magnitude of cell density. Yeh et al (2009) analyzed the nucleation efficiency of raw and vinyl modified silica particles, concluding that only the modified ones could serve as active heterogeneous nucleating agents in PMMA. Gorem and his collaborators (2010), also mixed PMMA with fluorinated and bare silica nanoparticles of different

sizes. They concluded that the smaller modified particles lead to the smallest cell sizes and highest cell densities. Zhai, Park and Kontopoulou (2006) used a PP-g-MA compatibilizer to improve the adhesion between non-modified silica particles and linear polypropylene concluding that a good dispersion of the particles could enhance the foamability of the linear PP.

All these papers are focused on the influence of silica particles at the microstructural level but there are little evidences of how its presence together with the improvement in cellular structure affects physical properties of such foamed nanocomposites.

So as far as we know, for silica/polymer foamed nanocomposites, multifunctional role of the nanoparticles and the effect on the properties have not been analyzed in detail. In addition, another aspect in which this paper presents novel results is because a non-polar semicrystalline polymer such as LDPE has not been used before to produce foamed nanocomposites containing silica.

Bearing all these ideas in mind, the main goal of this study is to produce solid and foamed LDPE/silica nanocomposites and to analyze the relationships between chemical composition, filler dispersion, cellular structure and physical properties. For this purpose a surface-modified silica as well as a compatibilizer (LLDPE-g-MA) have been used to improve particles-polymer interaction and dispersion. Samples have been foamed using a slightly modified version of the pressure quench method. The characterization of such samples will provide useful information about how chemical composition of the material affects them at microscopic and macroscopic levels.

Experimental

Materials

A low density polyethylene supplied by Sabic, (LDPE 2404) with a melt flow index of 3.95 g/10 min (measured at 190ºC and 2.16 kg), a density of 0.92 g/cm^3 and a melting temperature measured by DSC of 113.4 ºC was used as polymeric matrix. Nanosilica particles, (Aerosil R-974) were kindly provided by Evonik and they presented a primary particle size of 12 nm and a specific surface area of 200 m^2/g. In addition, the surface of the particles is modified with dimethyldichlorosilane in order to improve their dispersibility into the polymeric matrix.

Fusabond MB-226DE from DuPont was used as compatibilizer. It is a maleic anyhidride grafted linear low density polyethylene with a melt flow index of 1.5 g/10 min, (measured at 190 ºC and 2.16 kg), a melting point of 115ºC measured by DSC, a density of 0.93 g/cm^3 and a content of maleic anyhidride of 0.9 % by weight. As it was said in the introduction, the compatibilizer was added in order to improve the interfacial adhesion between the nanoparticles and the polymeric matrix. A small amount of stearic acid (Stearic Acid 301 from Renichem S.L.) was used as processing aid. In order to avoid polymer degradation, an antioxidant, (Irganox 1010 from Ciba) was also included.

Carbon dioxide with a high purity (99.95%) was used as physical blowing agent.

Compounding of Solid LDPE/Silica Nanocomposites

Before foaming step, solid nanocomposites have been melt-compounded in a batch mixer (Rheodrive 5000 from Haake Fisions). Compounding was carried out at a constant temperature of 130ºC and a screw speed of 50 rpm during 6 minutes.

In a first stage, two masterbatches have been produced. The first one, with a very high silica content (27 wt%) and a 4 wt% of compatibilizer and the second one with the same amount of silica but without compatibilizer. These initial composites were then diluted by melt blending with the LDPE in order to obtain several compounds with different silica contents, (0, 1, 3, 6 and 9 wt%). Solid nanocomposites will be called hereafter as S-NC1, S-NC3, S-NC6 and S-NC9 for the samples with compatibilizer and S-NS1, S-NS3, S-NS6 and S-NS9 for the samples without it. The sample corresponding to solid neat polymer, (without silica and without coupling agent) will be called S-LDPE. The chemical composition of each sample is detailed in table 1.

Foaming of LDPE/Silica nanocomposites using the pressure quench method

Pellets of the two types of solid nanocomposites are in a first step compression moulded in a two hot-plates press at 150ºC and 4 MPa to obtain discs with 20 mm in diameter and 3 mm in thickness. Such discs were used both as solid precursors for foaming experiments and for the characterization of solid materials.

Foaming step was conducted in a high pressure vessel using the pressure quench method. The precursors were foamed inside a mould which has the ability of controlling both geometry and density of the foams (Saiz-Arroyo 2012). Precursors after being placed in the mould are saturated with CO_2 at 18 MPa for 40 minutes at a constant temperature of 135 ºC. After saturation step, samples are cooled down until foaming temperature, (115 ºC) and foamed by a rapid pressure drop.

In order to focus the study on the effect of compatibilizer in the dispersability of the nanoparticles as well as on the effects of different silica amounts in foamed and un-foamed composites, nominal expansion ratio, (i.e. the density of the solid divided by the

density of the foamed material) was fixed at 1.6 for all the foamed samples. As a mould is used in the foaming step the density of all the foamed samples is very similar. Besides, due to their cylindrical shape, samples were suitable to perform compression tests.

Foamed samples designation is the same as for solid nanocomposites but with a capital F instead a capital S, this is, F-NC1, F-NC3, F-NC6 and F-NC9 for foamed nanocomposites containing compatibilizer and F-NS1, F-NS3, F-NS6 and F-NS9 for foams without it. Foamed neat polymer will be called hereafter as F-LDPE.

Density values of solid and foamed nanocomposites as well as experimental values of expansion ratio are summarized in table 2. As it can be observed values of expansion ratio are very close to nominal one, (1.6), regardless of the chemical composition of the samples, indicating a proper control of density during foaming.

Characterization of foamed and un-foamed LDPE/Silica composites

Density measurements of solid and foamed samples were performed by Archimedes principle using the density determination kit for the AT261 Mettler-Toledo balance following the standard UNE-EN 1183/1.

In order to analyze nanosilica dispersion in solid materials their morphology was studied using a high resolution scanning electron microscope, (ESEM Quanta 200FEG). Solid nanocomposites were frozen using liquid nitrogen and afterwards fractured.

Cellular structure of foamed materials with and without compatibilizer was analyzed by SEM using a Jeol JSM-820 scanning electron microscope. Samples were freeze-fractured in liquid nitrogen and the fractured surface was sputter-coated with gold. Cell

size and cell density were determined using an image processing tool based on the software ImageJ, (Pinto et al 2009).

Characteristic thermal properties of the materials were studied in order to analyze the effect of the presence of silica particles in the LDPE matrix. A Mettler DSC822^e differential scanning calorimeter previously calibrated with Indium, Zinc and n-Octane was used. The weight of the samples was around 5 mg. Samples were subjected to the following thermal program. A first heating step from -40ºC to 200ºC at a heating rate of 10 ºC/min in a nitrogen atmosphere followed by an isothermal step at 200 ºC during 3 minutes in order to erase thermal history of the samples. After that samples are crystallized from 200ºC to -40 ºC at a cooling rate of -20ºC/min also in an inert atmosphere. Finally samples are subjected to a second heating step from -40 ºC to 200 ºC at a heating rate of 10ºC/min in nitrogen atmosphere. The melting point was taken at the minimum of the heat flow-temperature curve. Crystallinity degree was calculated from the area of the DSC peak, by dividing the heat of fusion by the heat of fusion of a 100% crystalline material, (288 J/g for a 100% crystalline polyethylene (Wunderlich 1976)). A correction was introduced in the calculation of the crystallinity degree in order to account for the real polymer content in each material.

As the presence of nanofillers is known to enhance the thermal stability of the polymeric matrix thermogravimetric tests were carried out of both foamed and un-foamed materials. Measurements were carried out in a Mettler TGA/SDTA 851^e equipment. Samples were subjected to a heating program from 50ºC to 850ºC at a heating rate of 20ºC/min under nitrogen atmosphere. Samples mass was approximately 10 mg. The thermal stability of the samples was determined using the peak in the first derivate curve of the thermogram.

Mechanical properties in compression of both foamed and un-foamed composites can be determined in a very accurate way. Elastic modulus (E) and collapse stress (σ_c) and were determined from the stress-strain curves of the materials measured in a universal testing machine Instron model 5500R6025 following the standard ISO 604-2002 at a strain rate of 1 mm/min.

A more detailed description of the experimental methods used to characterize the foams has been published elsewhere (Rodríguez-Pérez 1999; Rodríguez Pérez 1997; Mills and Rodríguez-Pérez 2001; Almanza et al 2004).

Results

Influence of Chemical Composition at Microscopic Level

Particles Dispersion

As it was pointed out in the introduction, the dispersion degree of the filler in the polymeric matrix has a significant influence on the improvements accomplished by the use of nanoparticles.

In this study, high resolution scanning electron microscopy was used as a tool to quantify the dispersion level of the silica particles in samples with and without compatibilizer. Figure 1 shows several high resolution micrographs of solid LDPE/silica nanocomposites containing different amounts of silica particles. The micrographs in the first row correspond to samples with compatibilizer and the ones in the second row to samples without it.

Nanosilica particles can be appreciated in the micrographs as the bright white spots. It can be inferred from the figure that regardless of chemical composition, silica particles are not individually dispersed but forming well-scattered aggregates with a size between 100 and 200 nm. In addition, as it could be expected, with the increment in silica content, the number of aggregates also increases. Those results are in agreement with similar studies performed using LDPE as polymeric matrix and silica particles with similar diameters, (Barus et al 2009; García et al 2009).

However, the simple observation of the micrographs does not lead to any conclusion regarding the effect of the presence or not of the LLDE-g-MA based compatibilizer. Hence, it is necessary to perform a quantitative analysis. Such analysis may in first place account for dispersion degree of the nanofiller but also should be useful to explain how that dispersion affects both microstructure and mechanical properties of solid and foamed LDPE/silica nanocomposites.

The high resolution SEM micrographs can be used to quantify the real number of particle aggregates per unit surface. By raising the obtained value to the power of $\frac{3}{2}$ it is possible to calculate the real number of aggregates per unit volume. Those values are summarized in table 3. As it can be inferred, the quantitative analysis is in agreement with the qualitative one. As the silica concentration increases, the number of aggregates per unit volume also does, regardless of the presence of the compatibilizer.

In addition, it can be also point out that samples without compatibilizer present a number of aggregates per unit volume slightly higher than those samples containing compatibilizer. So, in this point it is possible to affirm that the melt-mixing technique is ineffective to disperse silica particles individually but it seems that the silane surface treatment of silica particles can contribute to accomplish a proper dispersion level. In addition, the presence of compatibilizer does not lead to higher dispersion levels,

therefore it seems that it does not contribute to increase the effect of the surface modification of the silica nanoparticles.

Moreover, the number of aggregates per unit volume can be compared with the theoretical one calculated assuming that the silica particles were individually dispersed. Presuming a complete dispersion of the filler the number of particles per unit volume can be calculated using the following equation, (Zhai et al 2006):

$$\frac{nucleants}{cm^3} = \frac{w_p}{\rho_p}\frac{\rho_c}{V_p} \qquad (1)$$

where w_p is the weight fraction of the particle in the composite, ρ_p and ρ_c are the density of the particle and the polymer composite respectively, and V_p is the volume of the individual particle. The values obtained from that calculation are also summarized in table 3. As it can be observed, they are much higher than the number of aggregates per unit volume regardless of the chemical composition of the samples. In addition, in figure 2a, this theoretical trend is compared with the real values accounting for the number of aggregates present in each type of sample. As it was previously mentioned the difference between NC and NS samples are not noteworthy, although for NS a slight better dispersion degree is achieved. On the other hand, there is a significant gap between the theoretical values accounting for a complete dispersion and the real obtained ones.

In this point and to quantify this difference a parameter called "*Agglomeration Ratio*" is defined. *Agglomeration Ratio* is defined as the ratio between these two values, this is, the theoretical number of particles per unit volume divided by the real number of particles, (aggregates) present in the sample. The parameter measures the average number of particles in each agglomerate.

Results for all these calculations are summarized in table 3 and in figure 2b. With the increment in silica concentration the trends for NC and NS samples are different. While for NC samples *Agglomeration Ratio* increases as silica content does, for NS ones it can be said that *Agglomeration Ratio* does not significantly change as silica concentration increases.

So, when compatibilizer is added to the LDPE/silica nanocomposites, larger aggregates are accomplished. On the other hand, when only the surface modification of the silica is acting, aggregates with similar sizes are achieved independently of the number of particles present in the sample.

Nanoparticles, tend to maintain agglomeration due to their high surface energy. Results obtained for NS samples indicate that despite the treatment of particles' surface with a silane coupling agent and the shear-forces generated during the melt-mixing step, it was not possible to obtain aggregates with less than 30 particles. In the case of NC samples, it seems that the presence of the compatibilizer lead to a re-agglomeration of the particles during the melt-mixing step and hence to the obtention of larger aggregates as the number of particles present in the sample increases.

Those results are in agreement with those found by Zhou (2009), Zhai (2006) and their respective co-workers. The first, found that the addition of a compatibilizer based in maleic anhydride polypropylene to nanocomposites containing surface-modified silica particles, does not lead to better dispersion of the nanofiller but to a higher degree of agglomeration due to the obtention of larger aggregates than when only surface-modified particles are used. On the other hand Zhai et al (2006) added surface-modified silica particles to a polycarbonate matrix. After analysing the microstructure of the solid nanocomposites, they concluded that as the number of particles decreases, the number of aggregates also did but their size and dispersion level did not change obviously.

Cellular Structure of Foamed Nanocomposites. Nucleating Effect

One of the most important reasons to add fillers or nano-fillers to polymeric foams is the achievement of improved cellular structures due to their nucleating effect. The results corresponding to the observation and analysis of cellular structure of foamed samples are presented in figures 3 and 4. Figure 3 corresponds to micrographs of foamed LDPE and LDPE/silica nanocomposites and figure 4 corresponds to average values of cell size (a) and cell density (b) of aforementioned samples.

Both pure LDPE and LDPE nanocomposite foams exhibit isotropic closed cell cellular structures. It is possible to observe also in figure 3 how the addition of small amounts of silica leads to a significant reduction in cell size and to an increase in cell density; moreover, this effect is more pronounced for samples without compatibilizer. Figures 4a and 4b quantify this effect. It is possible to observe in figure 4a that just with the addition of 1wt% of silica a reduction in cell size of 30%, (from around 65μm to around 45μm) can be reached. For silica contents higher than 1wt% samples with and without compatibilizer behave in a very different way. For NC samples, cell size increase as silica content increases, reaching values even higher than that of the pure LDPE. For NS samples, average cell size does not show any significant variation for samples with 3 or 6wt% of silica and slightly increase for F-NS9. Nevertheless, for NS samples values of cell size are always smaller than that of the neat polymer.

The results for cell density are in agreement with the effects observed for cell size. The presence of compatibilizer leads to smaller cell densities than that achieved for samples containing only surface-modified silica nanoparticles, and in some cases even smaller than that achieved for the control sample, (pure LDPE).

At this point it is necessary to analyze and quantify the efficiency as nucleating agents of silica particles either in the presence or not of the compatibilizer. It is known that the ability of particles to act as nucleation sites is determined by both their dispersion level along the polymeric matrix and by the degree of bonding between the particles and the polymer (Ibeh and Bubacz 2008; Lee et al 2005; Famili 2011). Regarding the effect of the dispersion level, the higher it is, the greater the nucleation effect that can be achieved with the nanofiller. On the other hand, if there is a high degree of bonding between the nanoparticles and the polymeric matrix, a large amount of energy is required to force the interface apart. However, if a poor bond exists, the interface between the matrix and the filler will have a lower surface tension and this will enhance nucleation (Famili 2011).

The effect of dispersion degree in the ability of silica particles to act as nucleating agents can be quantified by means of the *Nucleation Efficiency*. It is a parameter that can be defined as the ratio between the measured cell density and the potential nucleation density of the filler. Using the values presented in table 3 corresponding to real (measured by SEM) and estimated values (calculated using equation 1) of particles per unit volume it is possible to calculate both a theoretical and real value of *Nucleation Efficiency* for samples with and without coupling agent

Results are plotted in figures 5a and 5b together with the *Agglomeration Ratio* values calculated in the previous section. As it can be inferred from both figures, regardless of the presence or not of the compatibilizer, the nucleation efficiency considering the number of aggregates instead the number of potential nucleants is significantly higher. In addition, even considering the number of aggregates, nucleation efficiency in both systems reaches quite low values.

In samples containing compatibilizer, (figure 5a) it can be observed that as *Agglomeration Ratio* increases, nucleation efficiency decreases. This is, as dispersion degree is poorer a lower nucleating effectiveness of the nanoparticles is achieved. All these findings are in concordance with results presented in previous studies, (Zhai et al 2006, Siripurapu 2005, Siripurapu 2004) where it was reported that for high silica contents where aggregates are bigger and dispersion is lower, nucleating effect of nanofillers mitigates.

For samples without compatibilizer, (figure 5b) there is no significant variations in nucleation efficiency with the changes in silica concentration. This is in agreement with the results obtained for *Agglomeration Ratio*. As dispersion level remains approximately constant with the increment in silica concentration, nucleation efficiency also does.

As it was previously mentioned, the degree of bonding between the polymer and the nanofiller also determines the effectiveness of the nano-sized phase as nucleating agent. The dispersion level achieved for both types of samples is very similar, (although the trends with particle concentration are not), so the big differences achieved in cell size and cell density should be due to different degrees of bonding between the LDPE and the silica nanoparticles.

This effect can be simply quantified by calculating the Nucleation Ratio (*NR*) as follows (Famili 2011):

$$NR = \frac{N^*}{N_0} \qquad (2)$$

where N^* is the cell density of the sample containing the nanoparticles and N_0 is the cell density of the unmodified control sample, (neat LDPE in this case). Results are plotted in figure 6 as a function of silica content.

The first fact that can be inferred from the figure is that regardless of the presence of the compatibilizer, effective silica content to improve the cellular structure in both systems is 1wt%. Using higher amounts of silica does not lead to better improvements in terms of microstructure.

On the other hand, values of *NR* reached by samples without compatibilizer are much higher than those of samples containing it. In addition, for some silica concentrations, (6 and 9 wt %) values of *NR* indicates cell densities lower than the one achieved for the pure polymer.

As compatibilizers act enhancing the adhesion between the matrix and the filler it can be expected that in this case the LLDPE-g-MA based compatibilizer is improving the adhesion between the LDPE and the silica particles. Due to a higher degree of bonding between the two phases, a poorer nucleation effectiveness of the nanofiller is reached for the samples containing the compatibilizer.

The surface modification of silica particles with the silane coupling agent lead therefore to a poorer adhesion between the polymer and the nanoparticles which results in a higher effectiveness of the nanosilica as nucleating agent.

Polymer Morphology

The possible modification of polymer morphology in terms of thermal properties, (melting point, crystallinity degree and crystallization temperature) has been evaluated by DSC measurements. Experimental results are summarized in table 4.

There were not detected significant changes regarding melting or crystallization temperatures but a slight increase in the crystallinity degree in the first heating segment. To easily compare these results, the percentage of increment in crystallinity degree with

respect to pristine LDPE has been calculated for samples with and without compatibilizer, (figure 7).

As it can be observed, the increment reached for samples with compatibilizer is smaller than for samples without it. Surface-modified silica particles are by themselves (without the presence of compatibilizer) able to increase crystallinity up to 9%. This increment is achieved with the addition of 3wt% of SiO_2.

Influence of Chemical Composition at Microscopic Level

Thermal Stability

The influence of the presence of the silica particles in the decomposition temperature (T_d) has been analyzed for both foamed and un-foamed composites by means of thermogramvimetric analysis. Results are sumarized in table 5.

Regarding to solid samples, it is possible to observe two different trends depending on silica concentration. At SiO_2 concentrations lower than 3wt%, there is no improvement in thermal stability regardless of the presence of the compatibilizer. On the other hand, when silica content is higher than 3wt%, there is an increment of decomposition temperature. In addition this increment is higher for samples without compatibilizer.

The increment in thermal decomposition temperature reached by foamed samples is similar to those of solid composites. For silica contents higher than 3wt% but higher for silica contents lower than 3wt%. The presence of compatibilizer does not have a significant influence in the thermal degradation of foamed nanocomposites .

Mechanical Properties

Compression tests were performed for all types of foamed and un-foamed LDPE/Silica composites. Elastic modulus and collapse stress (figure 8), were calculated from the stress-strain curves, (Rodríguez-Pérez 2000).

Elastic modulus of nanocomposites is higher than that of pristine LDPE independently of the presence of the compatibilizer. On the other hand, as silica concentration increases, different behaviours are observed for samples with and without compatibilizer. As silica concentration increases, elastic modulus also does for S-NC samples up to a silica content of 6wt%. On the other hand, for samples without compatibilizer, (S-NS), elastic modulus does not follow any clear trend with the increment in silica concentration.

With regard to collapse stress, it can be observed how nanocomposites reach values substantially higher than neat LDPE. The presence of the compatibilizer can be detected also in the nanocomposites; while for samples with 1 and 9wt% of silica, S-NC and S-NS samples present similar values of collapse stress, for silica contents of 3 and 6wt% samples with compatibilizer exhibit slightly higher values.

To easily compare the differences between solid nanocomposites and neat LDPE, the increment in percentage of both elastic modulus and collapse stress has been calculated as follows:

$$\Delta E = \frac{E_{LDPE/SiO_2} - E_{LDPE}}{E_{LDPE}} x100 \qquad (3)$$

$$\Delta \sigma_C = \frac{\sigma_{C-LDPE/SiO_2} - \sigma_{C-LDPE}}{\sigma_{C-LDPE}} x100 \qquad (4)$$

where $E_{LDPE/SiO2}$ and $\sigma_{C\text{-}LDPE/SiO2}$ are the elastic modulus and collapse stress of each type of nanocomposite and E_{LDPE} and $\sigma_{C\text{-}LDPE}$ are the same parameters for neat LDPE. The results are presented in figures 9a and 9b.

21

The first fact that can be inferred from both figures, it is that silica particles lead to greatest improvement in terms of strength than in terms of stiffness independently of the presence of the compatibilizer in nanocomposites composition.

Figure 9a shows the results corresponding to samples with compatibilizer. To maximize stiffness is necessary to add a 6wt% of silica while for strength just a 3wt% is necessary. On the other hand when there is no compatibilizer in the composition of the samples, (see figure 9b), the optimum silica content to maximize both stiffness and strength is 9wt%.

S-NC this is samples with compatibilizer, present an overall improvement in mechanical response higher than S-NS ones. It was concluded after the analysis of the microstructure of the samples that the differences in dispersion level achieved for both types of samples were noteworthy although it was slightly better for NS ones. On the other hand, after the analysis of nucleation effectiveness of silica particles it was found that due to the presence of the compatibilizer, a higher degree of bonding between LDPE and silica nanoparticles was achieved for S-NC samples.

Results of mechanical response seem to indicate that dispersion level of the nano-sized phase is not significantly affecting the mechanical response of the samples. However, the presence of the compatibilizer leads to a better adhesion between both phases and its influence on mechanical response is detected in the higher increment achieved for S-NC samples due to the presence of the silica nanoparticles.

Experimental results corresponding to the characterization of mechanical properties of foams are plotted in figure 10. When compared to foamed LDPE, foamed nanocomposites exhibit higher values of elastic modulus and collapse stress.

For foamed samples it has been performed the same type of analysis as for solid ones. Using equations 3 and 4 the improvement in mechanical performance reached with the

addition of silica particles has been calculated. In addition as results for foamed nanocomposites are compared with the ones obtained for solid nanocomposites, it can be explored the presence of synergetic effects between the addition of nanoparticles and the foaming step.

Results corresponding to the increments reached in elastic modulus are presented in figures 11a and 11b. When samples include compatibilizer in their composition, (figure 11a), no synergetic effects can be observed. Similar improvements in stiffness for foams and for solids are reached up to a 3wt% of silica, and at higher concentrations, the gain in the solids is higher than that observed in the foams.

On the other hand, when there is no compatibilizer included in the chemical composition of the nanocomposites, (F-NC samples) the improvement reached with the addition of silica in foams is considerably higher than the one reached in the non-foamed samples, being the optimum silica content 3wt%, (figure 11b). Moreover, when compared with samples with compatibilizer, the overall increment in elastic modulus is higher for foams without it. It should be reminded at this point that in foams without compatibilizer nucleating effect of silica particles was more accused; hence, it seems that the gain in stiffness for foams without compatibilizer lies in an improved cellular structure in terms of cell size and cell density. So, it is possible to conclude that for samples without compatibilizer synergetic effects are reached by foaming the LDPE/silica nanocomposites.

In terms of strength, (figures 11c and 11d), although there is an overall improvement due to the presence of nanosilica in the samples, the gain reached in foams is always lower than that of the solids. On the other hand, to accomplish an improvement in foams collapse stress of around 19%, it is required a 1wt% of SiO_2 in samples with compatibilizer and silica contents higher than 3wt% in samples without compatibilizer.

Conclusions

LDPE/silica solid nanocomposites with and without compatibilizer have been prepared by melt-mixing. In addition, they have been successfully foamed using the pressure quench method using CO_2 as blowing agent.

The role played by silica nanoparticles in solid and foamed nanocomposites has been analyzed at micro and macro-structural levels concluding the following:

Microstructural Level

- In solid nanocomposites, silica particles are not individually dispersed but forming aggregates of 100 to 200nm in size. In addition, the results for *Agglomeration Ratio* indicate that the modification of silica surface with a silane coupling agent is enough to achieve a proper dispersion degree of the nanofiller. On the other hand, the presence of the compatibilizer does not contribute to increase the dispersability of the nanoparticles.
- Silica particles act as effective nucleating agents as results for cell size and cell density indicates. The effectiveness of silica particles as nucleating agents is greater for samples without compatibilizer due to a poorer adhesion between the polymer and the nanofiller. The presence of the compatibilizer enhances the bonding degree between the two phases mitigating their nucleating effect.
- Polymer morphology, (crystallinity degree) is also modified due to the presence of the SiO_2 particles in the LDPE matrix. An overall improvement in crystallinity degree is reached with the addition of such particles, being the increment higher when there is no compatibilizer in the composition of the nanocomposites.

Macrostructural Level

- A slight increment in thermal stability of LDPE can be achieved with the presence of silica particles. In this case, the presence of compatibilizer does not have a significant effect.
- Mechanical properties of foamed and un-foamed nanocomposites have been analyzed by performing compression tests. Results indicate that silica particles lead to an overall increase in mechanical response of all the analyzed samples. Nevertheless regardless if the samples are foamed or not, the effect of silica particles is greater in terms of strength than in terms of stiffness.
- The improvement in mechanical properties achieved in solids is always greater than that of the foams except in the case of elastic modulus of samples without compatibilizer, which indicates the presence of a synergetic effect. The synergetic effect is reached due to the combination of the use of nanoparticles and foaming the materials by the pressure quench method and are due to the multifunctional role played by nanoparticles which act both modifying the polymeric matrix morphology and the cellular structure of the foams.

Acknowledgements

Financial assistance from Spanish Ministry of Science and Education and Feder Program (MAT 2009-14001 CO2-01), Innocash Project (INC-0193) as well as the project founded by the European Spatial Agency (ESA) MAP AO 99-075 are gratefully acknowledged.

References

Almanza O, Rodríguez-Pérez M A, de Saja J A (2004) Measurement of the thermal diffusivity and specific heat capacity of polyethylene foams using the transient plane source technique. Polym Int 53: 2038-2044.

Barus S, Zanetti M, Lazzari M, Costa L (2009) Preparation of polymeric hybrid nanocomposites based on PE and nanosilica. Polymer 20: 2595-2600.

Cheng L, Schadler L S, Ozisik R (2011) An experimental and theoretical investigation of the compressive properties of multi-walled carbon nanotube/poly(methyl-methacrylate) nanocomposite foams. Polymer 52: 2899-2909.

Eaves D (2004) Handbook of polymeric foams. Rapra Technology. United Kingdom.

Famili M H N, Janani H, Enayati M S (2011) Foaming of a polymer-nanoparticle system: Effect of the particle properties. J App Polym Sci 119: 2847-2856.

Fu S Y, Feng X Q, Lauke B, Mai Y W (2008) Effects of particle size, particle/matrix interface adhesion and particle loading on mechanical properties of particulate-polymer composites. Compos Part B-Eng 39: 933-961.

García N, Hoyos M, Guzman J, Tiemblo P (2009) Comparing the effect of nanofillers as thermal stabilizers in low density polyethylene. Polym Degrad Stabil 54: 39-48.

Gibson L J, Ashby M F (1999) Cellular solids: Structure and properties. Cambridge University Press, United Kingdom.

Gorem K, Chen L, Schadler L S, Ozisik R (2010) Influence of nanoparticle surface chemistry and size on supercritical carbon dioxide processed nanocomposite foam morphology. J Supercrit Fluid 51: 420-427.

Ibeh C C, Bubacz M (2008) Current trends in nanocomposite foams. Cell Plast 44: 493-515.

Klempner D, Sendijarevic V (2004) Handbook of polymeric foams and foam technology, 2nd Edition. Hanser Publishers, Munich.

Lee L J, Zeng C, Cao X, Han X, Shen J, Xu G (2005) Polymer nanocomposite foams. Comp Sci Technol 65:2344-2363.

Lee Y H, Wang K H, Park C B, Sain M (2007) Effects of clay dispersion on the foam morphology of LDPE/clay nanocomposites. J Appl Polym Sci 103: 2129-2134.

Mills N J, Rodríguez-Pérez M A (2001) Modelling the gas-loos creep mechanisms in EVA foam from running shoes. Cell Polym 20: 79-100.

Pavlidou S, Papaspyrides C D (2008) A review on polymer-layered silicate nanocomposites. Prog Polym Sci 33: 1119-1198.

Pinto J, Rodríguez-Pérez M A, de Saja J A (2009) Development of an ImageJ macro to characterize the cellular structure of polymeric foams. XI Reunión del Grupo Especializado de Polímeros, (GEP), Valladolid, (Spain).

Ray S S, Okamoto M (2003) Polymer/layered silicate nanocomposites: A review from preparation to processing. Prog Polym Sci 28: 1539-1641.

Rodríguez-Pérez M A, Rodríguez-Llorente S, de Saja J A (1997) Dynamic mechanical properties of polyolefin foams studied by DMA techniques. Polym Eng Sci 37: 959-965.

Rodríguez-Pérez M A, de Saja J A (1999) The effect of blending on the physical properties of crosslinked closed cell polyethylene foams. Cell Polym 18: 1-20.

Rodríguez-Pérez M A, Arencon D, Almanza O, de Saja J A (2000) Mechanical characterization of closed-cell polyolefin foams. J Appl Polym Sci 75: 156-166.

Saha M C, Kabir Md E, Jeelani S (2008) Enhancement in thermal and mechanical properties of polyurethane foam infused with nanoparticles. Mat Sci Eng A-Struct 479: 213-222.

Saiz-Arroyo C, de Saja J A, Velasco J I, Rodríguez-Pérez M A (2012) Moulded polypropylene foams produced using chemical or physical blowing agents: Structure-properties relationship. J Mater Sci- *In press*, DOI 10.1007/s10853-0.12-63577-7.

Seraji S M, Aghjeh M K R, Davari M, Hosseini M S, Khelgati Sh (2011) Effect of Clay dispersion on the cell structure of LDPE/clay nanocomposites foams. Polym Composite 32: 1095-1105.

Shen J, Zeng C, Lee L J (2005) Synthesis of polystyrene-carbon nanofibers nanocomposites foams. Polymer 46:5218-5224.

Siripurapu S, DeSimone J M, Khan S A, Spontak R J (2004) Low-temperature surface-mediated foaming of polymer films. Adv Mater 16: 989-994.

Siripurapu S, DeSimone J M, Khan S A, Spontak R J (2005) Controlled foaming of polymer films through restricted surface diffusion and the addition of nanosilica particles or CO_2-philic surfactants. Macromolecules 38: 2271-2280.

Tjong S C (2006) Structural and mechanical properties of polymer nanocomposites. Mat Sci Eng R 2006; 53:79-197.

Urbanczyk L, Calberg C, Detrembleur C, Jérôme C, Alexandre M (2010) Batch foaming of SAN/clay nanocomposites with $scCO_2$: A very tunable way of controlling the cellular morphology. Polymer51: 3520-3531.

Vladimirov V, Betchev C, Vassilou A, Papageorgiou G, Bikiaris D (2006) Dynamic mechanical and morphological studies of isotactic polypropylene/fumed silica nanocomposites with enhanced gas barrier properties. Compos Sci Technol 66: 2935-2944.

Wunderlich B (1976) in Macromolecular Physics. Volumen 2: Crystal nucleation, growth, annealing. Academic Press, New York.

Yeh J M, Chang K C, Peng C W, Chand B G, Chiou S C, Huang H H, Lin C Y, Yang J C, Lin H R, Chen C L (2009) Preparation and insulation property studies of thermoplastic PMMA-silica nanocomposite foams. Polym Composite 30: 715-722.

Zeng C, Han X, Lee L J, Koelling KW, Tomasko D L (2003) Polymer-clay nanocomposite foams prepared using carbon dioxide. Adv Mater 2003; 15: 1743-1747.

Zhai W, Yu J, Wu L, Ma W, He J (2006) Heterogeneous nucleation uniformizing cell size distribution in microcellular nanocomposites foams. Polymer 47: 7580-7859.

Zhai W, Kuboki T, Wang L, Park C B, Lee E K, Naguib H E (2010) Cell structure evolution and the crystallization behaviour of polypropylene/clay nanocomposites foams blown in continuous extrusion. Ind Eng Chem Res 49:9834-9845.

Zhai W, Park C B, Kontopoulou M (2011) Nanosilica addition dramatically improves the cell morphology and expansion ratio of polypropylene heterophasic copolymer foams blown in continous extrusion. Ind Eng Chem Res 50:7282-7289.

Zhou H J, Rong M Z, Zhang M Q, Ruan W H, Friedrich K (2007) Role of reactive compatibilization in preparation of nanosilica/polypropylene composites. Polym Eng Sci 2007; 47: 499-509.

Zou H, Wu S, Shen J (2008) Polymer/sílica nanocomposites: Preparation, characterization, properties and applications. Chem Rev 108: 3893-3957.

Figure Captions

Figure 1: High resolution micrographs corresponding to solid nanocomposites with (superior row) and without (inferior row) compatibilizer in their chemical composition.

Figure 2: a) Number of aggregates per unit volume in un-foamed NC and NS samples compared with the theoretical number of particles calculated assuming that they are individually dispersed, b) *Agglomeration Ratio* calculated for solid nanocomposites.

Figure 3: SEM micrographs showing the cellular structure of foamed samples.

Figure 4: Cellular structure characterization of LDPE and LDPE/Silica nanocomposites. a) Average cell size, b) Average cell density.

Figure 5: Analysis of nucleation efficiency of silica nanoparticles in LDPE matrix for samples with (a) and without coupling agent (b).

Figure 6: Values of nucleation ratio for foams with and without compatibilizer.

Figure 7: Increment in crystallinity degree (measured in the first segment) for LDPE/Silica composites with respect to pure LDPE.

Figure 8: Experimental results from compression tests for solid LDPE/Silica nanocomposites.

Figure 9: Improvement (in percentage) in mechanical properties, (elastic modulus and collapse stress) for LDPE/Silica solid nanocomposites with respect to solid pure LDPE: a) Samples with compatibilizer (S-NC), b) Samples without compatibilizer, (S-NS).

Figure 10: Experimental results for elastic modulus and collapse stress for foamed nanocomposites with and without compatibilizer.

Figure 11: Analysis of the presence of synergetic effects between foaming and the addition of silica nanoparticles to LDPE. a) Elastic modulus for foams (F) and solids (S) with compatibilizer, b) Elastic modulus for foams (F) and solids (S) without

compatibilizer, c) Collapse stress for foams (F) and solids (S) with compatibilizer, d) Collapse stress for foams (F) and solids (S) without compatibilizer.

Figure 1
Click here to download high resolution image

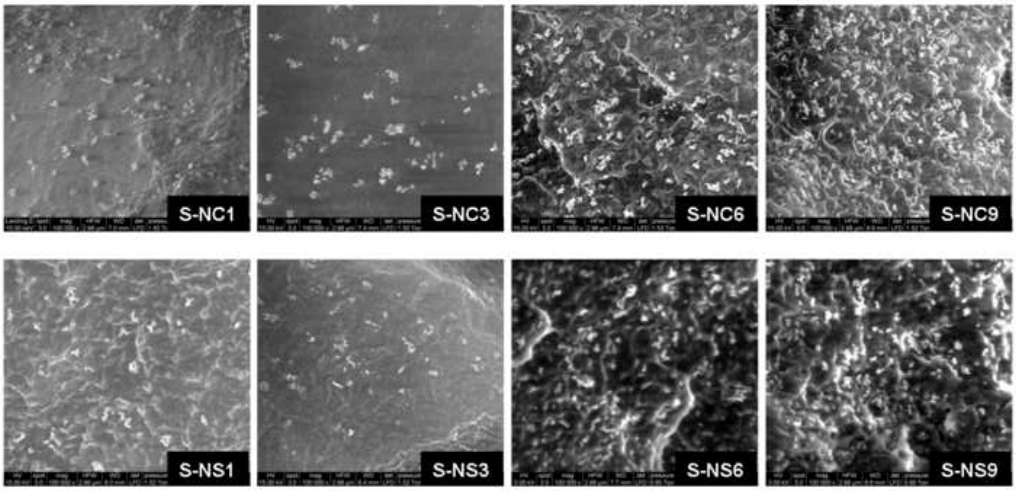

Figure 2
Click here to download high resolution image

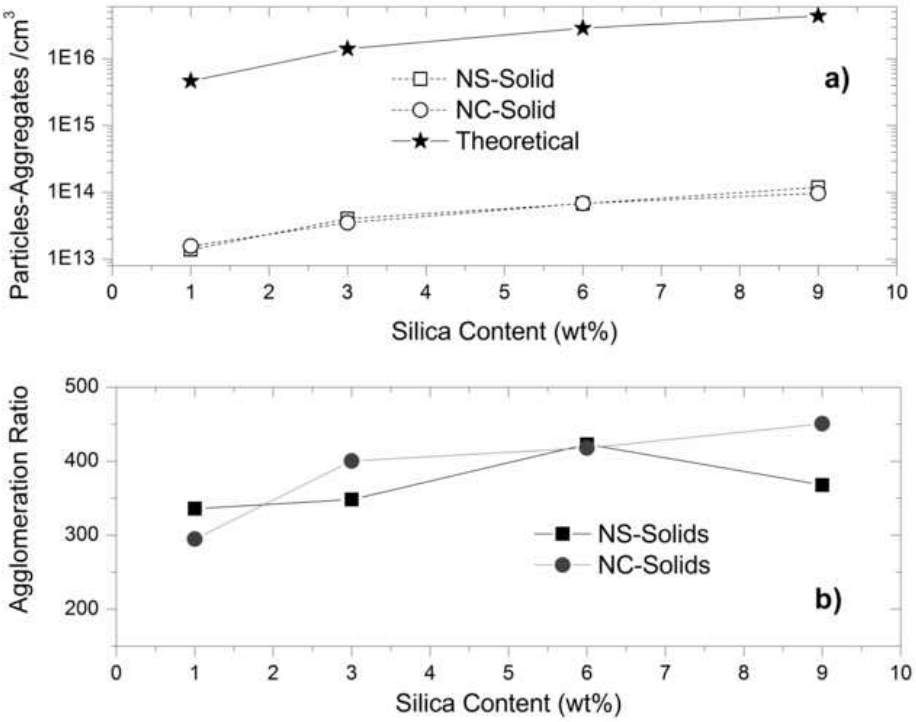

Figure 3
Click here to download high resolution image

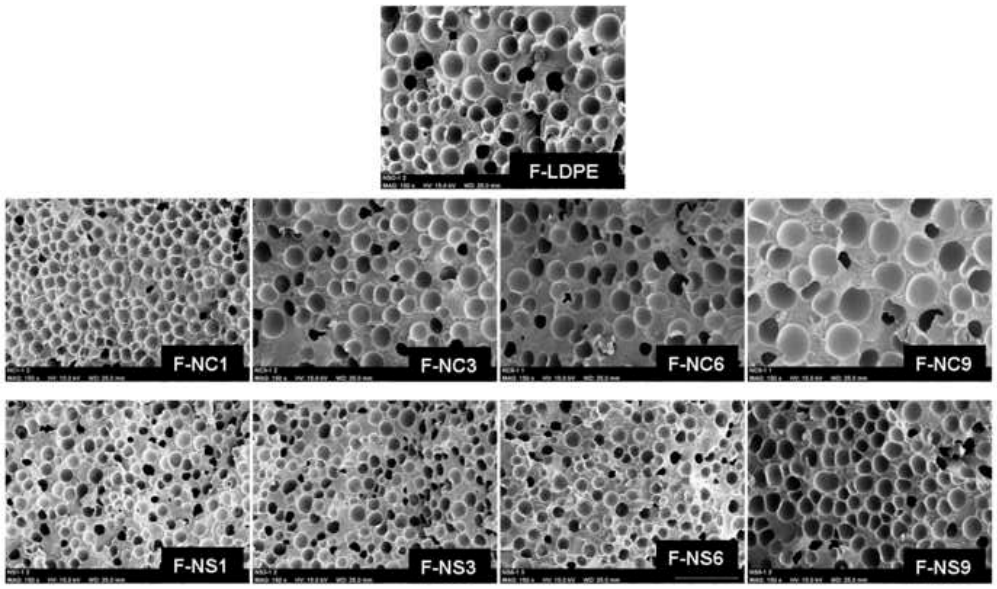

Figure 4 a
Click here to download high resolution image

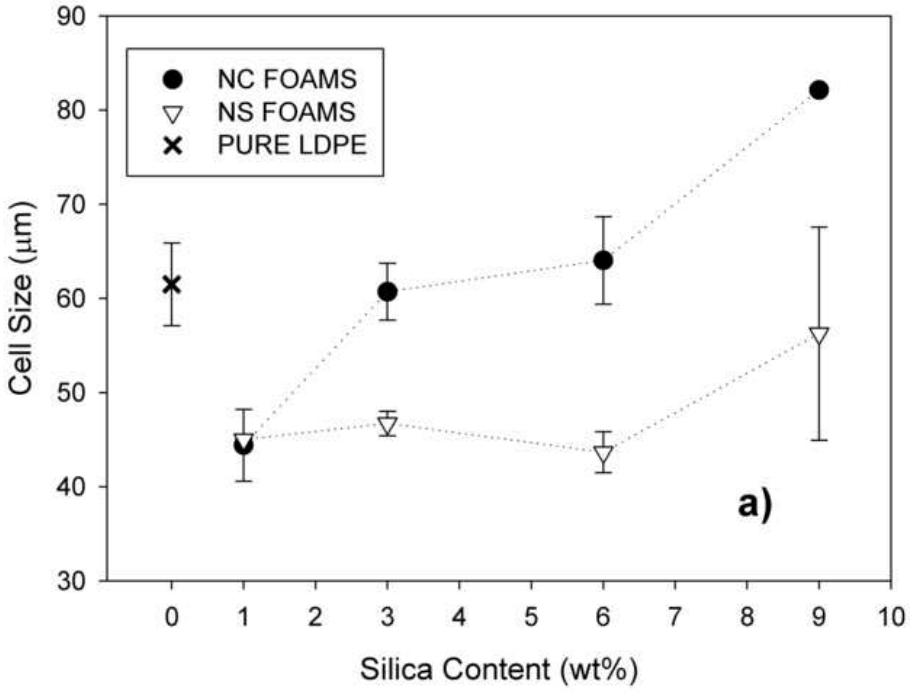

Figure 4b
Click here to download high resolution image

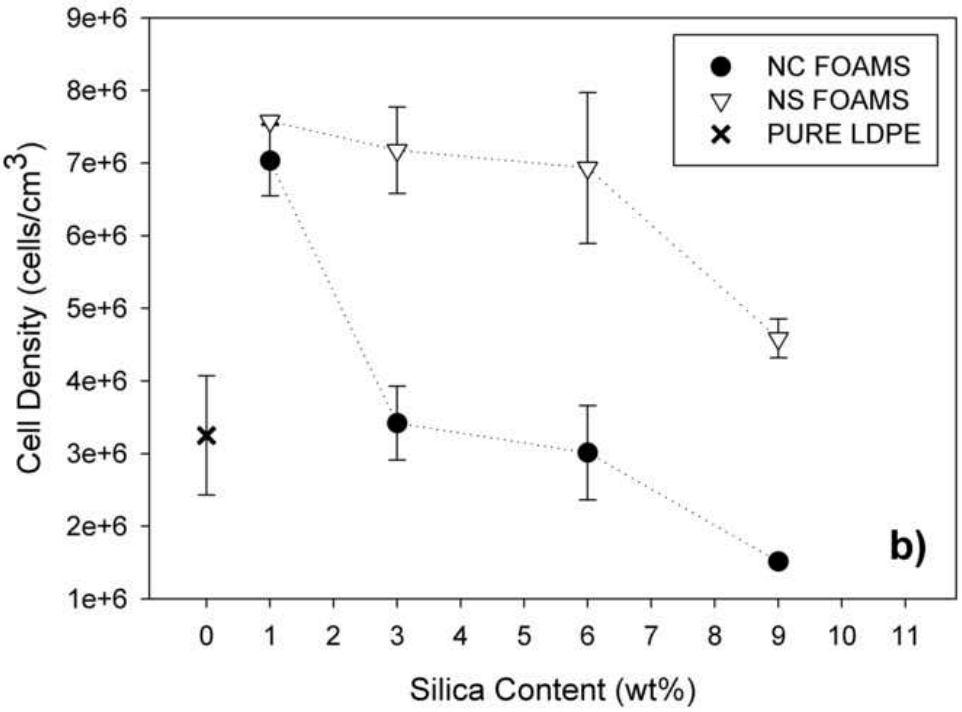

Figure 5a
Click here to download high resolution image

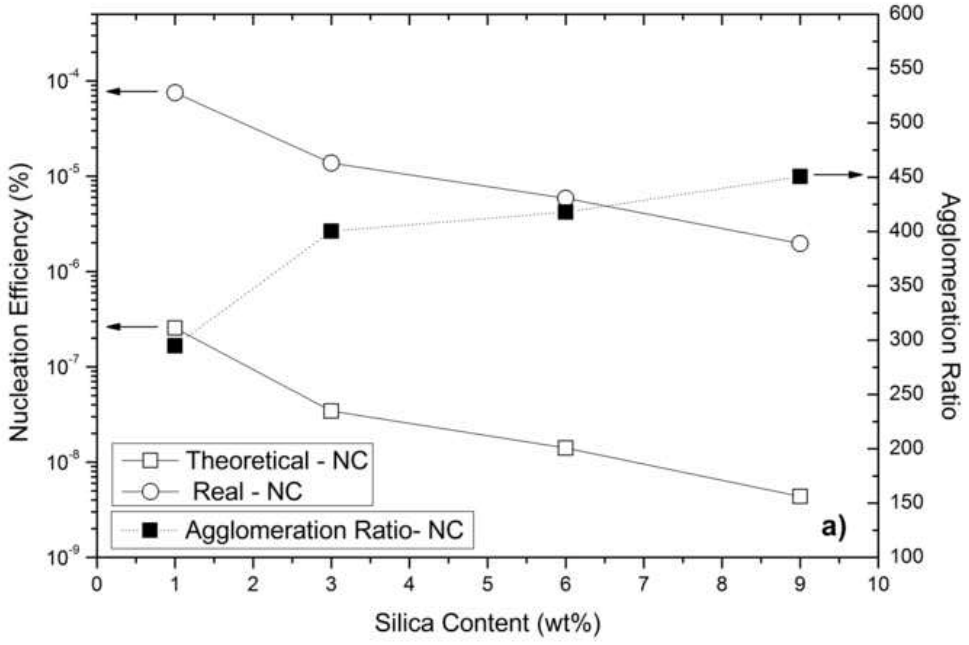

Figure 5b
Click here to download high resolution image

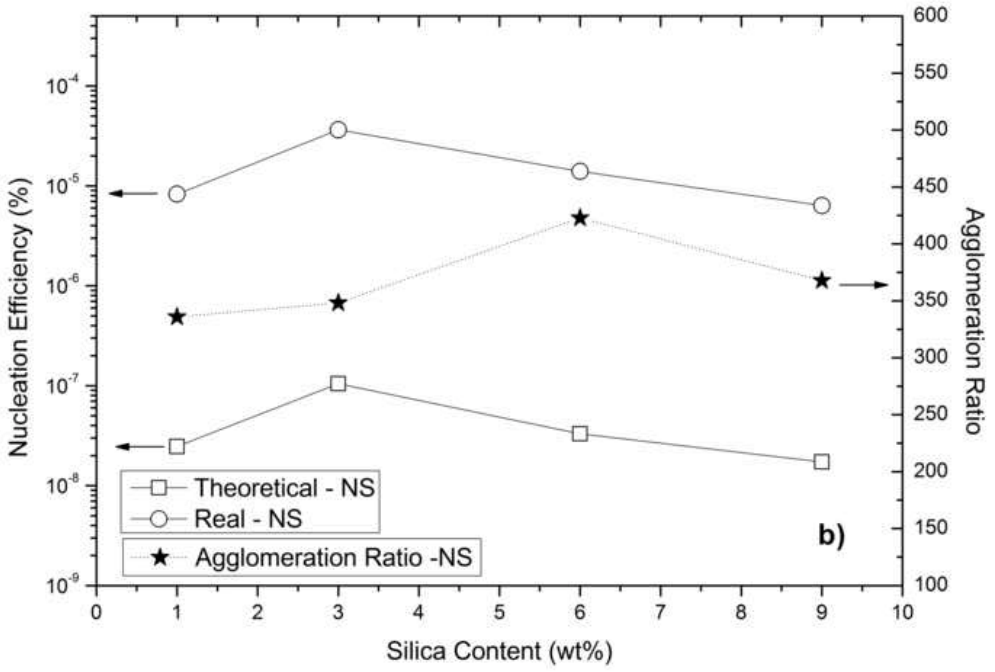

Figure 6
Click here to download high resolution image

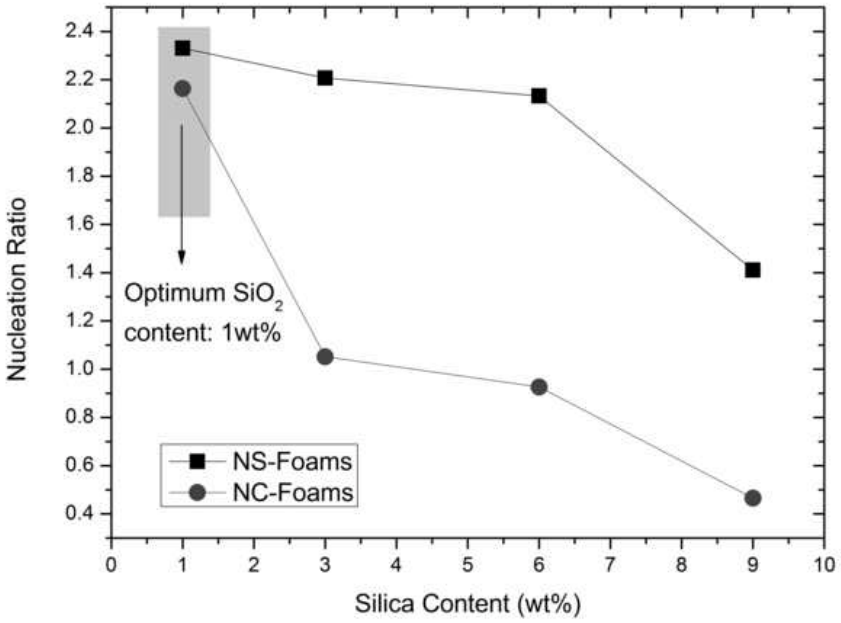

Figure 7
Click here to download high resolution image

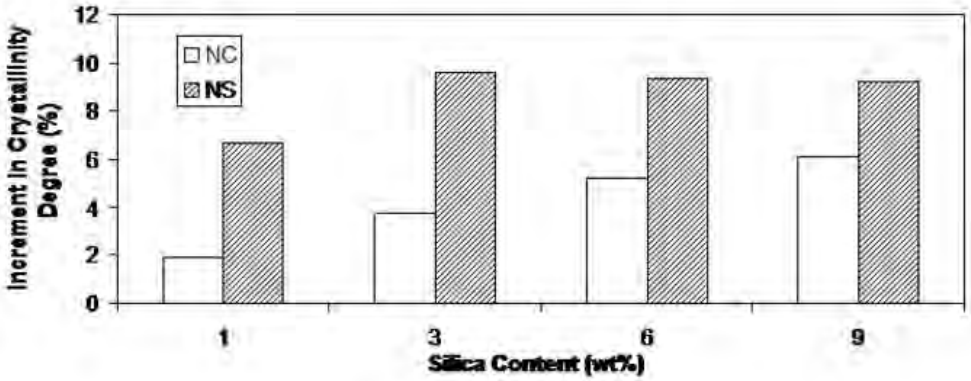

Figure 8
Click here to download high resolution image

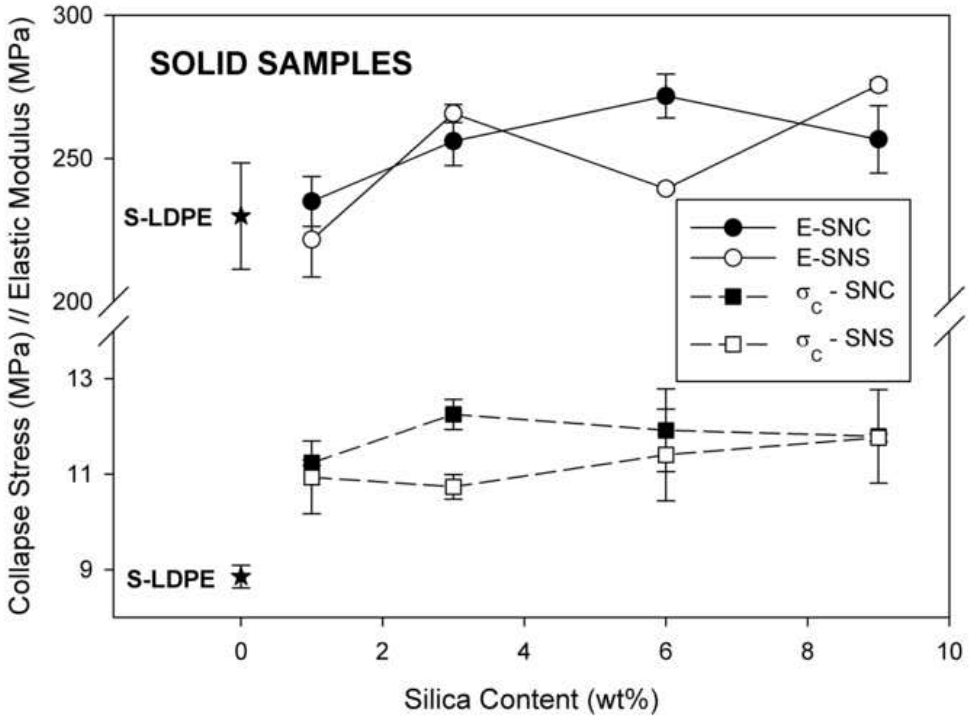

Figure 9
Click here to download high resolution image

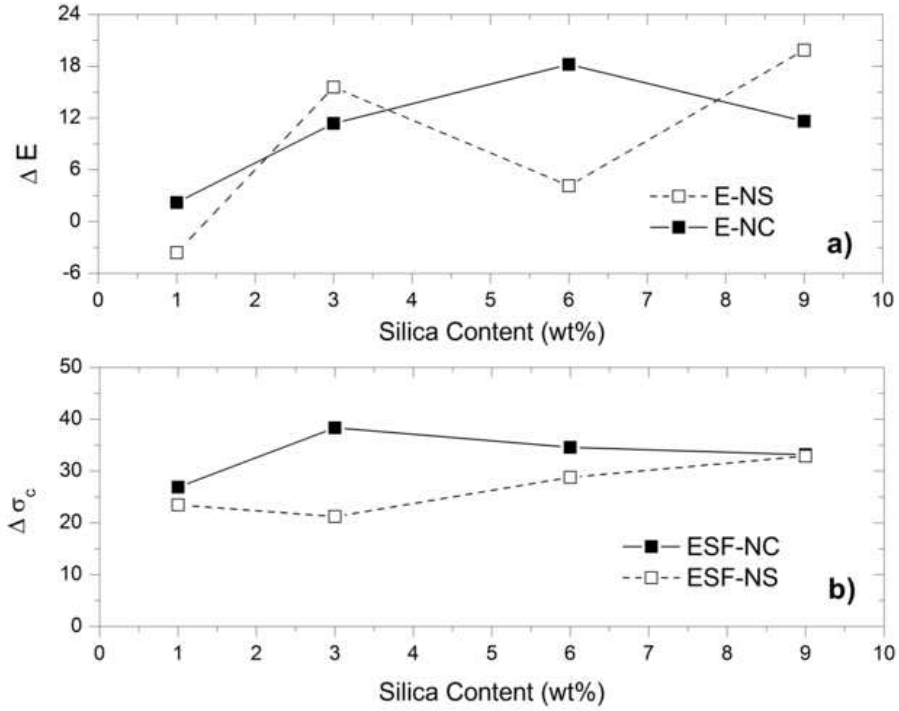

Figure 10
Click here to download high resolution image

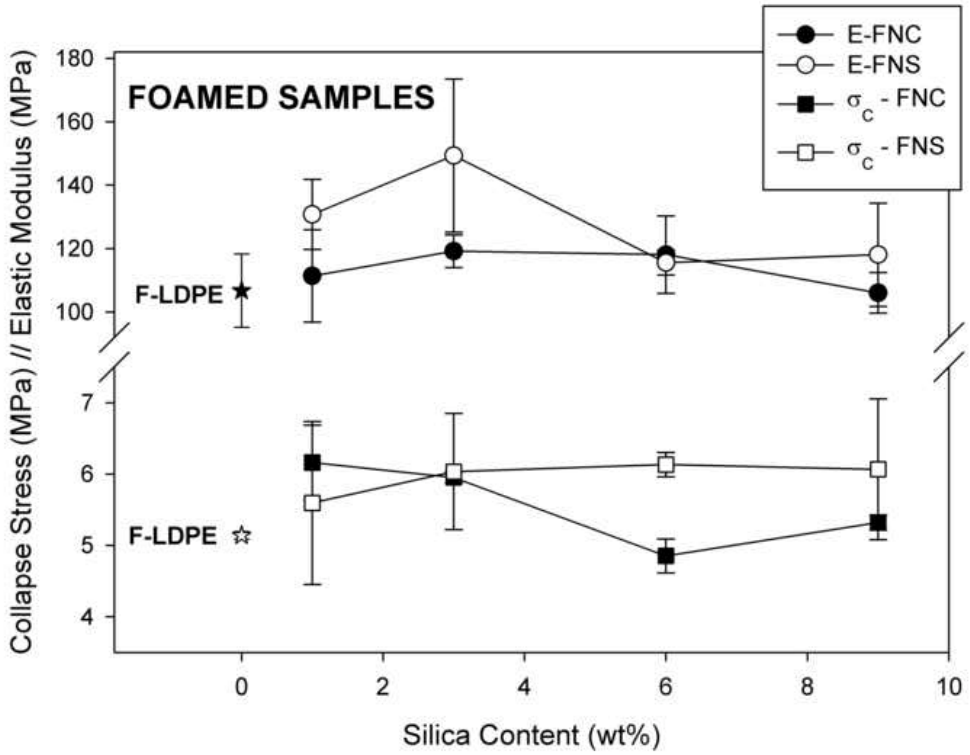

Figure 11 a-b
Click here to download high resolution image

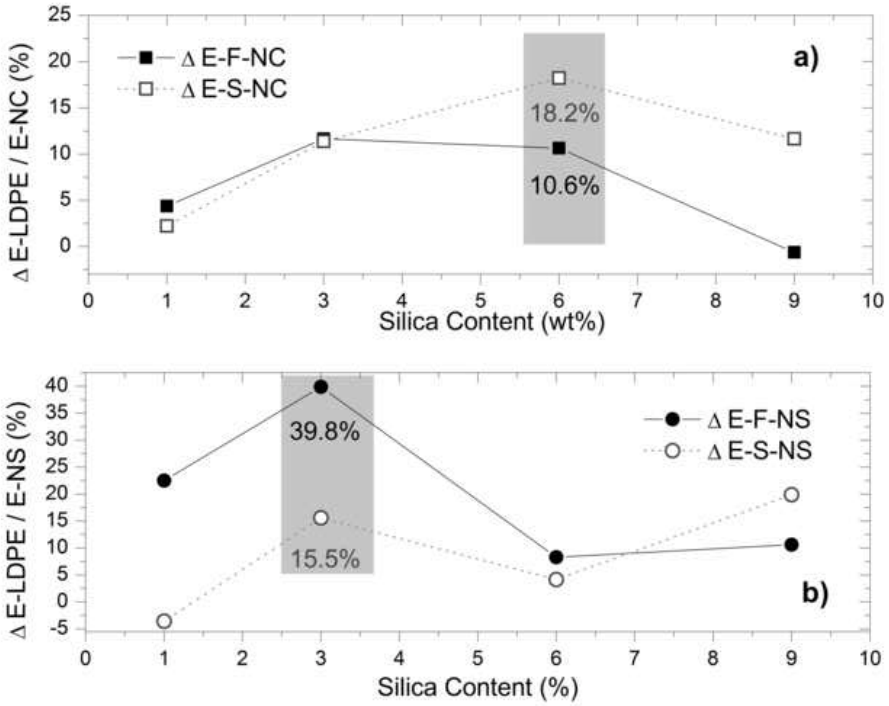

Table 1
Click here to download table: Table 1.doc

	SLDPE	SNC1	SNC3	SNC6	SNC9	SNS1	SNS3	SNS6	SNS9
LDPE	**99.75**	98.62	96.36	92.96	89.6	98.75	96.75	93.75	90.75
SiO_2	**0**	1	3	6	9	1	3	6	9
Coupling Agent	**0**	0.13	0.39	0.79	1.15	0	0	0	0
Stearic Acid	**0.15**	0.15	0.15	0.15	0.15	0.15	0.15	0.15	0.15
Antioxidant	**0.1**	0.1	0.1	0.1	0.1	0.1	0.1	0.1	0.1

Table 1: Chemical composition of LDPE/silica solid nanocomposites, (by weight)

Table 2
Click here to download table: Table 2.doc

Sample	ρ_{solid} (kg/m^3)	Sample	ρ_{foam} (kg/m^3)	Expansion Ratio
S-LDPE	**917.2 ± 3.2**	**F-LDPE**	**586.7 ± 31.2**	**1.56 ± 0.08**
S-NC1	924.8 ± 4.5	F-NC1	624.7 ± 32.7	1.48 ± 0.07
S-NC3	937.2 ± 0.2	F-NC3	582.9 ± 31.7	1.61 ± 0.08
S-NC6	945.5 ± 2.5	F-NC6	561.6 ± 7.2	1.68 ± 0.02
S-NC9	971.5 ± 15.5	F-NC9	563.6 ± 19.1	1.72 ± 0.05
S-NS1	923.4 ± 0.5	F-NS1	649.5 ± 51.0	1.54 ± 0.11
S-NS3	944.1± 1.7	F-NS3	650.5 ± 41.4	1.54 ± 0.09
S-NS6	952.5 ± 1.6	F-NS6	671.9 ± 26.5	1.48 ± 0.05
S-NS9	969.9 ± 1.7	F-NS9	631.1 ± 43.4	1.58 ± 0.11

Table 2: Experimental values of density of foamed and un-foamed nanocomposites and expansion ratio of foamed samples.

Table 3
Click here to download table: Table 3.doc

Sample	*Aggregates/cm³* Solids	*Particles / cm³*	*Aggregation Ratio* Solids
NC1	1.5×10^{13}	4.6×10^{15}	294
NC3	3.5×10^{13}	1.4×10^{15}	400
NC6	6.8×10^{13}	2.8×10^{16}	417
NC9	9.7×10^{13}	4.3×10^{16}	450
NS1	1.3×10^{13}	4.6×10^{15}	335
NS3	4.1×10^{13}	1.4×10^{15}	348
NS6	6.7×10^{13}	2.8×10^{16}	422
NS9	1.2×10^{14}	4.3×10^{16}	367

Table 3: Analysis of dispersion degree of silica particles in the LDPE matrix. (Measured number of aggregates per unit volume, number of particles per unit volume assuming that they are individually dispersed and *Agglomeration Ratio* for NC and NS samples).

Table 4
Click here to download table: Table 4.doc

Sample	1st Segment		2nd Segment		3rd Segment		ΔX_c(%)
	X_c (%)	T_m (°C)	X_c (%)	T_c (°C)	X_c (%)	T_m (°C)	
S-LDPE	43.1	113.5	37.1	96.92	40.9	111.2	-
S-NC1	45.3	115.6	46.2	96.7	45.7	111.8	1.89
S-NC3	46.2	114.8	47.6	97.0	45.5	111.1	3.72
S-NC6	46.8	115.1	50.9	93.3	51.2	112.6	5.25
S-NC9	47.2	115.1	47.2	94.6	48.2	112.5	6.13
S-NS1	45.5	113.4	46.7	96.8	45.9	111.2	6.71
S-NS3	47.2	113.4	45.6	96.8	45.9	111.4	9.62
S-NS6	47.0	114.6	46.5	95.6	47.0	111.4	9.32
S-NS9	47.0	113.7	46.0	93.6	48.2	112.3	9.20

Table 4: Experimental results for crystallinity degree (Xc), melting point (Tm) and crystallization temperature (Tc) for LDPE/silica solid nanocomposites with and without compatibilizer.

Table 5
Click here to download table: Table 5.doc

Sample	T_d (°C)	Δ (%)	Sample	T_d (°C)	Δ (%)
S-LDPE	480.5	-	F-LDPE	476.6	-
S-NC1	479.1	-0.31	F-NC1	485.5	1.87
S-NC3	489.4	1.84	F-NC3	486.6	2.10
S-NC6	490.2	2.01	F-NC6	487.1	2.20
S-NC9	493.6	2.71	F-NC9	488.2	2.42
S-NS1	478.8	-0.36	F-NS1	480.2	0.74
S-NS3	491.4	2.26	F-NS3	485.9	1.94
S-NS6	489.2	1.79	F-NS6	490.4	2.90
S-NS9	494.7	2.94	F-NS9	487.7	2.36

Table 5: Effect of silica nanoparticles in the degradation temperature of LDPE.

Capítulo 5

Obtención de Materiales Celulares con base LDPE Mediante Moldeo por Compresión en Dos Etapas. Adición de Silicatos Laminares.

Al igual que el capítulo anterior, éste se centra en la mejora de las propiedades de materiales celulares con base LDPE mediante la adición de cargas nanométricas. Las diferencias con los trabajos presentados en el capítulo 4 radican por un lado en la *morfología de la nanocarga* utilizada, (*silicato laminar*) y en el tipo de proceso de espumado utilizado para producir los materiales bajo estudio, que en este caso es el *moldeo por compresión en dos etapas*.

La descripción del proceso de producción y posterior caracterización de las propiedades físicas de nanocompuestos espumados basados en polietileno de baja densidad y nanopartículas de hectorita se ha publicado en el **Journal of Applied Polymer Science** bajo el título *"Foams based on Low Density Polyethylene/Hectorite Nanocomposites: Thermal Stability and Thermomechanical Properties"*.

Con este trabajo se intenta mejorar las propiedades de los materiales celulares con base LDPE producidos mediante moldeo por compresión en dos etapas. Por un lado, en ocasiones, las propiedades mecánicas de estos materiales no son suficientes como para dar respuesta a todas las necesidades del mercado y por otro, la estabilidad dimensional de estos materiales es bastante baja debido al alto coeficiente de expansión térmica de las espumas de celda cerrada de LDPE. La adición de nanopartículas de tipo laminar se presenta como una solución a ambos problemas, ya que su alta relación de aspecto y su alto módulo pueden hacer que estos materiales que actúen por un lado como refuerzo nanométrico de las paredes micrométricas y por otro, dado su bajo coeficiente de dilatación térmica, pueden actuar como elementos limitantes de la dilatación del polímero por acción de la temperatura. Al igual que ocurría con las partículas esféricas de sílice, para conseguir todas estas potenciales mejoras es necesario lograr un grado de dispersión y de exfoliación óptimo de las laminillas que conforman las nanopartículas dentro del polímero.

Los materiales bajo estudio se produjeron mediante un proceso convencional de moldeo por compresión en dos etapas reticulando la matriz polimérica con peróxido de dicumilo para así lograr densidades de unos 80kg/m^3, (ER~11). Como agente espumante químico se utilizó azodicarbonamida, (ADC) y se fabricaron muestras con dos porcentajes diferentes de un silicato laminar (hectorita), 3 y 7% en peso. Se incluyó también en la composición química de los materiales un compatibilizante, basado en polietileno de alta densidad funcionalizado con anhídrido maleico, (HDPE-g-MA). Como ya se mencionó en el capítulo anterior, la principal función de este tipo de compuestos es mejorar la interacción entre la matriz polimérica de tipo no polar y la arcilla organomodificada. Además de determinar la densidad y contenido en gel de las muestras, éstas se caracterizaron utilizando diversas técnicas experimentales, (DSC, TGA, SEM, WAXS, DMA y TMA) con el fin de dilucidar los efectos de las nanopartículas tanto en la microestructura del polímero como en las propiedades físicas de los

materiales. Con el fin de realizar un estudio más completo, dichos materiales se caracterizaron en cada una de las tres fases del proceso de fabricación, teniendo así probetas de tipo *preforma* (mezcla de los materiales sin entrecruzar y sin expandir), *pre-espuma*, (material sin entrecruzar pero con un grado de expansión, ER, de en torno a 3) y *espuma*, (material entrecruzado expandido unas 11 veces).

Al igual que en el caso de los nanocompuestos con partículas de tipo esférico, en este estudio se ha intentado fijar el valor de la densidad de los materiales en los dos estadios de expansión de los mismos, de este modo es más sencillo evaluar el papel que juegan las nanopartículas en la microestructura y propiedades de los materiales. La densidad de los materiales pre-espumados está en todos los casos en torno a unos 300-320 kg/m^3 y la de los materiales espumados en torno a unos 80 kg/m^3, aunque para los materiales que contienen el mayor porcentaje de cargas es ligeramente inferior. El contenido en gel de las muestras disminuye a medida que aumenta el porcentaje de nanoarcilla presente en los nanocompuestos espumados

Los experimentos de difracción de rayos X, (WAXS) demostraron que la exfoliación total de las laminillas de la nanoarcilla no se produce durante el proceso de mezclado en fundido sino durante el de expansión del polímero, (es detectada ya en las muestras pre-espumadas). Este resultado puede ser considerado un logro significativo; la separación de las laminillas que forman las nanoarcillas no es una tarea sencilla y raramente se logra la exfoliación completa mediante el proceso de mezclado en fundido. Se puede concluir por tanto que el proceso de espumado puede favorecer la inclusión de la matriz polimérica entre las láminas que forman la nanopartículas, (exfoliación).

No hay cambios significativos en el tamaño de celda de los materiales espumados o en la cristalinidad de la matriz polimérica debidos a la presencia de las partículas de hectorita, (no tienen efecto nucleante). Parece ocurrir en este caso también que la presencia del compatibilizante, (HHPE-g-MA) mitiga el efecto nucleante de las nanopartículas al producir un mayor grado de adhesión entre éstas y la matriz polimérica. Si que se detecta sin embargo un cambio en el grado de cristalinidad del LDPE debido al proceso de espumado. La cristalinidad de la matriz polimérica disminuye a medida que aumenta el grado de expansión del material. En un material celular, el polímero cristaliza en unas condiciones excepcionales, y dado el bajo espesor de la pared celular es lógico que la morfología de la fase cristalina sea muy diferente a la del correspondiente polímero sólido [1-3]. El análisis termogravimétrico muestra que la presencia de las partículas de hectorita mejora la estabilidad térmica de los materiales, aunque el porcentaje de mejora es más significativo en aquellos en los que las laminillas de la nanocarga están completamente exfoliadas, (espumas y pre-espumas).

Las propiedades mecánicas de todos los tipos de materiales se determinaron mediante análisis dinámico-mecánico en compresión, (DMTA). El análisis de los datos correspondientes al módulo de los materiales reveló un incremento en la respuesta mecánica de los mismos debido a la presencia de las nanopartículas. En las curvas obtenidas es posible observar el comportamiento típico de muestras con base LDPE, con una relajación en torno a -20 °C conocida como β, y otra alrededor de 60ºC conocida como α. No se observa desplazamiento de las temperaturas a las que se producen ambas relajaciones debido a la adición de las nanopartículas, aunque sí se puede observar un desplazamiento a mayores temperaturas de la relajación β así como un desplazamiento de la relajación α a menores temperaturas para las muestras espumadas. Estos cambios están asociados a las variaciones de la morfología de las fases cristalina, amorfa e interfase promovidas por el proceso de expansión del material. El espesor lamelar de las muestras no espumadas, (preformas) es mayor que el de las muestras espumadas, (independientemente de la presencia de las cargas) de ahí que se produzca un desplazamiento a mayores temperaturas de la relajación α a medida que aumenta el grado de expansión de los materiales. Por otro lado, la relajación β está asociada al movimiento de cadenas poliméricas presentes en la interfase existente entre la fase amorfa y la fase cristalina del polímero. En las muestras espumadas la cristalinidad es menor que en las no espumadas, por tanto es razonable suponer que la interfase entre ambas fases es mayor y de ahí que dicha relajación se desplace a temperaturas más elevadas.

La estabilidad dimensional de los materiales se determinó mediante análisis termomecánico, (TMA). Los efectos de las nanopartículas se reflejan en un menor porcentaje de expansión térmica en las muestras sólidas que continenen nanocargas. Sin embargo, en las muestras espumadas, no se detecta efecto alguno de las partículas debido a la importante contribución de la expansión de la fase gaseosa de los materiales que enmascara los posibles efectos asociados a la adición de las nanopartículas a la matriz polimérica.

Se puede concluir por tanto, que la adición de nanopartículas de tipo laminar a materiales celulares con base LDPE reticulado en los que se incluye un polímero compatibilizante y producidos mediante moldeo por compresión en dos etapas no induce cambios significativos a nivel microestructural aunque produce mejoras en las propiedades macroscópicas de los materiales (térmicas y mecánicas). El proceso de expansión de los materiales favorece la exfoliación de las laminillas además de inducir cambios en la morfología de la matriz polimérica.

BIBLIOGRAFÍA

[1]. O. Almanza, M.A. Rodríguez-Pérez, B. Chevnev, J.A. de Saja, P. Zipper. Comparative Study on the Lamellar Structure of Polyolefin Foams. European Polymer Journal 41: 599-609, (2005).

[2]. O. Almanza, M.A. Rodríguez-Pérez, J.A. de Saja. The Microstructure of Polyethylene Foams Produced by a Nitrogen Solution Process. Polymer 42: 7117-7126, (2001)

[3]. R. Campo-Arnáiz. Aplicación de Técnicas Espectroscópicas al Estudio de la Morfología Polimérica, Propiedades Térmicas y de Emisión de Espumas de Baja Densidad con Base Poliolefina. Tesis Doctoral, Universidad de Valladolid, (2011).

Foams Based on Low Density Polyethylene/ Hectorite Nanocomposites: Thermal Stability and Thermomechanical Properties

J. I. Velasco,[1] M. Antunes,[1] O. Ayyad,[1] C. Saiz-Arroyo,[2] M. A. Rodríguez-Pérez,[2] F. Hidalgo,[3] J. A. de Saja[2]

[1]*Centre Català del Plàstic, Departament de Ciència dels Materials i Enginyeria Metal·lúrgica, Universitat Politècnica de Catalunya, C/ Colom 114, E-08222 Terrassa, Barcelona, Spain*
[2]*Departamento de Física de la Materia Condensada, Cristalografía y Mineralogía, Facultad de Ciencias, Universidad de Valladolid, 47011 Valladolid, Spain*
[3]*Microcel S.A. Polígono de Villalonquejar, Burgos, Spain*

Received 13 September 2006; accepted 26 December 2006
DOI 10.1002/app.26254
Published online 25 April 2007 in Wiley InterScience (www.interscience.wiley.com).

ABSTRACT: Novel polymer nanocomposite foams made by a two step compression molding method are analyzed in this article. Nanocomposites of low density polyethylene and an organo-modified hectorite were first melt compounded and then foamed using a compression molding method. To study the influence of the presence and the amount of hectorite in both mechanical and thermal properties, samples with 3% and 7% content of hectorite were prepared. Polyethylene crystalline characteristics and thermal stability of the samples were studied by differential scanning calorimetry (DSC) and thermogravimetric analysis (TGA), respectively. Mechanical properties of foams and solid nanocomposites were analyzed by using dynamical mechanical analysis (DMA). Thermal expansion of the samples was analyzed by thermomechanical analysis. The results indicate that the exfoliation of hectorite platelets was achieved after the foaming process, but not during the melt mixing step. Foams with hectorite nanoparticles exhibit improved thermal stability and mechanical properties when compared with neat polymeric foams. © 2007 Wiley Periodicals, Inc. J Appl Polym Sci 105: 1658–1667, 2007

Key words: nanocomposites; polyolefin foams; dynamic mechanical analysis; LDPE

INTRODUCTION

Polymer-layered silicate nanocomposites have recently gained a great deal of attention as they offer new possibilities to provide superior properties when compared with pure polymers and conventional filled composites. The properties include high dimensional stability, high heat deflection temperature, reduced gas permeability, improved flame retardancy, and enhanced mechanical properties.[1,2] Polymer foams, on the other hand, are two-phase materials in which a gas is dispersed in a continuous macromolecular phase. These materials are important items in the economy, and, because of technical, commercial, and environmental issues, they represent an interesting dynamic in 21st century society.[3] However, the foam applications are limited by the inferior mechanical strength, poor surface quality, and low thermal and dimensional stability of these materials in comparison with dense solids.

To improve polymer foams properties, several researchers have focused their attention in how to combine the knowledge on foams and polymer nanocomposites.[1] By using a small amount of clay nanoparticles into the polymer matrix it is possible to obtain a significant improvement in a wide variety of properties. Furthermore, the nanometer dimension of nanoclays is especially beneficial for reinforcing foamed materials, considering the thickness of foam cell walls in the micrometer range. Most efforts related with this kind of experiments have been focused in the production of microcellular foams fabricated using a continuous process and studying the influence of the addition of nanoclays into the polymer matrix, both on foaming process and cellular structure.[4–9]

Shen et al.[4] used carbon nanofibers (CNFs) as nucleating agents to produce polystyrene nanocomposite foams. They obtained microcellular foams with uniform cell size distributions and proved that CNFs improved the nucleation efficiency in the foaming process. Lee et al.[5] investigated the effect of clay particles on the cell morphology of HDPE-clay

Correspondence to: M. A. Rodríguez-Pérez (marrod@fmc.uva.es).
Contract grant sponsor: Junta de Castilla y León, Spanish Ministry of Education and Science; contract grant numbers: VA026/03, MAT 2003-06,797.
Contract grant sponsor: FEDER.

Journal of Applied Polymer Science, Vol. 105, 1658–1667 (2007)

nanocomposite foams produced using a batch foaming process using supercritical CO_2. They demonstrated that in comparison with pure HDPE nanocomposites produced it was obtained much finer and more uniform cellular structures. Nam et al.[6] produced polypropylene/clay nanocomposites foamed in an autoclave in a batch process using supercritical CO_2. They studied the correlation between foam structure and rheological properties of the polypropylene clay composites. Mitsunaga et al.[7] successfully prepared intercalated polycarbonate/clay nanocomposites by using the melt intercalation method in the presence of a compatibilizer. After this, they foamed the nanocomposites using supercritical CO_2 as foaming agent. They obtained a significant improvement in most of the material properties. Reverchon et al.[8] and Zeng et al.[9] reviewed the use of supercritical fluids like CO_2 as foaming agent to produce foams from polymer nanocomposites.

On the other hand, interest in polyolefin nanocomposites has emerged due to their promise of improved performance in packaging and engineering applications. Chemical modification of these resins, in particular the grafting of pendant anhydride groups has been used successfully to overcome problems associated with poor phase adhesion in polyolefin/clay systems.[10] Nevertheless, in most cases using the most common methods to produce polymer nanocomposites the fabrication of polyolefin/clay composites leads to intercalated structures instead of the desired exfoliated ones.[5,10,11–17]

As it was previously mentioned, in most studies related with polymer nanocomposite foams, the solid nanocomposites are foamed using a batch foaming process with supercritical CO_2 as foaming agent. In this article, we introduce a commonly used foaming technique such as compression molding[18,19] using dycumil peroxide as crosslinking agent and azodicarbonamide (ADC) as foaming agent, as a tool to produce exfoliated low density polyethylene (LDPE) nanocomposite foams.[20] One of the main targets of this investigation is to gain knowledge on the effects of hectorite nanoparticles on the structure and physical properties of foamed polyethylene.

MATERIALS

Materials and compounding

At first, a low density polyethylene (LDPE), Stamylan LD 2404A (100.00 phr) (density 0,925 g/cm^3 and MFI 4.2 g/10 min at 190°C and 2.16 kg), manufactured by Sabic Europetrochemicals® (Germany), was compounded using a two-roll mill at a constant temperature of 120°C and constant speed of 60 rpm for no more than 5 min with the following materials

a. Azodicarbonamide (ADC, 18.50 phr) used as chemical blowing agent.
b. Dicumyl peroxide (DCP, 1.70 phr) used as crosslinking agent.
c. Stearic acid (0.11 phr) used as a lubricant.
d. Zinc oxide (0.075 phr) used as ADC activator.

An organic derivative of hectorite (Bentone 108, from Elementis Specialties, UK), chemically modified with dimethyl dehydrogenated tallow ammonium chloride (2M2HT), with a density of 1.7 g/cm^3, basal spacing (d_{001}) of 2.5 nm and an average specific area of 700 m^2/g, was used.

Secondly, a masterbatch was prepared by mixing the powdery hectorite and a compatibilizer polymer at 160°C and 160 rpm in a twin-screw extruder (Collin Kneter 25 × 36D). High density polyethylene grafted with maleic anhydride (Fusabond E MB100D, DuPont), with a density of 0.960 g/cm^3 and MFI of 2 g/10 min at 190°C and 2.16 kg was used as compatibilizer.

Finally, two composites were prepared using the hectorite masterbatch and the previously compounded LDPE: the first one (PE3) with a 3 wt % content of hectorite and the second one (PE7) with a 7 wt % content. The extrudates were water-cooled and pelletized.

Foaming process

Precursor materials for foaming were compression-molded in a hot-plate press (IQAP-LAP PL-15). Pellets were initially placed into a mold (3.5 mm deep and 74 mm in diameter) to slightly overfill it and subjected to heating at 110–115°C for 3 min until melting, followed by a final step at the same temperature and applying a constant pressure of 25 bar for 3 min. The resulting discs were cooled under pressure using recirculating water.

A two-step compression molding foaming process was used for all the studied specimens.[18,19] In the first step (prefoaming), the solid discs were placed in the circular mold and heated at temperatures ranging from 123°C to 140°C applying a constant pressure of 40 bar for 90 min. After this time, the pressure was released allowing the foam to partially grow. The expansion ratio in this prefoaming step was fixed in a value around three. The second step (foaming) consisted of the free expansion of the prefoamed samples at a higher temperature, typically between 140°C and 180°C, for no more than 30 min. An expansion ratio of 11 was set for this second step.

EXPERIMENTAL

Density

Density measurements were performed by Archimedes principle using the density determination kit for the AT261 Mettler balance.

Differential scanning calorimetry

Characteristic thermal properties of the materials were studied by means of a Mettler DSC822^e differential scanning calorimeter, previously calibrated with indium, zinc and *n*-octane. The weights of the samples were 2.5 mg.

To obtain both melting point and crystallinity of the samples the following heating program was chosen:

1st Segment: samples were heated from 30°C to 190°C at a heating rate of 20°C/min under nitrogen atmosphere. To remove the materials thermal history, an isothermal segment, (3 min), was added at the end of this heating segment.

2nd Segment: samples were cooled from 190°C to 30°C at 20°C/min under nitrogen atmosphere.

3rd Segment: after a second isothermal step, (1 min at 30°C), samples were heated a second time at 20°C/min, from 30°C to 190°C also under nitrogen atmosphere.

The melting point was taken at the minimum of the enthalpy-temperature curve. The crystallinity was calculated from the area of the differential scanning calorimetry (DSC) peak, dividing the heat of fusion by the heat of fusion of a 100% crystalline material, (288 J/g for a 100% crystalline polyethylene). In this calculation, a correction was introduced to take into account the real polymer content in each material.

Thermogravimetric analysis

Thermogravimetric analysis was used to determine the effect of addition of clays on the thermal stability of the samples. Tests were performed in a Mettler TGA/SDTA 851^e. Samples were heated from 50°C to 850°C at a heating rate of 20°C/min in nitrogen atmosphere. Samples mass was 5 mg.

Wide-angle X-ray scattering

Wide-angle X-ray scattering (WAXS) was used to analyze to determine the crystallinity of the materials. A Bruker D8 diffractometer with CuKα radiation, λ = 0,154 nm, 50 kV, and 20 mA was used. Scans were taken from 1° to 30° with a rotation step of 0.05° and a step time of 0.007 s.

Microscopy

Cell morphology was analyzed by using SEM. A JEOL JSM-820 scanning electron microscope was used. Samples were previously prepared by cutting 1 cm^2 specimens and making them conductive by sputtering deposition of a thin layer of gold. Nanocomposite morphology was analyzed using a Hitachi H-800 transmission electron microscope, (TEM) on ultra-microtomed sheets with a typical thickness of 60 nm.

Gel content

Crosslinking degree, (gel content), was measured following the ASTM D2765-90 standard. The procedure was as follows; the extraction was made in 400 mL of xylene at 140°C for 24 h, 300 ± 5 mg of material, (initial weight) were used. The remaining material, (gel) was dried for 1 h at 140°C and weighted. Gel content was calculated by using eq. (1) and corrected by using the polymer content present in each sample.

$$\text{Gel content} = 100 \times \frac{\text{gel weight}}{\text{initial weight}} \quad (1)$$

Dynamical–mechanical analysis

The DMA equipment (Perkin–Elmer DMA7) was calibrated according to the recommended procedures using the manufacture's software. The storage modulus, (E′), loss modulus, (E″), and loss tangent or loss factor, (tanδ), were obtained under compression geometry in a parallel plate measurement system for both prefoamed and foamed samples, while the nonfoamed samples were measured using a three point bending system.

All the experiments were performed at 1 Hz frequency, between −50°C and 110°C at a heating rate of 5°C/min. The applied static strain was 2% and it was chosen a dynamic strain of 0.11%.

For prefoamed and foamed samples test specimens were prepared in a cylindrical shape with a diameter of 8 mm and a thickness of 6 mm, approximately. For nonfoamed samples test specimens were bars of 20 mm width, 3.5 mm height, and 4 mm depth.

At least three experiments were carried out for each sample. For prefoamed and foamed samples tests were carried out in the thickness direction of the discs. For nonfoamed samples tests were performed with the applied force parallel to the thickness direction of the discs.

Thermal mechanical analysis

The experiments were performed in a DMA7 from Perkin–Elmer in the TMA mode. A parallel plate measuring system was used, with a plate diameter of 15 mm. For all the samples, cylindrical tests specimens were prepared with a diameter of 8 mm. The experiments were performed without applied force on the sample to measure the thermal expansion coefficient. The materials were studied between −40°C and 150°C at a heating rate of 5°C/min.

TABLE I
Materials Designation, Density, Expansion Ratio, and Gel Content Results

Material	Density (kg/m^3)	Expansion ratio	Gel content, (%)
Nonfoamed 0% Hectorite = NF0	969.2 ± 22.9	–	–
Nonfoamed 3% Hectorite = NF3	953.2 ± 14.0	–	–
Nonfoamed 7% Hectorite = NF7	990.5 ± 2.2	–	–
Prefoamed 0% Hectorite = PF0	289.5 ± 6.5	3.3	–
Prefoamed 3% Hectorite = PF3	315.2 ± 1.3	3.0	–
Prefoamed 7% Hectorite = PF7	341.2 ± 14.4	2.9	–
Foamed 0% Hectorite = F0	84.0 ± 4.4	11.4	35.3
Foamed 3% Hectorite = F3	86.6 ± 5.0	11.0	31.7
Foamed 7% Hectorite = F7	69.7 ± 3.2	14.2	27.8

For each sample at least three tests were carried out. Tests were performed in the same directions as the ones chosen for DMA experiments.

RESULTS AND DISCUSSION

Density and gel content

Table I summarizes the densities, expansion ratio, and gel content of the materials under study. It can be observed that for the same group of samples, (i.e., nonfoamed, prefoamed, and foamed samples) the density values were similar. The expansion ratio, obtained by dividing the density of nonfoamed samples between the densities of the foamed or prefoamed one, reached a value of three for prefoamed samples and 11 for the foamed ones. The main goal of this article is to compare the physical properties of materials with different contents of hectorite, the density and expansion ratio of materials with different hectorite content were keep constant.

As shown in Table I gel content of the foamed materials was slightly reduced when the hectorite was increased.

Micro-structure

It is well known that one of the targets for a successful polymer nanocomposite is to asses the complete exfoliation of the nanoclay into the polymer matrix. In a previous article[20] it was showed by using WAXS that the melt mixing compounding process used to produce the materials of this investigation was not enough to promote a complete exfoliation of the hectorite particles, only achieved during the prefoaming process. This exfoliation was maintained in the foamed samples.

DSC studies of the samples were carried out to study if the polymer crystallinity changed with the addition of nanoclays. DSC results are summarized in Table II. It can be observed that the crystallinity value (obtained on the first heating, cooling, and second heating segments) is not affected by the presence of hectorite, but it is clearly affected by the prefoaming and foaming steps. In general terms, the nonfoamed material has a higher crystallinity than the prefoamed and foamed materials. This result was also confirmed by the crystallinity values calculated by WAXS, (they are also collected in Table II).

The polymer in the foam, crystallizes in exceptional conditions, that is in the presence of a gas and in very thin walls, (these walls are usually thinner than 2 μm, which is smaller than the typical dimensions of the spherulites in a LDPE solid sheet), which has been stretched and crosslinked during foaming. Therefore, it should be expected that the solid polymer in the cell walls could have a different morphology and consequently different properties. Almanza et al.[21] and Rodriguez-Perez et al.[22] have studied this fact for LDPE foams produced by a nitrogen solution process, showing similar trends to those observed in the materials of this article.

The results for melting and crystallization temperatures are also collected in Table II. Differences between composites with different hectorite content and kind of sample are very small. Thus, there are no clear trends for these properties, which seem to be independent on the hectorite content and foaming steps.

TABLE II
DSC Results

	1st Segment		2nd Segment		3rd Segment		
Sample	X_c (%)	T_m (°C)	X_c (%)	T_c (°C)	X_c (%)	T_m (°C)	X_c (%) WAXS
NF0	38.2	113.0	38.8	96.6	36.0	111.7	47.4
PF0	33.9	112.3	35.7	96.0	34.4	111.4	36.7
F0	32.0	110.0	35.1	95.0	32.8	110.4	37.4
NF3	35.5	113.1	36.8	96.6	33.5	111.3	49.0
PF3	33.1	112.0	35.4	96.0	33.8	110.7	38.3
F3	28.7	109.6	31.2	94.8	29.4	110.5	37.0
NF7	36.3	112.0	38.3	95.6	35.9	110.4	45.9
PF7	36.1	111.7	37.1	95.6	35.2	111.1	37.1
F7	29.3	109.8	32.8	94.2	30.9	110.5	37.1

T_m, melting temperature; X_c, crystallinity; T_c crystallization temperature.

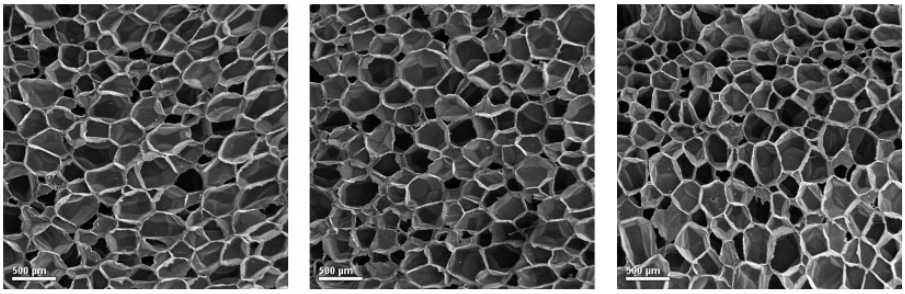

Figure 1 Micrographs of foamed samples: (a) PE0, (b) PE3, (c) PE7.

Other important aspect that has to be considered when foamed materials are analyzed is the cellular structure. Micrographs of foamed samples can be seen in Figure 1(a–c). A closed cell cellular structure characterized all the produced materials. Cell size was ~ 200 μm for all the studied foams. No significant differences in the cellular structure of samples with and without hectorite were found. Therefore, it has been concluded that hectorite nanoparticles did not play role as nucleating agents in the foaming behavior of these materials.[20]

Figure 2 shows a typical TEM picture of a foamed sample. The nanocomposite consisted of mixed dispersed individual hectorite and stacks of hectorite platelets. Foaming agent decomposition residues were also present in the form of regular particles of typical size 50 nm.

Thermal behavior

Thermogravimetric analysis

Thermograms corresponding to foamed samples are presented in Figure 3. Results corresponding to weight loss on each step and residues content are collected in Table III.

First and second steps in all the thermograms can be associated with the decomposition of foaming agent, additives, and residues of foaming agent. Third step is associated to the decomposition of the polymer matrix. Weight loss on each step for all the samples does not show significant differences (Table III). The used nanoclay, is organically modified, so approximately only the half hectorite content will appear in the residues, (the organic part decomposes during the experiment). The amount of residues increased as hectorite content increased. In this sense, if we take into account the amount of residues of samples without hectorite and subtract it from the amount of residues of samples with hectorite, the result is in agreement with the amount of hectorite that should remain after the decomposition of the organic part of the nanoparticle.

Generally, the incorporation of clay into the polymer matrix has been found to enhance thermal stability by acting as a superior insulator and mass transport barrier to the volatile products generated during decomposition.[2] The clay acts as a heat barrier, which enhances the overall thermal stability of the system, as well as assist in the formation of char after thermal decomposition. In the early stages of thermal decompositions the clay would shift the decomposition to higher temperature. Thermogravimetric studies of the samples were carried out to study if the previous effects showed in our materials.

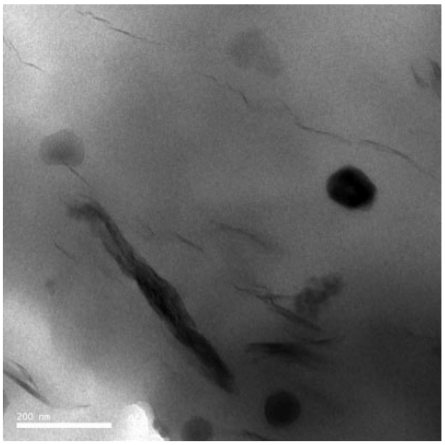

Figure 2 Typical TEM image for a foamed composite.

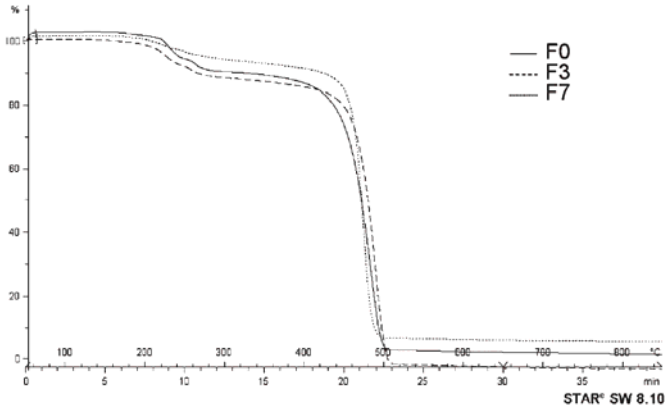

Figure 3 Thermograms of foamed samples.

It can be observed that the addition of nanoclays combined with the foaming improves thermal stability of the samples (an increase of 8°C was detected) (Fig. 3). In the case of solid materials and prefoamed materials this improvement is not so clear in the experimental data (improvement of 3°C for solid materials and no improvement for prefoamed materials). It has been previously explained that the best exfoliation is obtained after foaming the materials, this could be one of the reasons that justify why after foaming the thermal stability was improved in a higher extend.

Dynamic mechanical analysis

The experimental results corresponding to DMA tests of foamed and nonfoamed samples are shown in Figures 4 and 5. The storage modulus, (E′) and loss factor, (tanδ), are plotted as a function of temperature.

For both kinds of materials, it can be observed how all the curves present the typical DMA behavior of LDPE with the presence of β and α relaxations. The presence of hectorite can be detected in the storage modulus curve for both nonfoamed and foamed samples. As it can be observed, storage modulus increases as the hectorite weight content increases. This difference is more evident for the material with 7% weight content.

To partially eliminate the density differences between samples, the reduced specific storage modulus (i.e., storage modulus divided by the density of each sample) obtained at room temperature, was calculated. The value for the material without nanofiller was 3.5×10^4 Nm/kg, this value increased to a value of 1.5×10^5 for the material with a 7% filler content. Therefore, for foamed samples, mechanical properties of the material are clearly improved with the addition of 7% of nanoclays.

Relaxations of LDPE have been widely studied. At low temperatures, (around −20°C), β relaxation

TABLE III
TGA Results

	1st Step		2nd Step		3rd Step			
Sample	% w.1.	T (°C)	% w.1.	T (°C)	% w.1.	T (°C)	% Residues	T_{onset} (°C)
NF0	9.02	228.4	5.29	239.9	85.97	489.5	0.94	460.21
PF0	8.95	230.3	4.14	240.3	86.67	489.8	0.97	460.25
F0	7.08	232.3	4.84	240.4	88.72	486.4	1.26	456.50
NF3	8.02	229.3	3.79	239.8	87.45	475.1	2.28	462.08
PF3	7.14	229.9	3.18	259.9	88.95	474.1	2.02	459.84
F3	5.95	230.9	4.09	260.4	91.71	482.2	2.70	461.61
NF7	7.70	227.3	2.84	239.7	86.65	467.6	3.76	463.13
PF7	7.27	223.1	3.09	256.5	87.29	467.8	4.37	460.24
F7	4.18	227.3	2.44	254.1	89.07	477.7	5.13	464.67

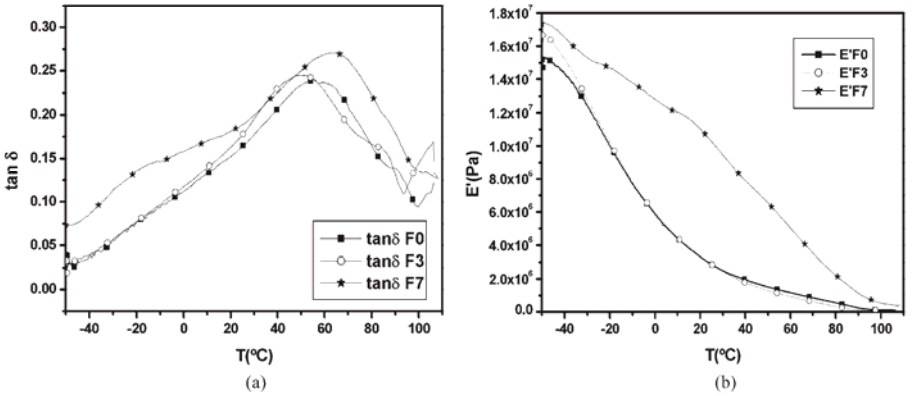

Figure 4 (a) Tanδ versus temperature for foamed samples, and (b) storage modulus versus temperature for foamed samples.

appears, and can be detected as a shoulder in the tanδ curve or as a peak in the loss modulus curve. In nonfoamed polyethylene, this relaxation results from motions of chain units located in the interfacial region and its existence is not universal in the different types of polyethylene, being conditioned by the presence of an interfacial content higher than about 7%. The α relaxation can be seen at higher temperatures, (between 30°C and 120°C).[23] It can be detected as a wide peak in the tanδ curve or a shoulder in the loss modulus curve. The α relaxation has been associated with the crystalline part of the polymer. In fact the position of the relaxation is controlled by the thickness of the lamellae.[23]

In the obtained DMA results α and β relaxations can be observed in the above described way for all the studied samples. In Table IV the temperatures at which α and β relaxations appear are summarized. It can be observed how β relaxation appears at higher temperatures for foamed samples than for nonfoamed samples and prefoamed samples. α-Relaxation appears at lower temperatures for foamed samples than for the other studied samples. The hectorite content seems not to have a significant effect on the shifting and intensity of the relaxations.

It was previously mentioned, that crystallinity values were affected by foaming process and not by hectorite content. Therefore one possible explanation

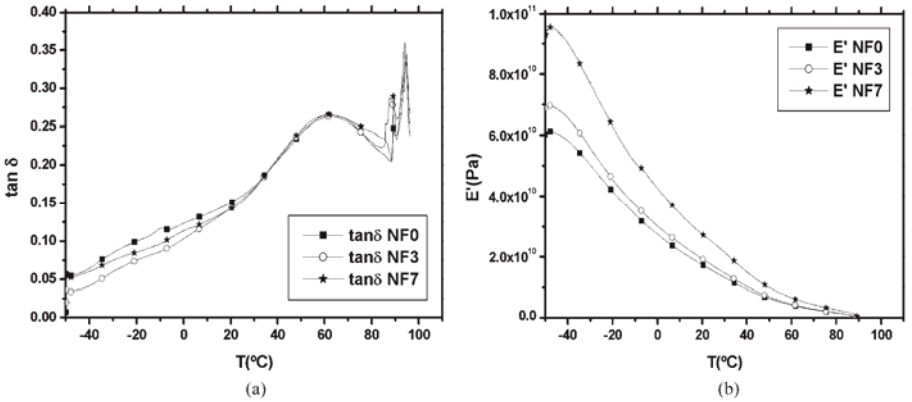

Figure 5 (a) Tanδ versus temperature for nonfoamed samples, and (b) storage modulus versus temperature for nonfoamed samples.

TABLE IV
Temperature and Intensity of α and β Relaxations Detected in the Tanδ Curve

Sample	T_β (°C)	tanδ (β)	T_α (°C)	tanδ (α)
F0	−20.44	0.074	55.41	0.23
F3	−19.83	0.077	49.67	0.24
F7	−17.04	0.140	63.39	0.27
PF0	−20.12	0.048	65.63	0.24
PF3	−20.64	0.054	64.23	0.21
PF7	−20.71	0.078	64.23	0.22
NF0	−28.15	0.088	62.52	0.26
NF3	−26.23	0.066	63.26	0.26
NF7	−29.99	0.074	62.02	0.26

of the relaxation shifting would be related with the different polymer morphology of the different materials. To prove if the thickness of the lamellae for foamed samples was smaller than that of nonfoamed samples, the thickness of lamellae for both kinds of samples were calculated using the model given by Alberola et al. using the DSC data.[24] In Figure 6(a–c), the distribution of lamellae thickness is presented for nonfoamed and foamed samples with different hectorite content. It can be observed that in all cases lamellae thickness is larger for nonfoamed samples than for foamed samples. This should be the reason of the displacement of α-relaxation to higher temperatures for nonfoamed samples.

On the other hand, foamed samples are the ones with lower crystallinity value and consequently with higher interfacial content between crystalline and amorphous phase, which would explain that β relaxation is displaced to higher temperatures for these materials, and particularly for F7 sample in which

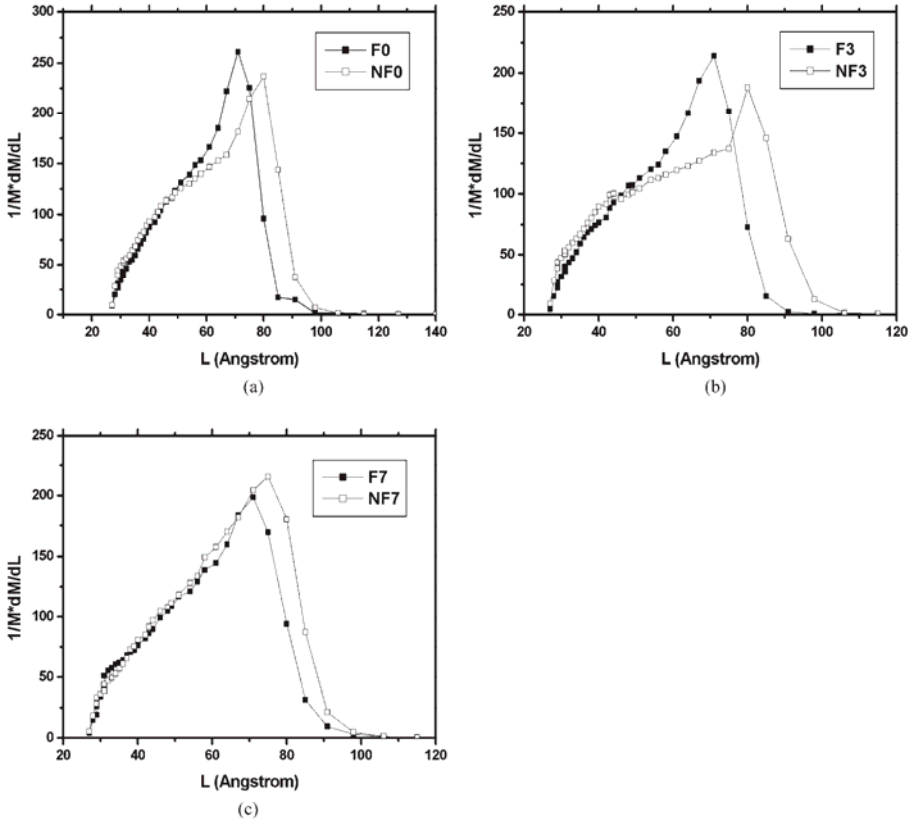

Figure 6 Distribution of lamellar thickness for both nonfoamed and foamed samples.

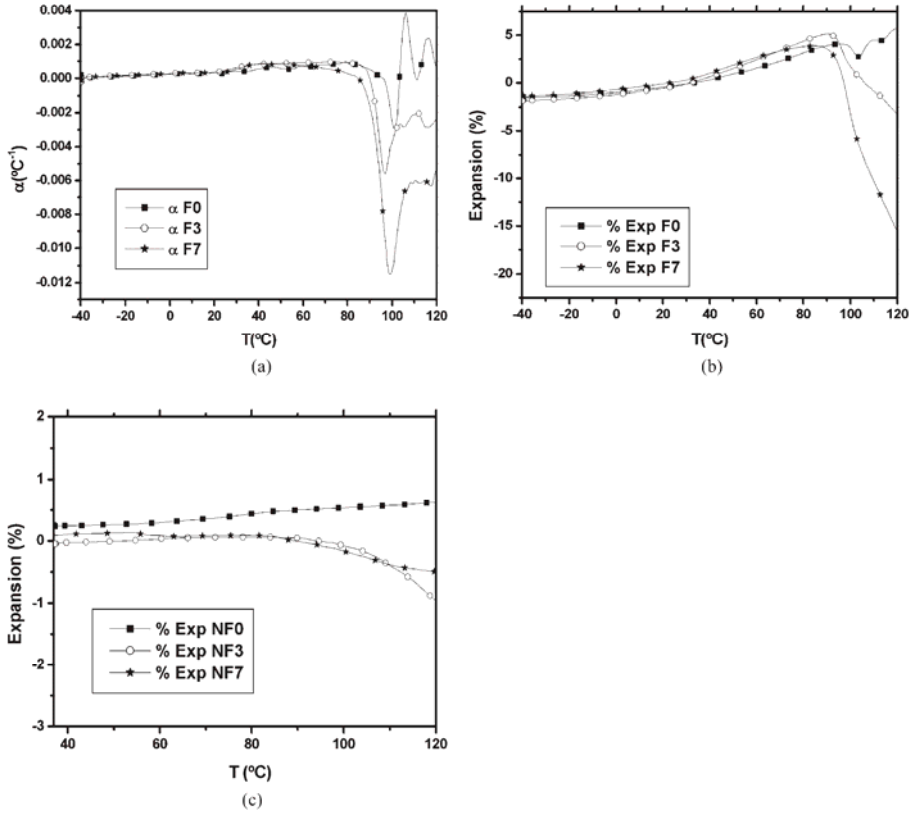

Figure 7 (a) Linear thermal expansion coefficient of foamed samples versus temperature, (b) percentage of expansion of foamed samples versus temperature, and (c) percentage of volumetric expansion of nonfoamed samples versus temperature.

the hectorite nanoparticle/polyethylene interface would be affecting.

Thermomechanical analysis

It is known that the addition of fillers or reinforcing agents into plastics mitigates to some degree the high thermal expansion of these materials by two different mechanisms: (a) volume dilution with a material of lower coefficient of thermal expansion, and (b) mechanical constraint by a dispersed phase with low coefficient of thermal expansion and higher modulus.

Polymer nanocomposites made by exfoliating the typical 1 nm thick aluminosilicate platelets of the clay-mineral, offer exciting possibilities for resolving the problem of the high thermal expansion coefficient that polymers posses. These nanoclays platelets have a high modulus and high aspect ratios for effective reinforcement and mechanical restraint of thermal expansion.[25]

The percentage of material expansion was calculated as follows:

$$\frac{l_i - l_0}{l_0} \times 100 \qquad (2)$$

where l_0 is the initial height of the sample and l_i is the height of the sample at a temperature T_i.

In Figure 7(a) linear thermal expansion coefficient corresponding to foamed samples is represented as a function of temperature, and in Figure 7(b) the per-

centage of material expansion is represented also as a function of temperature for the same kind of materials. It can be observed that there are no significant differences in the behavior of the samples with and without hectorite. The percentage of expansion for the foamed samples is almost the same in all cases. Therefore, the expected reduction of thermal expansion was not found in the foamed materials. The percentage of volumetric expansion of nonfoamed samples is represented as a function of temperature in Figure 7(c). As it was expected for the solid nanocomposites the presence of hectorite reduces the expansion of the material. However, this effect is not observed in the foamed materials.

Previous articles[26,27] on the thermal expansion of closed cell polyolefin based foams have showed that in addition to the contribution of the thermal expansion of the polymeric matrix there is an additional effect related with the expansion of the gas when the temperature increases. Therefore, the expected differences for the foams due to the polymer constraint by the hectorite platelets seem to be compensated in the samples under study by the expansion effect of the gas in the foamed materials.

CONCLUSIONS

As it has been established with this study the compression molding method can be an interesting tool in the production of polyolefin nanocomposite foams. From a practical point of view, with the procedure carried-out; there is no need for a complete exfoliation of the nanoclay in the compounding step. The exfoliation will occur during foaming.

Both thermal and mechanical properties of LDPE foams were improved because of the hectorite nanoplatelets. Thermal stability of the samples was enhanced for foamed samples; this is, when the exfoliation of the nanoclay is complete. On the other hand, mechanical properties were improved in both cases, when the nanoclay is intercalated, (nonfoamed samples) and when the nanoclay is exfoliated, (foamed samples). This effect was especially significant for the foamed sample with a 7% content of nanoclay. It was proved that crystallinity degree of the samples was not affected by the presence of hectorite but it was affected by the foaming process because of the different crystallization conditions of the polymer in the foams and in the solid nanocomposites. The different polymer morphology in the foamed materials also affected the position of the relaxations detected in the DMA tests.

References

1. Lee, J. L.; Zeng, C.; Cao, X.; Han, X.; Shen, J.; Xu, G. Compos Sci Technol 2005, 65, 2344.
2. Ray, S. S.; Okamoto, M. Prog Polym Sci 2003, 28, 1539.
3. Rodríguez-Pérez, M. A. Adv Polym Sci 2005, 184, 97.
4. Shen, J.; Zeng, C.; Lee, L. J. Polymer 2005, 46, 5218.
5. Lee, Y. H.; Park, C. B.; Wang, K. H. J Cell Plast 2005, 41, 487.
6. Nam, P. H.; Maiti, P.; Okamoto, M.; Kotaka, T.; Hasegawa, N.; Usuki, A. Polym Eng Sci 2002, 42, 1907.
7. Mitsunaga, M.; Ito, Y.; Ray, S. S.; Okamoto, M.; Hironaka, K. Macromol Mater Eng 2003, 288, 543.
8. Reverchon, E.; Volpe, M. C.; Caputo, G. Curr Opin Solid State Mater Sci 2003, 7, 391.
9. Zeng, C.; Ha, X.; Lee, L. J.; Koeling, K. W.; Tomasko, D. L. Adv Mater 2003, 20, 1743.
10. Gopakumar, T. G.; Lee, J. A.; Kontopoulou, M. Polymer 2002, 43, 5483.
11. Morawiec, J.; Pawlak, A.; Slouf, M.; Galeski, A.; Piorkowska, E.; Krasnikowa, N. Eur Polym J 2005, 41, 1115.
12. Zanetti, M.; Bracco, P.; Costa, L. Polym Degrad Stabil 2004, 85, 657.
13. Wang, K. H.; Choi, M. H.; Koo, C. M.; Xu, M.; Chung, I. J.; Jong, M. C.; Choi, S. W.; Song, H. H. J Polym Sci Part B: Polym Phys 2002, 40, 1454.
14. Alexandre, M.; Dubois, P.; Sun, T.; Garres, J. M.; Jérôme, R. Polymer 2002, 43, 2123.
15. Wang, K. H.; Choi, M. H.; Koo, C. M.; Choi, Y. S.; Chung, I. J. Polymer 2001, 42, 9819.
16. Kato, M.; Okamoto, H.; Hasegawa, N.; Tsukigase, A.; Usuki, A. Polym Eng Sci 2003, 43, 1312.
17. Liang, G.; Xu, J.; Bao, S.; Xu, W. J Appl Polym Sci 2004, 91, 3974.
18. Park, C. P. Handbook of Polymeric Foams; Klempner, D., Frisch, C., Eds.; Hanser Publishers: New York, 1991.
19. Puri, R. R.; Collington, K. T. Cell Polym 1988, 7, 219.
20. Velasco, J. I.; Antunes, M.; Ayyad, O.; López-Cuesta, J. M.; Gaudon, P.; Saiz-Arroyo, C.; Rodríguez-Pérez, M. A.; De Saja, J. A. Polymer, to appear.
21. Almanza, O.; Rodríguez-Pérez, M. A.; de Saja, J. A. Polymer 2001, 42, 7117.
22. Rodríguez-Pérez, M. A.; de Saja, J. A. J Macromol Sci Phys 2002, 41, 761.
23. Popli, P.; Glotin, M.; Mandelkern, L.; Benson, R. S. J Polym Sci Part B: Polym Phys 1984, 22, 407.
24. Alberola, N.; Cavaille, J. Y.; Pérez, J. J Polym Sci Part B: Polym Phys 1990, 28, 569.
25. Lee, H.; Fasulo, P. D.; Rodgers, W. R.; Paul, D. R. Polymer 2006, 47, 3528.
26. Rodríguez-Pérez, M. A.; Alonso, O.; Duijsens, A.; de Saja, J. A. J Polym Sci Part B: Polym Phys 1988, 36, 2587.
27. Almanza, O. A.; Masso-Moreu, Y.; Mills, N. J.; Rodríguez-Pérez, M. A. J Polym Sci Part B: Polym Phys 2004, 42, 3741.

Capítulo 6

Obtención de Materiales Celulares con base Polipropileno Mediante Moldeo por Compresión Mejorado

Este capítulo incluye la descripción y caracterización de materiales celulares con base polipropileno producidos utilizando el proceso de moldeo por compresión mejorado, (ICM) descrito en el capítulo 3 de esta memoria. Se incluyen dos trabajos, el primero de ellos titulado "*An Alternative Foaming Route to Produce Non-Crosslinked Thermoplastic Foams with Controlled Density and Cellular Structure*" ha sido enviado a la revista **Macromolecular Materials and Engineering** y el segundo titulado *"Structuture-Properties Relationship of Medium Density Polypropylene Foams"* y que ha sido enviado a la revista **Polymer International**.

El primer artículo, tal y como indica el título del mismo, se centra en la descripción del proceso de moldeo por compresión mejorado y para facilitar la compresión del mismo, se detallan los parámetros y condiciones de procesado utilizados para producir muestras con base polipropileno con dos geometrías diferentes, (discos y cilindros). Se han utilizado además diferentes porcentajes (1, 5, 10 y 15 % en peso) de un agente espumante químico, (azodicarbonamida, ADC) para producir materiales celulares con tres grados diferentes de expansión, (1.6, 2 y 3). Así es posible analizar la influencia de la composición química, de la densidad y de los parámetros de proceso tanto en la estructura celular como en la respuesta mecánica de discos y cilindros de PP producidos mediante la ruta ICM.

Se mencionó en el capítulo 3 que el proceso de moldeo por compresión mejorado permite producir materiales celulares en un amplio rango de densidad sin necesidad de entrecruzar la matriz polimérica. En estos estudios además, se ha utilizado un grado de polipropileno lineal (copolímero *random*) con un índice de fluidez (MFI) de 10g/min (medido a 230 ºC y 2.16 kg), que exhibe un comportamiento lineal de la viscosidad extensional en la zona de altas deformaciones, (es decir no presenta *strain hardening*). Tampoco han sido añadidos agentes nucleantes o cargas que aumenten la viscosidad del polímero y que por tanto favorezcan el proceso de nucleación y estabilización de la estructura celular. La razón principal para elegir este polímero no adecuado para procesos de espumado es analizar de forma más realista la influencia de la composición química y los parámetros de proceso en el tipo de estructura celular que se obtiene, ya que dicha influencia es mayor que en polímeros con mejores características para espumado, (como por ejemplo polímeros ramificados).

Dado que el objetivo principal de este primer trabajo es describir la ruta ICM, se ha incluido un análisis de los parámetros de proceso utilizados para producir los dos tipos de muestras, (discos y cilindros). Como para cada una de las geometrías la presión inicial aplicada (P_0) es significativamente diferente la evolución hasta la presión de espumado, (P_F) también lo es. Para los cilindros la presión inicial aplicada es menor y por tanto es posible apreciar un aumento lineal de P_F con el aumento en la concentración de agente espumante; sin embargo, para los cilindros, la elevada presión

inicial (P_0) hace que el aumento en la cantidad de azodicarbonamida no se refleje de forma evidente en los valores que alcanza P_F. El tiempo de espumado, (t_F) es ligeramente superior para las muestras cilíndricas, y respecto al efecto de la densidad, no se ha encontrado ninguna dependencia de los parámetros de proceso en relación a la misma. Con el fin de analizar la bondad del procedimiento en términos del control de la densidad de las piezas espumadas, se muestran los valores medios de la densidad y el grado de expansión de cada uno de los materiales así como el valor de %D, (definido en el capítulo 3). En general el control de la densidad de los materiales es bastante bueno, excepto quizá cuando se utilizan cantidades muy elevadas de agente espumante (10 o 15 %), donde el exceso de presión en el interior del molde puede producir pequeños escapes de material.

Tanto la densidad como el porcentaje de azodicarbonamida utilizado tienen una gran influencia en las características de la estructura celular de los materiales. Por un lado, al aumentar ambos, densidad y concentración de ADC, el tamaño de celda disminuye y la densidad celular aumenta. En términos de homogeneidad de la estructura, (distribución de tamaños de celda), se observa que para cualquiera de las densidades analizadas, la utilización de altos porcentajes de agente espumante promueve la obtención de estructuras celulares con distribuciones de tamaños de celda más homogéneas. Dada la gran influencia del contenido de celdas abiertas en la respuesta macroscópica de los materiales celulares, éste ha sido medido para todos los materiales utilizados. Para muestras de baja densidad, (ER=3), el contenido de celdas abiertas no depende del porcentaje de azodicarbonamida. Al someter al polímero a mayores ratios de estirado, las paredes de las celdillas se vuelven más finas y más propensas a las rupturas. Por otro lado a densidades mayores (ER=1.6 y ER= 2), a medida que aumenta la cantidad de agente espumante también aumenta el porcentaje de celdas abiertas debido a un exceso de presión dentro del sistema cuando se produce el llenado de la cavidad del molde.

Las propiedades mecánicas de los materiales se han medido utilizando diferentes configuraciones, (compresión, tracción y flexión). En este caso el análisis de la respuesta mecánica de los materiales se ha llevado a cabo estudiando las propiedades relativas de los mismos, (propiedad del material celular dividida entre la del sólido correspondiente). Se ha calculado el valor del parámetro *n* (ver capítulo 1) para el módulo medido en cada una de las configuraciones y para parámetros característicos de la zona de colapso plástico. Los resultados indican que la respuesta mecánica de los materiales está condicionada en primer término por la densidad, siendo para cada densidad superior la respuesta mostrada por los materiales producidos utilizando el menor porcentaje de agente espumante, (1%) debido al menor contenido de celdas abiertas que presentan. Teniendo en cuenta los valores que alcanza *n*, se puede decir

que los materiales producidos se comportan mejor en compresión y en flexión que cuando están sometidos a fuerzas de tracción.

La conclusión general que se puede extraer de este trabajo es que el moldeo por compresión es una técnica adecuada para producir materiales celulares termoplásticos moldeados, no entrecruzados con un control óptimo de la densidad final de los materiales. Mediante cambios en la composición química, (contenido de agente espumante) se pueden obtener estructuras celulares muy variadas en términos de tamaños de celda y grado de interconexión lo que permite generar materiales con densidades similares pero destinados a aplicaciones diferentes. Así por ejemplo un material con celda cerrada será más adecuado para aplicaciones de tipo estructural, mientras que uno con un alto grado de interconexión entre las celdillas tendría un interesente campo de aplicación como absorbedor acústico.

El segundo de los trabajos presentados en este capítulo complementa el trabajo descrito en primer lugar. El rango de densidad relativa de los materiales analizados varía entre 0.3 y 0.6, lo que les define como materiales celulares de densidad media (capítulo 2). La producción y utilización de materiales celulares de densidad alta y baja están muy extendidas, sin embargo los materiales celulares de densidad media no acaban de establecerse por completo en el mercado siendo una de las razones el que no existen procesos industriales adecuados para producir piezas moldeadas con buenas propiedades en dicho rango de densidad. La ruta ICM se presenta por tanto como una alternativa para producir materiales celulares en ese rango de densidades. La aplicación final del un material celular viene definida, (además de por su densidad) por la relación estructura-propiedades que éste presente. En este artículo se analiza de forma exhaustiva dicha relación con el fin de poder dilucidar posibles aplicaciones para materiales celulares de densidad media con base PP producidos mediante moldeo por compresión mejorado.

Tal y como se concluyó en el trabajo anterior, un aumento en la cantidad de agente espumante implica una disminución del tamaño de celda y un aumento de la densidad celular del material. Se define además en este artículo un parámetro denominado *Ratio de Degeneración de la Estructura Celular, (Cellular Structure Degeneration Ratio, CSDR).* Durante el proceso de expansión de un polímero se pueden producir fenómenos tales como la coalescencia, el engrosamiento de las paredes o drenaje del polímero. La coalescencia se produce debido a la ruptura de paredes celulares y el engrosamiento está causado por la difusión del gas de celdas más pequeñas (con elevada presión de gas) a otras más grandes (con menor presión). Ambos

fenómenos deben ser evitados si se desea obtener una estructura celular homogénea de celda cerrada. El parámetro CSDR puede ser considerado una medida cuantitativa de la degeneración que se produce en la estructura celular durante el proceso de crecimiento de la misma debido a los fenómenos mencionados anteriormente. En esta investigación se ha demostrado que los valores aumentan al disminuir la densidad y disminuyen al aumentar el porcentaje de espumante. Una mayor presión en el interior del sistema hace que se genere un mayor número de celdas. Curiosamente se ha probado que para elevadas presiones, las estructuras celulares son muy estables, dándose valores muy bajos del parámetro CSDR. El mecanismo físico que condiciona esta elevada estabilidad a alta presión es un tema aún por discernir.

La respuesta mecánica de los materiales espumados, del polímero puro y de los precursores, (polímero más distintos porcentajes de ADC) se ha medido en distintas configuraciones, (compresión, tracción, flexión e impacto Charpy). Los resultados obtenidos para los materiales sólidos indican que las partículas de azodicarbonamida aumentan la rigidez del polímero pero disminuyen su resistencia y ductilidad. Los ensayos de impacto Charpy dejan claro este punto, la adición de 1% de partículas de azodicarbonamida al polímero lleva asociada una pérdida de un 39% en la resistencia a impacto del material.

Debido a la reducción de densidad la respuesta mecánica de los materiales espumados es inferior a la que exhiben tanto los precursores como el polímero puro. Independientemente de la configuración de medida, los resultados indican que a densidad constante el porcentaje de celda abierta determina la respuesta mecánica. A medida que éste aumenta, la respuesta mecánica (rigidez, resistencia y tenacidad) de los materiales disminuye. Otro hecho que se observa en relación a los materiales espumados es que para densidades similares y contenidos de celda abierta similares las propiedades mecánicas (resistencia y tenacidad) disminuyen a medida que aumenta el contenido de azodicarbonamida. La azodicarbonamida, tal y como se comentó en el capítulo 2 se descompone liberando una mezcla de gases además de una cantidad bastante elevada de residuos. Dichos residuos quedan “atrapados” en el polímero que forma las paredes de las celdillas, y es de suponer que tengan un efecto similar al producido por las partículas de azodicarbonamida, es decir, que provoquen una reducción de la resistencia y tenacidad del polipropileno en este caso. Por otro lado, los resultados obtenidos indican que el tamaño celular y la distribución de tamaños celulares son parámetros con un peso despreciable frente al del contenido de celdas abiertas.

Se concluye de este trabajo que combinando la ruta ICM con distintos porcentajes de agente espumante se pueden obtener materiales celulares moldeados de densidad media con una amplia variedad de estructuras celulares para cada densidad. En

campos como la automoción esto podría ser una ventaja. La tendencia actual pasa por reducir el peso total de un vehículo, ya que al pesar menos también contamina menos, pero sobre todo debido a la reducción de costes en materia prima que lleva asociado. Así, para piezas que requieran una buena respuesta mecánica basta con utilizar porcentajes de agente espumante pequeños, (1%), pues así se consiguen materiales con estructuras celulares cuasi completamente cerradas. Por otro lado, cuando sea necesario producir piezas que combinen una buena respuesta mecánica con cierta capacidad de absorción acústica la solución pasa por utilizar mayores porcentajes de espumante dado que ese es el modo de obtener materiales con estructuras celulares altamente interconectadas.

An Alternative Foaming Route to Produce Non-Crosslinked Thermoplastic Foams with Controlled Density and Cellular Structure.

C. Saiz-Arroyo[1,2], M.A. Rodríguez-Pérez[1], A. López-Gil[1], J. Tirado[1], J.A. de Saja[1]

[1] Cellular Materials Laboratory, (CellMat). Condensed Matter Physics Department, University of Valladolid, Prado de la Magdalena s/n, 47011, Valladolid.

E-mail: csaiz@fmc.uva.es, marrod@fmc.uva.es

[2] Technological Centre of Miranda de Ebro, (CTME), C/ Montañana P R60-R61, 09200, Miranda de Ebro, Spain.

Abstract

The present paper deals with the description of a novel foaming process named "Improved Compression Moulding Route", (ICM). This process is suitable to produce non-crosslinked thermoplastic foams in a wide density range. The main advantage lies in an independent control of density and cellular structure in terms of average cell size, cell size distribution and type of cellular structure, (i.e. open or closed cells). According to that, the ICM route allows producing tailored cellular polymers with the suitable density and cellular structure for different applications. To easily understand how the process works and all the parameters that shall be controlled, a collection of a polypropylene foams, with densities ranging from 0.3 to 0.6 have been produced using the ICM process. It has been analyzed in detail the influence of foaming parameters, (pressure, temperature and chemical composition among others) on both microstructure and mechanical response of the foams.

Results have revealed that for similar densities foams with different open cell content and cell size can be achieved. In addition, it has been proved that mechanical behaviour strongly depends on the degree of interconnectivity of the cells. The analysis of the

relative mechanical properties allows determining the influence of microstructure on mechanical behaviour as well as well as quantifying the efficiency of the foaming process to produce light-weight stiff materials.

Keywords: foaming process, chemical blowing agent, thermoplastics, cellular structure, density control.

Introduction

Polymeric foams can be defined as two-phase materials in which a gas is dispersed in a continuous macromolecular phase [1]. Due to their outstanding properties, thermoplastic foams have become essential items and although they are mainly used as thermal insulators or impact absorbing elements, they have found applications in almost every field, [2-4].

Since their development in 1940s, both scientific and industrial communities have focused their attention on the development of foaming technologies able to satisfy the growing demand of thermoplastic foamed products [3]. Nowadays, no single foaming method dominates thermoplastic foam manufacture, and both continuous and batch processes are operated using either chemical or physical blowing agents. The most commonly used foaming processes to produce thermoplastic foams are extrusion, injection moulding, compression moulding or batch foaming, (dissolution of a physical blowing agent at high temperature and/or pressure) [1, 5].

The election of the foaming process is conditioned mainly by the final application of the material which at the same time strongly depends on its relative density (i.e. the density of the foam divided by that of the corresponding solid). It is well known that foaming

process itself as well as the intrinsic characteristics of the polymeric matrix heavily determines the cellular structure of the foamed product [4, 5].

According to this, depending on the final application of the foam and the desired expansion ratio, the most suitable process is chosen. Thus, extrusion using a physical blowing agent is a good choice to produce low or ultra-low density foamed sheets or profiles for heat insulation or damping applications [3]. Injection moulding is the best election to produce net-shaped foamed parts. However, density reductions are limited to a 40%, and in addition this weight reduction strongly depends on size and shape of the part [6]. The batch foaming process produces foamed products that have a very high quality, with fine cells and without residues coming from the blowing agent. However, the control of foam density is complicated in this type of process [7]; in addition, the investments are high due to the requirement of large high-pressure vessels and the cycle time to produce to foams are also very high.

Compression moulding is a versatile process suitable for a wide variety of thermoplastic polymeric matrices. Two different variations are commonly used at industrial level [4, 5, 7, 8]. The single stage process involves two steps, first compounding the polymer with the blowing agent and all the required additives, (using a extruder or a Bambury type mixer) and in the second one, the foamable compound is placed in a mould and subjected to a temperature higher than the decomposition temperature of the blowing agent, afterwards expansion takes place and the material is foamed. The main advantage of the single-stage variation is its simplicity, however it present several disadvantages being the most important the difficulty of controlling the final foam density. In addition when using low-melt strength thermoplastics, such as polyolefins, or when high expansion degrees are required, it is necessary to crosslink (either chemically or by irradiation) the polymer to bear the extensional forces occurring during expansion, thus

avoiding premature collapse of the foam or the presence of a high number of broken cell walls [4].

Using the single stage process, densities lower than 70 kg/m^3 can not be achieved. To obtain lower densities, a second variation known as two-stages compression moulding is used [5]. In this process, expansion takes place at two different times and this together with the crosslinking of the polymeric matrix allows lowering the density of the foamed products to values as low as 15 kg/m^3. Compounding is carried out as for the single stage process, and the foamable mixture is introduced in a mould and subjected to both pressure and temperature. The polymer is crosslinked and afterwards expanded between 4 and 7 times. Second expansion takes place at atmospheric pressure in a mould having the desired size and shape.

However, compression moulding, either the single or the two-stages variations presents several drawbacks. In the single-stage process, the control of density is made mainly by means of the blowing agent concentration, which effectiveness depends both on temperature and pressure, hence the control of foams density is far to be precise [4]. In the two-stages process, the control of density is much accurate than for the single stage one however, the foam blocks produced by this method are non-homogeenous, with density and cellular structure varying along the block thickness, (cells are smaller close to the surface of the blocks and density is higher in this zone) [9-13]. However, the main drawback of these two processes is the necessity of crosslinking the polymeric matrix, which harms its recyclability by conventional re-melting techniques [8].

According to the previous ideas, it can be said that the main drawbacks of current foaming technologies are the following: it is not possible to obtain net-shaped foams except at high relative densities, to reach low or ultra-low densities is is compulsory to

crosslink the polymeric matrix and finally that the control of density of foamed parts is not as precise at it should be desirable.

The Improved Compression Moulding Route, (ICM) can be considered as an alternative foaming route to provide a solution to aforementioned drawbacks. It allows obtaining non-crosslinked net-shaped foamed parts in a relative density range between 0.1 and 0.9, density is accurately controlled by mechanical means and moreover, it permits an excellent control of the cellular structure.

Therefore, this paper is focused on the analysis of the relationship between the ICM route and the structure and properties of polymeric foams. For this purpose, a collection of polypropylene foams with relative densities in the range between 0.3 and 0.6 and with different chemical compositions have been prepared using such process. Foamed discs and cylinders were prepared using a linear polypropylene grade (and without the addition of any additive to favour foamability), therefore it will be possible to show that it is not necessary to crosslink the polymer to obtain good quality foamed products which could be used for several applications depending on both their density and cellular structure.

The Improved Compression Moulding Route, (ICM).

The Improved Compression Moulding Route, (ICM) could be considered as a variation of the single stage process. It is based on a closed control of both temperature and pressure during foaming step as well as on a proper handling of the chemical composition of the sample.

The main difference between the ICM route and the conventional one-step compression moulding lays in the pressure applied to the foam during foam growing.

This difference promotes significant advantages of the ICM process over the conventional one. On one hand the possibility of achieving an accurate control of foam density and on the other hand the possibility of modifying the microstructure of the foamed part, (in terms of cell size, cell type and cell shape) by acting on both foaming parameters and chemical composition.

Foam density is controlled through the use of special moulds known as self-expandable moulds. Those moulds have the ability of applying and retaining a pressure to the polymer while the decomposition of the chemical blowing agent and subsequent dissolution into the polymer. In addition, moulds are capable of controlling the expansion degree of the material hence regulating in a very accurate way both size and shape of the foamed part. As the moulds can adopt different geometries, it is possible to obtain net-shaped foams using the ICM process.

With regard to the second main advantage, it is necessary to mention that the control of chemical composition, (mainly blowing agent concentration) time, pressure and temperature during the process make feasible the obtention of foamed products with tailored cellular structures in terms of cell diameters, cell type and cell shapes. Besides, the control of cellular structures can be achieved regardless of which is the density of the foam. Therefore using the ICM route it is possible to obtain customized foams with similar densities but with significantly different cellular structures. For example, for structural purposes samples with a good mechanical response, (i.e. with an almost zero open cell content) are desirable, while for sound absorption applications a high degree of interconnection between the cells is preferred.

Even though the independent control of density and microstructure is probably the greatest advantage of the ICM there are others that should be also taken into consideration. Any thermoplastic polymer or thermoplastic based composite or

nanocomposite can be foamed by this process without the necessity of crosslinking the polymeric matrix. Up to now, pure polymers such as LDPE or EVA, composites such as LDPE/ATH, EVA/ATH or mixtures of EVA and starch, and nanocomposites based on LDPE and silica nanoparticles have been successfully foamed using the ICM process [14-21].

The ICM route comprises the following steps. In the first one, all raw materials where is included the polymer, the chemical blowing agent and all the required or desired additives are melt-mixed in a twin-screw extruder or batch mixer at a temperature lower than the decomposition temperature of the blowing agent. So obtained pellets can either be directly foamed or used to produce a precursor that will be afterwards introduced in the final mould and foamed. Precursors are prepared using a mould with the same geometry as the final part but with different dimensions. A certain amount of the foamable compound is introduced in the mould and subjected to both temperature and pressure to form a solid sample. The applied pressure should be enough to assure a good compaction of the pellets and the temperature lower than the decomposition temperature of the blowing agent in order to prevent its prone decomposition. The final step is the foaming one, so, either pellets or precursors are introduced in the final mould which is at the same time introduced in a hot-plates press. An initial pressure (P_0) is applied to the system while it is heated until foaming temperature (T_F) which is usually higher than the decomposition point of the blowing agent. As the temperature increases, the blowing agent starts decomposing and the pressure inside the mould increases up to a higher value (P_F). After a certain time (t_F), when the blowing agent is fully decomposed, and P_F stabilizes, (does not continue increasing), the pressure of the press is released allowing the polymer to expand until the desired ratio. The mould is then introduced in cool water to cool-down the sample and hence stabilizing the cellular

structure as fast as possible. Foaming parameters, this is t_F, P_0 and T_F are chosen depending on the polymeric matrix type, chemical composition, (blowing agent concentration) and sample geometry.

The control of foam density is carried out by means of aforementioned self-expandable moulds. Figure 1 shows a schematic draw where it is represented the evolution of both sample and mould during a typical foaming experiment. In the first stage, the precursor or the pellets are introduced in the mould and the initial pressure applied, (P_0). Precursors or equivalently the cavity where pellets are introduced have a defined initial height, (h_0). As the blowing agent decomposes, (second step), the gas starts dissolving in the polymer and the pressure increases above P_0. After the complete decomposition of the blowing agent, the pressure is released allowing the piston to displace vertically and hence the material is able to expand. The distance covered by the piston is defined taking into account the desired expansion ratio, ($E.R. = \frac{h_f}{h_0}$). So, the final height of the sample is defined as follows:

$$h_f = h_0 + d \qquad (1)$$

The movement of the piston is restricted to such distance, (d) by the part named "*ER Control Part*". Such parts are interchangeable depending on the desired expansion ratio.

Materials

A random polypropylene copolymer, (200CA10 from Inneos) with a melt flow index of 10 g/min, (measured at 230ºC and 2.16 kg) was used to produce all the analyzed samples. Its melting point is 150.4 ºC and its crystallinity degree is 44.4 %, (both were

measured by DSC). Azodicarbonamide (Porofor ADC/M-C1 from Lanxess) with an average particle size of (3.9 ± 0.6) μm was used as blowing agent. In order to prevent thermal oxidation of the polymer a small amount of a commercial antioxidant, (Irganox B561 from Ciba) was used in all formulations. Stearic acid (Stearic acid 301 from Renichem) was used as processing aid.

Foaming Process

As it was mentioned in the introduction, polypropylene foams will be produced using the improved compression moulding process. It comprises the following three steps:

1. Melt-Compounding of Raw Materials

Polymer, blowing agent, the antioxidant and the processing aid were melt-mixed in a twin screw extruder, (Collin mod ZK25T). The temperature profile was varied from 135 ºC in the hopper to 155ºC in the die. Such profile was chosen in order to avoid premature decomposition of the blowing agent during the compounding steps. The material was water cooled and pelletized.

Pellets with four different blowing agent concentrations namely 1, 5, 10 and 15wt% were prepared. Varying blowing agent concentration will permit gaining more knowledge about the relationship foaming process-microstructure-mechanical properties.

2. Obtention of Solid Precursors

The second step of the process comprises the fabrication of solid foamable precursors using the previously obtained pellets. Solid cylinders with 20mm in diameter and 15 mm in height, and discs with 150 mm in diameter and 2 mm thickness were produced using stainless steel moulds and a two-hot plates press. For both cases the temperature of the press was fixed at 175 ºC (lower than the decomposition point of the ADC which is in the range between 200 and 220ºC [22]). The applied pressure (P_0) was 95MPa for cylinders and 50 MPa for discs. Those values were chosen in order to assure a proper compactaction of the pellets.

3. Foaming Step

Aforementioned foamable precursors are introduced in a stainless-steel mould with the ability of controlling the expansion ratio of the material (see figure 1). An initial pressure (P_0) of 95 MPa for cylinders and 3.5 MPa for discs were applied to the moulds. Foaming temperature (T_F) in both cases was 205ºC. As the temperature rises, azodicarbonamide starts decomposing and the pressure inside the mould increases up to a maximum value, (P_F), which varies depending on both geometry and azodicarbonamide concentration. After a certain time, (t_F), when P_F stabilizes and all the blowing agent is already decomposed, the pressure is released allowing the polymer to expand inside the mould. The mould is then rapidly introduced in a tank containing cool water to stabilize the cellular structure as fast as possible.

Foamed discs and cylinders with the four aforementioned ADC concentrations have been prepared. Samples were expanded to three different ratios 1.6, 2 and 3 which correspond to nominal densities of 562.5, 450 and 300 kg/m^2, (i.e. relative densities of around 0.6, 0.5 and 0.3 respectively).

Samples denomination is as follows, a capital C (for cylinders) or a capital D (for discs) followed by two numbers, first one indicates the ADC concentration, (1, 5, 10 or 15) and second one, the expansion ratio, (1 for 1.6, 2 or 3).

Characterization

Density

Density measurement of both solid precursors and foams was performed by the geometric method; this is by dividing the weight of each specimen between its corresponding volume, (ASTM Standard D1622-08).

Microstructural Characterization

Cellular structure of both foamed discs and cylinders was analyzed by using scanning electron microscopy (SEM). In order to keep the microstructure, samples were frozen in liquid nitrogen and afterwards fractured. Surface fracture was made conductive by sputtering deposition of a thin layer of gold and observed using a Jeol JSM-820 scanning electron microscope. Cell diameter as well as cell density were measured using an image processing tool based on the software Image J [23].

Open Cell Content

The analysis of open cell content of foamed samples is essential to understand their mechanical response. In addition, is very useful to be able to determine if they can be potentially used as sound absorbers. In this study, the percentage of open cells, (C) was measured with an Eijkelkamp 08.06 Lange air pycnometer according to ASTM D6226-10. The following equation, (1) was used according to the ASTM standard:

$$C = \frac{V_{Sample} - V_{Pycnometer}}{V_{Sample} \cdot p} \qquad (2)$$

where the geometrical volume, V_{Sample}, (calculated from the specimen dimensions) is substracted from the total volume measured with the pycnometer, $V_{Pycnometer}$, and divided by the volume of air contained in the sample, ($V_{Sample} \cdot p$), where p is the sample porosity calculated by $\left(1 - \frac{\rho_f}{\rho_S}\right)$; ρ_f is the foam density and ρ_S is the density of the polymeric matrix, in this case polypropylene (900 kg/m^3).

Mechanical Response

Mechanical response of foamed polypropylene was measured under different conditions, thus, compression, tensile, bending and impact tests were carried out. In addition precursor materials (polypropylene with different ADC contents) were also characterized.

Compression tests were performed in the solid and foamed cylinders using an universal testing machine (Instron model 5500R6025). Experiments were performed at room temperature and at a strain rate of 10s^{-1}. The maximum static strain was 75% for all the experiments. Elastic modulus and collapse stress were determined from the stress-strain curves.

Tensile tests were also performed using an Instron 5500R6025, in accordance with ISO 527, at a strain rate of 20mm/min. Type 1A specimens were machined from foamed and un-foamed discs and five replicates for each material were run in order to ensure the reproducibility of the results. Elastic modulus and yield strength were determined from tensile tests.

Flexural tests were performed using the same universal testing machine and in accordance with ISO 178 at a strain rate of 5mm/min. Flexural modulus as well as flexural strength were calculated from the resulting curves.

In all cases, samples were tested under controlled conditions of 23ºC and a 50% of relative humidity.

Further information about testing procedure can be found elsewhere [24-28]

Results and Discussion

Foaming Process

The hot-plates press in which the foaming experiments were conducted is equipped with a sensor able to measure the pressure during the experiments. Figure 2 shows how pressure evolves with time for foamed discs (a) and for foamed cylinders, (b). In both cases, the pressure increases as the experiment progresses. However, there is some differences between both types of samples. While for discs the increase is produced since the very beginning of the experiment for discs, it takes a longer time. This difference is related with the different size of both moulds. The mould used for disc is much bigger and then requires longer time to warm and to reach decomposition point of the ADC and then increasing the pressure.

There are other differences related with the total increment of pressure, ($\Delta P = P_f - P_0$) and foaming time, (t_f). Figures 3a and 3b summarize the average values of t_f for discs and cylinders respectively. Foaming time is slightly shorter for discs than for cylinders. Although the mould is bigger for cylinders, cylinders are thicker than discs (20 and 2

mm respectively) and hence they need a slight longer time for the ADC to be fully decomposed. Moreover, t_f remains approximately constant for each type of samples, (discs or cylinders) being not possible to observe any trend with density or with ADC concentration.

Pressure increment, (ΔP) has been calculated for the whole collection of samples and values are plotted as a function of ADC content in figures 3c (discs) and 3d (cylinders). For discs, ΔP increases linearly as ADC concentration does however, for cylinders this trend is not maintained. In addition, the values of ΔP reached by either discs or cylinders are significantly different, a maximum of 2MPa for discs and a maximum of around 120 MPa for cylinders.

As very different initial pressures were applied to both geometries, (4MPa for discs and 100 MPa for cylinders) it could be expected a very different pressure evolution during foaming step. It seems then, that the much higher applied pressure in cylinders hinders the real effect of ADC decomposition, leading to not linear trends between pressure and blowing agent concentration.

It was said in the introduction that one of the main advantages of the ICM route with respect to the conventional one is the accurate control of foam density that can be achieved. Table 1 summarizes average density values of both foamed discs and cylinders and their respective relative densities. Average density values are accompanied by the standard deviation calculated from density measurements of five different samples. So, error can provide information about the accuracy and repeatability of the process. In all cases, error is smaller than 8%, and it can be observed in the table that it increases as ADC content does and also it is higher for cylinders than for discs. The high pressures applied to the cylindrical samples during the foaming step can produce small leakages of polymer out of the mould leading then to samples with

densities smaller than nominal one. As the applied pressure to produce the discs is much smaller, a higher accuracy in density control is achieved. In addition it has been calculated a parameter called % Deviation, (*%D*) which gives account for the difference in percentage between the nominal expected density of the samples and the real one and has been calculated using equation 1:

$$\%D = \frac{\rho_{Real} - \rho_{Nominal}}{\rho_{Nominal}} x100 \qquad (3)$$

where ρ_{Real} is the measured density of the samples and $\rho_{Nominal}$ corresponds to expected nominal densities for the three considered expansion ratio, (i.e. 562.5 kg/m^3 for ER=1.6, 450 kg/m^3 for ER=2 and 300 kg/m^3 for ER=3). When *%D* is negative it means that the experimental value is lower than the expected one and when it reaches positive values, it means that experimental value is higher than nominal one.

The values in the table indicate that *%D* increases as ADC concentration does and it is higher for cylinders than for discs. As ADC content increases the pressure inside the mould also does and the polymer can easily escape from the mould. Negative values, this is experimental values of density lower than nominal one are in general due to leakages of material out of the mould, either because of high applied pressures, as in the case of cylinders or because the high pressure generated by the decomposition of high amounts of ADC, (samples with 15wt% of ADC). Positive values of *%D*, this is densities higher than expected ones, can be due to a non full decomposition of the blowing agent.

Microstructure

The analysis of the cellular structure of polypropylene foams produced by the improved compression moulding route has been focused on cylindrical shaped samples. SEM micrographs showing the cellular structure of foams with different densities and blown

using different ADC concentrations are shown in figure 4. As it can be observed, as both density or blowing agent concentration are varied a wide collection of different cellular structures can be achieved. Although all the samples exhibit an isotropic cellular structure some differences related with the effect of density and ADC concentration can be inferred from the micrographs. On one hand, as blowing agent amount increases, cell size decreases and cell density increases and on the other hand, as density decreases cell size increases and cell density decreases. To both quantify and easily understand those effects, cell density and cell size have been measured and the average values of both of them are plotted as a function of ADC content in figure 5.

As density decreases, cell size also does, being the cell size of samples with the higher relative density around three times lower than that of the samples with the lower relative density. With regard to cell density, it can be observed in figure 5 that it decreases as density does. As density decrease, the polymer has to expand to higher values and hence, cell walls are thinner and hence coalescence or coarsening phenomena can easily occur leading then higher cell sizes and lower cell densities, [4].

The variation in ADC concentration has also a great effect on both cell size and cell density. The increment in blowing agent concentration leads to significant cell sizes reductions, even reaching values of cell sizes below 100μm for samples with high ADC concentrations, (10 and 15 wt%). Chemical blowing agents such as azodicarbonamide are self-nucleating, [5], so as blowing agent concentration increases the number of available nucleating sites also does, hence leading to smaller cell sizes and higher cell densities.

Among cell density and cell size other parameters such as cell size distribution influences macroscopic response of foamed materials [2]. Typically, histrograms of cell size distributions are plotted and afterwards compared, however, due to the high number

of samples included in the study a parameter (*SD*) accounting for the width of the cell size distribution been calculated as follows:

$$SD = \sqrt{\sum_{i=1}^{n} \frac{(\phi_i - \phi)^2}{n}} \qquad (4)$$

where n is the number of counted cells, ϕ_i is the cell diameter of cell i and ϕ is the average diameter of the cells.

Results, (figure 6a) clearly indicate that as blowing agent concentration increases, more homogeneous cellular structures are achieved. In fact, it can be observed that samples with relative densities between 0.5 and 0.6 exhibit very similar values of *SD*. For lower densities, (ρ_R=0.3) values of SD significantly increase. For the latter samples the polymer, during expansion is subjected to higher stretching forces what can lead to more inhomogeneous cellular structures or a higher proliferation of coarsening or coalescence phenomena as it was previously mentioned.

Other important parameter to be taken into account is the open cell content percentage, (*C*) exhibited by the samples because it is known that this parameter can have a high influence on mechanical response of the samples. In addition, for the study it is used a conventional grade of PP, and hence it is worthy to know how the process itself or chemical composition of the samples affects to the open cell content of conventional polymer, (nor a filled one or a high melt strength grade). Experimental measurements were performed using an air pycnometer and results are plotted as a function of blowing agent concentration in figure 6b. As it can be observed there is a significant difference between samples with relative densities around 0.3 and the rest of samples. For those samples, open cell content remains constant (around a 60%) regardless of the azodicarbonamide concentration used to blown them. Those results indicate that at low densities, open cell content is conditioned by expansion degree more than by ADC

concentration. As polymer needs to expand to higher ratios, cell walls become thinner and hence easily breakable leading to a higher number of open cells. On the other hand, for samples with relative densities between 0.5 and 0.6 it can be observed how open cell content increases as blowing agent concentration does. In this case, an excess of pressure in the system can also leads to a higher degree of interconnection between the cells.

Analysis of the Relative Mechanical Response.

As it was said in the introduction, the way to obtain better quality foamed products is on one hand by optimising foaming process and on the other hand, by tailoring foams so that the most suitable foam could be used for each application. The analysis of mechanical response of ICM produced foams has been performed using relative values, this is considering the property of the foam divided by that of the solid. This type of analysis among analyzing the influence of density and blowing agent amount, allows accounting for the influence of cellular structure on the mechanical properties of the materials. Although mechanical properties of foamed products are always lower than that of the corresponding solid precursor materials due to density reductions, their relative properties, (i.e. the property of the foam divided by that of the solid) can reach higher values. It has been reported by several authors [2, 9, 10, 29-33] that properties of a cellular polymer can be predicted using the following equation:

$$\frac{P_f}{P_s} = C\left(\frac{\rho_f}{\rho_s}\right)^n \qquad (5)$$

where P_f is the property of the foam and P_s is the same property but for the solid polymer, and $\frac{\rho_f}{\rho_s}$ is the relative density of the foam. C and n are parameters that can be determined experimentally.

Most foamed products exhibit values of C close to 1 and values of n in a range between 1 and 2. n is closely related with the cellular structure of the foamed product, being closer to 1 for materials with closed cell cellular structures and small cell sizes and it is closer to 2 as open cell content and cell size increases. Hence equation 5 allows analyzing in a quite simple way the efficiency of the foaming process in terms of producing low density-stiff foams.

When the aforementioned property is the elastic modulus, (E) it can be concluded that for similar values of relative density ($\frac{\rho_f}{\rho_s}$) the foamed material reaching a value of n closer to n = 1 will exhibit better specific mechanical properties, (higher value of $\frac{E_f}{E_s}$).

As most foams exhibit values of n between 1 and 2, the reduction in mechanical properties is always greater than the corresponding density reduction. This means that the value of n can be considered as an index of under what conditions which of the analyzed foams will have a better mechanical performance.

Figures 7a, 7b and 7c shows the relative elastic modulus measured in compression, tensile and flexural tests represented as a function of relative density. n has been calculated considering the relative elastic modulus values measured in different configurations and results are presented in table 2. As it was expected n reaches values between 1 and 2 which is in agreement with the theoretical estimations.

It can be inferred from figure 7a that the cellular structure that maximizes stiffness is the one exhibited by samples blown using 1wt%; the value of n obtained for this samples is

the closest to 1. So, although those samples presented the highest cell sizes, its very low open cell content (close to 0, see figure 6b) lead to better mechanical performance than the one obtained for samples with lower cell sizes. This means that for the same relative density the role played by open cell content is more significant than the one played by cell size or cell size distribution homogeneity. This result is in concordance with previous studies of our group [9, 10] and from other researchers [33]. So in this case stiffer samples are not samples with very small cell sizes, (15wt% ADC ones) but the ones with a nearly complete closed cell microstructure.

When the same type of analysis is performed with the results obtained from tensile tests, (figure 7b) it can be concluded that in this case there is no significant differences between the samples made using different ADC concentrations. In fact, values of *n* are very similar although for 1wt% of azodicarbonamide is slightly smaller. It seems then that the different types of cellular structures achieved for the whole collection of samples do not have a significant effect on the mechanical response of the samples when they are subjected to uniaxial tensile forces.

Finally, when the results obtained from flexural tests are analyzed, (figure 7c) it can be concluded that once more the cellular structure showing the best mechanical performance is obtained using a 1wt% of azodicarbonamide. In fact the value of *n* showed by those samples is considerably smaller than for the other materials. As it happened for compression tests, open cell content plays a more important role than cell size or cell size distribution in mechanical response.

If values of *n* are compared now for the different measurement configurations, analyzed polypropylene foams seems to be have a better response in compression or bending than in tensile.

Besides the analysis of elastic modulus in relative terms, the same type of study can be performed for parameters accounting for plastic collapse, this is, collapse stress, yield stress or flexural strength. Figures 8a, 8b and 8c show those three parameters represented as a function of relative density. In addition, experimental data have been fitted to a power law according to equation 5. The results obtained for *n* are shown in these figures but also in table 3, in order to easily compare the behaviour of the materials under the three different types of deformation mechanisms.

As it can be observed in table 3 the highest values of *n* are obtained for yield strength, this is when samples are subjected to uniaxial tensile forces. On the other hand, the closer values to n=1 regardless ADC-concentration are reached by flexural strength.

As it happened for the zone of elastic behaviour, (table 2), the values of *n* closer to 1 are always obtained when the smallest amount of azodicarbonamide is used.

Therefore, results in table 3 are indicating that the samples under study have a superior performance in terms of strength when they are subjected to flexural forces. It seems then, that open cell content has a greater influence in the plastic collapse zone when samples are subjected to compressive or uniaxial tensile forces.

Conclusions

A detailed description of the improved compression moulding foaming route has been performed along the paper. In addition to easily understand all the concepts and parameters involved in the process, a collection of polypropylene foams with relative densities ranging from 0.3 to 0.6 have been produced using such foaming process.

It has been proved that the ICM route is then suitable to produce foams of a conventional lineal polyolefin without the necessity of crosslinking it achieving in

addition an accurate control of foam density due to the use of special moulds and a closed control of both pressure and temperature. In addition, it has been detected that reaching a lower deviation from density nominal values is achieved using lower initial pressures and/or lower blowing agent concentrations.

A proper set of foaming parameters together with the variation of chemical compositions, (by means of using different blowing agent concentrations) can lead to the obtention of a wide variety of cellular structures in terms of cell sizes, cell shapes or interconnection degree. It was found that using high initial pressures and high ADC concentrations, cellular structures with cell sizes below 100 μm and with a very narrow cell size distribution can be achieved. As density is lowered, the polymer is expanded to higher ratios leading to the obtention of samples with an open cell content of around 60% which can be potentially considered as good sound absorbers.

Mechanical response of the foams has been determined using different measuring configurations. Nevertheless, regardless of the type of test, the conclusions that can be inferred are very similar. Mechanical response of the foams produced by the ICM route is primarily determined by density but also depends on chemical composition and hence on open cell content. At high relative densities, (between 0.5 and 0.6) when high ADC concentrations are used, open cell content increases and mechanical response decreases. For the lightest samples, as open cell content remains constant regardless of blowing agent content, mechanical response also does.

The analysis of mechanical properties in terms of relative values can give an idea of the influence of microstructure on mechanical behaviour. The results, (regardless of measurement configuration) show that the cellular structure maximizing mechanical response is the one with the almost-zero open cell content which is presented by samples produced using the smallest amount of azodicarbonamide. So, for the same

density values, these results indicate that cell size plays a secondary role when compare to open cell, because samples with more homogeneous cell size distributions and very fine cell sizes but with higher open cell contents have a poorer mechanical performance. Regarding the general behaviour of the analyzed materials and taking into account the values of n parameter, it can be said that they behave better in compression and bending and slightly worst in tensile.

As a general conclusion it can be said that the ICM route is a very suitable foaming process to produce non-crosslinked net-shaped foams of a wide variety of polymeric matrices. The accurate control of density, together with the possibility of achieving different types of cellular structures are their main advantages. So, foams adequate for structural or damping applications or even for sound absorption purposes can be produced using the ICM route.

Acknowledgments

Financial assistance from Spanish Ministry of Science and Education and Feder program, (MAT 12009-14001), Innocash Project (INC-0193) as well as European Spatial Agentcy (ESA Project MAP AO-99-075) is gratefully acknowledged.

References

[1] M.A. Rodríguez-Pérez, Crosslinked Polyolefin Foams: Production, Structure, Properties and Applications. Adv. Polym. Sci. 184, 97-126 (2005).

[2] L. Gibson, F. Ashby. Cellular Solids. Structure and Properties. 2nd Edition. Cambridge University Press, United Kingdom, (1997).

[3] R. Gendrom, (Editor) Thermoplastic Foam Processing. Principles and Devlopment. CRC Press, Boca Raton, Florida, (2004).

[4] D. Klempner, V. Sendijarevic. Handbook of polymeric foams and foam technology. 2nd Edition. Hanser Publishers, Munich, (2004).

[5] D. Eaves. Handbook of polymeric foams. Rapra Technology. United Kingdom, (2004).

[6] K.T. Okamoto, Microcellular Processing, Hanser Publishers, Munich, (2004)

[7] R.R. Puri, K. T. Collington, *Cell. Polym.*, **7**, 57. (1988)

[8] R.R. Puri, K. T. Collington, *Cell. Polym.*, **7**, 219 (1988).

[7] C. Saiz-Arroyo, J.A. de Saja, J.I. Velasco, M.A. Rodríguez-Pérez. Moulded polypropylene foams produced using chemical or physical blowing agents: structure-properties relationship. Journal of Materials Science, Submitted-JMSC-25764.

[8] C. Saiz-Arroyo, J.A. de Saja, M.A. Rodríguez-Pérez. Production and characterization of crosslinked low density polyethylene foams using waste of foams with the same composition. Polymer Engineering and Science, DOI:10.1002/pen.22138, (2012). *In press.*

[9] J.A. Martínez-Díez, M.A. Rodríguez-Pérez, J.A. de Saja, L.O. Arcos y Rabago, O.A. Almanza. The termal conductivity of a polyethylene foam block produced by a compression Goulding process. Journal of Cellular Plastics 37, 21-42, (2001).

[10] J.L. Ruiz-Herrero, M.A. Rodríguez-Pérez, J.A. de Saja. Effective difusión coefficient for the gas contained in closed cell polyethylene based foams subjected to compression creep tests. Polymer, 46, 3105-3110, (2005).

[11] M.A. Rodríguez-Pérez, O. Almanza, J.L. Ruiz-Herrero, J.A. de Saja. The effect of processing on the structure and properties of closed cell polyethylene foams. Cellular Polymers 27, 179-200, (2008).

[12] M.A. Rodríguez-Pérez, J.I. González-Peña, J.A. de Saja. Anisotropic and heterogeneous termal expansion of polyethylene foam blocks. Effect of thermal treatments. European Polymer Journal 43, 4474-4485, (2007).

[13] M.A. Rodríguez-Pérez, J.I. González-Peña, J.A. de Saja. Modifiying the structure and properties of polyethylene foams using thermal treatments. Polymer International 58, 620-629, (2009).

[14] M.A. Rodríguez-Pérez, J. Lobos, C.A. Pérez-Muñoz, J.A. de Saja, L. González, B.M.A. del Carpio. Mechanical behaviour at low Straits of LDPE foams with cell sizes in the microcellular range: Advantages of using these materials in structural elements. Cellular Polymers, 27, 347-362, (2008).

[15] M.A. Rodríguez-Pérez, J. Lobos, C.A. Pérez-Muñoz, J.A. de Saja. Mechanical response of polyolefin foams with high densities and cell sizes in the microcellular range. Journal of Cellular Plastics, 45, 389-403, (2009).

[16] S. Román-Lorza, M.A. Rodríguez-Pérez, J.A. de Saja. Cellular strcutre of halogen-free flame retardant foams based on LDPE. Cellular Polymers, 28, 249-268, (2009).

[17] S. Román-Lorza, M.a. Rodríguez-Pérez, J.A. De Saja, J. Zurro. Cellular structure of EVA/ATH halogen-free flame retardant foams. Journal of Cellular Plastcis, 10. 1-21, (2010).

[18] S. Román-Lorza, J. Sabadell, J.J. García-Ruiz, M.A. Rodríguez-Pérez, J.A. de Saja. Fabrication and characterization of halogen free flame retardant polyolefin foams. Materials Science Forum, 636/637, 98-205, (2010).

[19] M.A. Rodríguez-Pérez, R.D. Simoes, C.J.L. Constantino, J.A. de Saja. Structure and physical properties of EVA/starch precursor materials for foaming applications. Journal of Applied Polymer Science, 212, 2324-2330, (2011).

[20] M.A. Rodríguez-Pérez, R.D. simoes, S. Román-Lorza, M. Alvarez-Lainez, C. Montoya-Mesa, C.J.L. Constantino, J.A. de Saja. Foaming of EVA/Starch blends: Characterization of the strcutre, physical properties and biodegradability. Polymer Engineering and Science, In press, (DOI: 10.1002/pen.22046), (2011).

[21] C. Saiz-Arroyo, J.A. de Saja, M.A. Rodríguez-Pérez. Influence of foaming process on the Structure-Properties relationship of foamed LDPE/silica nanocomposites. Submitted.

[22] A.S. Batthi, D. Dellimore. The thermal decomposition of azodicarbonamide. Thermochimica Acta, 76, 63, (1984).

[23] J.Pinto, M.A. Rodríguez-Perez, J.A. de Saja, Development o an Image J Macro to Characterise the cellular Structure of Polymeric Foams, XI Reunión del Grupo Especializado de Polímeros (GEP), 10-24 September 2009, Valladolid. (Spain).

[24] M.A. Rodríguez-Pérez, J.I. Velasco, D. Arencon, O. Almanza, J.A. de Saja. Mechanical characterization of closed cell polyolefin foams. Journal of Applied Polymer Science, 75, 156-166, (2000)

[25] M.D. Landete-Ruiz, J.A. Martínez-Díez, M.A. Rodríguez-Pérez, J.A. de Saja, J.M. Martín-Martínez. Improved adhesión of low density polyethylene/EVA foams using different surface treatments. Journal of Adhesion Science and Technology, 16, 1073-1101, (2002).

[26] N.J. Mills, M.A. Rodríguez-Pérez. Modelling the gas-loss creep mechanism in EVA foam from running shoes. Cellular Polymers 20, 79-100, (2001).

[27] O. Almanza, M.A. Rodríguez-Pérez, J.A. de Saja. Measurement of the termal diffusivity and specific heat capacity of polyethylene foams using the transient plane source technique. Polymer International 53, 2038-2044, (2004).

[28] J.I. Velasco, M. Antunes, O. Ayyad, J.M. López-Cuesta, P. Gaudon, C. Saiz-Arroyo, M.A. Rodríguez-Pérez, J.A. de Saja. Foaming behaviour and cellular structure of LDPE/hectorite nanocomposites. Polymer 48, 2098-2108, (2007).

[29] H. Sun, G.S. Sur, J.E. Mark. Microcellular foams from polyethersulfone and polypheniylsulfone. Preparation and mechanical properties. European Polymer Journal, 38, 2373-2381, (2002)

[30] J.I. Velasco, M. Antunes, V. Realinho, M. Ardanuy. Characterization of rigid polypropylene-based microcellular foams produced by batch foaming processes. Polymer Engineering and Science, DOI 10.1002/pen .22048 (2011)

[31] E. Herrera-Tejeada, C. Zepeda-Sahagun, R. González-Nuñez, D. Rodrigue. Morphology and Mechanical Properties of Foamed Polyethylene-Polypropylene Blends. Journal of Cellular Plastics, 41, 417-435, (2005)

[32] L.M. Matuana, C.B. Park, J.J. Balatinecz. Cell Morphology and property relationships of microcellular foamed PVC/wood-fiber composites. Polymer Engineering and Science, 38, 1862-1872, (1998)

[33] J.E. Weller, V. Kumar. Solid-State Microcellular Polycarbonate Foams. II. The Effect of Cell Size on Tensile Properties. Polymer Engineering and Science, 50, 2170-2175 (2010)

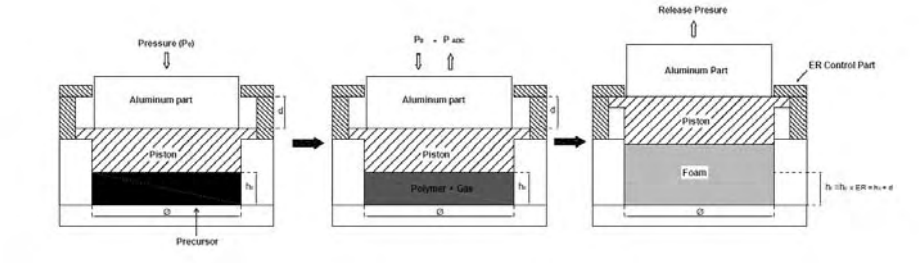

Figure 1: Schematic draw of one self-expandable mould used to produce polypropylene foams via the improved compression moulding route.

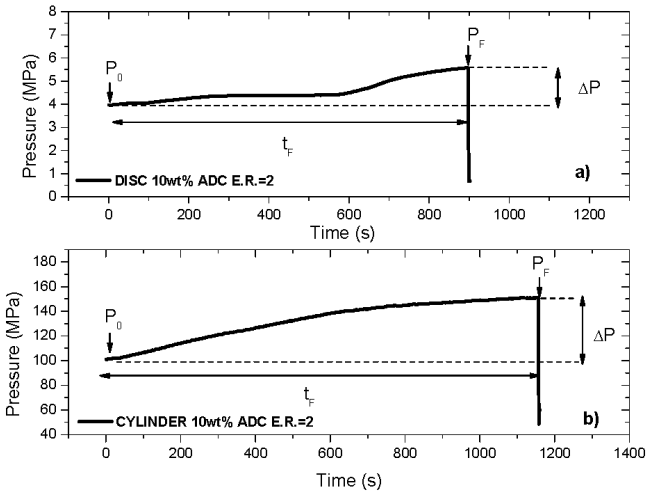

Figure 2: Curves showing the evolution of pressure with time during foaming experiments corresponding to discs and cylinders.

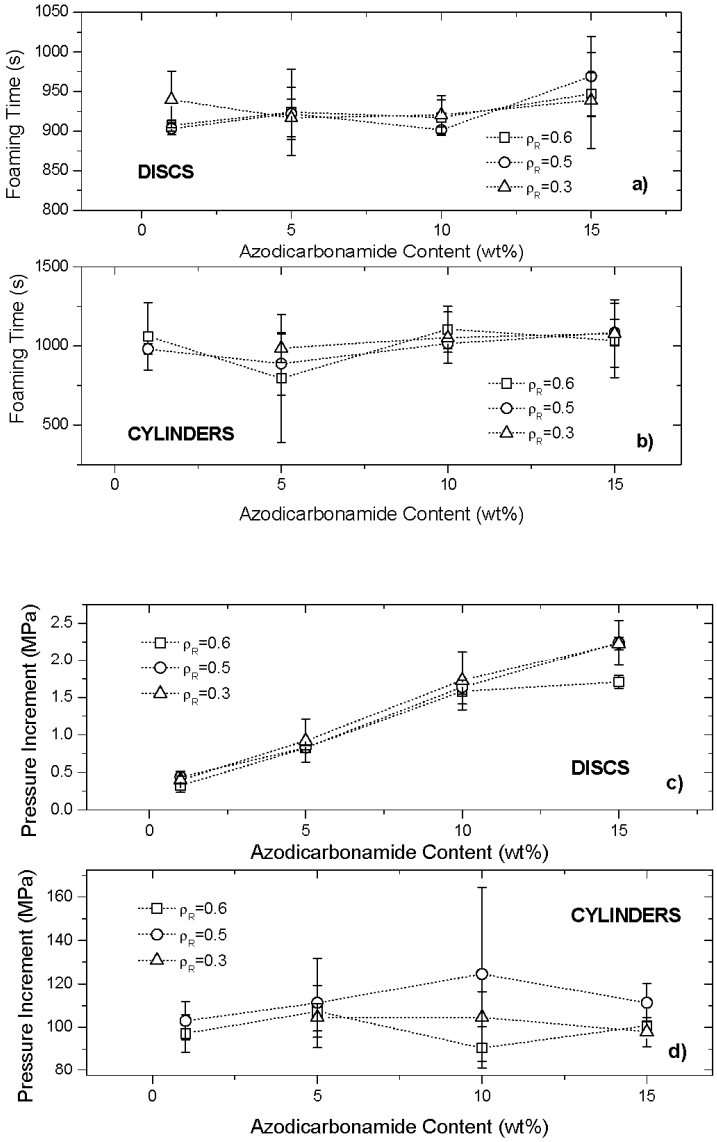

Figure 3: Average values of foaming time for PP foams,(a)Discs and b) cylinders) and average values of pressure increment, (c) discs and d) cylinders).

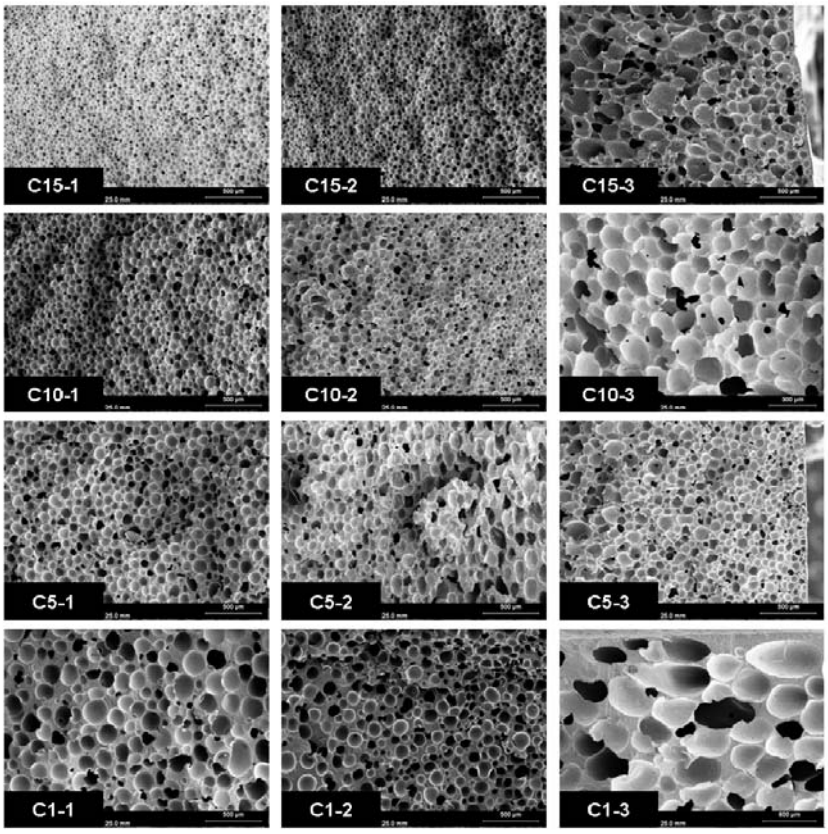

Figure 4: Micrographs corresponding to cylindrical shaped PP foams produced using the ICM route.

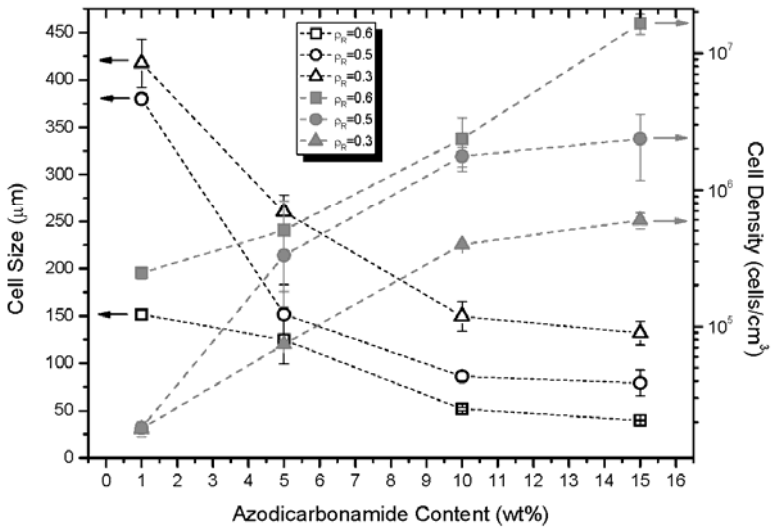

Figure 5: Cell size and cell density of cylindrical shaped polypropylene foams produced using the ICM route.

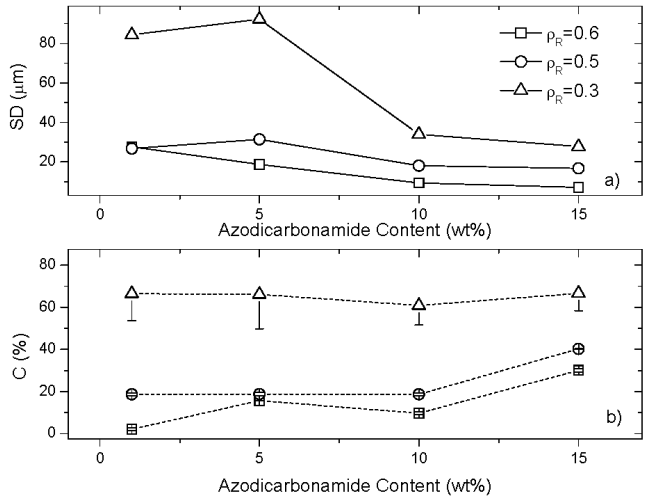

Figure 6: a) SD coefficient calculated for the analyzed cylinders. b) Open cell content of cylindrical samples.

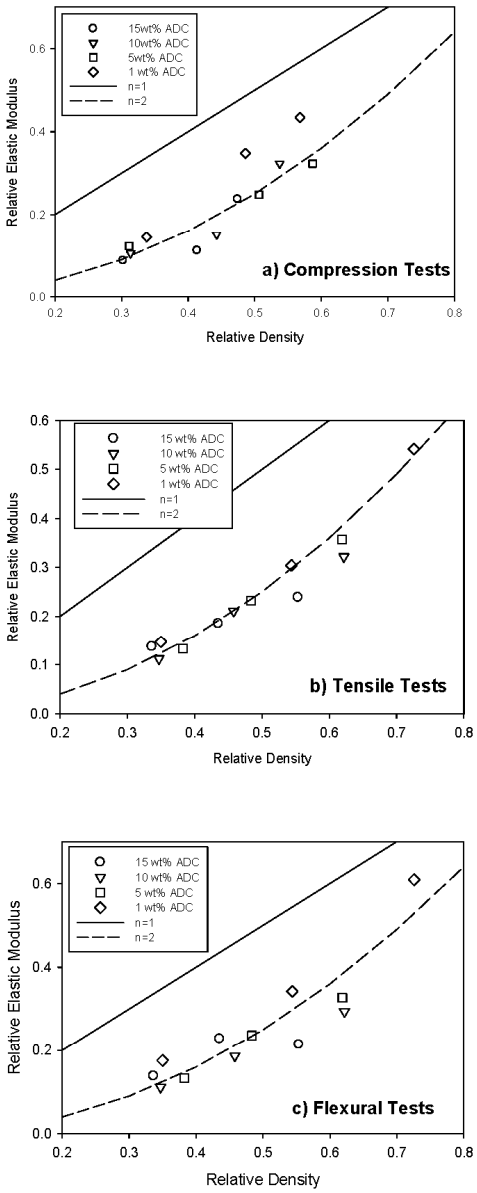

Figure 7: Relative elastic modulus measured in different configurations. a) Compression. b) Tensile. c) Three point bending.

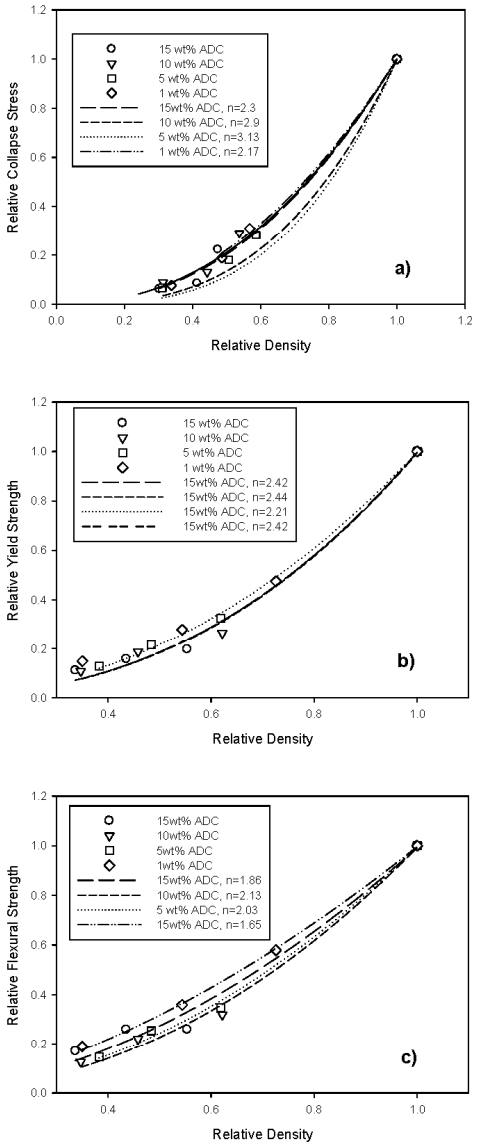

Figure 8: a) Relative collapse stress, b) Relative yield strength, c) Relative flexural strength.

CYLINDERS					DISCS				
	Sample	ρ (kg/m)^3	ρ_R	% Desv		Sample	ρ (kg/m)^3	ρ_R	% Desv
1wt% ADC	C1-1	525.2 ± 24.5	0.59	-6.61	1wt% ADC	D1-1	606.2 ± 15.0	0.72	7.78
	C1-2	423.8 ± 5.1	0.48	-3.81		D1-2	459.9 ± 19.9	0.54	2.20
	C1-3	294.0 ± 7.5	0.33	-1.97		D1-3	308.2 ± 3.0	0.35	2.67
5wt% ADC	C5-1	530.0 ± 20.7	0.58	-5.77	5wt% ADC	D5-1	541.7 ± 11.9	0.61	-3.68
	C5-2	461.3 ± 38.9	0.49	2.52		D5-2	426.6 ± 11.1	0.48	-5.17
	C5-3	284.0 ± 7.4	0.31	-5.31		D5-3	317.3 ± 2.6	0.38	5.79
10wt% ADC	C10-1	502.2 ± 34.1	0.57	-10.70	10wt% ADC	D10-1	539.8 ± 12.2	0.62	-4.01
	C10-2	424.5 ± 24.1	0.46	-5.66		D10-2	416.1 ± 9.1	0.45	-7.51
	C10-3	288.3 ± 4.3	0.31	-5.55		D10-3	303.8 ± 12.4	0.34	1.29
15wt% ADC	C15-1	450.8 ± 30.3	0.48	-19.84	15wt% ADC	D15-1	482.8 ± 32.1	0.55	-14.15
	C15-2	387.9 ± 36.8	0.42	-13.78		D15-2	382.4 ± 2.2	0.43	-15.00
	C15-3	287.9 ± 3.6	0.30	-7.00		D15-3	299.5 ± 15.5	0.33	-0.15

Table 1: Average density values, (ρ), relative density (ρ_R) and percentage of deviation with respect to the nominal density values, (i.e. 562.5, 450 and 300 kg/m^3 for 1, 2, and 3 samples).

n- Elastic Modulus	Compression	Tensile	Three-point bending
1 wt% ADC	1.55	1.90	1.67
5 wt% ADC	2.02	2.08	2.14
10 wt% ADC	2.00	2.17	2.32
15 wt% ADC	2.12	2.14	2.10

Table 2: Values of *n* obtained for the fitting of relative elastic modulus calculated in different configurations.

n- Plastic Collapse	Collapse Stress *Compression*	Yield Strength *Tensile*	Flexural Strength *Three-point bending*
1 wt% ADC	2.17	2.42	1.65
5 wt% ADC	3.13	2.21	2.13
10 wt% ADC	2.9	2.44	2.03
15 wt% ADC	2.3	2.42	1.86

Table 3: Values of *n* obtained for the fitting of collapse stress, yield strength and flexural strength.

Structure-Properties Relationship of Medium Density Polypropylene Foams

C. Saiz-Arroyo[1,2], J.A. de Saja[1], M.A. Rodríguez-Pérez[1]

[1] Cellular Materials Laboratory, (CellMat). Condensed Matter Physics Department, University of Valladolid, Prado de la Magdalena s/n, 47011, Valladolid.

E-mail: csaiz@fmc.uva.es, marrod@fmc.uva.es

[2] Technological Centre of Miranda de Ebro, (CTME), C/ Montañana P R60-R61, 09200, Miranda de Ebro, Spain.

Abstract

This paper is focused on the production and characterization of a collection of polypropylene (PP) foams with relative densities ranging from 0.3 to 0.6. Samples were foamed using the improved compression moulding method. The used process allows controlling density and cellular structure independently as well as permits obtaining PP foams without fillers, crosslinking or using special PP grades. The influence of blowing agent content, density, cellular structure and foaming conditions on the mechanical response measured in compression, tensile, bending and Charpy impact tests has been determined. Results have shown that among density, open cell content and blowing agent concentration have a significant influence on the mechanical performance of medium density polypropylene foams.

Key-words: medium density cellular plastics, polypropylene, mechanical properties, microstructure.

Introduction

Cellular plastics or plastic foams, generally consists of a minimum of two phases, a solid polymer matrix and a gaseous phase derived from a blowing agent, [1]. Polymer foams are commonly employed in the sporting, transport and building industries for weight reduction and passive safety applications due to their light weight, good energy absorption capability and low manufacturing cost. Moreover as they combine good mechanical properties with a relative low density, polymeric foams can be also used as light weight structural materials [2].

Nevertheless, whatever they are used for, their optimisation needs the understanding of the structure-properties relationship. In the case of the mechanical response it is known that it mainly depends on density, but also on cellular structure, (cell size and shape, open/closed cell ratio, cell density, cell size distribution, etc), as well as on the intrinsic properties of the material comprising the cell walls [3-5].

Polymeric foams are generally mechanically characterized by means of different conventional methods such as compression, tensile, bending or impact tests. Each type of test can provide information about the deformation mechanisms involved in foam response. A deep knowledge and understanding of the behaviour of foams under different conditions is very useful to select the most suitable application for a given material as well as to provide useful information useful to optimize foaming process and thus obtaining tailored foams. [4]

Density of a cellular material is known to play the most important role in controlling foam properties. Thus polymeric foams can be classified regarding to their relative density values, (this is the density of the foam divided by that of the solid) in three categories, low, (ρ_R <0.3), medium (0.3<ρ_R<0.6) and high density foams, (ρ_R >0.6). [1, 5]

Low density foams can be produced by batch foaming, compression moulding, reactive or direct extrusion using a physical blowing agent among others, and are mainly used as heat barriers and sound absorbers, in flotation applications and as energy absorbing elements because they can be subjected to impact energy or force without generating a high stress. Due to their main fields of application knowing its response to compressive forces is indispensable. On the other hand, high density foams are mainly produced by extrusion, batch foaming or injection moulding processes and are mostly employed for structural purposes. So, in the case of high density cellular polymers is even more important to understand how they will behave under different mechanical solicitations. [5, 6]

Although low and high density foams are widely used and studied materials with applications in almost every field, medium density foams are not still completely established in the market. One of the key reason lies in a lack of suitable industrial foaming processes able to produce foams of different polymeric matrices and with relative densities in this range (between 0.3 and 0.6) [5].

Moreover, even though medium density foams should exhibit lower mechanical properties in terms of strength and stiffness than high density foams, or lower performance as energy absorbent elements than low density foams, (they generate higher stresses), knowing their mechanical behaviour under a wide variety of different conditions is very important to establish those materials in applications such as core of sandwich panels or replacing some structural elements in industries such as the automotive one or even to find new areas in which these materials could play a decisive role.

Despite the fact that density clearly determines foams response, the role played by microstructure can not be neglected. Cellular structure of a foam is mainly determined

by the foaming process used to blown the polymer, so parameters such as foaming temperature, pressure or blowing agent type and amount are determinant for the development of the foam microstructure. [1-6]

In this study, foams have been produced using the improved compression moulding route [7, 8]. This foaming technique uses chemical blowing agents and allows obtaining shaped foams as well as controlling density of the foam independently of the formulation. Due to this reason density and cellular structure can be controlled in an independent way. Several polymers, composites and nanocomposites, such as low density polyethylene, (LDPE), blends of ethylene vinyl acetate copolymer with aluminium hydroxide or starch and nanocomposites based on low density polyethylene and silica nanoparticles have been successfully foamed using this technique [7-11]. Nevertheless, up to now, so foamed materials have been only characterized using compression tests, so it is worthy to know how this foaming process can affect the general mechanical performance of the produced materials.

As it was previously mentioned, together with density and microstructure of the foam, the intrinsic properties of polymeric matrix are also responsible of foam behaviour. In this study polypropylene will be used as base polymer. PP is a polyolefin which is widely used in many engineering applications owing to their excellent physical and mechanical properties, good reciclability and low cost [12]. Therefore, polypropylene foams are promising materials with a wide range of applications in many fields.

Nevertheless, when compared to other polymers, the development of polypropylene foams took longer time mainly due to its poor foamability. Linear grades of polypropylene exhibit a low melt strength which leads to the rupture of cell walls during cell growth, this, results in foams with a high amount of coalesced and open cells [12-16]. Nowadays, the solutions to overcome this handicap are focused on increasing melt

strength of the polypropylene by the addition of fillers, the use of special PP grades, (highly branched grades known as high melt strength resins) or the crosslinking of the PP matrix [17-21].

All those ideas have lead to improved foamed products but it should be also remarked that all of them involve increasing the cost of the original product such as in the case of high melt strength polymers which are more expensive than conventional ones. Crosslinking has the main disadvantage of producing non-recyclable polymers and fillers can contribute to enhance foamability but in some cases can harm the mechanical or thermal properties of the unfilled foam.

Bearing all this ideas in mind, the first objective of this paper is obtaining medium density polypropylene foams without using fillers, crosslinking or special polypropylene grades by the improved compression moulding route. The second and main objective of this paper is to investigate the relationship between processing, structure and properties for those medium density PP foams.

Foams of different densities and with different amounts of a chemical blowing agent, (azodicarbonamide) have been produced. Microstructure of such foams have been characterized in terms of cell size, cell density and open cell content and mechanical response of the foams have been measured in compression, tensile, bending, and Charpy impact tests.

Materials and Processing Methods

Materials

A random polypropylene copolymer grade named 200CA10 and commercialized by Inneos has been used in this work. It has a melt flow index of 10g/min, (measured at 230ºC and 2.16kg); its melting point and crystallinity, both measured by DSC are 150.4ºC and 44.4% respectively. Azodicarbonamide Porofor ADC/M-C1 from Lanxess with an average particle size of (3.9 ± 0.6) μm has been used as chemical blowing agent. In order to prevent thermal oxidation of the polymeric matrix an antioxidant, Irganox B561 from Ciba was added (0.1wt%). Stearic acid was used as processing aid, (0.1wt%).

Foaming Process

As it was mentioned in the introduction, polypropylene was foamed using the improved compression moulding route which comprises three main steps. (Although the process is here briefly described a more detailed description can be found in references, [7-9]).

In a first step, all raw materials were melt compounded in a co-rotating twin screw extruder, Collin Kneter model ZK 25T SCD15. Temperature profile was chosen in order to avoid premature decomposition of the blowing agent. It was varied from 130ºC in the hopper to 155ºC in the die. Material was water cooled and pelletized. Compounds with different amounts of blowing agent, (1, 5, 10 and 15wt%) were prepared in order to analyze its effect on both microstructure and mechanical response of polypropylene foams.

The second step comprises preparing "precursor" materials; it consists in producing solid samples using the pellets previously compounded. Two different types of solid samples were prepared, cylinders and discs. Cylinders with 20mm in diameter and 15mm in height, and discs with 150 mm in diameter and 2mm in height were

compression moulded in a two-hot plates press. A temperature of 175ºC and a pressure of 95MPa for cylinders and 4 MPa for discs were employed to prepare those precursors.

The third step is the foaming one. It is conducted under mechanical pressure using a special type of moulds known as "self-expandable moulds" [7-9] which are able to control the expansion of the material, this is the density of the foam. A temperature of 205ºC, high enough to decompose the blowing agent was used for both cylinders and discs and a pressure of 95MPa for cylinders and 4 MPa for discs were used to produce the foams.

Foamed discs and cylinders with expansion ratios of 1.6, 2 and 3, (i.e. relative densities, 0.56, 0.45 and 0.3) were prepared using the improved compression moulding route and different blowing agent amounts. Those expansion ratios correspond to nominal densities of 562.5, 450 and 300 kg/m^2. At least 5 discs and cylinders of each type were prepared.

Samples designation is as described. For discs, a capital D followed by two numbers, first indicates blowing agent amount, (1, 5, 10, or 15wt%) and second one the expansion ratio, (1 for 1.6, 2 or 3). For cylinders is the same but with a capital C instead of a D. For example C-5-1 is a cylinder produced using a 5wt% of azodicarbonamide and with an expansion ratio of 1.6.

Table 1 summarizes the average relative density of the foamed discs and cylinders under study.

Experimental

Density

The density of solid precursor and foams was determined by the geometric method, this is by dividing the weight of each specimen by its corresponding volume. (ASTM Standard D1622-08)

Structural Characterization

Microstructure of foamed discs and cylinders was analyzed by SEM. Samples were frozen in liquid nitrogen and fractured; fracture surface of the samples was made conductive by sputtering deposition of a thin layer of gold and observed using a Jeol JSM-820 scanning electron microscope. Average cell diameter and cell density, this is the number of cells per unit volume, were determined using an image processing tool based on the software ImageJ, [22].

Open Cell Content

The percentage of open cells, (C) was measured with an Eijkelkamp 08.06 Lange air pycnometer according to ASTM D6226-10. The following equation, (1) was used according to the ASTM standard:

$$C = \frac{V_{Sample} - V_{Pycnometer}}{V_{Sample} \cdot p} \qquad (1)$$

where the geometrical volume, V_{Sample}, (calculated from the specimen dimensions) is subtracted from the total volume measured with the pycnometer, $V_{Pycnometer}$, and divided by the volume of air contained in the sample, ($V_{Sample} \cdot p$), where p is the sample porosity calculated by $\left(1 - \frac{\rho_f}{\rho_S}\right)$; ρ_f is the foam density and ρ_S is the density of the polymeric matrix, in this case polypropylene.

Mechanical Tests

Mechanical response of foamed polypropylene was measured under different conditions, thus, compression, tensile, bending and impact tests were carried out. In addition precursor materials (polypropylene with different ADC contents) and pure solid polypropylene were also characterized.

Compression tests were performed in the solid and foamed cylinders using an universal testing machine (Instron model 5500R6025). Experiments were performed at room temperature and at a strain rate of $10s^{-1}$. The maximum static strain was 75% for all the experiments. Elastic modulus (E_c), collapse stress (σ_c) and absorbed energy per unit volume (W) were determined from the stress-strain curves.

Tensile tests were also performed using the Instron 5500R6025, in accordance with ISO 527, at a strain rate of 20mm/min. Type 1A specimens were machined from foamed and un-foamed discs and five replicates for each material were run in order to ensure the reproducibility of the results. Tensile modulus (E_T), and stress at yield (σ_y) and stress and strain at break (σ_b and ε_b) were determined from tensile tests.

Flexural tests were performed using the same universal testing machine and in accordance with ISO 178 at a strain rate of 5mm/min. Flexural modulus (E_F),as well as flexural strength (σ_F) were calculated from the resulting curves.

The impact strength of foams and their corresponding precursors was obtained using a Charpy Pendulum Impact Tester Frank model 53.566. Tests were carried out following the UNE EN ISO 179-1/1eA procedure.

In all cases, samples were tested under controlled conditions of 23ºC and a 50% of relative humidity.

A more detailed description of the experimental methods used to characterize the foams has been published elsewhere, [23-27].

Results and Discussion

Microstructure

Micrographs of polypropylene foams with different densities and produced using different azodicarbonamide contents are shown in figure 1.

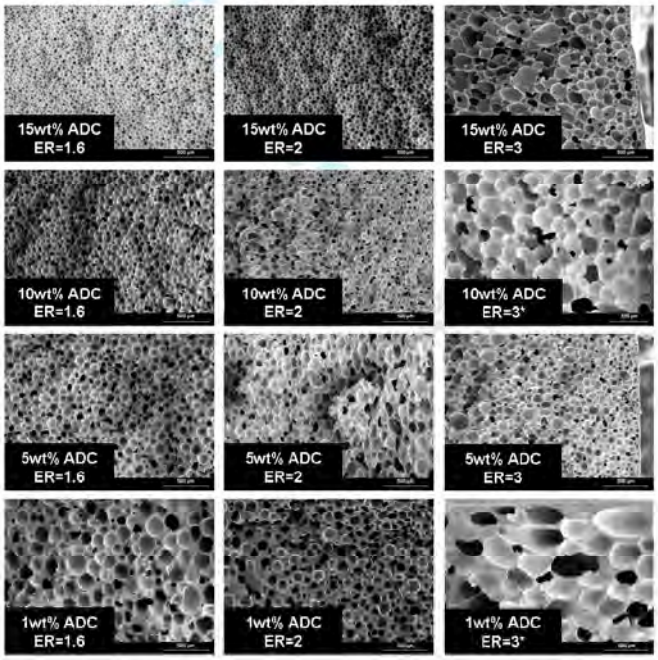

Figure 1: SEM micrographs of polypropylene foams with different expansion ratios (ER) foamed using different azodicarbonamide (ADC) contents.

Although the whole collection of samples exhibits a homogeneous and isotropic cellular structure, there is a clear dependence of cell size and cell density with both density and azodicarbonamide content. As it can be observed, cell size decrease and cell density increases when both density and blowing agent amount increase.

To easily understand these dependences, average values of cell size and cell density are represented as a function of blowing agent amount in figures 2a and 2b respectively. It can be clearly inferred that samples with higher densities exhibit smaller cell sizes regardless azodicarbonamide content used to blown them. For instance, samples with relative densities around 0.3 exhibit cell sizes three times higher than samples with relative densities around 0.6. On the other hand, cell density decreases as density does being the smallest values the ones exhibited by samples with the lowest relative density.

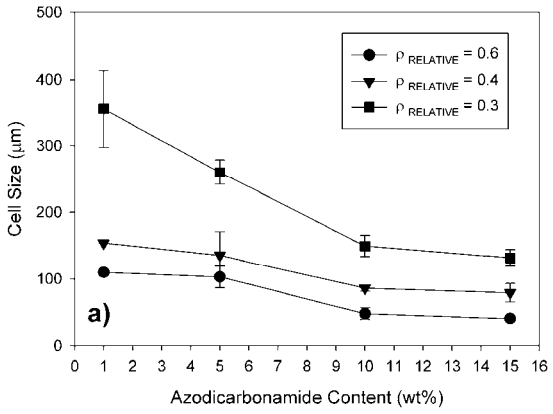

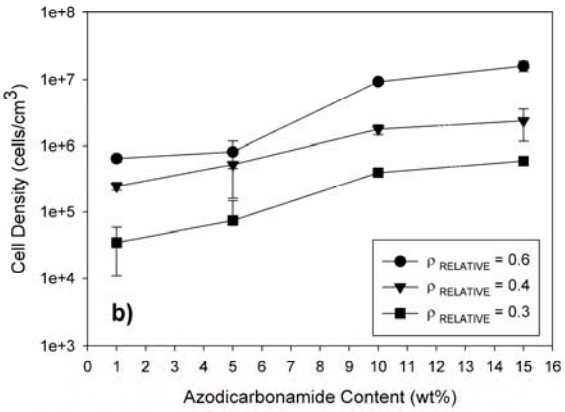

Figure 2: a) Cell size as a function of blowing agent amount for PP foams with different relative densities. b) Cell density as a function of ADC content.

The effect of azodicarbonamide content on cell size and cell density could be expected. Chemical blowing agents such as azodicarbonamide are self-nucleating the cells [6], so as blowing agent amount increases a higher number of nucleating sites are available, leading to higher nucleation rates and smaller cell sizes. In this case, the smallest cell sizes and the highest cell densities are obtained for samples with high relative density values, (0.6-0.4) blown using the highest azodicarbonamide contents, (10 and 15wt%). Moreover, for those samples cell sizes below 100μm are obtained.

In order to analyze in more detail the nucleating effect of azodicarbonamide particles its potential nucleation density can be estimated using equation 2, [28].

$$\frac{nucleants}{cm^3} = \frac{w_p \ \rho_c}{\rho_p \ V_p} \qquad (2)$$

where w_p is the weight fraction of the particle in the composite, ρ_p and ρ_c are the density of the particle and the polymer composite respectively, and V_p is the volume of the

individual particle. In this case it was assumed that azodicarbonamide particles are 3.9μm side cubes, being the density 1600 kg/m^3.

Table 2 summarizes the potential nucleation density of azodicarbonamide-polypropylene mixtures calculated according to equation 2. Those values are clearly higher than the cell densities exhibited by the produced polypropylene foams. This difference can be quantified by means of a parameter called "Cellular Structure Degeneration Ratio", (CSDR), which is defined as the ratio between the number of potential nucleating sites, (this is potential nucleation density) and the measured cell density.

During foaming step, several phenomena such as coalescence, coarsening, drainage among others can take place. For example, coalescence is caused by rupturing of cell walls during foaming step and should be suppressed in order to achieve a uniform and controlled cell growth. On the other hand cell coarsening leads to a reduction of cell density due to diffusion of gas from small cells to the larger ones. For example, excessive foaming time can promote this effect. [1] All these phenomena have a negative influence on the cellular structure development, leading to foams with cell densities lower than expected ones. Therefore, previously defined parameter (CSDR) can be considered as a quantitative measurement of the deterioration of the cellular structure during foam growth due to the previously mentioned mechanisms. CSDR values calculated for the whole collection of analyzed foams are presented in figure 3a. As it can be observed, once more, this parameter varies both with density and with azodicarbonamide content.

The lightest samples exhibit the highest values. As density decreases the stretching forces in the molten polymer should be higher in order to reach higher expansions

leading therefore to a higher number of broken cell walls. Regarding the effect of ADC concentration, as it decreases, CSDR parameter reaches higher values.

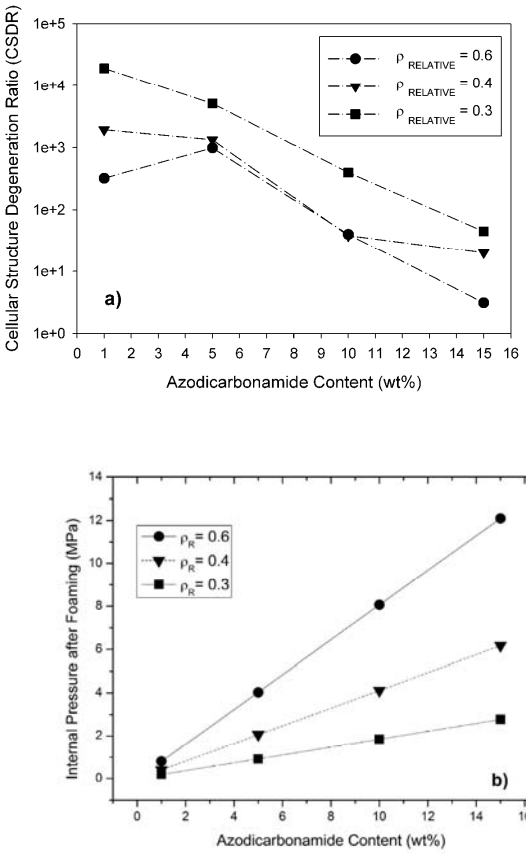

Figure 3: a) Cellular structure degeneration ratio, (CSDR), b) Internal pressure after foaming

This is an interesting new effect. Increasing the chemical blowing agent content results in a higher gas amount available for foaming. As a consequence the pressure after foaming (when the pressure is released and the material expands) increases, this is the foam is solidified under a significant pressure when high amounts of azodicarbonamide are used (see figure 3b). The experimental results seem to indicate that this external counter pressure is contributing in the stabilization of the cellular structure reducing the CSDR in a significant amount.

Other parameter which is closely related to the previously mentioned facts is the open cell content. Measuring the open/closed cell content ratio of a foam is essential to understand its macroscopic behaviour. Figure 4 shows the results.

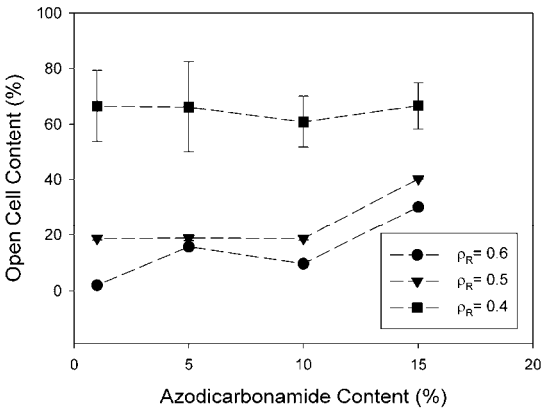

Figure 4: Open cell content of produced PP foams.

Open cell content increases as density decreases regardless of azodicarbonamide concentration. Once more, the reason of this behaviour can be attributed to the higher stretching forces required during foaming step, cell walls are thinner and thus easily breakable. It can be also inferred from figure 4 that open cell content keeps

approximately constant with the variation of ADC concentration although it increases for samples containing a 15wt% of chemical blowing agent..

Mechanical Response

Foamed samples as well as solid precursors and neat PP have been analyzed by performing the aforementioned measurements.

Compression Tests

Experimental results for elastic modulus and collapse stress are collected in figures 5a and 5b. When compared to neat polypropylene, solid precursors, (this is solid polypropylene with azodicarbonamide) present several differences. As ADC concentration increases, the materials become stiffer as the increase in elastic modulus indicates. On the other hand, the addition of ADC also leads to a loss of elasticity of the polymeric matrix due to a significant decrease in collapse stress just with the addition of 1wt% of blowing agent.

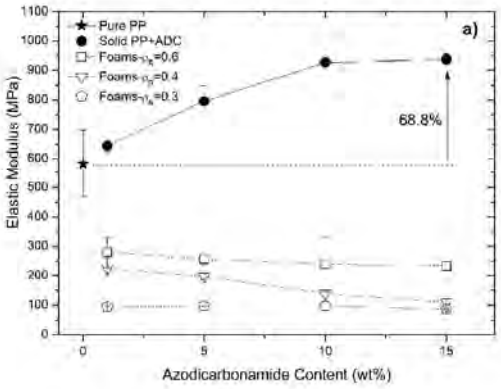

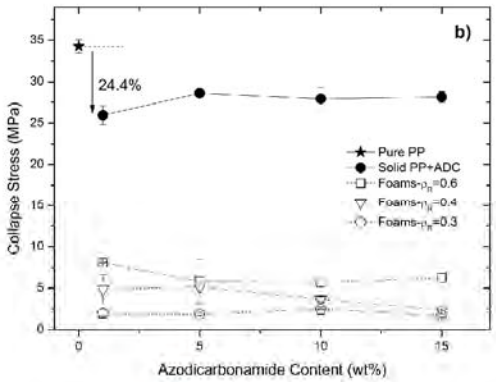

Figure 5: a) Results from compression tests, a) Elastic modulus, b) Collapse Stress.

As it could be expected, foamed samples exhibit smaller values of both elastic modulus and collapse stress than their corresponding precursors due to density reduction. With respect to the influence of azodicarbonamide content, it can be observed how for the lightest samples (ρ_R = 0.3) both E_C and σ_C remain constant independently of azodicarbonamide concentration. For denser samples ($\rho_R \geq 0.4$) the smallest values of those parameters are obtained when the highest amounts of azodicarbonamide content are used, (10 and 15wt%). This behaviour can be related with the higher open cell content of the samples containing higher amounts of ADC.

To clarify the previous fact, figure 6 shows both elastic modulus and collapse stress as a function of open cell content for each ADC concentration. This figure indicates that among density, mechanical response of foams is clearly conditioned by open cell content. The best mechanical response in terms of both strength and stiffness is reached for foams with very low open cell contents, (lower than 20%).

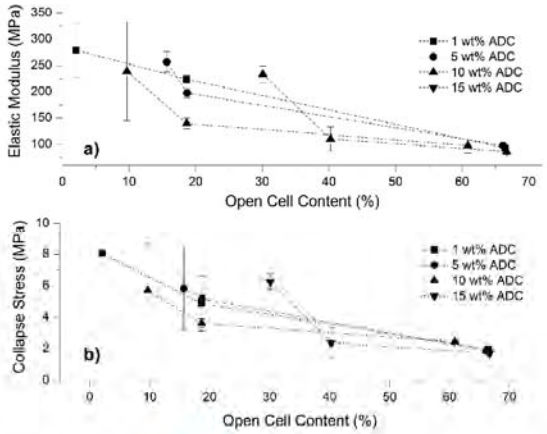

Figure 6: Relationship between open cell content and the compressive response of PP foams produced using different amounts of azodicarbonamide.

The value of absorbed energy per unit volume can be calculated as the area under the stress-strain curve. Taking into account that foams are typically used as energy absorbers, it is desirable to comprehend how both ADC concentration and density can affect the energy absorption capability of the analyzed PP foams. One well known method to analyze this characteristic is by using the so-called energy-absorption diagrams [2]. An energy-absorption diagram is obtained by plotting the absorbed energy, *W*, as a function of the stress. The absorbed energy (which is the area under the stress-strain curve) is calculated by:

$$W = \int_0^{\varepsilon} \sigma(\varepsilon) d\varepsilon \qquad (4)$$

By plotting together the absorbed energy-stress curves for the various foams it is simple to select the most adequate foam for packaging applications [2].

Figure 7aa shows energy-absorption diagrams for foams with different relative densities produced using a 1wt% of azodicarbonamide. The best foam for a given stress is the one that absorbs more energy up to this stress. Each foam has a stress value, (σ_p) for which it is the best choice; this value corresponds to the shoulder on the energy curve, (figure 7a). Moreover, the envelope of these points shows approximately a linear behaviour, ($W = a+b\sigma$), describing the relationship between absorbed energy and stress for an optimum choice of the foam [2].

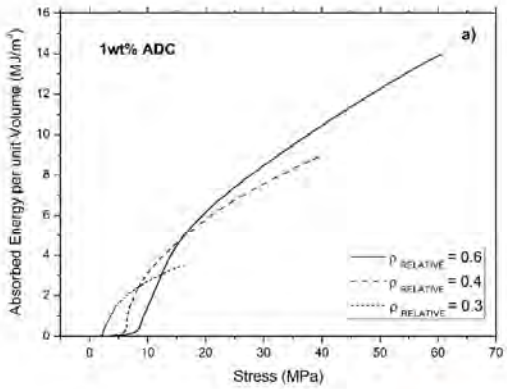

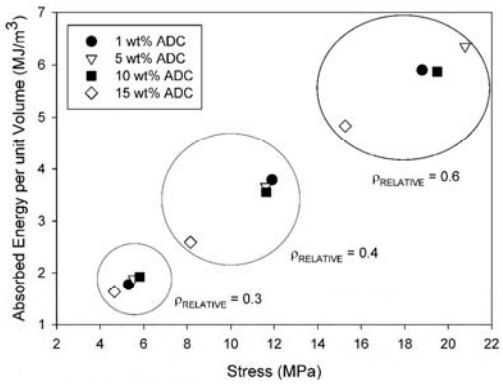

Figure 7: a) Energy absorption diagrams for samples with different relative densities blown using 1wt% of azodicarbonamide. b) Values of σ_p for the whole collection of analyzed PP foamed samples.

In this study, it is worthy to analyze the dependence of this linear trend with azodicarbonamide content. As for each azodicarbonamide content the three analyzed samples have similar densities the same linear function should be obtained. However the values of σ_p can give us an idea of which of the foams behaves better as energy absorbers.

σ_p has been calculated for all the analyzed samples and experimental results are shown in figure 7b. It can be observed the variation for each density with the ADC concentration. The dispersion in these values can give an idea of the influence of blowing agent amount in the absorption capability of the samples. For low density samples, there is a small influence of blowing agent concentration but as density increases, the dispersion in the values of σ_p increases considerably. As it can be inferred

from the figure values corresponding to 10 and 15wt% ADC-foamed samples are the ones out of the trend. It is detected that increasing the concentration of blowing agent amount leads to small cell sizes but not to better mechanical performance due to higher open cell contents.

By modifying the cellular structure it has been possible, for a given density, obtaining foams with different σ_p values. That would be suitable for being the optimum selection in different packaging applications.

Tensile tests

Average experimental values of tensile modulus (E_T), stress at yield (σ_y) and stress and strain at break (σ_B , ε_B) are plotted in figure 8 as a function of ADC concentration.

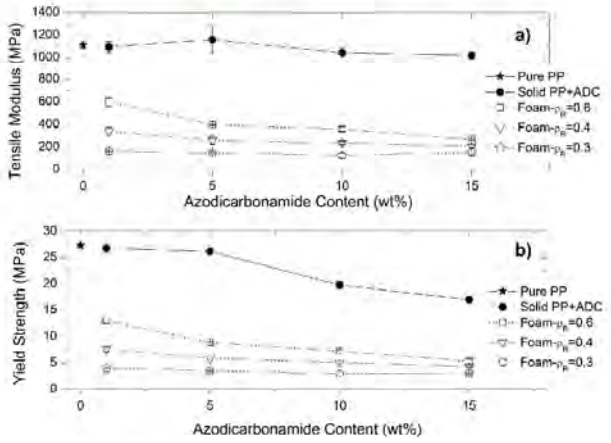

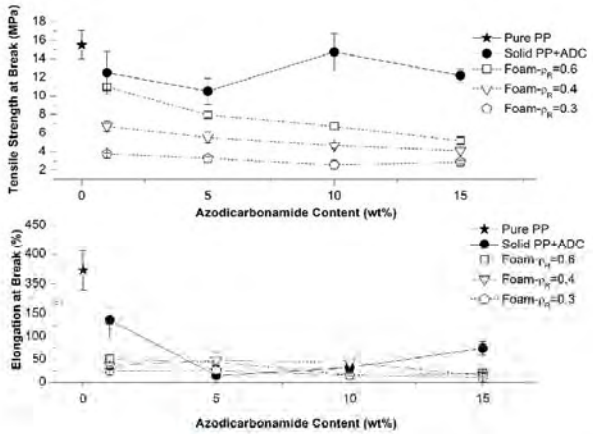

Figure 8: Experimental results from tensile tests. a) Tensile modulus, b) Tensile strength, c) Tensile strength at break, d) Elongation at break.

Solid precursors, (PP with different percentages of ADC) reach similar values of tensile modulus than that of the neat polymer. Unlike what happened for elastic modulus measured in compression tests, the presence of azodicarbonamide in the polymeric matrix does not affect the tensile response of the materials. As density is reduced, also tensile modulus decreases, so, foamed samples exhibit smaller values of tensile modulus than their corresponding solid precursors and of course than pure polymer. As it can be also observed in this figure, regardless of relative density, better mechanical response is reached when the smaller ADC concentration is used, (1wt%). This result is in agreement with the ones obtained in compression tests, and the explanation lies once more in the lower open cell content exhibited by such samples. At high ADC concentrations, (15wt%), samples show very similar values of tensile modulus regardless of the density. This behaviour can be due to two reasons. First one, is the very high open cell content present in these samples and the second one the presence of

ADC residues in the polymeric matrix comprising cell walls. It is known that after its decomposition, ADC can leave up to a 24% of its initial weight as a residue in the material [29]. The presence of such residues along the polymeric matrix could also contribute to reduce the elastic response of the polymer.

Yield strength is plotted in figure 8b. The presence of azodicarbonamide particles lead to lower values of both σ_y and ε_y. This result could be expected because in composite systems, the presence of a filler lead to a decrease in yield strength due to a non adequate adhesion between the non compatibilized filler and the polymeric matrix which produce cracks that become cavitations. With regard to foamed samples and as it was expected, density reduction induces a decrease in yield strength values. In addition, the increase in blowing agent concentration also contributes to decrease yield strength.

Similar trends are observed for tensile strength at break and elongation at break, (figures 8c and 8d). First one decreases for solids due to the presence of ADC particles and for foams due to density reduction and to the increment in ADC concentration. Second one (ε_b) also decreases for non-foamed materials due to the presence of the filler, (ADC) and for foamed materials remains approximately constant regardless of density and ADC concentration.

In foamed systems the explanation of fracture mechanisms is much more complicated than in solid ones due to the presence of the cells. It is well known that in foamed materials, the percentage of open cells has a significant influence on mechanical response; while in closed cell foams stresses are withstand by both walls and struts in open cell foams they are only borne by struts [2].

Moreover, a reduction in the amount of polymer leads to a decrease in the ability of the material to deform plastically. In addition, as filler amount increases, the material is stiffer and hence the transition from the linear regime to the fracture one is faster. As it

was said, a high open cell content, limit the plastic flow to cell struts leading to a decrease in mechanical performance [2].

All these facts can explain the results obtained for the analyzed foams. The presence of ADC residues in the polymeric matrix together with non-zero open cell content can contribute to have a poorer mechanical response for samples produced using high ADC concentrations, (10 and 15wt%) .

Flexural Tests

Flexural tests were also performed for the whole collection of samples; this is for foams, pure polypropylene and precursors, (solid polypropylene with different concentrations of azodicarbonamide). The obtained experimental data are collected in figures 9a and 9b.

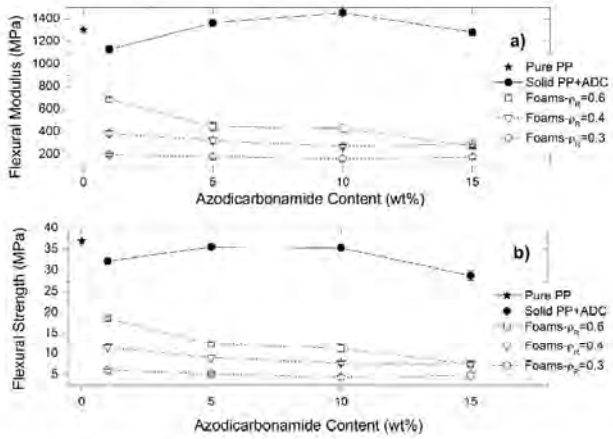

Figure 9: Results from bending tests. a) Flexural modulus, b) Flexural strength.

As in the case of tensile tests, for solid materials there was not found a clear tendency with the variation of ADC content indicating once again a poor interaction between azodicarbonamide particles and polypropylene matrix among a loose of elasticity of the polymeric matrix.

The response of analyzed polypropylene foams in flexural tests follows the trends previously observed for tensile tests. Mechanical response decreases with density decrease and at high relative densities also decreases with the increase in azodicarbonamide content.

Results are in agreement with the ones obtained for compression and tensile tests. Higher open cell content affects negatively the mechanical response. Besides, for bending tests it is even more evident the loose of ductility of the polymeric matrix due to the presence of azodicarbonamide decomposition residues in the polymer comprising cell walls. Samples with relative densities around 0.6 made using a 15wt% of ADC exhibit values of both flexural modulus and strength similar to samples of much lower relative density, (around 0.4).

Charpy Impact Tests

Charpy Imact test determines the amount of energy absorbed by a material during fracture and can be considered as a measure of materials toughness.

In figure 10 the results obtained for foamed specimens are compared with those obtained for solid precursors and pure polypropylene. As it can be observed the addition of 1wt% of azodicarbonamide to the polypropylene matrix leads to a significant decrease of impact resistance. As azodicarbonamide content increases the material becomes more brittle.

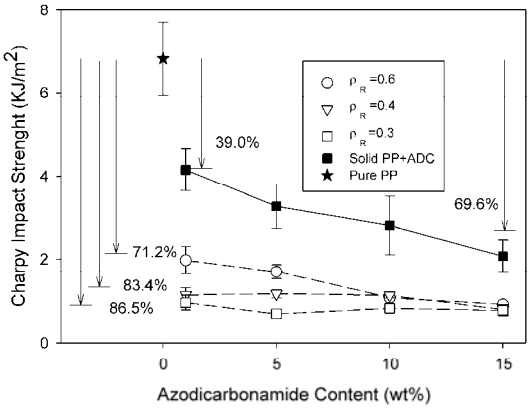

Figure 10: Charpy impact strength of foams and precursors.

Impact strength decreases when the material is foamed. Results for foams are around twofold lower than for their corresponding precursors but six times lower than the one corresponding to the neat polymer. Once again the properties are reduced when higher amounts of ADC are included and the density is reduced. The reasons for this behaviour are the same justifying the previous findings.

Conclusions

Medium density polypropylene foams (relative density between 0.3 and 0.6) have been produced using the improved compression moulding route with different blowing agent contents. In addition and as it was said in the introduction, any filler or special PP grade was used to produce such foams.

The relationship between mechanical response-microstructure-density and foaming process has been analyzed

Microstructure of the foams has been studied concluding that cell size and cell density depends on both density and azodicarbonamide concentration. The use to this foaming technique allows obtaining a wide variety of cellular structures by tunning density and chemical blowing agent concentration. For instance using high ADC concentrations, it can be obtained samples with cell sizes smaller than 100μm and significant open cell contents. In addition using very small ADC concentrations, samples with almost a completely closed cellular structure can be achieved.

Mechanical response of foams and solid precursors has been determined. Results have shown that the presence of ADC particles in the polymeric matrix lead to a decrease in polymer elasticity.

It has been observed that cell size or cell density do not have a significant influence on the mechanical response of foams while open cell content does. In addition with regard to foaming process influence, the addition of high amounts of ADC reduces mechanical performance of the material due to an increment in open cell content and to a loose of elasticity of polymeric matrix due to ADC residues.

Therefore, to maximize the response of medium density polypropylene foams produced by the improved compression moulding route, the best choice is using the smallest ADC concentration, (1wt%). Such concentration promotes foams with near-zero open cell contents and a insignificant amount of residues in the polymeric matrix, and as it was said this combination maximizes mechanical performance of the materials.

However, samples with non-negligible open cell contents can also find a place in applications related with sound absorption. For that purpose, it is desired a high degree of interconnection between cells. Therefore, the combination of a good mechanical response and a certain percentage of open cells can produce foams suitable for sound absorption applications in industries such as the automotive one.

Acknowledgements

Financial assistance from Spanish Ministry of Science and Education and Feder Program, (MAT 12009-14001), Innocash Project (INC-0193) as well as The European Spacial Agency (ESA) Project (MAP AO-99-075) are gratefully acknowledged.

References

[1] Klempner D, Sendijarevic V, Handbook of polymeric foams and foam technology. 2nd Edition, Hanser Publishers, Munich (2004).

[2] Gibson L, Ashby F. Cellular Solids: Structure and Properties. 2nd Edition, Cambridge University Press, United Kingdom, (1997).

[3] Gendrom R. Thermoplastic Foam Processing. Principles and Development. CRC Press, Boca Raton-Florida, (2004).

[4] Lee S T, Park C B, Ramesh N S. Polymeric Foams. Science and Technology. CRC Press, Boca Raton-Florida, (2007).

[5] Throne L. Thermoplastic Foams Extrusion. Hanser Publishers, Munich (2004)

[6] Eaves D. Handbook of Polymeric Foams. Rapra Technology, United Kingdom, (2004).

[7] Rodríguez-Pérez M A, Lobos J, Pérez-Muñoz C A, de Saja J A, *Cell Polym* **27**: 327-342, (2008)

[8] Rodríguez-Pérez MA, Lobos J, Pérez-Muñoz C A, de Saja J A. *J Cell Plast* **45**: 389-403, (2009).

[9] Rodríguez-Pérez M A, Román-Lorza S, Alvarez-Laínez M, Montoya-Mesa C, Contantino C, de Saja J A. *Polym Eng Sci* **52**: 62-70 (2012).

[10] Roman-Lorza S, Rodríguez-Pérez M A, de Saja J A. Cell Polym 28: 249-268 (2009)

[11] Rodríguez-Pérez M A, García de Acilu-Laa P, Arevalo-Gutierrez J, Saiz-Arroyo C, de Saja J A, Proceedings Antec 2009.

[12] Pasquini N, Polypropylene Handbook, Hanser Publishers, Munich (2005).

[13] Naguib H E, Park C B, Panzer U, Reichelt N, *Polym Eng Sci* **42**: 1481-1492 (2002)

[14] Naguib H E, Park C B, Reichelt N, *J App Polym Sci* **91**: 2661-2668 (2004)

[15] Xu Z M, Jian X L, Liu T, Hu G H, Zhao L, Zhu Z N, Yuan W K. *J Supercrit Fluid* **41**:299-310 (2007).

[16] Park C B, Cheung L K, *Polym Eng Sci* **37**: 1-10 (1997).

[17] Rodríguez-Pérez M A, *Adv Polym Sci* **184**: 1-30 (2005)

[18] Zheng W G, Lee Y H, Park C B, *J App Polym Sci* **117**: 2972-2979 (2010)

[19] Zhai W, Kuboki T, Wang L, Park C B, Lee E K, Naguib H E. *Ind Eng Chem Res* **49**: 9834-9845 (2010).

[20] Antunes M, Velasco J I, Realinho V, Solórzano E. *Polym Eng Sci* **49**: 2400-2413 (2009).

[21] Bhattacharya S, Gupta R K, Jollands M, Bhattacharya S N. *Polym Eng Sci* **49**: 2070-2084 (2009).

[22] J.Pinto, M.A. Rodríguez-Perez, J.A. de Saja, Development o an Image J Macro to Characterise the cellular Structure of Polymeric Foams, XI Reunión del Grupo Especializado de Polímeros (GEP), 10-24 September 2009, Valladolid. (Spain).

[23] Rodríguez-Pérez M A, Velasco J I, Arencon D, Almanza O, de Saja J A. *J App Polym Sci* **75**: 156-166 (2000).

[24] Mills N J, Rodríguez-Pérez M A. Cell Polym 20: 79-100 (2001)

[25] Landete-Ruiz M D, Martínez-Díez J A, Rodríguez-Pérez M A, de Saja J A, Martín-Martínez J M. *J Adhes Sci Technol* **16**: 1073-1101 (2002).

[26] Almanza O, Rodríguez-Pérez M A, de Saja J A. *Polym Int* **53**: 2038-2044 (2004)

[27] Velasco J I, Antunes M, Ayyad O, López Cuesta J M, Gaudon P, Saiz-Arroyo C, Rodríguez-Pérez M A, de Saja J A. *Polymer* **48**: 2098-2108 (2007)

[28] Zhai W, Yu J, Wu L, Ma W, He J, *Polymer* **47**: 7580-7589 (2005)

[29] Batthi A S, Dellimore D. *Thermochim Acta* **76**: 63 (1984)

CYLINDERS							
1 wt% ADC		5 wt% ADC		10 wt% ADC		15 wt% ADC	
Sample	ρ Relative	Sample	ρ Relative	Sample	ρ Relative	Sample	ρ Relative
C1-1	0.595	C5-1	0.588	C10-1	0.554	C15-1	0.493
C1-2	0.487	C5-2	0.492	C10-2	0.465	C15-2	0.389
C1-3	0.342	C5-3	0.317	C10-3	0.311	C15-3	0.306
DISCS							
1 wt% ADC		5 wt% ADC		10 wt% ADC		15 wt% ADC	
Sample	ρ Relative	Sample	ρ Relative	Sample	ρ Relative	Sample	ρ Relative
D1-1	0.725	D5-1	0.618	D10-1	0.621	D15-1	0.553
D1-2	0.543	D5-2	0.483	D10-2	0.458	D15-2	0.432
D1-3	0.350	D5-3	0.382	D10-3	0.347	D15-3	0.336

Table 1: Relative density of foamed discs and cylinders produced by the improved compression moulding technique.

Azodicarbonamide Content (wt%)	Potential Nucleation Density (cells/cm^3)
1	9.53×10^7
5	4.85×10^8
10	9.93×10^8
15	1.53×10^9

Table 2: Potential nucleation density of PP-ADC mixtures.

Capítulo 7

Estudio Comparativo de Materiales Celulares Basados en PP y LDPE/SiO_2 Producidos Mediante Disolución de CO_2 y Moldeo por Compresión Mejorado

En este capítulo se realiza un estudio comparativo entre los procesos de disolución de CO_2 (*pressure quench method en molde*) y moldeo por compresión mejorado. Para ello se utilizan dos sistemas distintos, por un lado en primer lugar materiales celulares basados en nanocompuestos de LDPE/SiO_2 y por otro materiales celulares con base polipropileno.

7.1.- MATERIALES CELULARES BASADOS EN NANOCOMPUESTOS DE LDPE/SiO_2

En esta sección se presenta un artículo titulado *"Influence of Foaming Process on the Structure-Properties Relationship of Foamed LDPE/Silica Nanocomposites"* enviado a la revista **Composites Part B: Engineering**.

El espumado de nanocompuestos mediante disolución de CO_2 o N_2 (batch foaming) es una práctica sumamente habitual y la mayoría de las publicaciones relacionadas con la fabricación y/o caracterización de nanocompuestos espumados está centrada en ese tipo de procesos. La utilización de agentes espumantes de tipo químico es mucho menos habitual aunque es posible encontrar algunos ejemplos. En este trabajo, se hace un estudio comparativo de la microestructura y propiedades de nanocompuestos espumados mediante dos procesos diferentes. Por un lado utilizando la versión modificada del *pressure quench method* (descrita en el capítulo 3 y que incluye el espumado en el interior de un molde) que se basa en el uso de un agente espumante de tipo físico y por otro lado, la ruta ICM, que como ya se ha mencionado utiliza un agente espumante de tipo químico.

Se han tomado como punto de partida los materiales descritos en el capítulo 4, más concretamente el sistema con compatibilizante y se han fabricado una serie de espumas con el mismo grado de expansión, (ER=1.6) y los mismos contenidos de nanopartículas de sílice (1, 3, 6, y 9 % en peso) que los previamente descritos, pero esta vez utilizando la ruta ICM y un 5% en peso de agente espumante, (azodicarbonamida).

Este tipo de estudios comparativos no son habituales debido a que en la mayoría de los casos las irregularidades que presentan las muestras hechas por disolución de gas limitan su caracterización al nivel microscópico. En este caso, dado que ambos procesos producen muestras moldeadas (cilindros) es posible caracterizar tanto su estructura como sus propiedades físicas, (respuesta mecánica). En general se puede decir que el objetivo principal es analizar de forma comparativa la influencia de la presencia de las nanopartículas en la relación estructura propiedades de nanocompuestos espumados utilizando agentes físicos y químicos.

El análisis mediante microscopía electrónica de transmisión y microscopía electrónica de alta resolución de los nanocompuestos sólidos revela que las partículas no están dispersadas de forma individual sino formando agregados con un tamaño aproximado de entre 100 y 200nm. Además se observa en ambos tipos de micrografías que el tamaño de los agregados aumenta al aumentar la concentración de nanopartículas.

Todas las muestras (independientemente del proceso de producción) presentan una estructura celular isótropa y bastante homogénea. En ambos tipos se produce un descenso del tamaño de celda y un aumento en la densidad celular debido a la presencia de las nanopartículas aunque la tendencia con el aumento de la concentración de las mismas difiere considerablemente según se utilice CO_2 o ADC. El contenido óptimo de sílice es del 1% para las muestras producidas utilizando CO_2 y del 6% para las producidas usando ADC, si bien, el porcentaje de reducción al que se llega es aproximadamente el mismo. Para contenidos superiores al óptimo, en ambos casos, el efecto nucleante de las partículas se mitiga. La efectividad como agentes nucleantes de las nanopartículas de sílice en cada uno de los sistemas se puede cuantificar calculando un parámetro conocido como *Nucleation Ratio*, el cual compara el valor de la densidad celular de una muestra cargada con el de otra sin partículas. Los resultados indican que el efecto nucleante en el sistema que utiliza un agente espumante de tipo químico es superior al producido en el que utiliza un agente de tipo físico.

La obtención de estructuras con distribuciones de tamaños de celda más homogeneos es otra de las razones para utilizar nanocargas. En este caso, se ha calculado el valor del parámetro SD (capítulo 2) para comparar ambos tipos de muestras. En los materiales sin carga, (LDPE puro espumado), la distribución más homogenea se obtiene utilizando CO_2, sin embargo, tras añadir partículas esta tendencia se invierte, pasando a ser más homogénea en los materiales producidos utilizando azodicarbonamida.

La estabilidad térmica de todos los tipos de materiales, (nanocompuestos sólidos y aligerados) aumenta debido a la presencia de nanopartículas de sílice en la matriz polimérica siendo el porcentaje óptimo en todos los casos 9%. El porcentaje de mejora es aproximadamente igual para los nanocompuestos sólidos y los espumados utilizando CO_2 y ligeramente inferior para aquellos producidos con ADC.

La respuesta mecánica de los materiales ha sido medida realizando ensayos de compresión. Las curvas esfuerzo-deformación de ambos tipos de materiales revelan una respuesta mecánica superior de los materiales producidos por disolución de CO_2, ya que éstos presentan un contenido de celda abierta cercano a cero. Se ha calculado el módulo de elasticidad, el esfuerzo de colapso y la densidad de energía absorbida para

cada material. En cada caso, la concentración óptima de sílice para maximizar cada uno de los parámetros es diferente. De cualquier manera, aunque la respuesta mecánica de los materiales producidos por disolución de gas es superior, el porcentaje de mejora conseguido al incluir las partículas nanométricas en las muestras fabricadas con azodicarbonamida es considerablemente superior. El análisis de las propiedades relativas pone de manifiesto una vez más que la presencia de un cierto porcentaje de celdas abiertas afecta de forma negativa a la respuesta mecánica de los materiales celulares.

Se puede concluir por tanto que la presencia de nanopartículas mejora en general las características de materiales celulares con base LDPE, sin embargo dichas mejoras están sumamente condicionadas por el tipo de proceso de espumado utilizado, ya que en último término el proceso de espumado condiciona el tipo de estructura celular obtenida en cada caso.

Influence of Foaming Process on the Structure-Properties Relationship of Foamed LDPE/silica Nanocomposites

C. Saiz-Arroyo[1, 2],M.A. Rodríguez-Pérez[1], J.I. Velasco[3], J.A. de Saja[1]

[1] Cellular Materials Laboratory, (CellMat), Condensed Matter Physics Department, University of Valladolid, 47011, Valladolid, Spain. Email: csaiz@fmc.uva.es, marrod@fmc.uva.es

[2] Technological Centre of Miranda de Ebro, (CTME), 09200, Miranda de Ebro, Burgos, Spain.

[3] Centre Catalá del Plástic. Universitat Politècnica de Catalunya. C/Colom 114. E-0822, Terrassa, Barcelona, Spain.

Abstract

In this paper LDPE/silica nanocomposites are foamed by two different processes. First one is the pressure quench method which is based on the use of a physical blowing agent and second one is the improved compression moulding technique. As the latter process uses a chemical blowing agent, both types of foamed nanocomposites will provide very useful information about the relationship between foaming process-microstructure and macroscopic properties. Results have revealed how silica nanoparticles are able to act as nucleating sites during foaming step in both processes; however, the optimum amount of particles strongly depends on the foaming route. Thermal and mechanical properties of solid and foamed nanocomposites have been analyzed by means of thermogravimetric analysis and compression tests. Results have revealed that nanosilica particles act as effective nucleating agents, no only reducing cell size and increasing cell density but also achieving more homogeneous cellular

structures. Thermal and mechanical properties are improved due to the presence of silica nanoparticles. It has been found that the improvement degree reached for samples produced using chemical blowing agents is greater than that achieved for samples produced using physical blowing agents.

Key-words

A. Foam; A. Particle-reinforcement; B. Microstructures; B. Mechanical properties.

Introduction

The combination of functional nanoparticles and polymer foaming technologies has generated a new class of materials known as nanocomposite foams. Those materials exhibit enhanced thermo-mechanical properties as a result of the multifunctional role played by nanoparticles in such systems. Nanofillers act as nucleating agents for bubble formation promoting an improved cell morphology which at the same time lead to an overall increase in macroscopic properties. [1, 2].

Due to these outstanding characteristics, the amount of papers dealing with the production and characterization of polymeric nanocomposite foams has rapidly increased in the last few years. Thus, it is possible to find a wide variety of polymeric matrices such as polypropylene, polylactic acid, polystyrene, polyurethane, polycarbonate, poly-methyl-methacrylate, polyethylene, etc., infused with several types of nanoparticles, namely, nanoclays (mainly montmorillonite), carbon nanotubes, carbon nanofibers or silica particles. [3-13]

Polymer nanocomposites can be foamed by any of the existing foaming processes using either physical or chemical blowing agents [2]. Nevertheless the vast majority of the

published studies use the one or two steps batch foaming process which is based on the dissolution of a physical blowing agent in a polymer under high temperature and/or pressure. This foaming route presents several advantages and it is appropriate to analyze the nucleating effect of nanofillers as no other additives have to be introduced in the formulation. However it presents a severe drawback; it is not easy to obtain samples with a defined shape or geometry and therefore, the possibilities of measuring the macroscopic properties of foamed materials are limited. In previous papers [14] we have presented a solution to overcome this problem. It consists in introducing the precursor of solid nanocomposite in a mould with the ability to control both density and shape of the foamed product.

The use of chemical blowing agents to produce nanocomposite foams is not very common, however, it is possible to find some examples using injection moulding, extrusion and compression moulding processes [15-23].

Foaming injection moulding processes allow obtaining very well shape-defined materials. There is a huge amount of parameters involved in the process and several authors such as Guo et al [15] have proved that an accurate control of such parameters can lead to the same degree of improvement that the addition of nanoparticles to the polymeric matrix.

Foam extrusion can be carried out in single or twin-screw extruders, but regardless of the machine type, it is necessary to have a very high pressure drop at the die in order to have a material with an optimum cellular structure [24]. Due to their nucleating effect, nanoparticles can contribute to enhance the homogeneity of the microstructure, but the requirements concerning the high pressure drops limits the shape and size of the extruded foams. Thus, it is possible to find, ultra-low density foamed sheets, (density around 20-30kg/m^3) [24] or filaments, with higher densities, but with such small

diameter, (between 0.5 and 2mm) that are only suitable for the analysis of the cellular structure; it is not possible to measure the mechanical properties [16, 17].

Single or two-steps compression moulding have been widely used both for scientific and industrial purposes due to their relatively simplicity [19-23]. Two-steps process usually involves crosslinking the polymeric matrix to be able to obtain low density foams. Although this is beneficial for the process, it is not adequate from an environmental point of view, because turns the polymer non-recyclable by conventional methods [19, 20, 23]. The single-step process only comprises the addition of a chemical blowing agent to the nanocomposite and after that foaming it by applying temperature [21].

The improved compression moulding route was developed in the CellMat laboratory several years ago and it is a modified version of the single-step compression moulding process. It permits obtaining net-shaped foamed materials with homogeneous cellular structures. In addition, it is not necessary to crosslink the polymeric matrix to produce foams of different densities, due to the combination of a close control of both temperature and pressure together with the use of specific moulds. This foaming route has been used to produce foams of several pure polymeric matrices such as LDPE or PP, or conventional composites such as LDPE with high concentrations of aluminium or magnesium hydroxide, or EVA with starch, but up to now it has never been reported its use to produce foams of polymeric nanocomposites [25-31].

Bearing all this ideas in mind, it is possible to define the main objectives of this paper. The first one will be the production of LDPE/silica nanocomposites by the melt-compounding route. The second objective will be to foam such nanocomposites using the pressure quench method and the improve compression moulding route. The third

objective is to gain knowledge on the relationship foaming process-microscopic-macroscopic properties for the foamed nanocomposites.

Experimental

Materials

Low density polyethylene supplied by Sabic, (LDPE 2404) with a melt flow index of 3.95 g/10min (measured at 190ºC and 2.16kg), a density of 0.92 g/cm^3 and a melting point of 113.4ºC, (measured by DSC) was used. Silica nanoparticles were kindly provided by Evonik and presented a primary particle size of 12nm and a specific surface area of 200m^2/g. In addition particles' surface was modified with a silane coupling agent (dimethyldichlorosilane).

In order to improve the interfacial adhesion between the silica particles and the LDPE matrix a compatibilizer, (Fusabond MB-226DE from Dupont) was used. It is a maleic anhydride grafted linear low density polyethylene with a melt flow index of 1.5g/10min (measured at 190ºC and 2.16kg), a melting point of 115ºC (measured by DSC), a density of 0.93 g/cm^3, and a content of maleic anhydride of 0.9 % by weight. A small amount of stearic acid, (Stearic Acid 301 from Renichem S.L.) was used as processing aid. In order to prevent thermal oxidation of the polymer, an antioxidant (Irganox 1010 from Ciba) was also added to the compounds.

As chemical blowing agent azodicarbonamide (ADC), (Uquifoam L, kindly supplied by Uquinsa), with an average particle size of 4.9 μm was used. Zinc oxide (Silox Active grade provided by Safi Alcan) was used as ADC activator. Carbon dioxide with a high purity, (99.95%) was used as physical blowing agent.

Foaming: Improved Compression Moulding

This foaming route comprises three main steps.

1st Stage: Blending

The first stage of the process involves the production of the LDPE/silica solid nanocomposites by the melt-compounding route. A high concentration of silica particles, (27wt%) and a 4wt% of compatibilizer as well as the rest of the raw materials were mixed in a batch mixer, (Rheodrive 500 from Haake Fisions) at a constant temperature of 130ºC and a screw speed of 50 rpm during 6 minutes. Such masterbatch was afterwards diluted with the LDPE matrix under the same conditions in order to obtain several compounds with different silica contents, (namely, 0, 1, 3, 6 and 9wt%). Those solid nanocomposites will be called hereafter as S-0, S-1, S-3, S-6 and S-9. The density and the chemical composition of solid LDPE/SiO_2 nanocomposites are detailed in table 1

2nd Stage: Production of solid precursors.

The solid nanocomposites fabricated in the first stage are first of all blended with the chemical blowing agent as well as with the activator, (ZnO) in the same way as they were produced, this is in a batch mixer at 130ºC during 6 minutes at a constant screw speed of 50rpm. Blowing agent concentration was fixed for all the experiments at a constant value of 5wt%. So obtained pellets were used to produce cylindrical shaped precursors of 15mm in height and 20 mm in diameter in a two hot-plates press at a temperature of 130ºC. A pressure of 4 MPa was applied during 10 minutes.

Precursors for each silica concentration were produced. Their density was measured in order to assure an accurate densification of the materials.

3rd Stage: Foaming

Cylindrical precursors were introduced in a special mould which has the ability to control the final density of the material [31]. The mould is subjected to both temperature and pressure in a two-hot plates press. An initial pressure of 8 MPa is applied and as the temperature rises up to the foaming temperature (170ºC). The chemical blowing agent decomposes and the pressure inside the mould increases above the initial value. After a certain time, when ADC is fully decomposed pressure inside the mould stabilizes. At this point, the applied pressure is relaxed allowing the polymer to expand. The mould is cooled down in cold water in order to stabilize the cellular structure as fast as possible.

At least five foams per each silica concentration were fabricated. The samples produced using this foaming route will be called hereafter as ICM followed by a number indicating the silica concentration, this is ICM-0, ICM-1, ICM-3, ICM-6 and ICM-9.

To focus the analysis on the effect of the silica particles, relative density (this is the density of the foam divided by that of the solid precursors) of the samples was fixed at a constant value of around 0.6. Chemical composition as well as average relative density of ADC blown foams are detailed in table 2.

Foaming: Pressure Quench Method

Solid LDPE/silica composites were prepared following the procedure described before. They were used as solid precursors to obtain foams by the pressure quench method. Pellets of each composition were in a first stage compression-moulded using a two-hot

plates press to produce discs of 3mm in height and 15 mm in diameter. A temperature of 130ºC and a pressure of 4 MPa were applied during 10 minutes.

Solid precursors are introduced in a mould [14] which at the same time is placed in a high pressure vessel. Samples are saturated with CO_2 at 18MPa for 40 minutes at a constant temperature of 135ºC. After saturation time, samples were cooled down until foaming temperature, (115ºC) and foamed by a rapid pressure drop.

As it was carried out for ADC-blown samples, relative density of foams produced by the pressure quench method was fixed at a constant value of 0.6. Due to the use of a mould, a very accurate control of samples density can be achieved. Table 3 summarizes both chemical composition and density of foams blown using CO_2.

Such samples will be denoted as GD followed by a number indicating SiO_2 concentration, (i.e. GD-0, GD-1, GD-3, GD-6 and GD-9).

Characterization of Solid and Foamed LDPE/Silica Composites

Density measurements of foams and solids were performed by Archimedes principle using the density determination kit for the AT261 Mettler-Toledo balance, following the standard UNE-EN 1183/1.

The dispersion degree of silica nanoparticles in solid nanocomposites was analyzed by high resolution scanning electron microscopy, (ESEM, Quanta 200FEG) as well as by transmission electron microscopy, (TEM-Hitachi H-800). Samples for high resolution SEM were frozen using liquid nitrogen and afterwards fractured. Samples for TEM observations were cut into very thin sheets (typical thickness of 60 nm) using an ultramicrotome, (Ultracut E from Reichert-Jung).

Cellular structure of samples produced by using either ADC or CO_2 was analyzed by SEM. A Jeol JSM-820 scanning electron microscopy was used. Samples were freeze-fractured in liquid nitrogen and the fractured surface was made conductive by sputtering deposition of a thin layer of gold. Cell size and cell density were determined using an image processing tool based on the software Image J [32].

The percentage of open cells, (C) was measured with an Eijkelkamp 08.06 Lange air pycnometer according to ASTM D6226-10. The following equation, (1) was used according to the ASTM standard:

$$C = \frac{V_{Sample} - V_{Pycnometer}}{V_{Sample} \cdot p} \qquad (1)$$

where the geometrical volume, V_{Sample}, (calculated from the specimen dimensions) is subtracted from the sample volume measured with the pycnometer, $V_{Pycnometer}$, and divided by the volume of air contained in the sample, ($V_{Sample} \cdot p$), where p is the sample porosity calculated by $\left(1 - \frac{\rho_f}{\rho_S}\right)$; ρ_f is the foam density and ρ_S is the density of the polymeric matrix, in this case polypropylene, (ρ_S = 910 kg/m^3).

The effect of silica particles on thermal stability of foamed and non-foamed composites was analyzed by thermogravimetric analysis. Measurements were performed in a Mettler TGA/SDTA 851^e equipment. Samples were heated from 50ºC to 850ºC at a heating rate of 20ºC/min under nitrogen atmosphere. Samples mass was approximately 10mg. The thermal stability of the samples was determined using the peak of the first derivate curve of the thermograms.

As both foams and solids exhibit a perfect regular shape, (cylinders), it was possible to carry out compression tests to determine how silica content and foaming process type affect the mechanical response of the materials. Experiments were performed in a universal testing machine, (Instron 5500R6025) at a strain rate of 1mm/min up to a

maximum strain of 75%, (following the standard ISO 604-2002). Elastic modulus, (E), collapse stress, (σ_c) and density of absorbed energy, (W) were calculated from the stress-strain curves.

A more detailed description of the experimental methods used to characterize the foams has been published elsewhere, [33-36]

Results and Discussion

Density

Density and relative density values of foamed and non-foamed samples are summarized in tables 1, 2 and 3. It can be observed that relative density of ADC-blown samples is slightly lower than those of the CO_2 ones. The reason is related with the foaming process itself; using the improved compression moulding route, small amounts of material can sometimes leak out of the mould leading to samples with densities slightly lower than the nominal one.

However, the accuracy of both processes to obtain samples with customized densities is very good. The whole collection of samples presents relative densities very similar to the expected one, (0.6). As far as we now, no papers have reported or achieved such accuracy in obtaining net-shaped samples with controlled density using the pressure quench method.

Dispersion Degree of Silica Particles in Solid Nanocomposites

Quantifying the dispersion degree of nanoparticles in a nanocomposite is extremely important because it can determine if the potential improvements achievable with the

nanofillers are reached [1, 2]. As in this study solid nanocomposites are used as precursors to produce foams, analyzing the dispersion degree is even more important. A good dispersion can lead to a positive nucleating effect, while a high degree of agglomeration can reduce the effectiveness of nanoparticles as bubble nucleators [1, 2].

The study of the microstructure of solid LDPE/silica nanoparticles has been carried out by means of transmission electron microscopy and high resolution scanning electron microscopy.

TEM micrographs corresponding to composites with 1 and 9 wt% of silica are presented in figure 1. It can be clearly observed how silica nanoparticles are not individually dispersed but forming aggregates of around 100-200 nm in size. The number of aggregates increases as silica concentration does; it is possible to clearly observe in the figure that in the sample with higher silica concentration, the number of aggregates is higher, and in addition such aggregates present a larger size.

Those results are in concordance with the dispersions levels achieved by other researchers which also uses the melt-mixing technique to prepare LDPE/silica nanocomposites. [37, 38].

High resolution scanning electron micrographs support TEM results, (figure 2). Silica particles are forming well-scattered aggregates along the LDPE matrix. The number and size of the aggregates increases as silica concentration does. These results indicates that the shear forces produced during the melt-mixing are not enough to achieve the completely dispersion of the silica particles. However, the presence of the compatibilizer together with the surface-modification of the particles with a silane coupling agent are suitable to obtain well-scattered small aggregates.

Cellular Structure of Foamed LDPE/Silica Nanocomposites

SEM micrographs showing the microstructure of foams produced by both the improved compression moulding route and the pressure quench method appear in figure 3.

Regardless of either silica content or foaming process, samples exhibit an isotropic closed cell cellular structure. The effect of silica particles can be detected in the micrographs, the increment in silica concentration is accompanied by a decrease in cell size and an increase in cell density. Nevertheless, in order to quantify the influence of both foaming process and silica particles concentration, cell size and cell density were measured. Average values of both parameters are summarized in figures 4a and 4b.

Figure 4a shows how for neat LDPE cell size is slightly smaller when the gas dissolution technique is used. However this trend is not maintained for each silica concentration. When the gas dissolution technique is used, the smallest cell size is reached at the smallest silica concentration, (1wt%); at higher nanofiller contents, cell size increases reaching values even higher than that of the pure polymer.

On the other hand, for the improved compression moulding route, it can be observed how as silica content increases, cell size start decreasing up to a silica concentration of 6wt% where the smallest value is obtained. At higher silica concentrations, cell size starts increasing again.

Therefore, for both processes it has been found a very similar behaviour. Cell size decreases up to the optimum silica content and from this value increases reaching values even higher than for the neat polymer. The main difference between the two processes lies in the optimum silica content; 1wt% using CO_2 and 6wt% using ADC.

The effectiveness of each optimum silica concentration can be simply quantified by calculating the percentage of reduction in cell size with respect to the neat polymer, (values are written in figure 4a). Results show that optimum concentrations lead to very

similar reduction in cell size although is slightly higher for ADC-blown samples, (29.9 % for ADC-blown samples compared to a 27.6% for CO_2 blown ones).

Cell density values are plotted in figure 4b. Results follow the trends detected for cell size. The highest values are reached for the optimum silica content and a decreased in cell density is observed as silica content increases to higher concentrations. In addition, the improved compression moulding route lead to higher cell densities both for the neat polymer and for the sample with the optimum filler concentration.

To easily understand the cross-effects between silica concentration and foaming process, *Nucleation Ratio* was calculated [39]. This parameter gives account of the effect of a filler as nucleating agent and is defined as follows:

$$Nucleation\ Ratio = \frac{N}{N_0} \qquad (2)$$

Where N is the cell density of the sample containing the additive and N_0 is the cell density of the un-modified control sample, (in this case pure LDPE). Results are plotted in figure 5a. For the optimum silica content, nucleation ratio of any of the two process reach very similar values, (2.16 for gas dissolution and 2.23 for improved compression moulding). However, for non-optimum silica contents, nucleation ratio is higher for ADC blown samples than for CO_2 ones. For all the ADC-blown samples, the chemical blowing agent concentration was the same, (5wt%), nonetheless, it seems that the combination of chemical blowing agents and nanoparticles can lead to higher nucleation ratios than physical blowing agents.

The nucleating effect of nanofillers is focused not only in reducing cell size and increasing cell nucleation rates but also in achieving more homogeneous structures, this is samples with narrower cell sizes distributions, [1, 2]. In order to be able to easily compare the results obtained for both processes a dispersion coefficient, (*SD*) has been calculated according to equation 3:

$$SD = \sqrt{\sum_{i=1}^{n} \frac{(\phi_i - \phi)^2}{n}} \qquad (3)$$

where n is the number of counted cells, ϕ_i is the single cell diameter and ϕ is the average diameter of the cells. This parameter gives an idea of the dispersion of cell sizes in each sample. (figure 5b).

Results for pure LDPE indicates that the gas dissolution technique lead to more homogeneous materials than the improved compression moulding route. Regarding the effect of the nanofiller, just with the addition of 1wt% of silica nanoparticles, SD considerably decreases, being the decrease more pronounced for ADC-blown samples. So, although for both types of samples the optimum silica concentration maximizing the homogeneity of the structures is 6wt%, up to this value, SD is smaller for ADC-blown samples. Once more, it can be observed how the combination of silica particles and the chemical blowing agent leads to a more optimized cellular structure than the use of nanofillers and physical blowing agents. At higher silica concentrations, (9wt%), more inhomogeneous structures appear for both types of materials.

Thermal Stability of Solid and Foamed LDPE/Silica Nanocomposites

The presence of a nano-sized phase in a polymeric matrix used to be accompanied by an increment in thermal stability of the corresponding polymer, [2]. The possible increment in thermal stability of LDPE due to the presence of silica particles was analyzed by thermogravimetric analysis. Results corresponding to degradation temperature of solid and foamed LDPE/silica based nanocomposites are plotted in figure 6.

With regard to solid samples, it can be observed, that as silica content increases degradation temperature also does. The maximum increment (around 11ºC) is achieved when the highest silica concentration is used, (9wt%).

The same behaviour is observed for both types of foamed samples, degradation temperature shifts to higher values due to the presence of silica particles. The higher silica concentration leads to the greatest improvement in both cases, being of 7.7ºC for ADC-blown samples and of 10.3ºC for CO_2 ones.

Mechanical Response of Foamed and Solid LDPE/SiO_2 Nanocomposites

Besides the improvement in thermal properties, the other main reason to add nanoparticles to polymers is to improve the mechanical performance. In addition, the analyzed foamed samples due to their relative density values are suitable for structural applications; hence an improvement in mechanical response would be advantageous.

As it was previously mentioned, both solid and foamed samples present a perfect cylindrical shape, so it was possible to measure mechanical response of the samples by performing compression tests.

Compressive stress-strain curves from samples produced using any of the two processes are shown in figures 7a and 7b. As it can be observed regardless of the presence of the silica particles there is a great difference between the curves obtained for CO_2 blown samples and ADC-blown ones. The mechanical performance exhibited by GD samples is clearly higher than that of ICM ones. The reason of this behaviour lies in the results obtained from open cell measurements. While for GD samples open cell content is almost 0%, for ICM ones it reaches values near to a 25% in some cases, (see table 2).

In order to easily understand the role played by silica particles, elastic modulus (E), collapse stress (σ_c) and density of absorbed energy (W) were calculated for the whole collection of samples. Elastic modulus, (E) was calculated as the slope of the initial part of the stress-strain curve. Experimental results for solid and foamed samples are plotted in figure 8a. It can be observed how elastic modulus of solid nanocomposites increases as silica content does up to a concentration of 6wt%; for higher silica contents, elastic modulus decreases.

As it could be expected, and due to density reduction, foamed samples exhibit smaller values of elastic modulus than their respective solid precursors. Experimental results also highlights differences between samples foamed using ADC or CO_2 as blowing agents. Samples produced by the pressure quench method are stiffer than the ones produced using the improved compression moulding route, regardless of silica concentration. After the observation of the stress-strain curves it can be concluded that the reason of this behaviour is the open cell content exhibited by both types of samples. It is known that open cell content has a negative impact on mechanical response of foams, [40]. While samples produced by the pressure quench method present an almost zero open cell content, for samples produced by the improved compression moulding route and as it was previously mentioned, this parameter can not be neglected. Open cell content varies from around 12% to 28% for ADC blown samples, (see table 2), but there is no evident relationship between open cell content and silica concentration.

The second difference between both types of foams lies in the optimum silica content which maximizes the stiffness. It is a 3wt% for CO_2 blown samples and a 6wt% for ADC ones. Thus, for samples produced using chemical blowing agents, optimum silica concentration coincide with the one for solid nanocomposites, but for samples produced using physical blowing agents is lower than for the solids.

Besides of the optimum nanofiller concentration is worthy to quantify the improvement degree due to the presence of silica particles in either solid or foamed nanocomposites. A simple way to perform this analysis is to calculate the percentage of variation with respect to samples without silica, using the following equation:

$$\%Increment - E = \frac{E_{NC} - E_0}{E_0} x100 \qquad (4)$$

Where E_{NC} is the elastic modulus of the sample containing silica and E_0 is the elastic modulus of the control sample, (pure LDPE in this case). Results for calculations for foamed and non-foamed composites are plotted in figure 9a.

When compared to either solid or CO_2-foamed samples, ADC-blown foams achieve the greatest improvement degree due to the presence of infused silica particles in the polymeric matrix. For optimum silica content, an increment in elastic modulus of 86.5% is reached for ADC-blown samples, while for CO_2 ones is 11.6% and for solid nancomposites 18.4%. Therefore, as it was found for the microstructure, in terms of stiffness, the combination of nanoparticles and chemical blowing agents lead to the best results.

The analysis of mechanical response in terms of strength has been performed by calculating collapse stress for the whole collection of samples. Experimental results are plotted as a function of silica content in figure 8b. An increment in collapse stress is detected due to the addition of silica particles to solid LDPE. Even tough the highest values is reached adding a 9wt% of nanoparticles, there is no a marked improvement by adding silica concentrations larger than 3wt%.

Due to density reduction, foams exhibit values of collapse stress significantly lower than solid nanocomposites. Optimum silica concentration to maximize strength is lower for CO_2 blown samples, (1wt%) than for ADC ones, (6wt%). Such optimum concentrations coincides with the one maximizing stiffness in the case of ICM-samples

18

but is lower for GD ones. Collapse stress values reached by samples produced using physical blowing agents are two times higher than those reached by samples produced using chemical blowing agents. The reason of this behaviour lies in two reasons, first one the higher open cell content exhibited by ADC-blown samples and second one the presence of solid residues coming from ADC decomposition in the polymeric matrix. It is known that after decomposing around a 24% of the initial weight of ADC can remain as residues inside the polymeric matrix, [41]. It has been proved in previous studies that such residues can harm mechanical response of foams in terms of strength due to a loss of elasticity of polymeric matrix [14].

Moreover, the same type of analysis than for elastic modulus has been performed for collapse stress. The effective increment in terms of strength due to the presence of silica nanoparticles has been calculated as follows:

$$\%Increment-\sigma_c = \frac{\sigma_{C-NC} - \sigma_{C-0}}{\sigma_{C-0}} x100 \qquad (5)$$

Where $\sigma_{C\text{-}NC}$ is the collapse stress of the samples containing silica particles and $\sigma_{C\text{-}0}$ is the collapse stress of control samples, (without fillers). Results of these calculations are presented in figure 9b. As it was previously mentioned, the increase for the solids is approximately constant from a silica concentration of 3wt%. For CO_2-blown samples, the higher improvement is reached by adding just a 1wt% of silica; at higher silica contents percentage of increment starts decreasing reaching values even lower than that of the control sample. ADC-blown samples reach the higher increment degree at the optimum silica content; a 72.2% in comparison with a 19.9% achieved for GD-samples and a 21.7% for solid nanocomposites.

Those results together with the ones obtained for elastic modulus indicates the presence of synergetic effects due to the combination of the improved compression moulding route and the infusion of the polymeric matrix with nanofillers. The improvement

reached in the foamed nanocomposites is greater than that of the solid ones. The explanation to this effect lays in the fact that silica particles are, on the one hand, improving both stiffness and strength of the polymer comprising cell walls of the foams, (as it has been demonstrated for solid composites) and on the other hand, silica particles acting as effective nucleating agents, both favouring bubble nucleation, (decreasing cell size and increasing cell density) and improving homogeneity of the cell size distribution.

The last mechanical parameter that has been determined from the stress-strain curves is the density of absorbed energy, (i.e. the absorbed energy per unit volume). Experimental data are shown in figure 8c. Similar trends as those found for E and σ_C can be detected for this parameter. An increase in W is detected with the addition of silica particles in solid nanocomposites being the optimum concentration 6wt%. A decrease due to foaming is achieved for foamed samples. Optimum silica content for GD-samples is 1wt%, at higher concentration, energy absorption capability of the samples decrease significantly reaching values smaller than that of the sample without fillers.

The behaviour in terms of energy absorption of samples produced using ADC as blowing agent does not significantly change due to the presence of silica particles. Although the highest value is reached using a silica concentration of 9wt%, the differences with other silica concentrations or with the sample without particles are very small. It seems also that ADC residues are playing here a significant role; as their presence is accompanied by a loss of polymer's elasticity, the energy absorption capability is reduced.

The increment in percentage for W due to the addition of silica particles for both solid and foamed nanocomposites, (same type of analysis as for E and σ_C) has been calculated using equation (6).

$$\%Increment - W = \frac{W_{NC} - W_0}{W_0} x100 \qquad (6)$$

Where W_{NC} and W_0 are absorbed energy per unit volume of samples with and without silica particles. Results (figure 9c) show that in this case, regardless of the silica content, the increment reached by solid nanocomposites is higher than that of both types of foamed samples. In addition, at high silica concentrations, there is a significant decrease in absorption capability of CO_2 blown foams.

Relative Mechanical Properties of LDPE/Silica Foamed Nanocomposites. Influence of Cellular Structure

The analysis of mechanical properties in terms of relative values, (i.e. the property of the foam divided by that of the solid) allows obtaining information related with the effectiveness of foaming process as well as quantifying the influence of cellular structure on mechanical properties, [42].

Mechanical properties of foamed products are always lower than that of the corresponding solid precursor materials due to density reductions; nevertheless, their relative properties can reach higher values. Several authors [14, 25, 26, 42] have reported that properties of a cellular polymer can be predicted using the following equation:

$$\frac{P_f}{P_s} = C\left(\frac{\rho_f}{\rho_s}\right)^n \qquad (7)$$

where P_f is the property of the foam and P_s is the same property but for the solid polymer; $\frac{\rho_f}{\rho_s}$ is the relative density of the foam. C and n are parameters that can be determined experimentally.

Most foamed products exhibit values of C close to 1 and values of n in a range between 1 and 2. n is closely related with the cellular structure of the considered foamed product, reaching values close to 1 for materials with closed cell cellular structures, small cell sizes and/or homogeneous cellular structures and closer to 2 as open cell content and cell size increases and/or cell homogeneity decreases. [45]. So, as most foams exhibit values of n between 1 and 2, the reduction in mechanical properties is always greater than the corresponding density reduction. From a technical point of view, n value can quantify the efficiency of a foaming process.

Figure 10 summarizes the relative mechanical properties of foams produced using either the improved compression moulding route or the pressure quench method plotted as a function of silica content. As it can be observed for both elastic modulus and collapse stress, relative properties of CO_2 blown samples are higher than those of ADC ones; relative absorbed energy per unit volume is very similar for both types of foams at high silica concentrations. This effect is mainly due to the non-zero open cell content exhibited by ICM samples, which affects negatively the mechanical response of these materials.

As it was said, the analysis of mechanical properties in relative terms gives information about the optimum cellular structures to maximize the mechanical response. It was found that a 1wt% of silica particles infused in the LDPE matrix can have an effective nucleating effect when physical blowing agents are used. However, as it can be observed in figure 10, GD-1 samples, only maximize stiffness, nor strength or energy absorption capability. In addition, for the latter parameters, the higher values are reached by the sample without silica particles.

On the other hand, ICM samples exhibit a different behaviour, the sample maximizing both stiffness and strength is the one reaching the higher value of *Nucleation Ratio*, (this

is ICM-6 sample). In addition, it seems that the sample with the optimum cellular structure to maximize energy absorption capability is ICM-9.

Those results indicate that only when chemical blowing agents are used the optimization of cellular structure due to the addition of nanoparticles plays a significant role in improving mechanical performance. Besides, the addition of silica particles combined with the use of physical blowing agents involves in some cases (addition of 1wt% of silica) improvements in cellular structure; however, in this case better microstructures does not imply a better mechanical performance.

To analyze the effectiveness of foaming process, relative elastic modulus, collapse stress and density of absorbed energy have been plotted as a function of relative density, (figures 11a, 11b and 11c).

Relative elastic modulus of GD samples is higher than that of ICM ones in the analyzed density range. This effect is mainly due to the almost zero open cell content exhibited by these samples, and not to the addition of silica particles or improvements in cellular structure. The presence of open cells is also highlighted in the results obtained after fitting experimental data to equation 6. As it is written in figure 11a, for GD samples n is 1.67 and for ICM ones 2.39.

The same analysis has been performed for collapse stress, (figure 11b). As it happened for elastic modulus, samples produced using CO_2 as blowing agent reach higher values than the ones produced using ADC. Fitting experimental results to equation 6, are obtained values for n=1.49 for GD samples and n=2.45 for ICM ones.

As it can be inferred from equation 7, as n reaches values closer to 1, foamed materials exhibit better specific mechanical properties, [45]. So, in this case, results shows that pressure quench method seems to be more efficient under this point of view. Thus, the isotropic and closed cell cellular structures generated using the pressure quench method

are more suitable than those generated by the improved compression moulding to maximize mechanical response of the materials.

The previous information is supported by the results obtained for relative absorbed energy per unit volume (figure 11c). The highest values are reached for GD samples, although in this case the cellular structure maximizing energy absorption capability is the one exhibited by GD-0, this is the foam without silica particles in the formulation.

Conclusions

LDPE/Silica nanocomposites have been prepared using the melt-mixing technique and afterwards foamed by applying two different technologies. On the one hand it was used a physical blowing agent, (CO_2) and the pressure quench method and on the other hand, a chemical blowing agent, (azodicarbonamide) and the improved compression moulding route.

Results showed that the melt-mixing route is not enough to achieve a complete dispersion of the silica particles along the polymeric matrix, however, the shear forces combined with the presence of the compatibilizer and the surface modification of the particles lead to a dispersion degree adequate to produce an effective nucleating effect.

The addition of SiO_2 nanoparticles to the LDPE matrix implies an improvement of cellular structure, not only in achieving reduced cell sizes and increased cell densities but also in cell size distribution homogeneity. Moreover, *Nucleation Ratio* values indicate that nucleation effectiveness is higher in the improved compression moulding route than in the pressure quench method. The optimum silica content to reach the higher nucleating effect is different in both cases, a 1wt% for CO_2 blown samples and a 6wt% for ADC ones.

Thermal and mechanical properties are improved due to the presence of silica particles in both foamed and solid nanocomposites. Elastic modulus, collapse stress and density of absorbed energy increases as silica content does up to the optimum concentration. For higher values, it is obtained a worse response of the materials, sometimes even lower than for the samples without particles. Optimum concentration varies depending on foaming process. In addition, the improvement degree reached with respect to the neat polymer due to the addition of silica is much higher for ICM samples than for GD ones.

The analysis of mechanical properties in relative terms has revealed that the improvement of cellular structure due to the presence of silica particles does not contribute to enhance mechanical response in CO_2- blown samples but it does for ADC ones. In addition, the samples produced using the improved compression moulding route exhibit a poorer mechanical response, mainly due to two effects, the non-completely closed cellular structures and the presence of ADC residues in the polymeric matrix comprising cell walls.

Acknowledgements

Financial assistance from Spanish Ministry of Science and Education and Feder Program (MAT 2009-14001 CO2-01) as well as Innocash Project (INC-0193) are gratefully acknowledged.

References

1. Ibeh C C, Lee S W. Current trends in nanocomposite foams. J Cell Plast 2008; 44: 498-515.

2. Lee L J, Zen C, Cao X, Han X, Shen J, Xu G. Polymer nanocomposite foams. Compos Sci Technol 2005; 65: 2344-2636.

3. Zhai W, Park C B, Kontopoulou M. Nanosilica addition dramatically improves the cell morphology and expansion ratio of polypropylene heterophasic copolymer foams blown in continous extrusion. Ind Eng Chem Res 2011; 50: 7282-7289.

4. Zhai W, Kuboki T, Wang L, Park C B, Lee E K, Naguib H E. Cell structure evolution and the crystallization behaviour of polypropylene/clay nanocomposite foams blown in continous extrusion. Ind Eng Chem Res 2010; 49: 9834-9845.

5. Zeng C, Han X, Lee L J, Koelling K W, Tomasko D L. Polymer-clay nanocomposite foams prepared using carbon dioxide. Adv Mater 2003; 15: 1743-1747.

6. Lee Y H, Wang K H, Park C B, Sain M. Effects of clay dispersion on the foam morphology of LDPE/clay nanocomposites. J App Polym Sci 2007; 103; 2129-2134.

7. Seraji S M, Aghjeh M K R, Davari M, Hosseini M S, Khelgati Sh. Effect of clay dispersion on the cell structure of LDPE/clay nanocomposite foams. Polym Compos 2011; 32: 1095-1105.

8. Shen J, Zeng C, Lee L J. Synthesis of polystyrene-carbon nanofibers nanocomposites foams. Polymer 2005; 46: 5218-5224.

9. Saha M C, Kabir Md E, Jeelani S. Enhancement in thermal and mechanical properties of polyurethane foam infused with nanoparticles. Mat Sci Eng A-Struct 2008; 479: 213-222.

10. Cheng L, Schadler L S, Ozisik _R. An experimental and theoretical investigation of the compressive properties of multi-walled carbon nanotube/poly(methyl methacrylate) nanocomposite foams. Polymer 200; 52: 2899-2909.

11. Zhai W, Yu J, Wu L, Ma W, He J. Heterogeneous nucleation uniformizing cell size distribution in microcellular nanocomposite foams. Polymer 2006; 47: 7580-7859.

12. Yeh J M, Chang K C, Peng C W, Chand B G, Chiou S C, Huang H H, Lin C Y, Yang J C, Lin H R, Chen C L. Preparation and insulation property studies of thermoplastic PMMA-Silica nanocomposite foams. Polym Compos 2099; 30: 715-722.

13. Gorem K, Chen L, Schadler L S, Ozisik R. Influence of nanoparticles surface chemistry and size on supercritical carbon dioxide processed nanocomposite foam morphology. J Supercrit Fluid 2010; 51: 420-427.

14. Saiz-Arroyo C, de Saja J A, Velasco J I, Rodríguez-Pérez M A. Moulded PP foams produced using chemical or physical blowing agents. Structure-Properties Relationship. J Mater Sci 2012 *Accepted for publication*

15. Guo M C, Heuzev M C, Carreau P J. Cell structure and dynamic properties of injection molded polypropylene foams. Polym Eng Sci 2007; 47: 1070-1081.

16. Chaudhary A K, Jayaraman K. Extrusion of linear polypropylene clay nanocomposite foams. Polym Eng Sci 2011; 51: 1749-1756.

17. Zhai W, Park C B. Effect of nanoclay addition on the foaming behaviour of linear polypropylene-based soft thermoplastic polyolefin foam blown in continuous extrusion. Polym Eng Sci 2011, 51: 2387-2397.

18. Guo G, Wang K H, Park C B, Kim Y S, Li G. Effects of nanoparticles on the density reduction and cell morphology of extruded metallocene polyethylene wood fiber nanocomposites. J App Polym Sci 2007; 104: 1058-1063.

19. Velasco J I, Antunes M, Ayyad O, Lopez-Cuesta J M, Gaudon P, Saiz-Arroyo C, Rodríguez-Pérez M A. de Saja J A. Foaming behaviour and cellular structure of LDPE/Hectorite nanocomposites. Polymer 2007; 18: 2098-2108.

20. Velasco J I, Antunes M, Ayyad O, Saiz-Arroyo C, Rodríguez-Pérez M A. Hidalgo F, de Saja J A. Foams based on low density polyethylene/hectorite nanocomposites: Thermal stability and thermomechanical properties. J App Polym Sci 2007; 105: 1658-1667.

21. Antunes M, Velasco J I, Realinho V, Solórzano E. Study of the cellular structure heterogeneity and anisotropy of polypropylene and polypropylene nanocomposite foams. Polym Eng Sci 2009; 49: 2400-2413.

22. Riahinezhad M, Ghasemi I, Karrabi M, Azizi H. Morphology and tensile properties of crosslinked nanocomposite foams of low density polyethylene and poly(ethylene-co-vinyl acetate) blends. J Vinyl Addit Technol 2010; 16: 229-237.

23. Abbasi M, Khorasani S N, Baheri R, Esfahani J M. Microcellular foaming of low-density polyethylene using nano-$CaCO_3$ as a nucleating agent. Polym Compos 2011; 32: 1718-1725.

24. Throne J L. Thermoplastic Foams Extrusion. An Introduction. Munich: Hanser Publishers, 2004.

25. Rodríguez-Pérez M A, Lobos J, Pérez-Muñoz C A, de Saja J A, González L, del Carpio B M A. Mechanical behaviour at low strains of LDPE foams with cell sizes in the microcellular range: Advantages of using these materials in structural elements. Cell Polym 2008; 27: 347-362.

26. Rodríguez-Pérez M A, Lobos J, Pérez-Muñoz C A, de Saja J A. Mechanical response of polyolefin foams with high densities and cell sizes in the microcellular range. J Cell Plast 2009; 45: 389-403.

28

27. Roman-Lorza S, Rodríguez-Pérez M A, de Saja J A. Cellular structure of halogen-free flame retardant foams based on LDPE. Cell Polym 2009; 28: 249-268.

28. Roman-Lorza S, Rodríguez-Pérez M A, de Saja J A, Zurro J. Cellular structure of EVA/ATH halogen-free flame retardant foams. J Cell Plast 2010, 10: 1-21.

29. Roman-Lorza S, Sabadell J, García-Ruiz J J, Rodríguez-Pérez M A, de Saja J A. Fabrication and characterization of halogen free flame retardant polyolefin foams. Materials Science Forum 2010; 636/637: 98-205.

30. Rodríguez-Pérez M A, Simoes R D, Constantino C J L, de Saja J A. Structure and physical properties of EVA/Starch precursor materials for foaming applications. J App Polym Sci 2011; 212: 2324-2330.

31. Rodríguez-Pérez M A, Simoes R D, Roman-Lorza S, Alvarez-Lainez M, Montoya-Mesa C, Constantino C J L, de Saja J A. Foaming of EVA/Starch blends: Characterization of the structure, physical properties and biodegradability. Polym Eng Sci 2011, *In press* (DOI: 10.1002/pen.22046), (2011).

32. Pinto J, Rodríguez-Pérez M A, de Saja J A. Development of an Image J macro to characterize the cellular structure of polymeric foams. XI Reunion del Grupo Especializado de Polímeros, (GEP) 10-24 September 2009, Valladolid-Spain.

33. Rodríguez-Pérez M A, de Saja J A. The effect of blending on the physical properties of crosslinked closed cell polyethylene foams. Cell Polym 1999; 18: 1-20.

34. Rodríguez-Pérez M A, Rodríguez-Llorente S, de Saja J A. Dynamic mechanical properties of polyolefin foams studied by DMA techniques. Polym Eng Sci 1997; 37: 959-965.

35. Mills N J, Rodríguez-Pérez M A. Modelling the gas-loos creep mechanisms in EVA foam from running shoes. Cell Polym 2001; 20: 79-100.

36. Almanza O, Rodríguez-Pérez M A, de Saja J A. Measurement of the thermal diffusivity and specific heat capacity of polyethylene foams using the transient plane source technique. Polym Int 2004; 53: 2038-2044.

37. Barus S, Zanetti M, Lazzari M, Costa L. Preparation of polymeric hybrid nanocomposites based on PE and nanosilica. Polymer 2009; 20: 2595-2600.

38. García N, Hoyos M, Guzman J, Tiemblo P. Comparing the effect of nanofillers as thermal stabilizers in low density polyethylene. Polym Degrad Stabil 2009; 54: 39-48.

39. Famili M H N, Janani H, Enayati M S. Foaming of a polymer-nanoparticle system: Effect of the particle properties. J App Polym Sci 2011; 119: 2847-2856.

40. Rodríguez-Pérez M A, Alvarez-Lainez M, de Saja J A. Microstructure and physical properties of open-cell polyolefin foams. J App Polym Sci 2009; 114: 1176-1186.

41. Batthi A S, Dellimore D. The thermal decomposition of azodicarbonamide. Thermochim Acta 1984; 76: 63-68.

42. Gibson L J, Ashby M F. Cellular Solids: Structure and Properties. United Kingdom 1997: Cambridge University Press.

Figure Captions

Figure 1: TEM micrographs of solid nanocomposites containing 1 and 9 wt% of silica nanoparticles.

Figure 2: High resolution micrographs showing silica particles infused in the LDPE matrix.

Figure 3: SEM micrographs of foams produced by both foaming processes. (Magnification of ICM samples x150 and magnification of GD samples, x90).

Figure 4: Results regarding cellular structure characterization of LDPE/Silica foams. a) Cell size, b) Cell density.

Figure 5: Effect of addition of silica in LDPE foams. a) Nucleation ratio, b) SD parameter.

Figure 6: Degradation temperature of solid and foamed LDPE/Silica composites measured by thermogravimetric analysis.

Figure 7: Stress-strain curves corresponding to foams produced by either of the two processes. a) Pure LDPE, b) LDPE with a 3wt% of silica nanoparticles.

Figure 8: Mechanical properties of LDPE/Silica composites: foams and solids. a) Elastic modulus, b) Collapse stress, c) Density of absorbed energy.

Figure 9: Improvement in mechanical response due to the addition of silica nanoparticles. a) Elastic modulus, b) Collapse stress, c) Density of absorbed energy.

Figure 10: Relative mechanical properties of LDPE/Silica foams analyzed as a function of silica content.

Figure 11: Relative mechanical properties of LDPE/Silica foams analyzed as a function of relative density. a) Relative elastic modulus, b) Relative collapse stress, c) Relative density of absorbed energy.

Table 1

Sample	LDPE	SiO_2	Compatibilizer	Antioxidant	Stearic Acid	Density(kg/m^3)
S-0	99.75	0	0	0.1	0.15	915.57
S-1	98.62	1	0.13	0.1	0.15	926.60
S-3	96.36	3	0.4	0.1	0.15	940.66
S-6	92.96	6	0.8	0.1	0.15	950.41
S-9	89.71	9	1.18	0.1	0.15	973.84

Table 1: Chemical composition (wt%) and density of solid LDPE/Silica Nanocomposites.

Table 2

Sample	LDPE	SiO_2	Compatibilizer	Antioxidant	Stearic Acid	ADC	ZnO	C (%)	Relative Density
ICM-0	94.71	0	0	0.1	0.15	5	0.04	27.9	0.536
ICM-1	93.48	1	0.13	0.1	0.15	5	0.04	13.4	0.555
ICM-3	91.02	3	0.4	0.1	0.15	5	0.04	18.7	0.562
ICM-6	87.33	6	0.8	0.1	0.15	5	0.04	11.7	0.559
ICM-9	83.64	9	1.18	0.1	0.15	5	0.04	23.5	0.567

Table 2: Chemical composition (wt%), open cell content (C) and relative density of LDPE/SiO_2 foams produced using azodicarbonamide, (ADC) as blowing agent and the improved compression moulding technique.

Table 3

Sample	LDPE	SiO_2	Compatibilizer	Antioxidant	Stearic Acid	Relative Density
GD-0	99.75	0	0	0.1	0.15	0.639
GD-1	98.62	1	0.13	0.1	0.15	0.675
GD-3	96.36	3	0.4	0.1	0.15	0.621
GD-6	92.96	6	0.8	0.1	0.15	0.594
GD-9	89.71	9	1.18	0.1	0.15	0.581

Table 3: Relative density and chemical composition, (wt%) of LDPE/silica foams produced by the pressure quench method.

Figure 1
Click here to download high resolution image

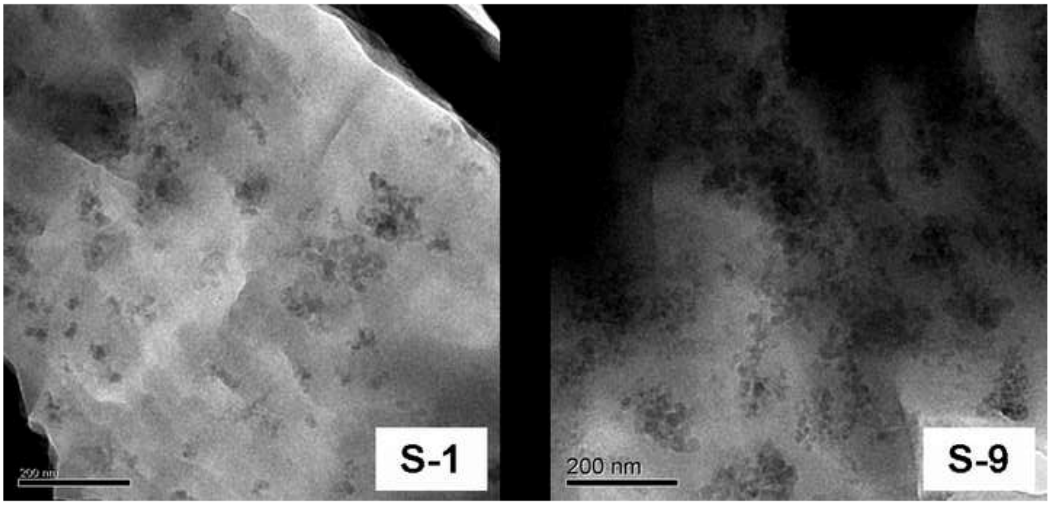

Figure 2
Click here to download high resolution image

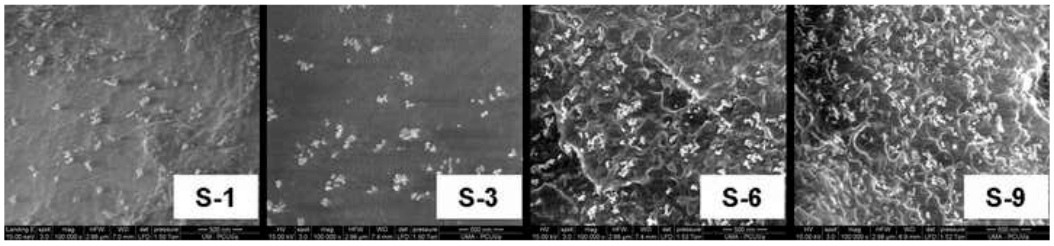

Figure 3
Click here to download high resolution image

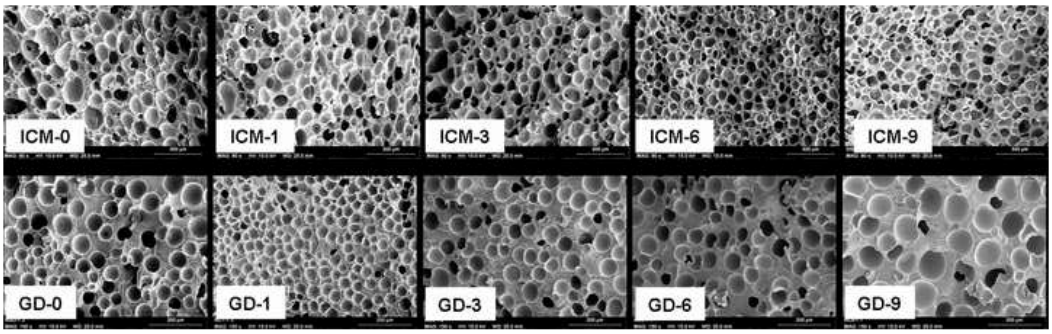

Figure 4a
Click here to download high resolution image

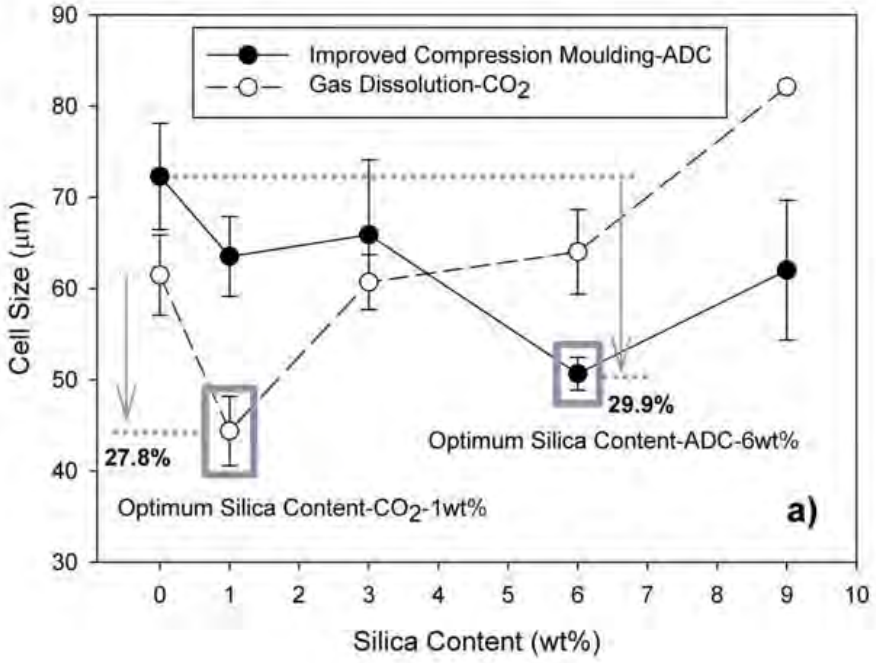

Figure 4b
Click here to download high resolution image

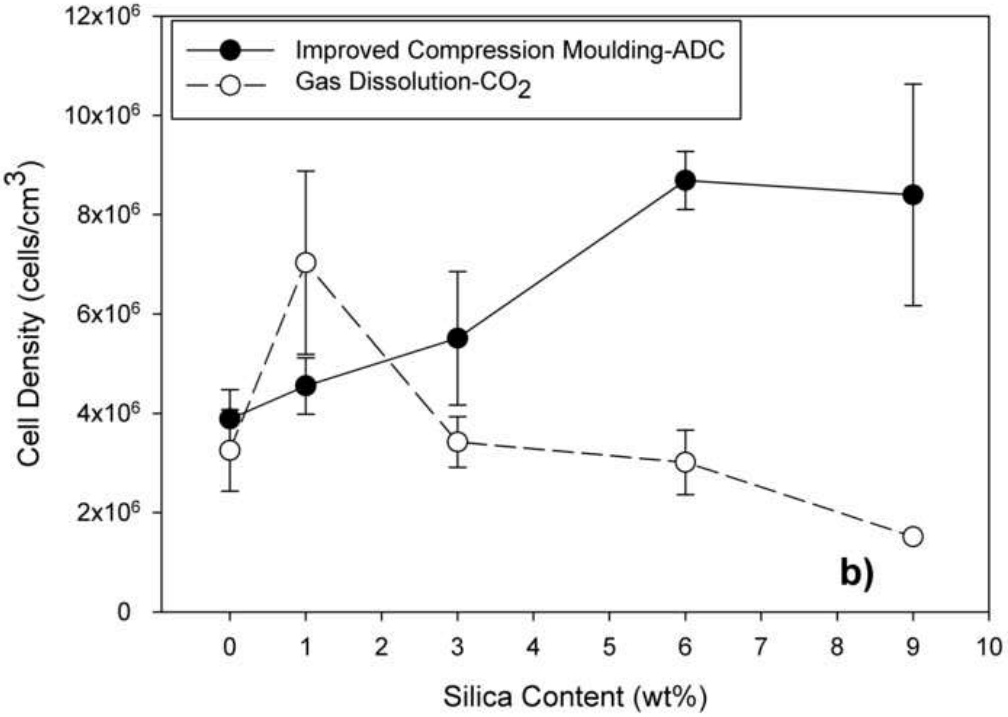

Figure 5
Click here to download high resolution image

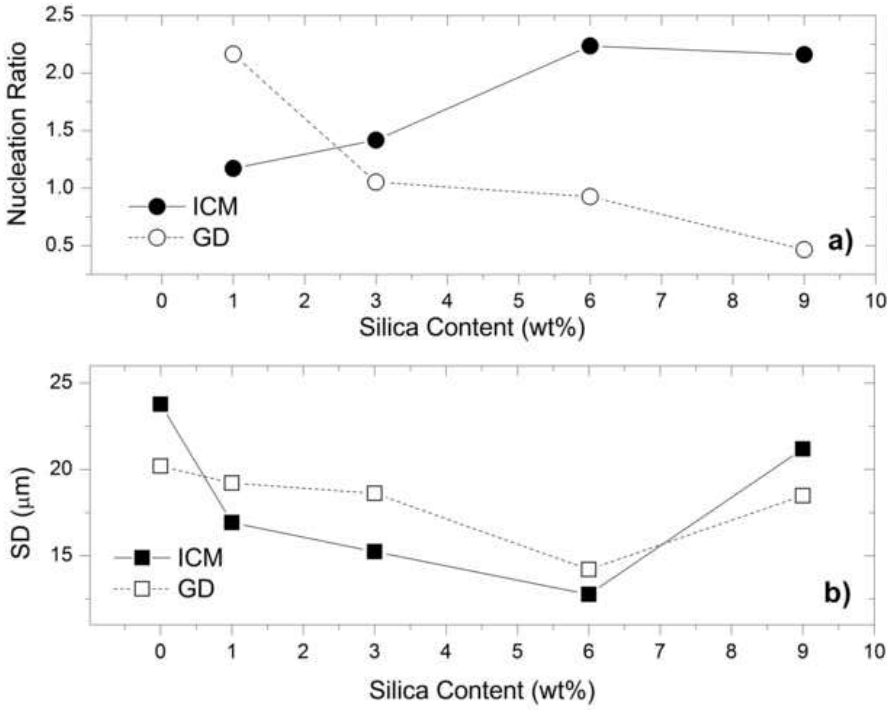

Figure 6
Click here to download high resolution image

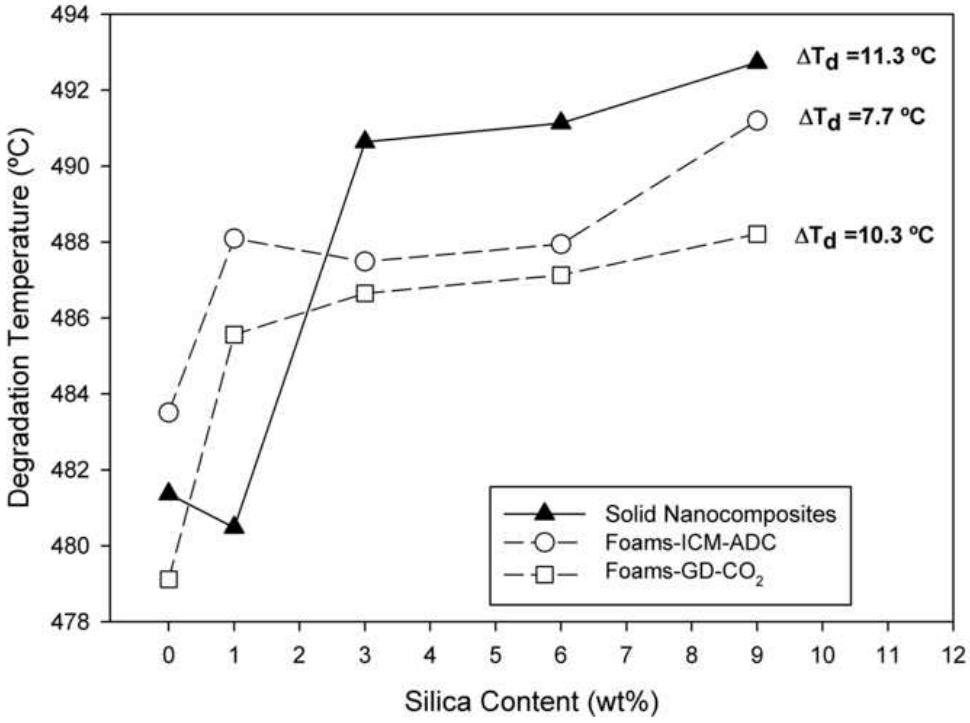

Figure 7
Click here to download high resolution image

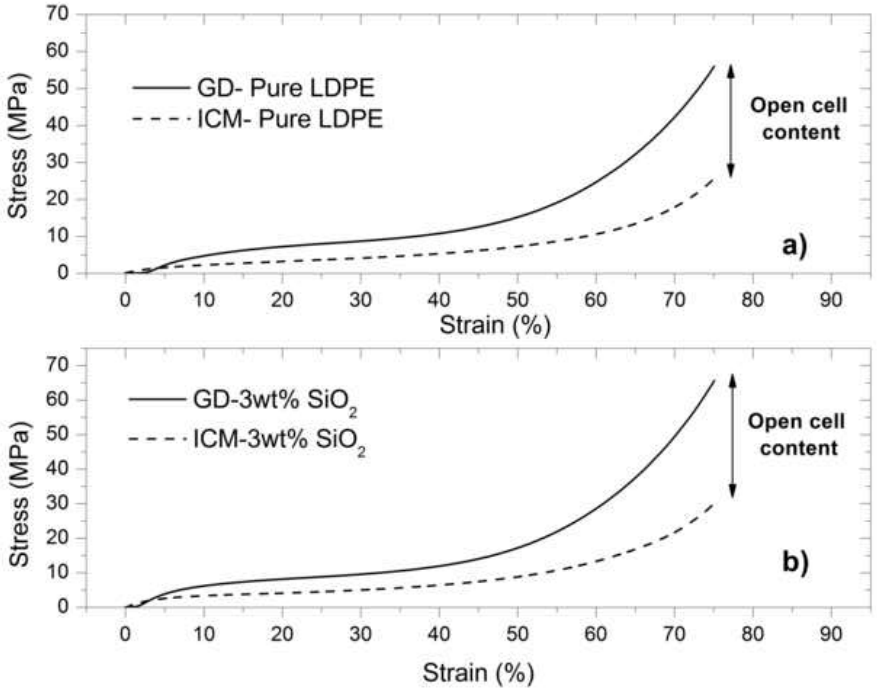

Figure 8a
Click here to download high resolution image

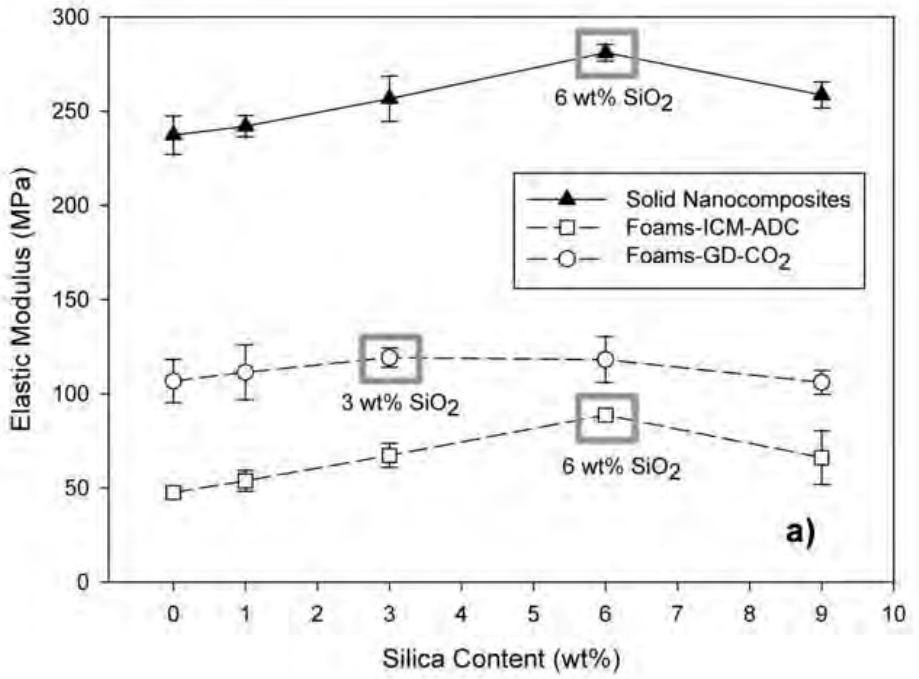

Figure 8b
Click here to download high resolution image

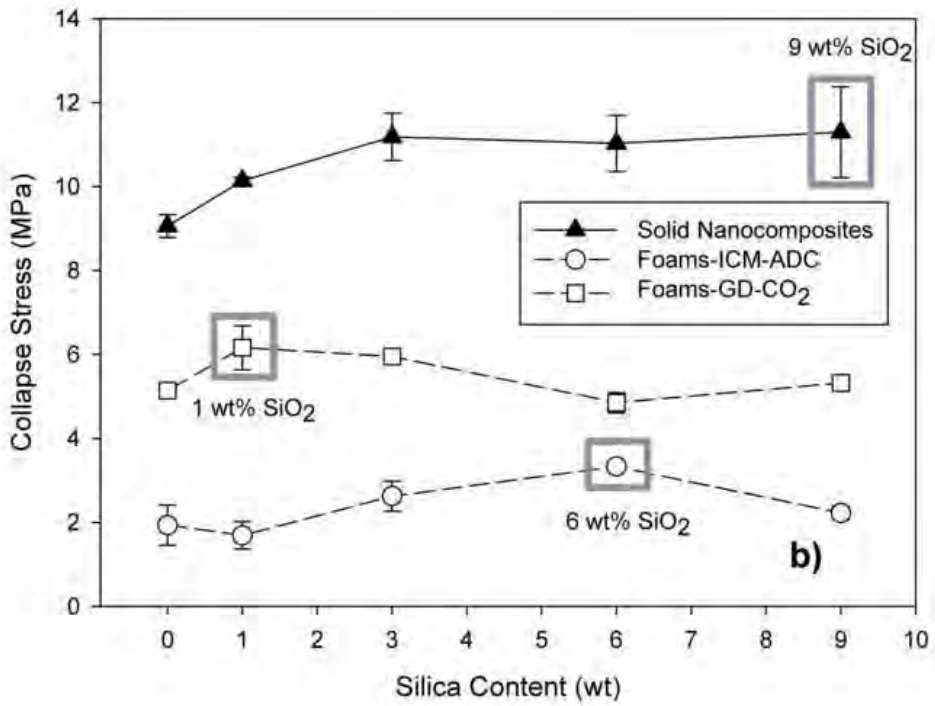

Figure 8c
Click here to download high resolution image

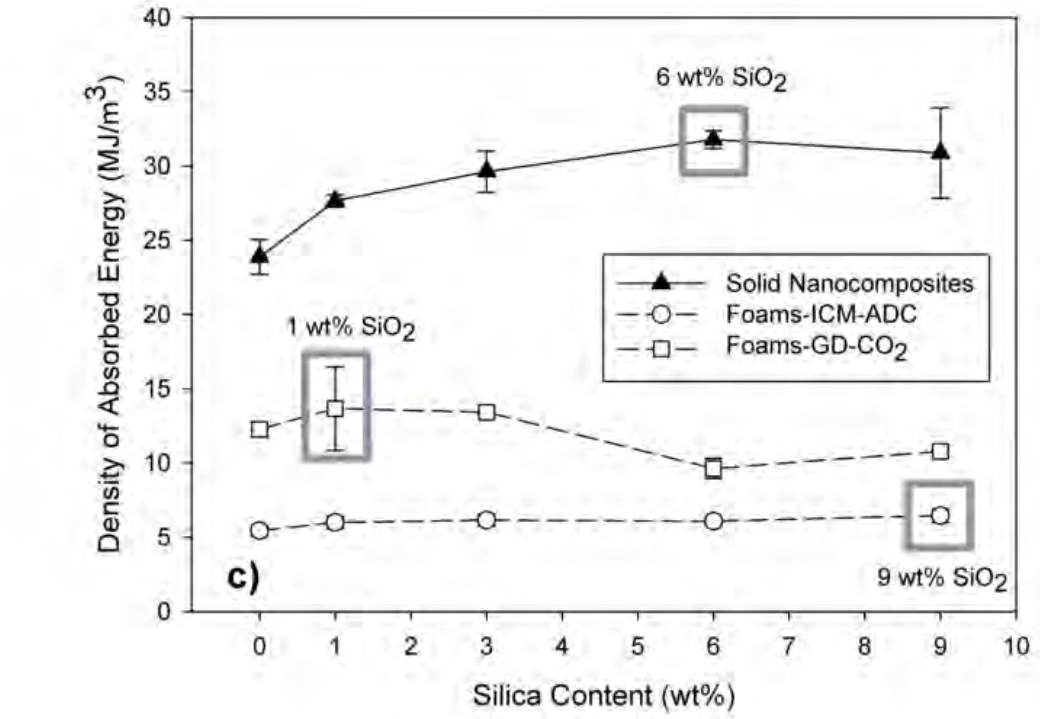

Figure 9a
Click here to download high resolution image

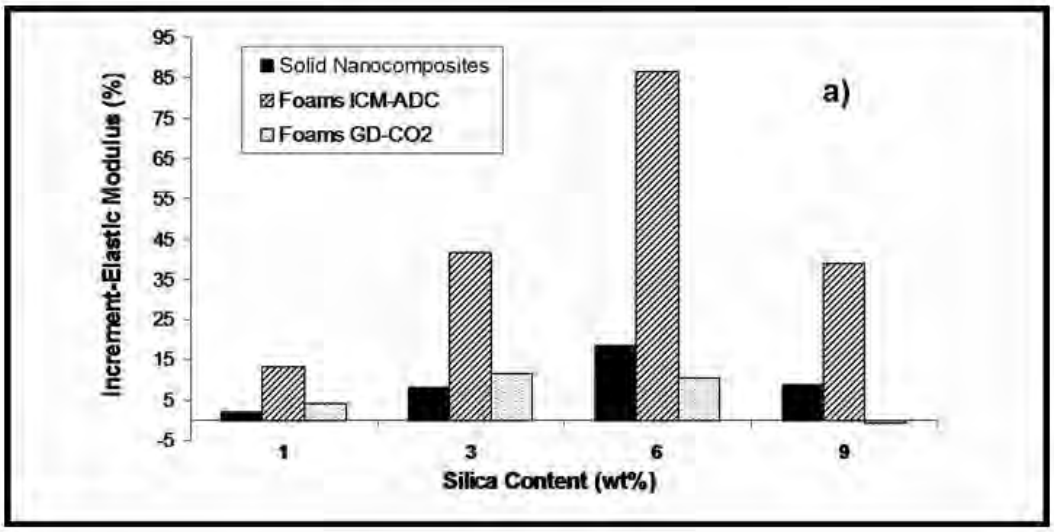

Figure 9b
Click here to download high resolution image

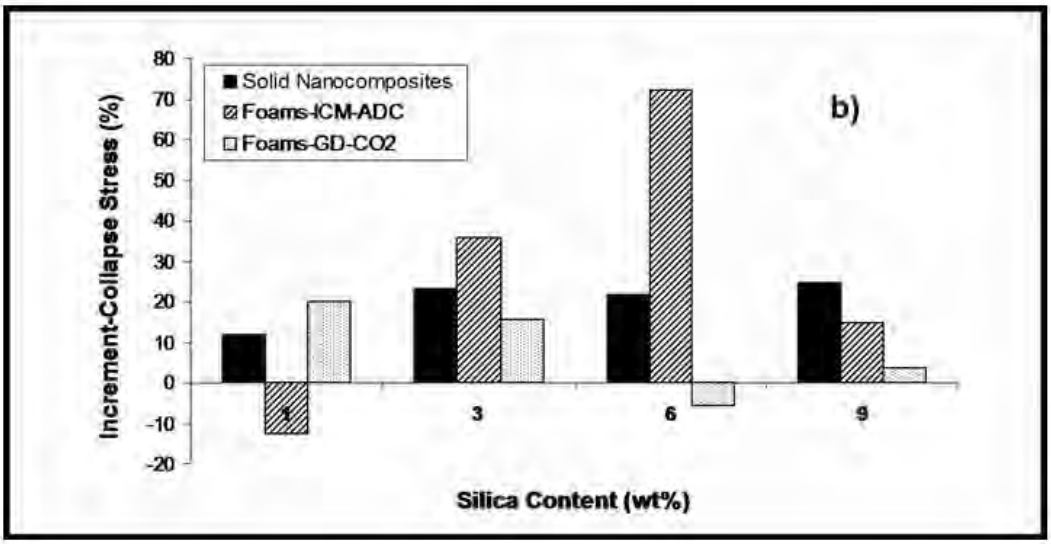

Figure 9c
Click here to download high resolution image

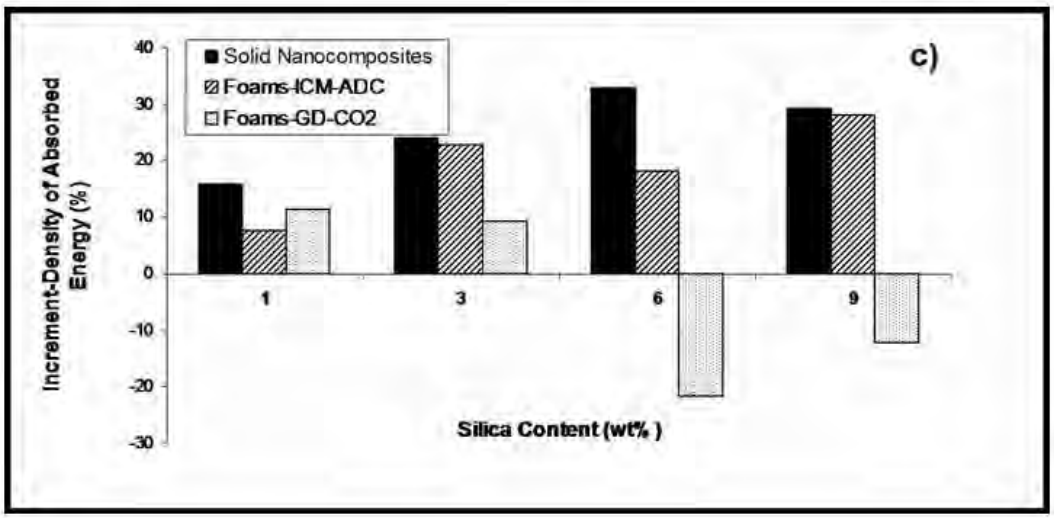

Figure 10
Click here to download high resolution image

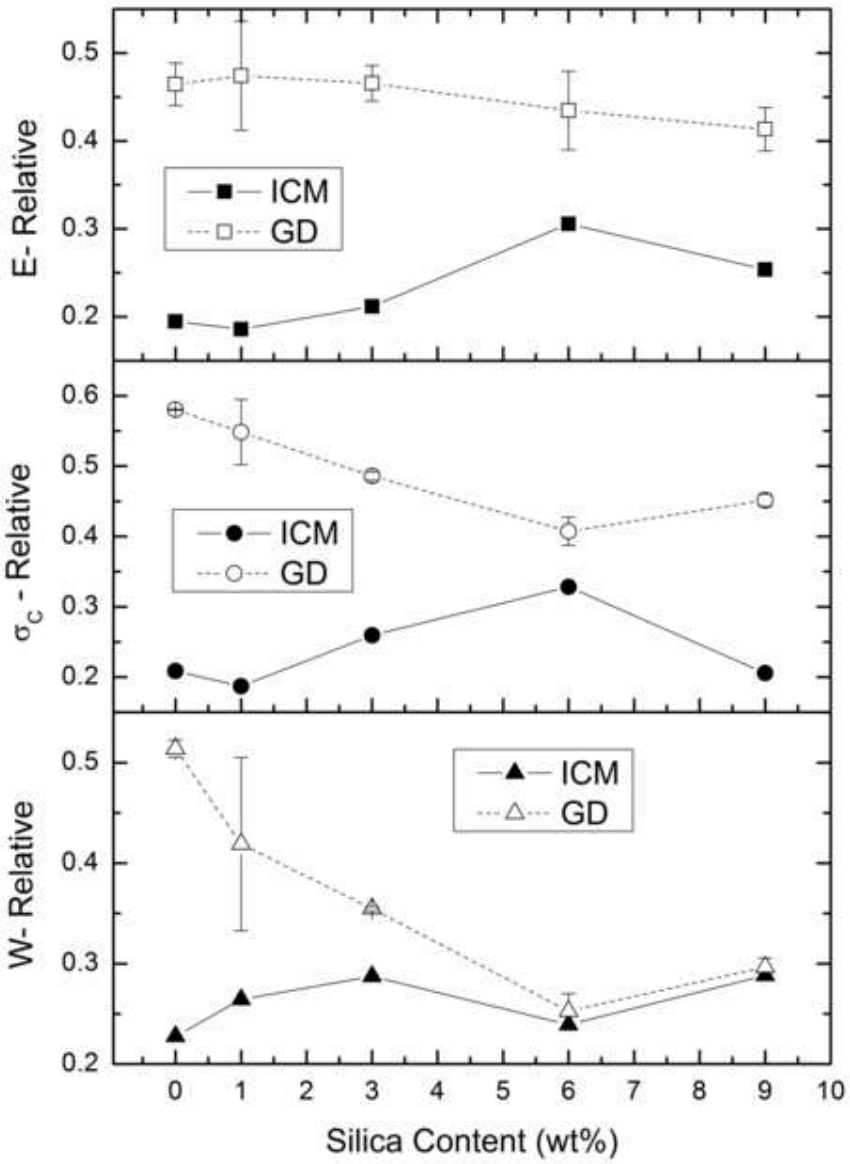

Figure 11a
Click here to download high resolution image

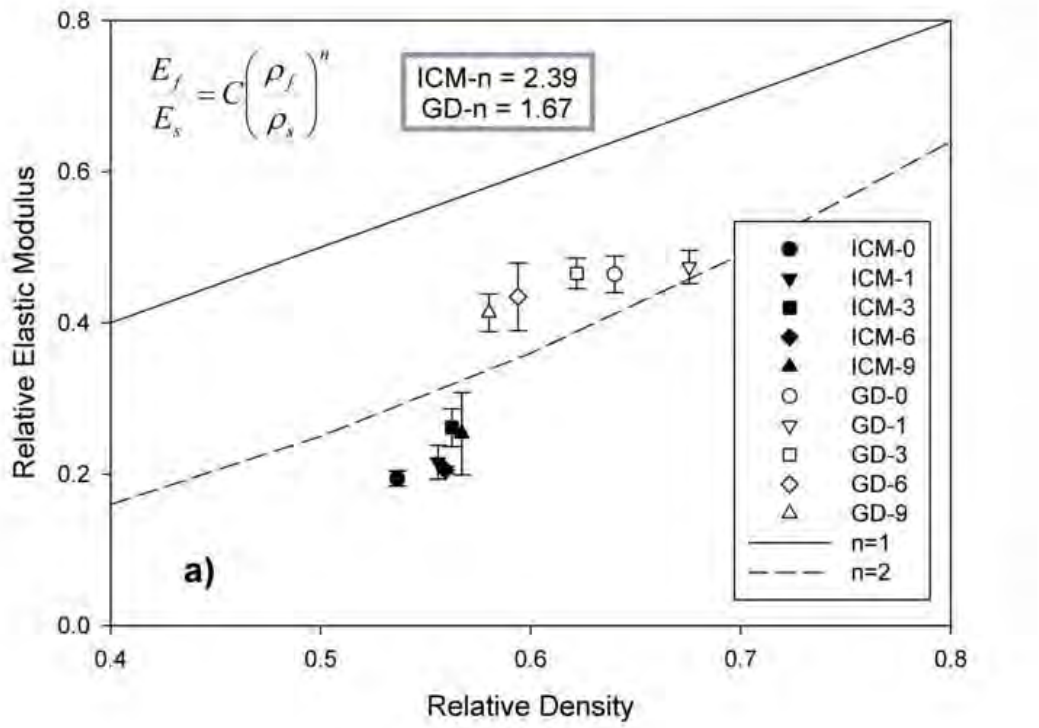

Figure 11b
Click here to download high resolution image

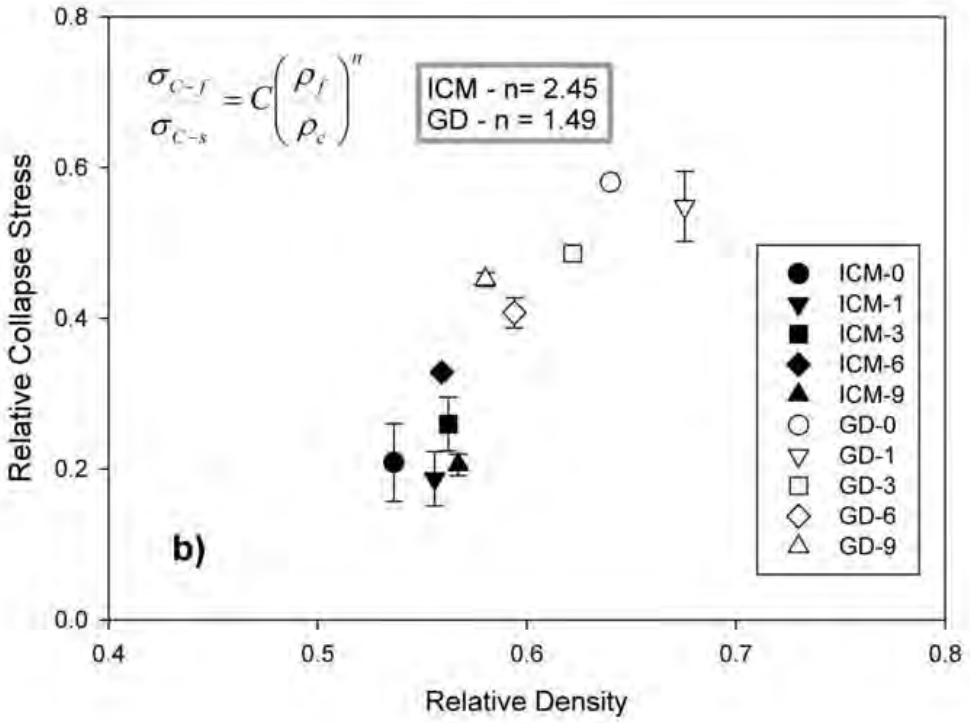

Figure 11c
Click here to download high resolution image

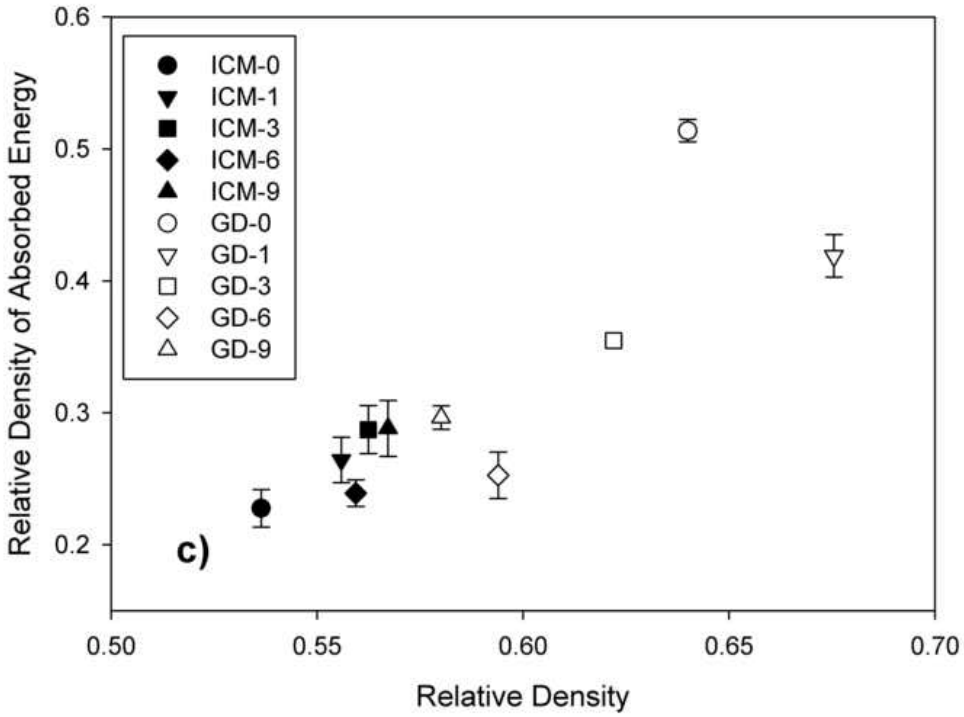

7.2.- MATERIALES CELULARES BASADOS POLIPROPILENO

De forma similar a lo hecho para el sistema LDPE/SiO_2, en esta sección se realiza un estudio comparativo de la relación estructura-propiedades de materiales celulares con base polipropileno producidos utilizando ambos tipos de procesos, disolución de CO_2 y moldeo por compresión mejorado utilizando azodicarbonamida como agente espumante. Dicho estudio se recoge en un artículo publicado en la revista **Journal of Materials Science** con el título *"Moulded Polypropylene Foams Produced using Chemical or Physical Blowing Agents: Structure-Properties Relationship"*.

Uno de los aspectos más novedosos de este trabajo es la obtención de materiales celulares moldeados con diferentes densidades mediante disolución de CO_2 (*pressure quench method*). Por otro lado dado que la ruta ICM también permite obtener muestras moldeadas con una amplia variedad de estructuras celulares en función de la composición química del material, es interesante comparar el comportamiento de ambos tipos de materiales celulares. Como añadido, hay que recordar que en todos los casos se utiliza el mismo tipo de matriz polimérica, un polipropileno copolímero *random* con un MFI de 10g/min, (210ºC y 2.16 kg). Tampoco en este caso se han añadido cargas o agentes nucleantes o entrecruzantes de ningún tipo.

El procedimiento seguido para producir ambos tipos de materiales está descrito en los capítulos 3 (*pressure quench method* en molde) y 5 (ruta ICM-cilindros). Todas las muestras se han caracterizado desde un punto de vista microscópico, (estructura celular) y macroscópico, (propiedades mecánicas medidas en compresión).

Como se señaló en el capítulo 5, la estructura celular de las muestras producidas por la ruta ICM es generalmente isótropa, y tanto el tamaño de celda como la densidad celular dependen de la composición química, (porcentaje de agente espumante) y de la densidad. Por el contrario, para las muestras producidas mediante disolución de gas, se observa que a medida que aumenta el grado de expansión, la estructura celular presenta una orientación preferencial de las celdillas en la dirección de crecimiento. Para el menor grado de expansión, (ER=1.6) el ratio de anisotropía es aproximadamente igual a la unidad (muestra isótropa), pero crece hasta alcanzar un valor aproximadamente igual a 2 para el mayor ratio de expansión analizado, (ER=4). Claramente, dicha orientación celular parece estar inducida por el crecimiento del material en el interior de un molde (expansión unidireccional).

Respecto al tamaño de celda y la densidad celular, se observa una tendencia aparentemente contraria a la encontrada para las muestras obtenidas en la ruta ICM. A medida que disminuye la densidad, disminuye el tamaño de celda y aumenta la

densidad celular, excepto para la muestra con menor densidad (ER=4). Para disminuir la densidad es necesario aumentar la presión de saturación lo que equivale a un aumento de la cantidad de agente espumante. Al disolver una cantidad de gas mayor en el material, se nuclear un mayor número de celdillas. Por tanto, para ambos tipos de materiales se observa una tendencia similar, al aumentar la cantidad de agente espumante se reduce el tamaño de celda. Respecto a la muestra con mayor grado de expansión, puede ocurrir que al ser mucho más finas las paredes celulares, (debido al mayor ratio de estiramiento del polímero) estén ocurriendo fenómenos asociados con la degeneración celular tales como coalescencia o engrosamiento. Por otra parte, la elevada presión de saturación de estas muestras induce una gran plastificación de la matriz polimérica, (reducción de la viscosidad), lo que favorece la ruptura de las paredes celulares durante el proceso de expansión. Además existe otro factor a tener en cuenta, para este tipo de muestras, la presión remanente tras la despresurización del sistema es nula, (autoclave abierto), lo que puede contribuir a una mayor degeneración de la estructura celular.

El contenido de celdas abiertas de los materiales producidos mediante disolución de gas es próximo a cero, sin embargo para los producidos utilizando azodicarbonamida, existe una dependencia de dicho contenido tanto con la densidad como con el contenido de agente espumante. Otro parámetro relacionado con la estructura celular que se ha analizado es la distribución de tamaños de celda, al igual que en el caso anterior dicho análisis se ha realizado con la ayuda del parámetro SD, (capítulo 2). En este caso se han detectado de nuevo tendencias aparentemente opuestas entre ambos tipos de materiales. Mientras que para aquellos producidos utilizando ADC, a medida que aumenta la densidad se obtienen distribuciones de tamaños de celda más homogéneos, en aquellos fabricados utilizando CO_2, la distribución de tamaños de celda se hace más homogénea a medida que disminuye la densidad, (excepto para las muestras con ER=4). Un aumento en la concentración de agente espumante implica una reducción de la anchura de la distribución de tamaños de celda. Es necesario tener en cuenta que para las muestras hechas con CO_2 la reducción de la densidad equivale a un aumento de la cantidad de agente espumante, por lo que se puede concluir que desde este punto de vista ambos tipos de materiales se comportan de un modo similar.

Las propiedades mecánicas de los materiales han sido analizadas en términos absolutos y relativos, sin embargo es el análisis de las propiedades relativas el que mejor clarifica el comportamiento de todos los tipos de muestras. En términos de rigidez (módulo de elasticidad), se observan dos tendencias claras con respecto a la densidad relativa. Para densidades relativas mayores de 0.4, los materiales más rígidos son aquellos producidos utilizando la ruta ICM y más concretamente los fabricados

utilizando un 1 % de azodicarbonamida. Dichos materiales exhiben un contenido de celda abierta casi nulo, lo que les iguala en ese sentido a los materiales fabricados por disolución, sin embargo la razón de su comportamiento mecánico superior parece residir en una distribución de tamaños de celda más homogénea. Por otro lado para densidades relativas menores de ese valor, son los materiales fabricados mediante disolución de gas los que exhiben una respuesta mecánica superior. En este caso, la razón de dicho comportamiento radica en las estructuras celulares cerradas altamente anisotrópicas de los materiales producidos por disolución de gas.

En términos de resistencia, todos los materiales presentan un comportamiento bastante similar para las distintas densidades relativas. Esto permite deducir que la resistencia de los materiales celulares se ve influenciada en menor grado por el contenido de celdas abiertas o por la presencia de estructuras anisotrópicas.

Se puede concluir por tanto que es posible obtener materiales moldeados de celda cerrada mediante disolución de gas con un rango de densidades relativas comprendido entre 0.2 y 0.6. El crecimiento restringido del material en el interior de los moldes induce estructuras altamente anisotrópicas. Este estudio es bastante interesante desde un punto de vista práctico, en función de la densidad y de la respuesta mecánica deseada se podrá elegir uno u otro proceso de modo que se obtenga una estructura celular tal que sea capaz de adecuar la respuesta del material a las necesidades de la aplicación considerada. Así, a altas densidades (entre 0.4 y 0.6) el moldeo por compresión mejorado presenta una respuesta mecánica superior, mientras que a bajas densidades (entre 0.3 y 0.6) es más acertado utilizar el proceso de disolución de gas en un molde.

J Mater Sci
DOI 10.1007/s10853-012-6357-7

SYNTACTIC & COMPOSITE FOAMS

Moulded polypropylene foams produced using chemical or physical blowing agents: structure–properties relationship

Cristina Saiz-Arroyo · José Antonio de Saja · José Ignacio Velasco · Miguel Ángel Rodríguez-Pérez

Received: 22 October 2011 / Accepted: 16 February 2012

Abstract Polypropylene (PP) foams have become essential items due to their excellent properties. Nevertheless, obtaining net-shaped PP foams with medium relative densities is a complicated issue. In this article, two processes able to produce moulded PP foams in this density range are presented. One of them is based on a modification of the pressure quench foaming method and therefore uses a physical blowing agent (CO_2). The second one is the improved compression moulding technique which uses a chemical blowing agent (azodicarbonamide). PP foams with relative densities in the range between 0.25 and 0.6 and cylindrical shape were prepared using these foaming techniques. A common PP grade (instead a highly branched one) was used to obtain the samples, showing, that by combining the appropriate foaming technique, the adequate moulds, suitable blowing agent and proper foaming parameters, net-shaped PP foams with excellent properties can be produced starting from a conventional PP grade. Samples were characterized by analyzing their cellular structure and their mechanical properties. Results have showed that depending on the chosen foaming route isotropic or anisotropic structures with cell sizes ranging from 40 to 350 μm and open cell content in the range between 0 and 65% can be obtained. Moreover, mechanical properties are highly influenced by the production route and chemical composition of the foams. For instance, the stiffer materials at relative densities higher than 0.4 are the ones produced using the chemical blowing agent while at relative densities lower than 0.4 are the ones produced using the physical blowing agent.

C. Saiz-Arroyo (✉) · J. A. de Saja · M. Á. Rodríguez-Pérez
Cellular Materials Laboratory (CellMat), Condensed Matter Physics Department, University of Valladolid, Prado de la Magdalena s/n, 47011 Valladolid, Spain
e-mail: csaiz@fmc.uva.es

C. Saiz-Arroyo
Technological Centre of Miranda de Ebro (CTME), C/Montañana P R60-R61, 09200 Miranda de Ebro, Burgos, Spain

J. I. Velasco
Departament de Ciencia dels Materials i Enginyeria Metal lúrgica, Centre Català del Plàstic Universitat Politécnica de Catalunya, C/Colom 114, 08222 Terrassa, Barcelona, Spain

Published online: 01 March 2012

Introduction

Polymeric foams can be defined as two-phase materials in which a gas is dispersed in a continuous macromolecular phase [1–3]. Foams, owing to the combination of excellent properties and costs savings have found an application in almost every field [2, 3].

Polypropylene (PP) is a commodity polymer that due to its outstanding functional characteristics and low material costs has been considered as a substitute for other thermoplastic polymers [4]. However, foaming PP is not a simple task [5–7] mainly due to two reasons; first, PP is a semicrystalline polymer, and as it is known that gases do not dissolve in crystalline regions. This hinders obtaining a homogeneous polymer/gas solution in solid state and hence controlling foaming process is much more difficult than for amorphous polymers when the solid state foaming process is used [8]. The second reason lies in the weak melt strength exhibited by PP. Low melt strength leads to a rupture of the cell walls under the elongational forces occurring during cell growth; as a result, final foam has a high amount of coalesced and open cells which harms their mechanical properties and makes it unsuitable for many applications [8, 9].

The main solutions proposed up to now are based in increasing melt strength of the polymer through different

ways. On the one hand, by filling PP with inorganic compounds such as talc or nanoparticles [10–12] and on the other hand by using special PP grades known as high melt strength PPs, on which by promoting a high degree of branching the melt strength is significantly increased [6, 11, 13]. Finally the less desirable solution because turn the polymer non-recyclable, is crosslinking the PP matrix [1].

Regardless the aforementioned handicaps, both linear and highly branched PP grades have been foamed with more or less success using different foaming processes such as extrusion, compression moulding, injection moulding or batch foaming [2, 3, 5–11]. Nonetheless, when the final application of the foamed part requires a certain final shape, the number of suitable foaming processes becomes limited.

In the literature it is possible to find examples of extruded PP foams; they can be classified in two types, low density foamed sheets [2, 3] or foamed filaments, [6, 7, 9–11]. Low density extruded sheets can be shaped by thermoforming but the need for a secondary process can contribute to increase the cost of the final part and thermoforming is only limited to simple shapes. Extruded filaments are made using the process developed by Park and co-workers [6, 7, 9–11] which is based on obtaining fine celled PP foams in a wide range of relative densities (between 0.1 and 0.9). For this purpose they use high melt strength PP grades or add fillers to the base PP. Regarding to the shape, they used to work with a filamentary die with a very small diameter (around 0.45 mm [6]), so that the obtained foam is only suitable for scientific purposes.

Xu [8], Jian [14], Zhai [15] and their respective co-workers have proved that despite its semicrystalline character, PP pellets or very thin sheets (50 μm thickness) can be foamed by gas dissolution using supercritical CO_2 as blowing agent. Nevertheless, all those works only deal with the structural characterization of the foamed samples. Results regarding mechanical or thermal properties of the foams are not provided. The limitations imposed by the non-regular shape and small size of so-obtained PP foams have resulted in a lack of information about the influence of foaming parameters in the structure–properties relationship. Thus, although very good cellular structures (in terms of cell size and homogeneity) are obtained by using gas dissolution as foaming process [8, 14] it is unknown its influence on the physical response of PP foams.

Taking into account the previous facts, it seems that nowadays the most suitable foaming process to obtain moulded PP foams is injection moulding. It is possible to use a conventional injection moulding machine with small modifications and physical or chemical blowing agents to produce PP foamed parts. Although foaming injection moulding offers several advantages such as the absence of sink marks on the final part surface, reduced weight, lower back pressure, faster production cycle or higher stiffness to weight ratio there are also several disadvantages. Maximum weight reduction is limited to a 40%, samples have a wide distribution of cell sizes what can negatively affect to their properties, and moreover, the quality of foamed part surface is not as good as for solid parts [16–19].

During the last years efforts have been focused in microcellular injection moulding process, also known as Mucell process [20]. It allows producing microcellular foams but weight reduction is limited to around a 25% and it is not suitable for producing big parts. Thus, it seems that injection moulding is adequate to produce moulded foams but with the main disadvantage that operating density range is very limited (usually relative density values higher than 0.6).

The main objectives of this article are connected with some of the previous topics in which a lack of knowledge has been detected in the literature. So, the first goal is to produce shaped PP parts with medium relative densities (between 0.25 and 0.6). To cover this objective, two different foaming methods have been used, a modified pressure quench method and the improved compression moulding technique.

The second goal is to gain knowledge on the structure–property relationships for these materials. As the produced samples have a cylindrical geometry with a significant thickness, it has been possible to measure the mechanical properties analyzing them as a function of the foams structure. A comparative study of the materials produced from both methods is also presented.

Finally, the third objective is to analyze if by using adequate formulations and processing parameters it is possible to produce foamed parts with relative densities in the range 0.2–0.6 with a good quality using a conventional linear non-filled PP avoiding the use of high melt strength PPs.

Materials and foaming processes

Materials

A random PP copolymer (200CA10 from Inneos) with a melt flow index of 10 g/min (measured at 230 °C and 2.16 kg) was used to produce all the analyzed samples. Its melting point is 150.4 °C and its crystallinity degree is 44.4% (both were measured by DSC). Azodicarbonamide (Porofor ADC/M-C1 from Lanxess) with an average particle size of (3.9 ± 0.6) μm was used as chemical blowing agent and CO_2 with a high purity was used as physical blowing agent. In order to prevent thermal oxidation of the polymer a commercial antioxidant (Irganox B561 from Ciba) was added. Stearic acid (Stearic Acid 60/40 from Renichem) was used as processing aid.

Foaming processes

Modified pressure quench method

In a first step, PP pellets were re-extruded in a twin-screw extruder (Collin Kneter 25X36D) at a rotating speed of 160 rpm and with a temperature profile varying from 130 °C in the hopper to 155 °C in the die. Extruded material was water cooled and pelletized. A 0.1 wt% of both antioxidant and processing aid (stearic acid) were added to the polymer.

In a second step, discs with 20 mm in diameter and 3 mm thickness were compression moulded in a two hot-plates press at 170 °C and 40 bars. The so-obtained discs are placed in a mould which is at the same time disposed inside a high pressure vessel.

This mould has the ability of controlling the final density of the foams as well as allows producing a shaped foamed part (cylindrical in this paper, although other geometries could be produced using the same process). Figure 1 shows a schematic draw of such mould. As it can be observed, it is a cylindrical mould with an internal cavity of 20 mm in diameter and 12 mm in height made of stainless steel. There are also several cylindrical inserts with different heights but with the same diameter of the cavity (20 mm). Those inserts allow reducing the volume of the mould internal cavity to increase the foam density.

To control the density of the foam, the volume of the precursor (solid PP discs), is kept constant while the volume of the cavity of the mould is varied using the previously mentioned inserts. So, precursors always have the same weight and dimensions but they are expanded to different heights which are controlled by the height of mould cavity.

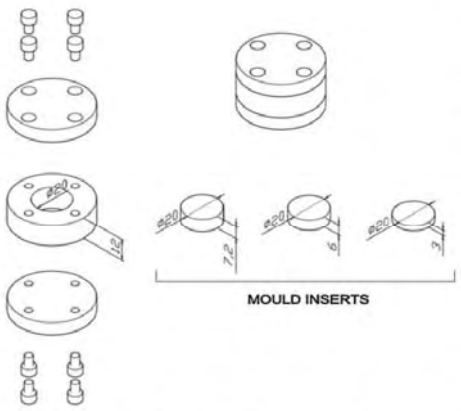

Fig. 1 Schematic draw of the mould use to produce foams by the modified pressure quench method

It has been possible to obtain foams with expansion ratios of 1.6, 2, 3 and 4, which corresponds to nominal densities of 562.5, 450, 300 and 225 kg/m^3. The use of a mould inside the pressure vessel to produce net-shape parts is not a common practice, although as it is shown in this paper is a promising technique.

As it was previously mentioned, samples were produced by the pressure quench method. This method comprises two steps. First, a thermoplastic sample is placed in a high pressure vessel and saturated with an inert gas, typically CO_2 in the supercritical region. For an amorphous polymer gas saturation is performed at a temperature slightly below its glass transition temperature, while for semicrystalline polymers, in order to increase gas sorption it is done at a temperature slightly above its melting point. Then, upon a prolonged exposure to supercritical CO_2 at high pressure a polymer/gas solution is formed. In a second step, the system is rapidly depressurized. The rapid pressure quench decreases the gas solubility in the polymer and causes bubble nucleation due to supersaturation.

In this study, PP discs placed inside the mould were saturated with CO_2 at different pressures varying from 170 to 240 bar. Saturation pressure was chosen depending on the final density of the sample; as density should be lower, saturation pressure was higher. Gas dissolution step was performed at a constant temperature of 155 °C. After 40 min, polymer/gas solution was cooled down until foaming temperature. Then, samples were foamed by rapid depressurization of the autoclave. Sample density (expansion ratio) was controlled with the mould dimensions, pressure drop (ΔP) and foaming temperature. In addition, along the experiments, final pressure (remnant pressure in the autoclave after depressurization step) was also tuned to have a more accurate control of the expansion degree of the sample.

Table 1 shows the main processing parameters used to produce foams with the four different density values allowed by the mould. Saturation temperature was kept constant along the experiments while saturation pressure, foaming temperature and pressure drop were adjusted for each expansion ratio value. It can be also observed that both saturation pressure and pressure drop were increased as density decreases.

It can be also concluded from Table 1, that as density decreases, residual pressure inside the autoclave after depressurization was lower. In fact, for the lightest materials, the autoclave remains open after depressurization to assure the complete expansion of the samples. Regarding to foaming temperature, it can be seen how as expansion ratio increases, foaming was performed at lower temperatures. As the density decreases the base polymer is stretched to

Table 1 Foaming conditions used to produce moulded polypropylene foams using CO_2 as blowing agent

Sample	$\rho_{Theoretical}$ (kg/m^3)	$T_{Saturation}$ (°C)	$t_{Saturation}$ (min)	$P_{Saturation}$ (bar)	$T_{Foaming}$ (°C)	$P_{Foaming}$ (bar)	Pressure drop (ΔP, bar)	Final pressure (bar)
D1	562.5	155	40	185	125	155	100	55
D2	450	155	40	200	125	170	120	50
D3	300	155	40	235	120	180	160	20
D4	225	155	40	240	115	190	190	0—Open

higher ratios and hence it is necessary to increase the melt strength of the polymer by decreasing foaming temperature. Moreover, it should be taken into account that at high pressures, gas concentration is higher leading to lower viscosities and therefore reducing temperature is needed to increase polymer viscosity.

Designation of CO_2 blown samples will be as follows. A D followed by a number that indicates expansion ratio value, so samples will be named as D1 (for expansion ratio of 1.6), D2, D3 and D4.

Table 2 summarizes the expected values of density, real density, relative density, and theoretical and real expansion values. Comparing expected and obtained values of both density and expansion ratio, it can be concluded that foaming parameters were suitably chosen and an accurate control of foaming process was achieved.

Improved compression moulding

In this foaming route, the first step comprises melt compounding of raw materials. Thus, PP, blowing agent (azodicarbonamide), stearic acid and antioxidant were melt-mixed in a twin-screw extruder (Collin Kneter 25X36D) with a temperature profile varying from 130 °C in the hoper to 155 °C in the die and at a rotation speed of 160 rpm. Material was water cooled and pelletized.

Pellets with different blowing agent contents (1, 5, 10 and 15 wt%) were produced. The use of different contents of azodicarbonamide was aimed to analyze the effect of blowing agent amount in both cellular structure and mechanical properties of so-produced foams.

The second step comprises the preparation of precursor materials which in this case are cylinders with 20 mm in diameter and 15 mm in height. They were produced using a cylindrical shaped mould and a two hot-plates press at a temperature of 175 °C and using a pressure of 3 Tn during 10 min.

Foaming step was conducted under mechanical pressure using the so-called self-expandable moulds. Those moulds allow controlling density of the foamed sample. A temperature of 205 °C and an initial pressure of 95 MPa were used to produce foams with different azodicarbonamide contents. A more detailed description of this foaming process can be found elsewhere [21–23].

For azodicarbonamide blown samples, designation is as described. An A followed by two numbers, first one indicates azodicarbonamide amount (1, 5, 10 or 15 wt%) and second one the expansion ratio value (1 for 1.6, 2 and 3). For example sample A-5-2 was foamed using a 5 wt% of azodicarbonamide and an expansion ratio of 2.

Foams with expansion ratios of 1.6, 2 and 3 were produced using this method. Average density and relative density values of so-produced foams are summarized in Table 3.

Table 2 Values of density, relative density and expansion ratio (E.R. $= \frac{\rho_{Solid}}{\rho_{Foam}}$) of moulded polypropylene foams

Sample	ρ_{REAL} (kg/m^3)	$\rho_{RELATIVE}$ (kg/m^3)	E.R. (Theoretical)	E.R (Real)
D1	534.8 ± 33.5	0.594	1.6	1.69 ± 0.09
D2	447.9 ± 17.5	0.497	2	2.01 ± 0.07
D3	290.4 ± 5.4	0.322	3	3.10 ± 0.05
D4	218.5 ± 2.8	0.242	4	4.12 ± 0.05

Experimental

Density

Density measurements of both precursors and foamed samples were performed by the geometric method; this is by dividing the weight of each specimen between its corresponding volume (ASTM standard D1622-08).

Structural characterization

Cell morphology of the samples was analyzed by using scanning electron microscopy. Samples were frozen with liquid nitrogen and fractured. Fractured surface of the samples was made conductive by sputtering deposition of gold and observed using a Jeol JSM-820 scanning electron microscope. Average cell diameter and cell density were determined using an image processing tool based on the software ImageJ [24]. In addition, anisotropy ratio (R) which can be defined as the ratio of the mean intercept

Table 3 Main characteristics of foams produced by the improved compression moulding route using azodicarbonamide as blowing agent: density, relative density and real expansion ratio (theoretical expansion ratios were 1.6, 2 and 3)

Sample	ρ (kg/m^3)	ρ_R	E.R.$_{REAL}$
1 wt% Azodicarbonamide			
A1-1	525.7	0.595	1.60
A1-2	432.2	0.483	1.97
A1-3	294.1	0.337	3.01
5 wt% Azodicarbonamide			
A5-1	512.5	0.571	1.61
A5-2	444.2	0.498	1.98
A5-3	279.2	0.313	3.04
10 wt% Azodicarbonamide			
A10-1	474.0	0.525	1.71
A10-2	424.5	0.456	2.01
A10-3	281.8	0.307	3.01
15 wt% Azodicarbonamide			
A15-1	436.8	0.469	1.73
A15-2	387.9	0.420	2.01
A15-3	287.9	0.306	3.08

length in the longitudinal direction to that in the perpendicular plane [25] was also measured using the aforementioned software

Open cell content

The percentage of open cells (C) was measured with an Eijkelkamp 08.06 Lange air pycnometer according to ASTM D6226-10. The following equation (1) was used according to the ASTM standard:

$$C = \frac{V_{\text{Sample}} - V_{\text{Pycnometer}}}{V_{\text{Sample}} \cdot p} \quad (1)$$

where the geometrical volume, V_{Sample} (calculated from the specimen dimensions) is subtracted from the sample volume measured with the pycnometer, $V_{\text{Pycnometer}}$, and divided by the volume of air contained in the sample ($V_{\text{Sample}} \cdot p$), where p is the sample porosity calculated by $\left(1 - \frac{\rho_f}{\rho_S}\right)$; ρ_f is the foam density and ρ_S is the density of the polymeric matrix, in this case PP ($\rho_S = 900$ kg/m^3)

Mechanical tests

Mechanical response of solid precursors and foamed samples was analyzed by compression tests. Stress–strain curves were measured in a universal testing machine (Instron model 5500R6025). Experiments were performed at room temperature and at a strain rate of 10 s^{-1}. The maximum static strain was 75% for all the experiments.

Three mechanical properties were obtained from these experiments, elastic modulus, calculated as the slope of the initial zone of the stress–strain curves, density of absorbed energy, defined as the area under the stress–strain curve up to a 75% strain, and collapse stress, measured in the intersection between a parallel line to the stress–strain response at low strains and a parallel line to the plateau region of the stress–strain curve.

Results and discussion

Cellular structure

Cell size, cell density and anisotropy

Although the properties of a cellular material are mainly determined by its density, microstructure also plays an important role in the behaviour of a foam, so a careful analysis of foam cellular structure can be useful for the comprehension of its response.

In this study, as different foaming processes are being used, it is necessary to know how each of them affects to the microstructure. Therefore, in the case of CO_2 dissolution, it should be analyzed the effect of density, and in addition if the restricted growth could affect in somehow the cellular structure of so-produced materials. On the other hand, in the case of samples made using azodicarbonamide, the effect of density as well as the influence of blowing agent content should be analyzed.

Figure 2 shows micrographs of PP foams produced using CO_2 as blowing agent. Several assertions can be pointed out from the observation of those micrographs.

First of all, as it can be observed, foams exhibit a completely closed cell cellular structure (this was confirmed afterwards with open cell content measurements). As it was mentioned in "Introduction", the base polymer used was a linear PP, therefore accomplishing closed celled foams indicates a proper control of foaming parameters (mainly foaming temperature and pressure drop).

On the other hand, it is easily inferred from the previous micrographs (Fig. 2) that as density decreases more anisotropic structures are obtained. The more dense samples (D1) exhibit an isotropic cellular structure, but as density of the samples decreases (expansion ratio increases) cells become oriented in the expansion direction (Fig. 1). In order to quantify this effect, the anisotropy ratio (R) of the samples was measured (Fig. 3a). While for D1 samples anisotropy ratio value is close to 1 (isotropic material) for D4 samples values around 2 are reached. Obtaining such anisotropic structures is connected with the restricted growth of the foam inside the mould. As diameter of the precursor is equal to the diameter of mould

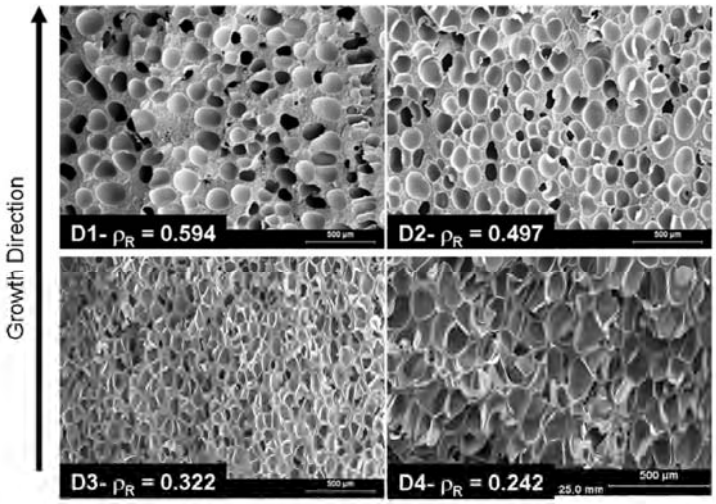

Fig. 2 Micrographs showing the cellular structure of polypropylene foams produced using CO_2 as blowing agent

cavity, expansion of the sample may occur only in one direction.

Cell size as well as cell density of those foams were measured. Results are shown in Fig. 3b. It can be observed how cell size decreases as density does except for D4 samples where cell density increases as density does, once more except for D4 samples. So it seems that the lightest samples do not follow the same tendency as the others being the reason the foaming process itself.

The results obtained for D4 samples can be due to the combination of various effects. On one hand, for those samples, autoclave remains open after depressurization steps and the absence of a counter pressure could lead to larger cell sizes. On the other hand, a decrease in foaming temperature and an increase in the saturation pressure can lead to an increase in the amount of CO_2 dissolved in the polymer allowing cells to be able to grow large. Finally, D4 samples are the ones with the highest expansion ratio; as the cell expansion increases, cell wall thickness decreases, and the rate of gas diffusion between cell walls can increase leading to coalescence phenomena and thus decreasing cell density.

Figure 4 shows micrographs of PP foams with similar relative densities (around 0.5) blown using different amounts of azodicarbonamide. All of them exhibit an isotropic cellular structure being cell size smaller and cell density higher as azodicarbonamide content increases. This effect is achieved for all the analyzed density values, and can be evaluated in Fig. 5 where cell size (a) and cell density (b) are plotted as a function of azodicarbonamide content. Chemical

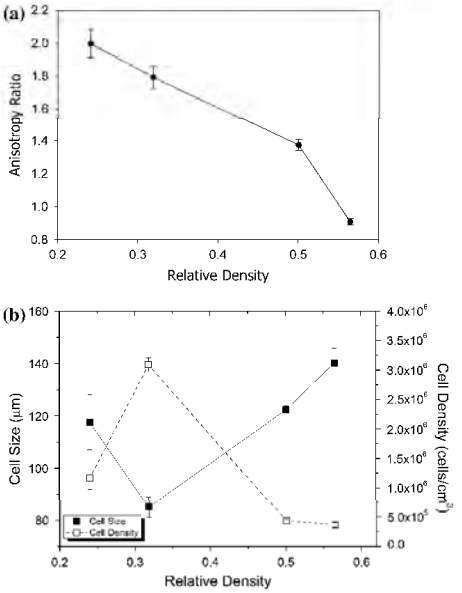

Fig. 3 **a** Variation of anisotropy ratio with relative density for polypropylene foamed by the modified pressure quench method. **b** Cell size and cell density of polypropylene foams produced using CO_2 as blowing agent

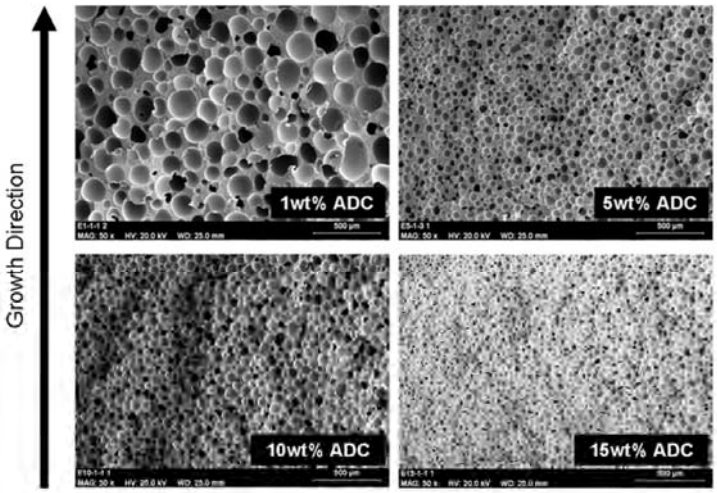

Fig. 4 Cellular structure of polypropylene foams with relative density 0.5 and produced using different amounts of azodicarbonamide

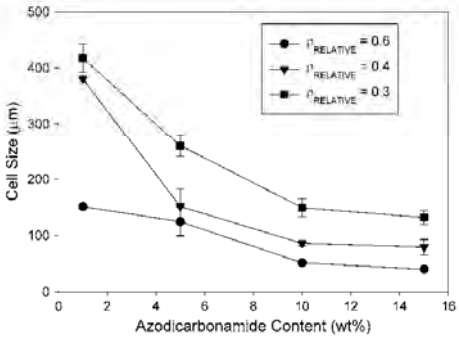

Fig. 5 Cell size of azodicarbonamide blown samples

blowing agents such as azodicarbonamide are known to be self-nucleating [2] so as blowing agent content increases a higher number or nucleating sites are available leading to higher nucleation rates and smaller cell sizes.

Comparing the results obtained using both types of processes (Figs. 3, 5), it can be concluded that the restricted growth only lead to anisotropic structures in the case of CO_2. Moreover, using chemical blowing agents, smaller cell sizes and higher cell densities are achieved.

Cell size distribution

It is known that large and non-uniform cells can have a negative influence on mechanical response [2, 3, 25]. Typically, histograms of the cell size distributions are plotted and afterwards compared. Due to the high amount of samples included in this study and in order to be able to easily compare the results obtained for both processes a standard deviation coefficient of the cell size distribution (SD), has been calculated according to Eq. 2 [26, 27]:

$$SD = \sqrt{\sum_{i=1}^{n} \frac{(\phi_i - \phi)^2}{n}} \quad (2)$$

where n is the number of counted cells, ϕ_i is the cell diameter of cell i and ϕ is the average diameter of the cells. This parameter measures the width of the cell size distribution.

Results (Fig. 6) show clear differences between the samples produced using azodicarbonamide or CO_2. For relative densities higher than 0.4, smaller values of SD are achieved using azodicarbonamide while for relative densities smaller than 0.4, smaller values of SD are obtained for CO_2 blown samples. Moreover, as density decreases SD increases for samples made using ADC. On the contrary, for samples made using CO_2, SD decreases as density does.

There is also a clear influence of blowing agent amount. The smallest values of SD are obtained for high azodicarbonamide content (10 and 15 wt%) while when lower amounts of blowing agent are used, SD values are between two and three times higher.

Open cell content

It was found that open cell content for PP samples made using CO_2 was very close to 0%; on the contrary for samples produced using azodicarbonamide (Fig. 7) it was observed that this parameter increases as density is

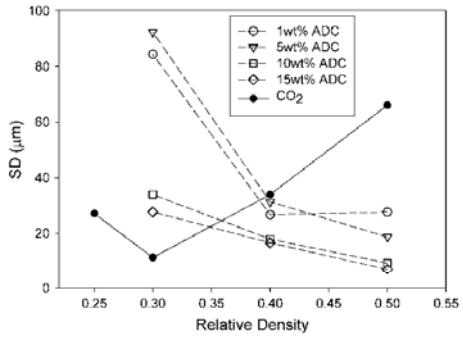

Fig. 6 SD coefficient for the whole collection of polypropylene foams

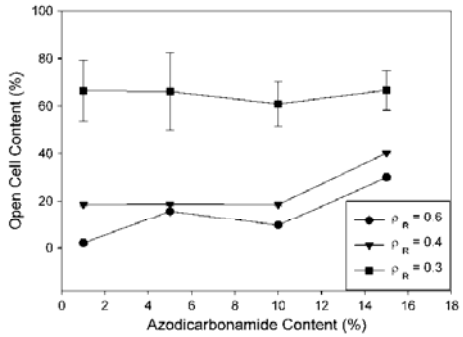

Fig. 7 Open cell content as a function of blowing agent amount for polypropylene foams with different relative densities

reduced. Regarding the influence of blowing agent amount, the higher values of open cell content are reached when the highest percentage of azodicarbonamide (15 wt%) is used. When such high amounts of ADC are used (15 wt%), the pressure generated inside the mould is much higher than for lower ADC contents. Due to this, the pressure drop during foaming is higher, and could lead to a significant opening of cell walls.

In addition, higher open cell contents are reached in the lightest samples ($\rho_R = 0.3$). As expansion ratio increases, the polymer is subjected to stronger elongational forces, hence, cell walls are thinner and consequently easily breakable.

Mechanical response

Using any of the two foaming processes it is possible to obtain perfectly moulded foams, so their mechanical properties could be determined by performing compression tests. Moreover, solid precursors from which each foam was produced were also analyzed. In the case of gas dissolution it was pure PP and for the improved compression moulding process, PP with the corresponding azodicarbonamide content.

Elastic modulus (E), collapse stress (σ_e) and density of absorbed energy (W) were determined for both precursors and foams from the stress–strain curves. Results corresponding to foams produced using CO_2 are summarized in Table 4. As it was expected, E, σ_e and W decrease when the density is reduced.

Experimental results corresponding to samples made using different percentages of ADC are presented in Table 5. In order to better understand the relationship between mechanical properties, density and blowing agent amount, experimental results for E, σ_e and W for foams, precursors and pure PP have been plotted as a function of ADC concentration (Fig. 8).

Comparing the results obtained for neat solid PP and precursors of PP with different percentages of ADC it is possible to detect that increasing the amount of blowing agent improves the stiffness (Fig. 8a). As it is marked in Fig. 8, PP with 15 wt% of ADC has an elastic modulus a 40.7% higher than pure PP.

On the other hand, there is a decrease in elastic modulus due to density reduction; this reduction varies from 52 to 84% in the analyzed interval of relative density. In addition, there is a slight decrease in E with the increase of ADC concentration. Samples made using 15 wt% of azodicarbonamide exhibit a poorer stiffness than samples produced using lower amounts of blowing agent.

Figure 8b shows the results corresponding to collapse stress. While solid PP becomes stiffer as ADC is added to the polymeric matrix, the addition of the chemical blowing agent has a negative effect in samples strength. By adding only 1 wt% of ADC to the PP matrix, collapse stress is reduced by around a 25%. This result indicates a loss of elasticity of the polymeric matrix with the addition of small amounts of azodicarbonamide.

Table 4 Results of compression tests for PP foams produced using CO_2 as blowing agent

Sample	E (MPa)	σ_c (MPa)	W (MJ/m^3)
Pure PP	582.44	34.27	44.20
D-1	208.19	9.87	20.35
D-2	138.51	7.04	15.10
D-3	99.90	3.08	5.20
D-4	68.82	1.48	2.70

All the values correspond to averages of three experiments performed in the same conditions

Table 5 Results of compression tests for PP foams produced using azodicarbonamide as blowing agent

Sample	E (MPa)	σ_c (MPa)	En_{ABS} (MJ/m^3)
Azodicarbonamide 15 wt%			
PP-15	983.10	28.16	38.86
A15-1	263.55	6.25	9.15
A15-2	110.26	2.38	5.52
A15-3	86.34	1.72	2.89
Azodicarbonamide 10 wt%			
PP-10	926.98	27.95	39.96
A10-1	178.97	5.70	10.11
A10-2	139.88	3.62	6.40
A10-3	97.79	2.45	3.36
Azodicarbonamide 5 wt%			
PP-5	795.74	28.62	40.35
A5-1	141.82	5.82	10.40
A5-2	197.90	5.17	8.12
A5-3	97.83	1.87	3.59
Azodicarbonamide 1 wt%			
PP-1	644.08	25.95	38.06
A1-1	279.49	8.05	13.02
A1-2	224.16	4.88	9.32
A1-3	93.24	1.96	3.65

All the values correspond to averages of three experiments performed under the same conditions

On the other hand, there is a significant decrease of collapse stress for foamed samples due to density reduction (between 76 and 94.4% for the analyzed density range). In this case, there is no significant variations with the changes in blowing agent amount although slightly higher values are obtained for samples produced using a 1 wt% of ADC.

Finally, Fig. 8c presents the results corresponding to the absorbed energy per unit volume (W). The results follow a similar trend to that observed for collapse stress. Once more, it seems that the addition of small amounts of ADC lead to a loss of elasticity of the PP matrix. In this case, foams produced using the smallest amount of ADC exhibit the highest values of W.

The results presented in Fig. 8a–c indicate that there are cross-effects of density, blowing agent amount and cellular structure affecting the mechanical performance.

With regard to the differences between materials from both processes, it can be observed (Tables 4, 5) that for similar relative densities, samples with 1 wt% of chemical blowing agent are stiffer than the foams produced using CO_2. However, samples made using CO_2 present a better mechanical performance in terms of strength (collapse stress) and energy absorption capacity. The presence of residues coming from ADC decomposition in cell walls of PP foams produced by the improved compression moulding

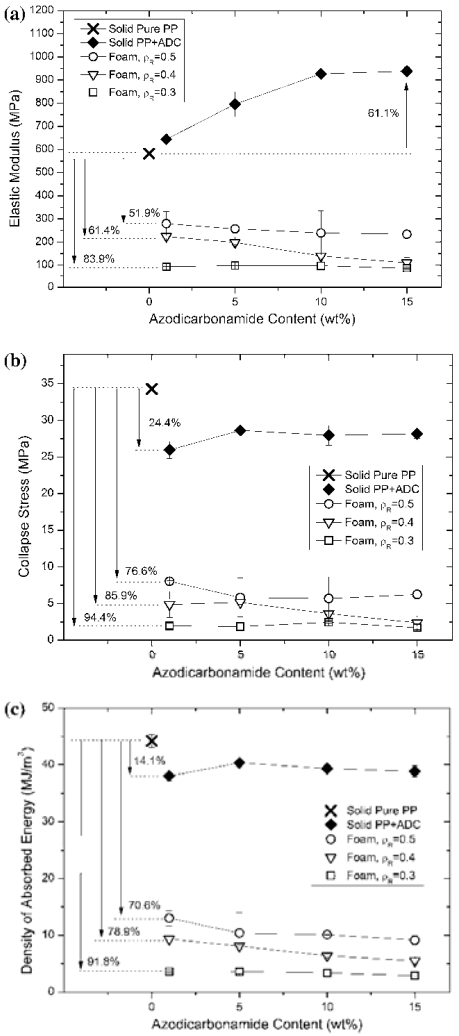

Fig. 8 Mechanical properties of PP foams with different densities produced by the improved compression moulding using different ADC contents. **a** Elastic modulus, **b** collapse stress, **c** density of absorbed energy

route, lead to a detriment of polymer elasticity and hence to a poorer mechanical response above the elastic limit.

In order to analyze if cell size is affecting the mechanical response, elastic modulus of PP foams produced using both foaming routes has been plotted as a function of

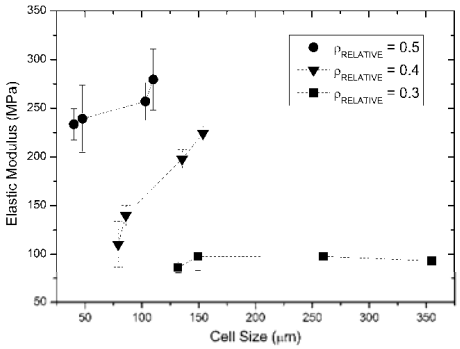

Fig. 9 Elastic modulus as a function of cell size for foams produced using the chemical blowing agent

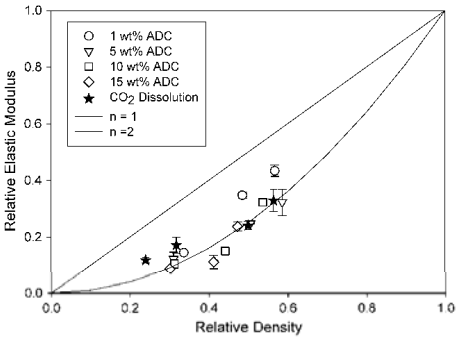

Fig. 10 Relative elastic modulus of polypropylene foams versus relative density

average cell diameter (Fig. 9). There is a significant decrease in elastic modulus as cell size decreases for ADC-blown foams at relative densities equal or higher than 0.4. On the other hand, for relative densities lower than 0.3, elastic modulus is almost constant. As it was previously mentioned, smallest cell sizes are obtained when high ADC concentrations are used; at the same time, this high concentrations lead to higher open cell contents and hence to a decrease in mechanical performance. At low relative densities, although cell size decreases as ADC content increases, open cell remains constant (Fig. 7) thus leading to a similar mechanical response of the foams.

To better understand the effect of cellular structure on the mechanical response of the whole collection of studied foams, experimental data have been also analyzed in terms of relative properties, i.e. the property of the foam divided by the property of a reference solid. The solid from which each type of foams were produced (pure PP for CO_2 blown samples and PP with ADC for azodicarbonamide blown samples) has been used as reference material.

The analysis of mechanical properties in terms of relative values, apart of clarifying results can provide information about the effect of cellular structure on the mechanical response of produced PP foams.

In addition, experimental data have been compared with theoretical estimations obtained using a potential law of relative elastic modulus versus relative density (Eq. 3) with exponent $n = 1$ and exponent $n = 2$. C was assumed to be 1 in these estimations [21, 22, 25]

$$\frac{E_F}{E_S} = C\left(\frac{\rho_F}{\rho_S}\right)^n \tag{3}$$

where E_F and ρ_F are the foam elastic modulus and density and E_S and ρ_S are the modulus and density of the reference material used in each case.

Values of n between 1 and 2 are typical for a wide amount of cellular materials [25], therefore it is expected that most foams, including the analyzed ones would have properties between these two limits.

Relative elastic modulus of the analyzed foams as a function of relative density is shown in Fig. 10. As it can be observed, both gas dissolution foams and azodicarbonamide blown foams exhibit values of n between 1 and 2. Moreover, it can be inferred that mechanical properties clearly depend on the foaming technique used to produce them.

At relative densities higher than 0.4 the stiffer materials are the foams made using the lowest amount (1 wt%) of azodicarbonamide while at relative densities lower than 0.4 the stiffer materials are the ones produced by CO_2 dissolution. Samples made using the smallest amount of azodicarbonamide are the ones with the smaller open cell content (see Fig. 6). Thus, although samples containing higher azodicarbonamide amounts (10 and 15 wt%) present smaller cell sizes, they exhibit a poorer stiffness.

It was previously said that samples produced using the physical blowing agent exhibit a closed cell structure so, although samples made using 1 wt% of azodicarbonamide present a higher open cell content, their mechanical response is much better.

The explanation of this behaviour lies in the differences found in cell sizes distribution (see Fig. 6). It was concluded after analyzing sample's microstructure that at relative densities higher than 0.4, the samples produced using a chemical blowing agent exhibited a more uniform cell sizes distribution (this is smaller values of SD).

It is known that a lower dispersion in cell sizes enhances mechanical behaviour of cellular materials [25, 26], and in this case, this narrower cell size distribution has a greater effect on stiffness than open cell content.

On the other hand at relative densities lower than 0.4, the behaviour of produced PP foams is the opposite, being the stiffer materials the ones produced by the gas dissolution technique. The results seem to be due to several reasons: an almost zero open cell content, a very uniform cell sizes distribution (for $\rho_R < 0.4$ they exhibit the smallest values of SD, Fig. 6), and the presence of a highly oriented cellular structure induced by foaming inside a mould.

According to Gibson and Ashby [25] Eq. 3 becomes the following one (4) when it is considered the elastic modulus measured in the direction where cells are oriented:

$$\frac{E_{f-Z}}{E_S} = C\left(\frac{\rho_f}{\rho_S}\right)^n \cdot R \tag{4}$$

where E_{f-Z} is the elastic modulus measured in the direction in which the cells are oriented, E_S is the modulus of the solid polymeric matrix, ρ_f and ρ_S are, respectively, foam and solid density and R is the anisotropy ratio.

Therefore, at equal relative density, an anisotropic foam ($R > 1$) will exhibit higher specific properties than an isotropic one ($R = 1$).

Collapse stress values obtained from compression tests have been also analyzed in relative terms and are shown in Fig. 11. Moreover, experimental data have been fitted to a power law equation (Eq. 5):

$$\frac{\sigma_F}{\sigma_S} = C\left(\frac{\rho_F}{\rho_S}\right)^n \tag{5}$$

where σ_F is collapse stress value of the foam, σ_S is collapse stress of solid material (each precursor in this case) and $\frac{\rho_F}{\rho_S}$ is the relative density of the foams [22, 25].

Values for n obtained from the fitting of experimental data are also given in Fig. 11. Values of n close to 2 are in agreement with predictions for an elastic collapse of the cellular structure [22]. In this study, the closest values to $n = 2$ are obtained for samples produced using the gas dissolution technique ($n = 2.24$) and the ones produced using 1 wt% of chemical blowing agent ($n = 2.17$) and those produced using 15 wt% of chemical blowing agent ($n = 2.3$).

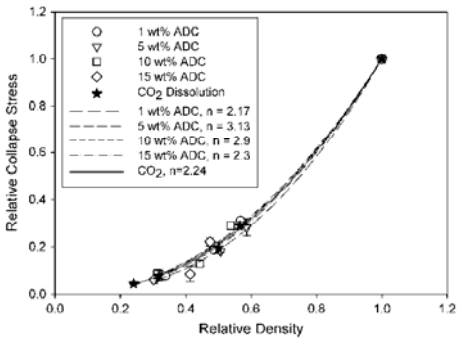

Fig. 11 Relative collapse stress of PP foams versus relative density

Gibson and Ashby [25] define the Young's modulus anisotropy ratio as the ratio between the modulus measured in the direction of maximum orientation of pores (E_L) and the modulus measured in the transversal direction (E_T). This parameter is a function of anisotropy ratio (R) and is defined as:

$$\frac{E_L}{E_T} = \frac{2R^2}{1+(1/R)^3} + (1-\phi)\frac{2R}{1+(1/R)} \tag{6}$$

where R is the anisotropy ratio, E_L and E_T are the elastic modulus in the longitudinal direction (LD) and the transverse direction (TD), respectively. ϕ is the fraction of solid in the cell edges.

Performing a similar analysis for plastic collapse stress they find the following equation:

$$\frac{\sigma_L}{\sigma_T} = \frac{2R}{1+1/R} \tag{7}$$

where σ_L and σ_T are collapse stress measured in longitudinal and transversal direction and R the anisotropy ratio.

Therefore, the modulus depends strongly on anisotropy than strength; cells with an R value of 2 have a modulus anisotropy of nearly 8 and a strength anisotropy of around 2.6. On the other hand, Eq. 7 indicates that cells are stronger in the orientation direction, even though the anisotropy in strength is not as large as that in stiffness (Eq. 6).

Hence, in our case, we can observe a great effect of anisotropy in the elastic modulus but not in the collapse stress for CO_2 blown samples. The good behaviour of these samples in terms of strength should be due to their more elastic cell walls (there is no residues from blowing agent) and to their zero open cell content.

On the other hand, samples made using 1 and 15 wt% of ADC have a mechanical performance similar to CO_2 blown samples. Samples with 1 wt% have a very small amount of ADC residues in cell walls (so elasticity of cell walls should be similar to that of neat polymer), and they combine a small open cell content with a fine cell size. PP foams made using 15 wt% of azodicarbonamide have the highest open cell content and a huge amount of residues of ADC in their cell walls but they have the most uniform cell size distribution (see Fig. 6) which seems to compensate the previous effects giving a reasonable strength.

These results seem to indicate that cell size distribution plays a key role in the mechanical response in terms of strength of PP foams.

Finally, Fig. 12 shows values of relative density of absorbed energy as a function of relative density. In this

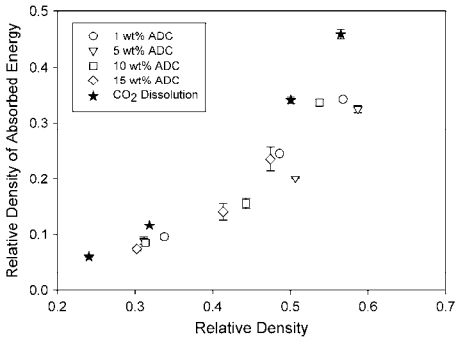

Fig. 12 Relative density of absorbed energy of polypropylene foams versus relative density

case, it can be clearly inferred from the figure that the materials produced by gas dissolution have the higher absorption capacity along the whole range of analyzed densities. Between materials made using ADC, the better performance in terms of energy absorption is obtained for samples containing 1 wt% of chemical blowing agent.

So, in this case it seems that the key parameter is a high elasticity and a zero open cell content. Foams made by the improved compression moulding route present open cells as well as residues of the chemical blowing agent in their cell walls which became them less elastic and hence they exhibit a poorer energy absorption capacity.

Conclusions

Moulded PP foams with relative densities between 0.25 and 0.6 have been successfully manufactured using two different foaming processes, gas dissolution and improved compression moulding. It has been proved that by means of both processes final density of the foams can be controlled. The accuracy of experimental density values compared with nominal ones demonstrates a proper control of the foaming parameters involved in both processes. Moreover, it should be mentioned that one of the goals of this work was obtaining moulded foams by the gas dissolution technique. Up to now, and as far as we know no papers reported such accurate control of final density and shape of CO_2 blown PPs.

It has been proved that depending on the chosen foaming process, blowing agent type and blowing agent amount a wide variety of cellular structures can be obtained. Combining the restricted growth in a mould and the pressure quench method highly anisotropic structures can be achieved. It was also observed that this combination leads to completely closed celled PP foams which could be considered a significant achievement taking into account that a linear conventional PP grade was used for the study (instead a highly branched one).

By using different amounts of chemical blowing agents, foams with different open cell content and diverse cell sizes can be manufactured.

Mechanical response of the samples has been analyzed, concluding that mechanical properties of the materials strongly depend on the method and formulation used to produce the foams. Stiffness at high relative densities can be improved using the improved compression moulding technique due to the more uniform cell size distribution obtained for 1 wt% ADC samples, however, at low relative densities the optimum cellular structure to maximize stiffness is the one obtained by the gas dissolution technique due to their high anisotropy ratio and zero open cell content. The differences obtained in strength are small. In terms of strength, the best materials are the ones made by the gas dissolution followed by the ones made using the lowest azodicarbonamide content. In addition samples produced using CO_2 have a better performance in terms of energy absorption. Those last results can be explained considering the loss of elasticity of PP matrix due to the presence of residues coming from ADC decomposition in the samples produced using chemical blowing agents.

Acknowledgements Financial assistance from Spanish Ministry of Science and Education and Feder Program (MAT 2009-14001 CO2-01) as well as Innocash Project (INC-0193) and ESA Project AO-99-075 "Advanced foams unless Microgravity" are gratefully acknowledged.

References

1. Rodríguez-Pérez MA (2005) Adv Polym Sci 184:1
2. Eaves D (2004) Handbook of polymeric foams. Rapra Technology, Shawbury
3. Klempner D, Sendijarevic V (2004) Handbook of polymeric foams and foam technology, 2nd edn. Hanser Publishers, Munich
4. Naguib HE, Park CB, Song SW (2005) Ind Eng Chem Res 44:6685
5. Doroudiani S, Park CB, Kortschot MT (1996) Polym Eng Sci 36:2645
6. Naguib HE, Park CB, Panzer U (2002) Polym Eng Sci 42:1481
7. Naguib HE, Park CB, Reichelt N (2004) J Appl Polym Sci 91:2661
8. Xu ZM, Jian XL, Liu T, Hu GH, Zhao L, Zhu ZN, Yuan WK (2007) J Supercrit Fluid 41:299
9. Park CB, Cheung LK (1997) Polym Eng Sci 37:1
10. Zheng WG, Lee YH, Park CB (2010) J Appl Polym Sci 117:2972
11. Zhai W, Kuboki T, Wang L, Park CB, Lee EK, Naguib HE (2010) Ind Eng Chem Res 49:9834
12. Antunes M, Velasco JI, Realinho V, Solorzano E (2009) Polym Eng Sci 49:2400
13. Bhattacharya S, Gupta RK, Jollands M, Bhattacharya SN (2009) Polym Eng Sci 49:2070

14. Jian XL, Liu T, Xu ZM, Zhao L, Hu GH, Yuan WK (2009) J Supercrit Fluid 48:167
15. Zhai W, Wang H, Yu J, Dong JY, He J (2008) Polymer 49:3146
16. Osswald TA, Turn LS, Gramman PJ (2002) Injection moulding handbook. Hanser Publishers, Munich
17. Lee JWS, Wang J, Yoon JD, Park CB (2008) Ind Eng Chem Res 47:9457
18. Touleshkow N, Djoumaliisky S, Kotzev G (1989) Polym Degrad Stab 24:327
19. Guo MC, Heuzev MC, Carreau PJ (2007) Polym Eng Sci 47:1070
20. Okamoto KT (2003) Microcellular processing. Hanser Publishers, Munich
21. Rodríguez-Pérez MA, Lobos J, Pérez-Muñoz CA, de Saja JA (2008) Cell Polym 27:327
22. Rodríguez-Pérez MA, Lobos J, Pérez-Muñoz CA, de Saja JA (2009) J Cell Plast 45:389
23. Rodríguez-Pérez MA, Simoes RD, Roman-Lorza S, Alvarez-Lainez M, Montoya-Mesa C, Constantino CJL, de Saja JA (2011) Polym Eng Sci. doi:10.1002/pen.22046
24. Pinto J, Rodríguez-Pérez MA, de Saja JA (2009) In: XI Reunión del Grupo Especializado de Polímeros (GEP), 10–14 September 2009, Valladolid, Spain
25. Gibson LJ, Ashby MF (1997) Cellular solids: structure and properties. Cambridge University Press, Cambridge
26. Rodríguez-Pérez MA, Alonso O, Duijsens A, de Saja JA (1998) J Appl Polym Sci 36:2587
27. Gong W, Gao J, Jiang M, He L, Yu J, Zhu J (2011) J Appl Polym Sci 122:2907

Capítulo 8

Proceso de Recuperación de Materiales Celulares con base Polietileno de Baja Densidad Entrecruzados.

En este capítulo se presenta un proceso de recuperación de residuos de materiales celulares con base LDPE entrecruzado. La gran demanda de materiales celulares en los últimos años ha ido acompañada de la generación de una gran cantidad de residuos que no en todas las ocasiones son fácilmente recuperables. Estos residuos pueden proceder de productos ya utilizados, (en muchos casos los materiales celulares debido a sus aplicaciones, tienen un ciclo de vida muy corto) o a productos defectuosos o recortes generados durante el proceso de fabricación.

Cuando se trata de un material termoplástico sin entrecruzar, el proceso es sencillo, basta con moler los residuos, volverlos a procesar en una extrusora y el polímero es válido de nuevo para producir nuevas piezas, ya sea aligeradas o no. Sin embargo, cuando se trata de materiales celulares entrecruzados el proceso se complica ya que no se pueden volver a fundir y reprocesarlos sin más. Se pueden encontrar algunas opciones como son el molido y la inclusión de un porcentaje de dicho polvo como material de relleno o la producción de nuevos materiales mediante la compresión en caliente de virutas de residuos. En cualquiera de los dos casos, el material obtenido no tiene propiedades similares a las del material de partida, ya que la densidad del material recuperado suele ser considerablemente más elevada.

El artículo incluido en este capítulo se ha publicado en la revista **Polymer Engineering and Science** y se titula "*Production and Characterization of Crosslinked Low-Density Polyethylene Foams using Waste of Foams with the Same Composition*". El objetivo principal de este trabajo es por tanto, optimizar un proceso de recuperación de residuos de materiales celulares de baja densidad con base LDPE entrecruzado. Como novedad, se pretende mantener la densidad de los productos recuperados lo más baja posible de modo que éstos puedan ser utilizados para aplicaciones similares a las de los materiales de partida.

Además de virutas de espuma, se ha introducido otro tipo de residuo, al que se ha denominado "piel" y que es la capa exterior de bloques de espuma de LDPE entrecruzada producidos en un proceso de moldeo por compresión en dos etapas. El proceso consiste en introducir una cierta cantidad de residuos en un molde de sección cuadrada que se introduce a su vez en un horno precalentado a 140ºC. Cuando en el interior del molde se alcanza una temperatura de 120ºC, se saca el molde del horno y se coloca en una prensa hidráulica, donde se comprime el material hasta obtener una pieza con la altura deseada. El material se deja enfriar lentamente bajo presión para que adopte una forma regular.

Se han producido materiales recuperados con diferentes relaciones de porcentaje piel-virutas y con tres densidades distintas. La densidad de los materiales recuperados es similar a la que presentan productos comerciales producidos utilizando el mismo

proceso de fabricación, de modo que se han comparado las propiedades de los materiales recuperados con las de dichos productos comerciales así como con las de los materiales de partida (virutas y piel). De este modo es posible cuantificar cómo afecta el proceso de recuperación tanto a la microestructura como a las propiedades físicas (térmicas, mecánicas y acústicas) de los materiales.

El grado de adhesión entre las virutas se analizado mediante microscopía electrónica de barrido, (SEM). Se puede observar que los trozos de espuma están perfectamente unidos unos a otros mediante unas uniones que en ningún caso superan las 200 μm de espesor. Esto sólo se consigue gracias a la baja presión utilizada durante el proceso, indicando además el buen grado de adhesión una selección adecuada de los parámetros de proceso. Respecto a la estructura celular hay dos efectos importantes inducidos por el proceso de recuperación. Por un lado, una reducción del tamaño de celda de los materiales recuperados respecto al del material de partida y por otro lado, la aparición de estructuras celulares altamente orientadas, ($R \approx 2$ para los materiales recuperados frente a $R \approx 1$ para los materiales de partida). La compresión de las virutas calientes durante el proceso de recuperado induce ambos efectos que permanecen en el material al ser éste enfriado bajo presión. Además, dicha compresión en caliente junto con la presencia de algunos huecos entre las virutas conlleva un aumento del contenido de celda abierta en los materiales recuperados.

Dado que los materiales de partida son utilizados típicamente como aislantes térmicos, se ha cuantificado el efecto del proceso de recuperado en la conductividad térmica de los materiales. Las espumas recuperadas presentan valores de conductividad térmica superiores a los del material de partida debido al aumento de densidad. También exhiben valores ligeramente superiores a los obtenidos para productos comerciales con densidades similares, lo cual se ha relacionado con mayor porcentaje de celda abierta de los materiales recuperados.

Las propiedades mecánicas de los materiales recuperados han sido medidas en dos direcciones diferentes, una paralela a la de compresión durante el proceso de recuperado y otra perpendicular a ésta. En cualquiera de las dos direcciones, las propiedades de los materiales recuperados son superiores a las del material de partida debido al aumento de la densidad, sin embargo, en ambos casos son ligeramente inferiores a las de los materiales comerciales, debido principalmente al aumento del grado de interconectividad entre las celdillas y a la orientación celular previamente descrita.

Aunque los materiales de partida no son utilizados típicamente como absorbedores acústicos debido a un insuficiente porcentaje de celdas abiertas, al detectarse un aumento del mismo debido al proceso de recuperado se decidió medir el

coeficiente de absorción acústica de los materiales recuperados. Tanto el material de partida como los comerciales presentan un máximo de absorción localizado en una frecuencia. El aumento del grado de interconexión entre las celdillas promovido por el proceso de recuperado hace que el rango de frecuencias donde los materiales son capaces de atenuar el sonido se amplíe.

Para concluir se puede decir que se ha puesto a punto un proceso sencillo de recuperado de espuma reticulada de LDPE, que no implica una gran inversión económica y que puede ser viable desde un punto de vista industrial. La densidad de los materiales no se incrementa de forma crítica debido al proceso de recuperación, sino que se mantiene dentro del rango de productos comerciales producidos por la misma vía que los materiales de partida. Desde un punto de vista científico se ha analizado la relación estructura-propiedades para estos nuevos materiales y se ha probado que los productos recuperados se pueden utilizar en aplicaciones similares a las de los productos originales. Esto supone una gran ventaja, ya que un posible productor no tendría que buscar un nuevo mercado para dichos productos.

Production and Characterization of Crosslinked Low-Density Polyethylene Foams using Waste of Foams with the Same Composition

C. Saiz-Arroyo,[1,2] J.A. de Saja,[1] M.A. Rodríguez-Pérez[1]
[1] *Cellular Materials Group (CellMat), Condensed Matter Physics Department, University of Valladolid, Prado de la Magdalena s/n, 47011, Valladolid, Spain*

[2] *Technological Centre of Miranda de Ebro (CTME), Miranda de Ebro, Spain*

A process to recover residues of crosslinked polyolefin foams is described in this paper. Low-density foam scraps coming from discarded products or cuts from secondary manufacturing processes are heated and pressed to obtain a new material. The main target to reach with the used recovering process was to keep the density of the recycled specimens as low as possible, and similar to that of the starting products. The structure and properties of both recovered and virgin commercial materials with similar densities have been analyzed. It has been found that due to the recovering process cell size slightly decreased and at the same time the cells become orientated. Mechanical properties of recovered foams were lower than those of commercial products, even though thermal conductivity remained in the range of the values presented by virgin products, and recovered products were better sound absorbers than virgin foams. It is concluded that due to its low density and good balance of properties the recovered materials can substitute virgin materials in applications in which the key properties are excellent thermal insulation, good acoustic absorption, and medium compressive strength. POLYM. ENG. SCI., 52:751–759, 2012.

INTRODUCTION

Polymer foams are two-phase materials in which a gas is dispersed in a continuous macromolecular phase [1]. The markets for foams have been growing worldwide, with North America, European countries, and Japan as the leading producers and consumers of foams [2].

Polyolefins are tough, flexible, and resistant to chemicals and abrasion. Foams made from polyolefins inherit these properties. Although polyolefin foams are relatively recent compared with, for instance, polyurethane or polystyrene foams, they are used in almost every industry. Areas of application include packaging, sports and leisure, toys, thermal insulation, automotive, military, aircraft, buoyancy or cushioning [3]. The typical density range for these products is between 25 and 100 kg/m^3. In terms of sales, foamed plastics demand in USA in 2008 was 7.4 billion pounds and it is expected to grow 2.7% annually through 2013 to 8.4 billion pounds. Foamed urethane will remain the largest segment while foamed low-density polyethylene will grow the fastest [4].

The tremendous growth in the use of foams in the last three decades has created a serious problem of waste disposal. A number of methods have been developed for the utilization of foam scrap. In the case of thermoplastic foams, they can be reprocessed either by extrusion, thermoforming or by molding; another option is the recovery of the respective monomers by thermal degradation. Foam scrap has also been widely used as fill material.

Some of the processes used to produce polyethylene foams, involve crosslinking the polymeric matrix before expansion of the cells. Crosslinking extends the rubbery plateau of the polymer melt, widening the temperature range in which a stable foam can be produced [1–3]. Crosslinking is advantageous for stabilizing bubbles during foam expansion. Some foam properties such as resistance of the cellular product to thermal collapse are enhanced by crosslinking polymeric matrix. Moreover, by crosslinking, polyethylene foams can extend their working temperature range. Improving thermal stability of the foams is important in some final applications of the materials such as thermoforming [2]. Other properties that are improved by crosslinking the matrix are resistance to chemicals, stability against weathering and ultraviolet radiation; mechanical properties are also positively affected by crosslinking [5, 6].

Crosslinking polyolefins produces thermoset materials. This is the main disadvantage of crosslinking; the materials become nonrecyclable by melting of the polymer phase [1].

Correspondence to: C. Saiz-Arroyo; e-mail: csaiz@fmc.uva.es
DOI 10.1002/pen.22138
Published online in Wiley Online Library (wileyonlinelibrary.com).

Residues of crosslinked polyolefin foams are originated in the manufacturing processes or from already used products. Some applications of these materials, such as packaging, have a very short life cycle; this involves producing large amounts of residues in a very short period of time. Also manufacturing process generates significant quantities of residues, mainly from parts cut from the manufactured foams or from products with defects.

Noncrosslinked polyolefin foams can be readily recycled by granulation and re-extrusion. There are many patents describing different ways for grinding foams and after extrusion the material is pelletized [7–10]. Pellets can be used to produce foams or different types of products. For instance, the recycled material can be incorporated with virgin polymer at levels of 10–20% to produce a new foam with a little effect on its properties [7–10].

On the contrary, crosslinked foams cannot be easily recovered and are used to manufacture new products, since crosslinking interferes with melt flow [3]. In the literature, it is not possible to find much information related to the recycling or recovering of crosslinked polyethylene foams. The possible solutions to recover this crosslinked waste can be divided into two options.

First one consists in producing powders from the foam residues. This powder can be used as filler in new formulations. This procedure could be advantageous, because there will be an acceptable compatibility between filler and matrix if this material is a polyolefin. Tamboli et al. [6] measured the properties of high-density polyethylene filled with residues of crosslinked foam. The authors used a mixture of crosslinked LLDPE (linear low-density polyethylene) and LDPE with a gel content between 75 and 80%. The mixture was pulverized into fine powder and used as filler. They concluded that the addition of waste foam as a filler had an effect similar to crosslinking the base HDPE. Liu et al. [11] studied the influence of adding wastes of crosslinked LDPE in the foaming process of electron beam-irradiated LDPE blends. It was concluded that under the irradiation doses used for crosslinking the base material it was not possible to make foams with smooth surface and uniform cell sizes, with a recycled material content higher than 10%.

The second solution to recover this kind of materials is similar to a thermoforming process. It consists in heating foam scrap and pressing it to obtain a new item. It is possible to find some patents describing how to obtain some articles by using this method. Those patents [12–15] describe processes for producing foam sheets using scraps or chips from crosslinked polyethylene foams. In most of the described processes, scraps are heated at high temperatures (above 200°C), and after that pressed to obtain the aforementioned sheets. The so-obtained products are used as lagoon covers and floating wetland structures in water remediation.

Recovering process detailed in these patents typically leads to foam sheets with a higher density than that of the waste used for their production. Density of described products depends on their final use, but in the aforementioned patents the range of densities is between 200 and 600 kg/m^3. Consequently, recovered products manufactured using the described recovering processes have very different properties to those of the original foams (with densities around 30 kg/m^3) and cannot be used for thermal insulation or packaging applications due to their high density. It is interesting to mention the patent by Svirklys [16] in which a continuous process to produce foams from scraps with a density range between 32 and 190 kg/m^3 is claimed.

In this paper, low-density crosslinked polyolefin foams produced from waste of the same material are produced and characterized. The main novelty of this research is that the recovering process is designed to keep the density of the final products in a range of values similar to that of the wastes used as precursors. As a consequence, recovered materials should maintain some of the properties of the original materials and could be used in the same applications as the virgin products. In order to check how physical properties of the foams are affected by the recovering process, structure and properties of the recovered materials are compared with those of virgin products with similar densities.

MATERIALS

Crosslinked polyolefin foams can be obtained by different technologies such as nitrogen gas dissolution, compression molding, semicontinuous process where the crosslinking is done by chemicals or by irradiation, and injection molding [1, 2]. In this paper, all the analyzed foams were produced by the compression molding process.

This process comprises four steps. First of all, low-density polyethylene, LDPE with a density of 0.92 g/cm^3 and melt flow index of 4.2 g/10 min at 190°C; the foaming agent, which in this case is azodicarbonamide (18.5 per hundred resin, phr); dycumil peroxide (crosslinking agent, 1.7 phr); and other additives such as carbon black are mixed in a Bambury equipment at a temperature above the melting point of the polymer (LDPE) and below the decomposition temperature of the crosslinking and blowing agents. The obtained material is in the second stage placed in a two-roll mixer to obtain a sheet of nonfoamed and noncrosslinked material (pre-form). In the third stage, a given amount of pre-form material is placed inside a two plates press, where it is heated and compressed to crosslink and to pre-expand the material. In the last step, the pre-expanded material is again heated at atmospheric pressure in a mold. The material expands to fill the mold due to the decomposition of the foaming agent. A more detailed description of this method can be found in Refs. [1, 3, 17, 18].

Four kinds of foams produced by the above-described process have been used in this study. The virgin materials are named as PE10, PE15, PE20, and PE40, where PE means that they are made from polyethylene and the two numbers represent the expansion ratio. All the materials

 DOI 10.1002/pen

TABLE 1. Main characteristics of the virgin materials under study.

Sample	Density (kg/m^3)	ϕ (μm)	CA	C (%)
PE40	22.4 ± 0.4	264 ± 20	0.98 ± 0.08	8
PE20	36.9 ± 5.7	207 ± 6	0.96 ± 0.04	7
PE15	57.5 ± 5.9	198 ± 10	1.00 ± 0.08	6
PE10	83.1 ± 0.4	125 ± 10	1.03 ± 0.04	5.5
Skin	70.7 ± 6.8	—	—	—

Density, pore size (ϕ), anisotropy coefficient (CA), and open cell content (C).

were kindly supplied by Microcel S.A. (Burgos, Spain). The main characteristics of the commercial foams used in the study are shown in Table 1.

All the recovered foams were produced from residues of the PE40 foam. Scraps, discarded foam blocks, and remaining trims were used. Furthermore, foam blocks have a "skin" after the manufacturing process. When blocks are sold to customers, a 5-mm thick skin is usually removed. Skin is formed by a combination of foamed material together with a very thin layer (thickness lower than 1 mm) of solid material; skin shows an average density of 70.7 kg/m^3. As this skin is an additional source of waste that manufacturers have to overcome different percentages of skin were introduced in the recovering process (Table 2).

The procedure used to obtain the recovered foams was as follows (Fig. 1). Waste pieces from PE40 foam were cut into chips of nonregular shape of approximately 5 mm in size. They were introduced in a prismatic mold with dimensions 7 × 7 × 15 cm^3 previously impregnated with a silicone-water solution to easily remove the sample from the mold. A thermocouple was placed inside the mold in contact with the foam scraps. The mold was then introduced in a preheated oven at 140°C. The system is placed there until the temperature measured in the thermocouple reached 120°C. This temperature was chosen according to previously reported works of our group [19, 20], where it was concluded by using thermomechanical analysis that 120°C is the optimum temperature to achieve good-quality specimens in thermoforming. Once the temperature was 120°C, the mold was removed from the oven and placed in a press where the foam scraps were pressed using a piston entering the upper part of the mold until the desired thickness was reached. After that the sample was

TABLE 2. Main characteristics and processing parameters of the recovered materials produced in this study.

Sample	m_{foam} (g)	m_{skin} (g)	T (°C)	t (min)	P (bar)	ρ (kg/m^3)
100% foam (100-F)	5	-	120	9.5	50	40.3 ± 4.4
50% foam (50-F)	5	5	120	10	50	61.1 ± 3.6
100% skin (100-S)	—	12	120	11	50	78.9 ± 5.8

m_{foam} represents the foam mass used to produce the recovered sample, m_{skin} indicates the skin mass introduced in the corresponding recovered sample. T is heating temperature of the scraps, t indicates time needed to reach aforementioned temperature, P is the pressure used during processing, and ρ is density for each type of recovered foam.

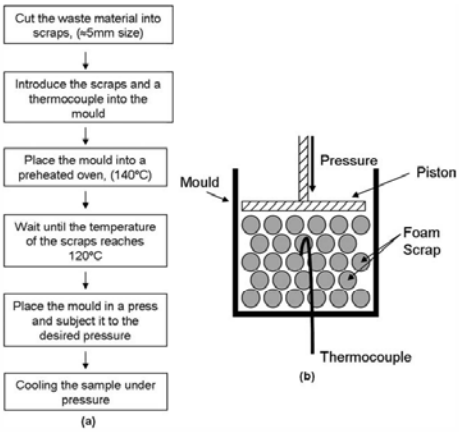

FIG. 1. (a) Diagram showing the main steps of the recovering process. (b) Schematic diagram of the set-up used to produce the samples.

cooled under pressure using compressed air and removed from the mold. A schematic diagram of the recovering process and the used set-up are shown in Fig. 1.

Three kinds of recovered samples were produced. Samples designation, composition (weight percentage of foam and skin), processing parameters (pressure, temperature, and the time needed to reach 120°C), as well as their density are shown in Table 2. At least five samples of each type were produced. 100-F foams were produced of foam scraps; 50-F was formed using half foam scraps and half skin scraps, and, finally, 100-S foams are completely produced from skin scraps. As it can be observed, the whole collection of samples was produced at the same temperature (120°C). Time to reach this temperature is also indicated in the table and increases as mass of the samples increases. A pressure of 50 bars was used to join the scraps in all cases.

Table 2 shows average density values of recovered samples. Density range is between 40 and 78 kg/m^3.

The similitude of density between recovered samples and commercial products can be observed comparing Tables 1 and 2. This was one of the targets of this research and makes possible to perform a comparative analysis between the properties of recovered products and those of virgin ones. Thus, due to their density values, 100-F samples can be compared with PE20 foams, 50-F samples with PE15 foams, and finally 100-S samples with PE10 foams.

EXPERIMENTAL

Scanning Electron Microscopy (SEM)

Scanning electron microscopy was used to observe the effect of recovering process on two characteristics of the

cellular structure such as cell size and cell anisotropy. The joints between scraps of foams were also observed by using this technique.

Samples were cooled using liquid nitrogen to cut them without modifying their structure; after they were vacuum coated with a thin layer of gold to make them conductive. A Jeol JSM-820 scanning electron microscope was used to observe the samples morphology.

Density. Density measurements of virgin materials were performed using Archimedes' principle using the density determination kit for the AT261 Mettler balance. For recovered materials, density measurements were performed by geometric method, that is by dividing mass of the samples by their volume.

Open Cell Content. The percentage of open cells (C) was measured with a Eijkelkamp 08.06 Langer air pycnometer according to ASTM D2856-94. The following equation was used according to the ASTM standard:

$$C = \frac{V_{\text{sample}} - V_{\text{pyc}}}{V_{\text{sample}} \cdot p} \quad (1)$$

where the geometrical volume, V_{sample} (calculated from the specimen dimensions) is subtracted from the total volume measured with the pycnometer, V_{pyc}, and divided by the volume of air contained in the sample (V_{sample}·p) , where p is the sample porosity calculated by $\left(1 - \frac{\rho_f}{\rho_s}\right)$; ρ_f is the foam density, and ρ_s is the density of the polymeric matrix.

Differential Scanning Calorimetry (DSC)

Thermal properties of both recovered and virgin materials were studied by means of a Mettler DSC822^e differential scanning calorimeter, previously calibrated with indium, zinc, and *n*-octane. The weight of the samples was approximately 2.5 mg.

To obtain both melting point and crystallinity of the samples, the following heating program was chosen:

- First segment: Samples were heated from −40°C to 200°C at a heating rate of 10°C/min under nitrogen atmosphere. In order to remove materials thermal history, an isothermal segment (3 min), was added at the end of this heating segment.
- Second segment: Samples were cooled from 200°C to −40°C at 20°C/min under nitrogen atmosphere.
- Third segment: Samples were heated a second time from −40°C to 200°C at a heating rate of 10°C/min, also under nitrogen atmosphere.

The melting point was taken at the minimum of the heat flow–temperature curve. The crystallinity was calculated dividing the heat of fusion in the DSC curve by the heat of fusion of a 100% crystalline material (288 J/g for a 100% crystalline polyethylene) [21].

Thermal Conductivity. A Hot-Disk TPS thermal constant analyzer was used for the measurement of thermal conductivity. This equipment is based on the transient plane source method (TPS). The method is based on the use of a sensor, which acts both as heat source and as temperature sensor. This element is built from an electrical conducting pattern of thin nickel foil in the form of a double spiral embedded by an insulation kapton layer. The hot disk sensor is located between two layers of the material under study and applies a constant electrical powder during a period of time; the increase in the temperature of the sensor is directly associated with the variation in the sensor resistance. Thermal conductivity is obtained from the temperature curve of the sensor versus time, solving the heat conduction equation. A more detailed description of this technique can be found in previous papers [22–25].

Each sample was measured five times with the same sensor (Radius= 3.189 mm). Both power and measuring time were optimized for the different types of materials to account for their different thermal conductivity.

Mechanical Tests. In order to check if the recovered materials could be used in applications such as packaging, mechanical properties in compression were measured. Stress (σ) strain (ε) curves were measured with an Instron machine (model 5500R6025) at room temperature and at a strain rate of 10 s^{-1}. The maximum static strain was 75% for all the experiments.

Three mechanical properties were obtained from these experiments. Young's modulus was calculated as the slope of the initial zone of the stress–strain curve, density of absorbed energy was defined as the area under the stress–strain curve up to a 75% strain, and collapse stress was measured in the intersection between a parallel line to the stress–strain response at low strains and a parallel line to the plateau region of the stress–strain curve.

Acoustic Characterization. The possibility of using the recovered samples as acoustic absorbers was analyzed by measuring their acoustic absorption coefficient. Determination of normal incident absorption coefficient was performed in a two microphone impedance tube (Type 4206) of Brüel & Kjaer. Experimental assembly and measurements were fixed according to the standard procedure detailed in ISO(10534-2). Frequency range of measurements was from 500 to 6400 Hz.

Samples were disks of approximately 10 mm thickness and 29 mm diameter. Two samples of each material were used to determine the absorption coefficient. Each specimen was measured twice by both sides.

Moreover in order to have a better understanding of the experimental results, normalized absorption coefficient was calculated as follows in (*Eq. 2*):

$$\tilde{\alpha} = \frac{\int_{f_1}^{f_2} \alpha(f)df}{f_2 - f_1} \quad (2)$$

DOI 10.1002/pen

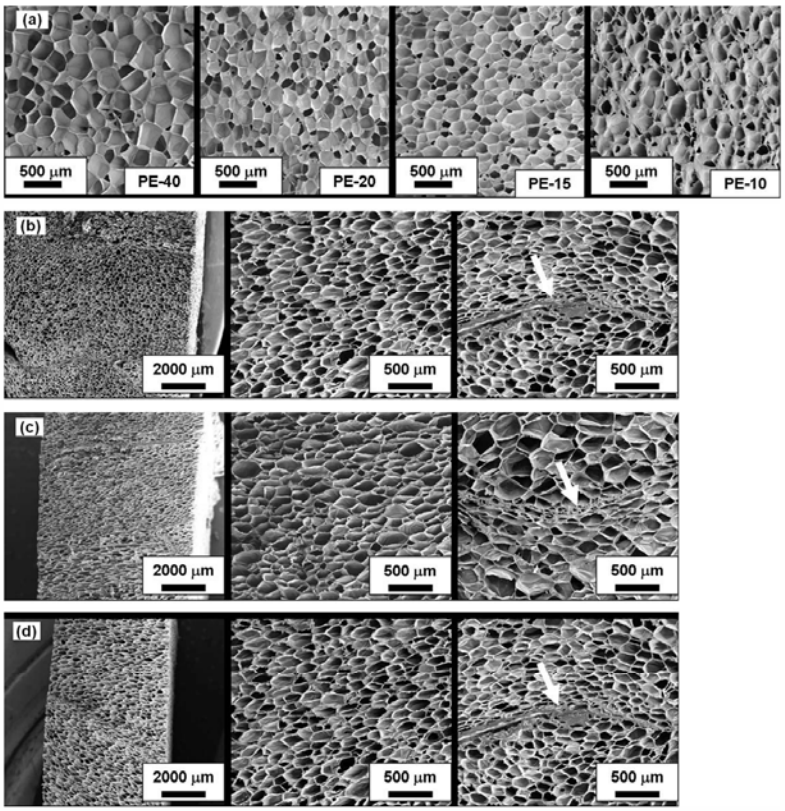

FIG. 2. (a) SEM micrographs of virgin and commercial foam samples. (b) SEM micrographs of 100-F samples. (c) SEM micrographs of 50-F samples. (d) SEM micrographs of 100-S samples.

where α is the absorption coefficient as a function of frequency (f), f_1 is the lower frequency limit (500 Hz for these measurements), and f_2 the upper frequency limit (6400 Hz in this case).

EXPERIMENTAL RESULTS AND DISCUSSION

This section has been divided into two parts, one comprising the results related with microscopic aspects and the other one related with the macroscopic properties.

Microscopic Characterization

By using the micrographs obtained with SEM and the results obtaining by using DSC it is possible to evaluate the effect of recovering process on the cellular structure and in the base polymer morphology.

Regarding the cellular structure of the samples, Fig. 2 shows micrographs of both recovered and virgin samples, and Table 3 summarizes pore size, anisotropy coefficient, joints thickness, and open cell content of recovered samples. There are three main differences between virgin and recovered samples.

First of all, a clear decrease of cell size is detected. The cell size for precursor material (PE40 foam) is around 265 μm. On the contrary, for recovered materials, cell diameter varies between approximately 100 μm for 100-F samples and 150 μm for 100-S samples. When compared with commercial products with similar densities also cell size is slightly smaller for recovered samples. For example, PE20, that has a similar density to 100-F foam, presents a cell size of approximately 205 μm which is higher than the value presented by 100-F samples (147 μm). Also, 50-S samples present a pore size of 115 μm while the

DOI 10.1002/pen

TABLE 3. Microscopic characteristics of recovered samples.

Sample	ϕ (μm)	AC	Joints thickness (μm)	C (%)
100-F	100	2.1	199	19.8
50-F	113	1.7	120	20.0
100-S	147	2.3	76	36.3

Pore size (ϕ), anistropy coefficient (AC), joints thickness, and open cell content (*C*).

commercial product with a similar density (PE15) has a cell size of around 198 μm.

Therefore, cell size of recovered samples is smaller than the one corresponding to both precursor materials and commercial products with similar densities. This could be expected, because recovering process involves steps of heating and pressing the scraps, which causes a cell size reduction.

The second difference related to the cellular structure is cell anisotropy. As it can be observed in Fig. 2, commercial products do not show any preferential orientation of the pores, i.e., these are isotropic materials. On the contrary, as it can be seen in these micrographs, the whole collection of recovered samples presents a cellular structure highly Oriented. Thus, after recovering process foams with a high anisotropy degree are obtained. For commercial products, anisotropy coefficient is around 1 in all cases (see Table 1), while for recovered materials, is around 2 (see Table 3). It seems that the deformation induced in the pores by applying pressure when scraps are hot remains once the sample is cooled down, thus obtaining a highly anisotropic cellular structure.

Finally, a third important aspect related to the cellular structure of the recovered foams is the presence of joints between the scraps. Some micrographs included in Fig. 2 show these joints. As it can be observed in all cases, a very good adhesion between scraps was obtained. This is an important result that indicates a proper selection of processing parameters (pressure, temperature, and time).

Other aspect related with these joints is their thickness. As it can be seen in the micrographs, the thickness of the joints is small (below 200 μm). Table 3 summarizes average values of this thickness for all recovered samples. These small values of joints thickness were obtained due to the low pressure used during fabrication. It was not desirable to produce samples with very thick joints due to an increase of density. As it was mentioned in the introduction of the paper, one of the main objectives was to tune a process to recover foamed crosslinked LDPE wastes but keeping density as low as possible in order to use the materials in similar applications as the virgin ones.

DSC provides information related with the crystallinity and melting point of the base polymer. Experimental results are shown in Table 4. Values of crystallinity degree calculated in heating and cooling steps, melting point calculated in heating steps and crystallization temperature for recovered and commercial products are summarized in this table. Results for precursor materials, that is skin and PE40, are also presented. As it was expected, there are no significant differences between recovered and virgin materials. This means that recycling process does not affect the base polymer morphology in terms of crystallinity and melting point.

Other structural characteristic that could have an effect on properties is the open cell content (Table 1 for virgin foams and Table 3 for recovered foams). It has been found that open cell content for recovered samples is much higher than for virgin samples. This could be due to two reasons; first, some cell walls can break during recovering process incrementing open cell content. Second, although it was said that scraps are very well joined, that is, foam scraps are perfectly stacked, there are some areas in the inner part of the samples where some voids between scraps can be found (see Fig. 2a and c). These voids can also contribute to increment open cell content of recovered samples. Moreover, open cell content increases for recovered samples with the increase in density and with the addition of skin scraps to recovered samples.

Macroscopic Characterization

Thermal conductivity values for recovered materials, precursor foam, and commercial products are shown in Fig. 3.

It is well known that thermal conductivity of foams increases when density does [26–28]. The conductivity for virgin materials increases when density does. For recovered foams, a similar trend was observed, although slightly higher values (8-10% higher) were found for 50-F and 100-S samples in comparison with PE15 and PE10. These two materials (50-F samples and 100-S samples) include a proportion of skin in their composition that contributes to increase the density and also the thermal conductivity. Moreover, these two materials have a higher open cell content than virgin foams of similar densities, this fact could also contribute to increase thermal conductivity.

Nevertheless, thermal conductivity values obtained for recycled samples are in the range of the ones for commercial low-density polyethylene foams with similar densities. In fact, for one of the materials (100-F) the conductivity is

TABLE 4. DSC results.

	First segment		Second segment		Third segment	
Sample	X_c (%)	T_m (°C)	X_c (%)	T_c (%)	X_c (°C)	T_m (°C)
100-F	43.45	108.54	37.48	94.25	41.37	109.88
PE20	42.96	107.71	36.38	91.48	39.02	108.88
50-F	40.98	109.03	35.31	94.61	39.54	109.03
PE15	41.67	107.74	36.04	91.98	37.60	108.65
100-S	41.02	108.5	35.85	92.27	39.83	109.72
PE10	41.70	109.20	37.19	91.98	40.66	110.86
PE40	41.53	109.35	34.39	94.96	36.53	109.85
Skin	36.41	107.5	32.52	153.37	34.99	106.27

T_m, melting temperature, X_c, crystallinity, T_c, crystallization temperature.

DOI 10.1002/pen

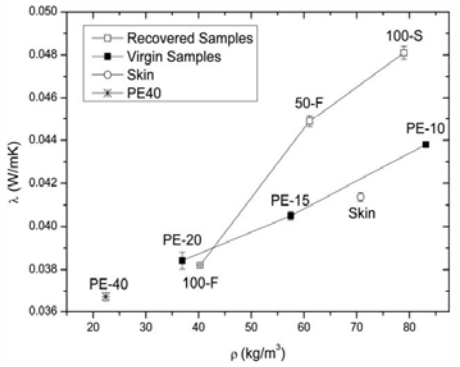

FIG. 3. Comparison of thermal conductivity values of virgin and recovered samples.

lower than that of the virgin foam of similar density (PE20). Therefore, we can conclude that recovered foams could be used as thermal insulators with a similar performance than virgin ones.

A second important property that has been analyzed is the compressive mechanical response, closely related with the applicability of these materials in packaging. Due to the highly anisotropic structures obtained after recovering process, mechanical tests were carried out in two perpendicular directions. First, parallel to the direction of the applied pressure during fabrication and second perpendicular to this direction.

Young's modulus of recovered materials in the two directions and of commercial products is collected as a function of density in Fig. 4.

Experimental data shows the typical tendency of this kind of cellular materials, that is, Young's modulus increases as density does. In addition, it can be also observed that Young's modulus measured in parallel direction is very low in comparison with the one calculated in the perpendicular direction. This is a consequence of the highly oriented structure obtained for recovered foams (see previous section). Moreover, the whole collection of recovered foams exhibit higher values of Young's modulus (measured in perpendicular direction) than precursor foam (PE40). This improvement in mechanical properties in the perpendicular direction of recovered foams in comparison with precursor material is clearly due to the higher density values of recovered foams and the anisotropic structures present in this direction.

The Young's modulus of virgin materials is higher than that of recovered products with similar densities. There are several causes for this behavior. First, the presence of voids between scraps in the inner part of the samples, second the higher open cell content of recovered samples, and finally the presence of cell walls and edges which were deformed plastically during recovering process.

Results of collapse stress for recovered samples and virgin foams are shown in Fig. 5. As it can be observed, similar trends to the ones observed for Young's modulus can be detected. The higher values correspond to commercial products in all cases. Once again this could be due to the presence of voids, the higher open cell content, and the plastic deformation induced during the processing of recovered foams. In addition the anisotropy in the cellular structure is also detected in the results of collapse stress, showing higher values in perpendicular direction than in the parallel one.

Figure 6 shows the experimental results for the density of absorbed energy as a function of density. The observed trends are similar to those of Young's modulus and collapse stress. Recovered materials absorb more energy when compressed in the perpendicular direction due to the anisotropic structure obtained during fabrication. When recovered materials are compared with commercial ones, it can be seen that absorbed energy is lower for recovered materials, except for 100-S samples that show a very high density of absorbed energy, equal to the one of the corresponding commercial product (PE10). The lower values of absorbed energy should be due to the same effects mentioned to understand the results of Young's modulus and collapse stress.

Crosslinked polyethylene foams due to their closed cell cellular structure are not used as acoustic absorbers. However, acoustic properties of recovered materials were measured to examine if the modifications in the structure induced by the processing method could improve this property.

The results of normal incidence absorption coefficient are shown in Fig. 7. There are some differences between the behavior of recovered and virgin foams. Virgin products show the typical curve of closed cell foams, that is poor absorption in all the range of frequencies except in a narrow range in which a peak appears [29]. For recovered materials, although the absorbance in the analyzed frequency range is low (when compared with typical acoustic absorbers such as polyurethane flexible foams), the

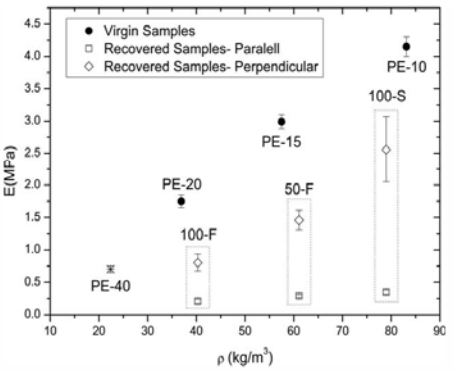

FIG. 4. Young's modulus as a function of density.

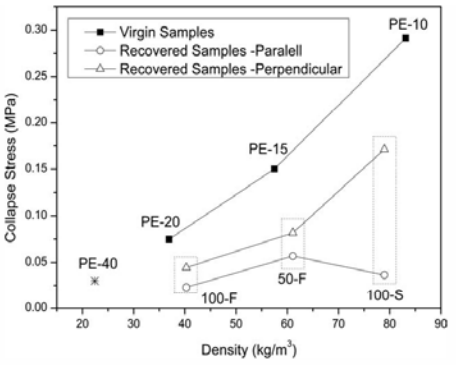

FIG. 5. Collapse stress as a function of density.

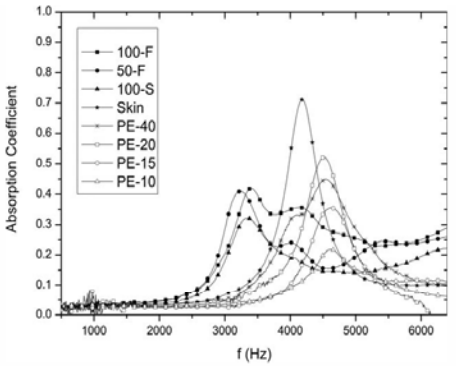

FIG. 7. Absorption coefficient of recovered and virgin foams.

frequency range where absorption shows higher values is wider than for virgin foams. This fact can be more clearly appreciated in Fig. 8, where the normalized absorption coefficient of the samples is plotted as a function of foams density. It can be observed that precursor material, that is PE40 foam is the material with higher absortion capacity, due to its low density. It can be observed for virgin foams that as density increases, absorption capacity decreases. This result is in concordance with other research works of our group, [29]. For recovered samples, normalized absorption coefficient follows the same tendency but recovered samples are better sound absorbers than virgin foams, a twofold increase in this value is detected. This interesting result should be due to the higher open cell content of recovered foams.

CONCLUSIONS

A process for recovering low-density crossslinked polyethylene foams using waste of foams with the same chemical composition as raw materials has been described. The main novelty of this process is that it allows producing foams with low densities and similar to those of commercial low-density crosslinked polyethylene foams.

Recovered samples have been characterized from a microscopic and macroscopic point of view analyzing their cellular structure and mechanical, thermal, and acoustic properties. The anisotropy induced in the material during recovering process, the presence of joints inside the materials, and the open cell content have a significant influence on the physical properties. The measured properties are in the range of those for virgin foams, which should allow using the foams produced in this paper in similar applications to the ones of low-density crosslinked polyethylene foams.

Thermal conductivity values of recovered samples are slightly higher than those of virgin materials when skin is included in the recovering process. In terms of mechanical behavior, it has been observed that recovered foams

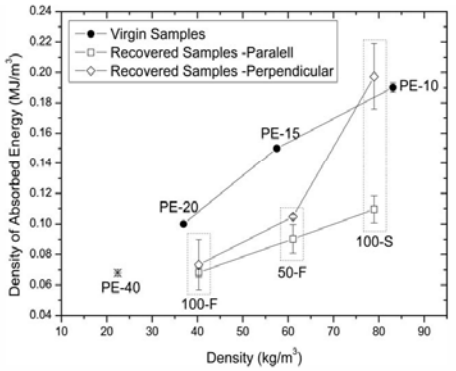

FIG. 6. Density of absorbed energy as a function of density.

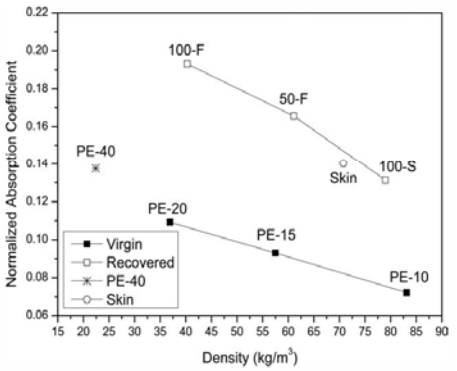

FIG. 8. Normalized absorption coefficient as a function of density.

DOI 10.1002/pen

exhibit lower values of mechanical properties when compared to virgin materials. On the contrary, the presence of a certain degree of open cells in recovered materials leads to better acoustic behavior for recovered samples than for virgin ones.

From a scientific point of view, it has been proved that samples can be used in similar applications than virgin ones. From an economical or industrial point of view, the recovering process described in this paper is simple and economically viable. Its industrial implantation should not involve very high investments. In fact the same type of machinery than the one used for making virgin foams can be used to obtained the recovered products. Moreover, maintaining density values could help manufacturers to find markets for recovered products.

ACKNOWLEDGMENTS

Financial assistance from the Local Government (Excellence group GR39). Spanish Ministry of Education and Science FECYT and FEDER program (Innocash Project INC0193 and MAT 2009-14001-C02-01) and Technological Centre of Miranda de Ebro (CTME) are gratefully acknowledged.

REFERENCES

1. M.A. Rodríguez-Pérez, *Adv. Polym. Sci.*, **184**, 97 (2005).
2. D. Klempner and V. Sendijarevic, *Handbook of Polymeric Foams and Foam Technology*. 2nd ed., Hanser, Munich, (2004).
3. D. Eaves, *Handbook of Polymer Foams*, Rapra, United Kingdom (2004).
4. Foamed Plastics to 2013 Study performed by Freedonia Group. (Study ID: 2532) (2009).
5. M.A. Rodríguez-Pérez, J.I. González-Peña, and J.A. de Saja., *Eur. Polym. J.*, **43**, 4474 (2007).
6. S.M. Tamboli, S.T. Mhsake, and D.D. Kale, *J. Appl. Polym. Sci.*, **91**, 110 (2004).
7. W. Kühnel, U.S. Patent 4,246,211 (1981).
8. N. Tatsuda, K. Fukumori, N. Sato, S. Sahara, and H. Ono, U.S. Patent 6,090,862 (2000).
9. L. Bourland, R.A. Freundlich, R.G. Nwana, and V.W. Herrant, U.S. Patent 6,384,093 B1 (2002).
10. F. Shutov, G. Ivanov, and H. Arastoopour, U.S. Patent 5,395,055 (1995).
11. L.-C. Liu, C.-K. Chuang, and R. Chien-Choo Tsiang, *J. Polym. Res.* **11**, 149 (2004).
12. F. Svirklys and D. Shanklin, U.S. Patent 6,932,540B2 (2005).
13. F. Svirklys, W. McGregor, R. Marsh, and D. Shanklin, U.S. Patent 6,558,548B2 (2003).
14. F. Svirklys and D. Shanklin, U.S. Patent 7,314.562B2, (2008).
15. H.U. Breitschidel, P. Spielau, and F.W. Alfter, U.S. Patent 4,417,932 (1983).
16. Svirklys, Patent Aplication CA2586224 A1 2007/10/26 (2007).
17. R.R. Puri, and K.T. Collington, *Cell. Polym.*, **7**, 57 (1988).
18. R.R. Puri, and K.T. Collington, *Cell. Polym.*, **7**, 219 (1988).
19. J.I. González-Peña, Effect of Thermal Treatments in Low Density Polyethylene Foam Blocks Manufactured by Compression Moulding, PhD Thesis, University of Valladolid (2006).
20. F. Hidalgo, Design and Optimization of Process Parameters Involved in the Manufacturing of Crosslinked Polyolefin Foams by Using the Compression Moulding Technique, PhD Thesis, University of Valladolid (2008).
21. B. Wunderlich, Macromolecular Physics, Vol. **2**. Academic Press, New York (1973–1976).
22. O. Almanza, M.A. Rodríguez-Pérez, and J.A. de Saja. *J. Polym. Sci. Pol Phys.*, **42**, 1226 (2004).
23. O. Almanza, M.A. Rodríguez-Pérez, and J.A. de Saja. *Polym. Int.*, **53**, 2038 (2004).
24. T. Log, and S.E. Gustafsson. *Fire Mater.*, **19**, 43 (1995).
25. M. Gustavsson, E. Karawacki, and S.E. Gustafsson. *Rev. Sci. Instrum.*, **65**, 12 (1994).
26. O. Almanza, M.A. Rodríguez-Pérez, and J.A. de Saja. *Cell. Polym.*, **18**, 385 (1999).
27. J.A. Martínez-Diez, M.A. Rodríguez-Pérez, J.A. de Saja, L.O. Arcos y Rabago, and O. Almanza. *J. Cell. Plast.* **37**, 21 (2001).
28. L.J. Gibson and M.F. Ashby, *Cellular Solids: Structure and Properties*, Cambrigde University Press, United Kingdom, (1997).
29. M.A. Rodríguez-Perez, M. Alvarez-Laínez, and J.A. de Saja. *J. Appl. Polym. Sci.* **114**, 1176 (2009).

Capítulo 9

Conclusiones y Líneas Futuras de Investigación.

9.1.- CONCLUSIONES

En esta sección se recogen las principales conclusiones que se pueden extraer de las distintas líneas de trabajo incluidas en esta memoria.

Producción de Nanocompuestos Espumados Mediante Disolución de Gas en un Molde.

- Se han producido dos tipos de *nanocompuestos* basados en polietileno de baja densidad y nanopartículas esféricas de sílice mediante la técnica de mezclado en fundido, uno conteniendo partículas de sílice modificadas con silanos y otro conteniendo además de dichas partículas un compatibilizante, (LLDPE-g-MA).
- Ambos tipos de nanocompuestos han sido *espumados* utilizando la técnica de disolución de gas en un molde, utilizando para ello como agente espumante, CO_2. Esta técnica permite obtener un *alto grado de precisión en el control de la densidad*, por lo que ha sido posible fijar el grado de expansión de los materiales en un valor de 1.6, con el fin de centrar el estudio en los efectos de la concentración de nanopartículas.
- El grado de dispersión de las nanocargas en ambos sistemas se ha analizado de forma exhaustiva estableciendo una metodología de trabajo que permite relacionar el grado de dispersión en el nanocompuesto sólido con los efectos que producen las nanopartículas en los materiales celulares. En ninguno de los sistemas se ha logrado la dispersión individual de las partículas; éstas se encuentran formando agregados de un tamaño de entre 100 y 200nm. La presencia del compatibilizante no mejora el grado de dispersión.
- Se ha comprobado que las nanopartículas juegan un *papel multifuncional* en materiales celulares con base LDPE/SiO_2. La presencia de la fase nanométrica va asociada a multiples efectos tales como: reducción del tamaño de celda e incremento de la densidad celular, aumento de la viscosidad elongacional y grado de cristalinidad del polímero base, y mejora de las propiedades térmicas y mecánicas.
- Se ha analizado el papel que juega la *compatibilización polímero/partícula* en el papel multifuncional de las nanopartículas. La presencia del

compatibilizante induce un alto grado de adhesión entre ambas fases lo que mitiga el efecto nucleante de la fase nanométrica debido a una reducción de la zona de interfase. Por otro lado, el efecto como materiales de refuerzo de las nanopartículas es superior en los nancocompuestos sólidos que contienen compatibilizante debido a una mejor transmisión de esfuerzos entre ambas fases. Cuando no se añade compatiblizante se consigue una peor adhesión entre la matriz polimérica y las partículas lo que resulta en una mayor efectividad como nucleantes de estas últimas debido a la generación de una mayor interfase. El mayor grado de mejora inducido en la estructura celular se traduce en una respuesta mecánica superior de los nanocompuestos espumados que no contienen compatibilizante.

- La fabricación de las probetas espumadas en un molde ha permitido realizar un estudio comparativo entre las mejoras inducidas por la adición de partículas nanométricas de sílice en nanocompuestos sólidos y aligerados a nivel macroscópico detectando en algunos casos porcentajes de mejora mayores en estos últimos. La combinación de técnicas de espumado con la adición de una fase nanométrica genera *efectos sinérgicos* debido al papel multifuncional que juega dicha fase.

Producción de Nanocompuestos Espumados Mediante Moldeo por Compresión en Dos Etapas

- Se han producido y caracterizado nanocompuestos basados en polietileno de baja densidad y nanopartículas de hectorita, (silicato laminar). mediante moldeo por compresión en dos etapas para lo cual se ha sometido a la matriz polimérica a un proceso de entrecruzamiento químico. Los materiales se han analizado durante los tres estadios que implica el proceso de fabricación con el fin de determinar cómo influye la presencia de las cargas en cada uno de ellos.
- El proceso de mezclado en fundido en una extrusora de doble husillo no es suficiente para obtener una exfoliación completa de las laminillas de la nanoarcilla, si bien, ésta se ve favorecida por el proceso de expansión de la matriz polimérica. Mediante difracción de rayos X se puede observar que los nanocompuestos espumados, (ya en las fases inciales de expansión) se caracterizan por presentar un grado de exfoliación adecuado de las

laminillas, que se traduce en una mejora superior de las propiedades térmicas de dichos materiales.

- No se ha observado efecto nucleante de las nanopartículas laminares; no se han detectado reducciones de tamaño de celda, aumentos en la densidad celular o incrementos del grado de cristalinidad de la matriz polimérica asociados a la presencia de las nanocargas.
- El análisis mediante calorimetría diferencial de barrido de la morfología del polímero en cada una de las fases del proceso de fabricación ha permitido dilucidar que el porcentaje de cristalinidad sí que se ve afectado por el proceso de expansión del material. La cristalinidad de la matriz polimérica disminuye a medida que aumenta el grado de expansión ya que el proceso de cristalización en un material celular está confinado a la pared de las celdillas, lo que genera esferulitas de menor tamaño.
- La presencia de las nanopartículas genera un aumento de las propiedades mecánicas que han sido analizadas mediante análisis dinámico-mecánico, (DMTA). Las curvas presentan el aspecto típico de un material con base LDPE si bien se han detectado desplazamientos de las relajaciones α y β asociados con los cambios de cristalinidad de la matriz polimérica durante el proceso de fabricación.
- La estabilidad dimensional de los nanocompuestos sólidos se ve favorecida por la presencia de una fase nanométrica en la matriz de LDPE; sin embargo en los nanocompuestos aligerados este efecto queda mitigado por la expansión del gas ocluido en el interior de las celdillas.

Producción de Materiales Celulares con base Polipropileno Mediante Moldeo por Compresión Mejorado

- Se ha descrito y optimizado un proceso de fabricación de materiales celulares sin necesidad de entrecruzar la matriz polimérica y con un control adecuado de la densidad final de la pieza moldeada producida.
- Utilizando dicho proceso, se han producido materiales celulares con base polipropileno con distintas geometrías y con densidades relativas en el rango comprendido entre 0.3 y 0.6, (rango de densidades medias). Para ello se ha utilizado un grado convencional de polipropileno lineal; en

ningún momento se han utilizado agentes nucleantes o cargas que aumenten la viscosidad del polímero en estado fundido.

- Se ha comprobado que tanto los parámetros de proceso como la composición química de los materiales influyen significativamente en el tipo de estructura celular que presenta el material. Así, mediante la elección adecuada de parámetros tales como presión, temperatura, tiempo y composición química del material, (porcentaje de agente espumante químico) se puede producir una colección de materiales con una amplia variedad de estructuras celulares. A bajas densidades es posible fabricar materiales con un alto grado de interconexión entre las celdillas, mientras que a altas densidades utilizando altos porcentajes de agente espumante se pueden producir materiales con tamaños de celda muy pequeños y con altos grados de interconexión, por otro lado utilizando porcentajes más pequeños de espumante se pueden generar materiales con contenidos de celda cerrada cercanos a cero. La utilización de altos contenidos de agente espumante favorece además la generación de estructuras celulares con distribuciones de tamaños de celda más homogéneas.
- Se ha caracterizado la respuesta mecánica del polímero puro así como de los materiales precursores, (polímero más distintos porcentajes de agente espumante) utilizando diferentes configuraciones de medida. Los resultados de la medida de resistencia a impacto de los materiales sugieren que la presencia de las partículas de azodicarbonamida auque aumentan la rigidez del polímero, (aumento del módulo), provocan una disminución de la elasticidad del mismo. De la misma forma, los residuos que genera durante su descomposición al quedar atrapados en las paredes de las celdillas contribuyen a disminuir la respuesta elástica de los materiales celulares.
- Aunque las propiedades mecánicas de los materiales producidos está determinada en primer grado por su densidad, el porcentaje de celda abierta que estos presenta condiciona la respuesta de materiales con densidades similares. La influencia de este parámetro es superior a la que pueden ejercer el tamaño de celda o la distribución de tamaños celulares.
- La efectividad del proceso de moldeo por compresión mejorado ha sido estudiada mediante el análisis de las propiedades relativas de los materiales en las zonas de bajas deformaciones, (módulo elástico) y post-colapso plástico. Los resultados indican que los materiales celulares así

producidos presentan una respuesta superior cuando son sometidos a fuerzas de compresión o de flexión que a fuerzas de tracción.

- La variedad de estructuras celulares y tipos de respuestas mecánicas que se pueden generar mediante este proceso lleva a pensar en la multitud de aplicaciones que pueden encontrar los materiales celulares generados utilizando este proceso.

Análisis Comparativo de Materiales Celulares Producidos Utilizando Agentes Espumantes Químicos (Ruta ICM) y Físicos (Disolución de CO_2 en Molde).

Materiales Celulares con base LDPE/SiO_2

- Se ha realizado un análisis comparativo del efecto que promueve la presencia de nanopartículas de tipo esférico, (sílice) en la microestructura y propiedades físicas de probetas producidas utilizando agentes espumantes de tipo físico y químico. Utilizando la ruta ICM se han fabricado una serie de muestras con identica densidad y contenido de nanopartículas que las producidas mediante disolución de gas en un molde (sistema con compatibilizante).
- Las nanopartículas de sílice tienen efecto nucleante independientemente del tipo de proceso utilizado, si bien el contenido óptimo para conseguir la máxima reducción, (que es similar en ambos casos) es considerablemente inferior en el caso del agente espumante físico, (1% frente a 6%). En cualquier caso, la mejora general de la estructura celular para cualquier concentración de nanopartículas es superior cuando se utiliza un agente espumante de tipo químico.
- La presencia de una fase inorgánica nanométrica mejora la estabilidad térmica de los nanocompuestos sólidos y aligerados de cualquier tipo, aunque es ligeramente superior en los producidos mediante disolución de CO_2.
- Las propiedades mecánicas que exhiben los materiales producidos utilizando un agente espumante físico son superiores a las de los materiales producidos con un 5% de agente espumante químico debido a la presencia de un cierto porcentaje de celdas abiertas en éstos últimos. Las nanopartículas actúan como agentes de refuerzo en todos los casos,

aunque mejoran en mayor medida la resistencia que la rigidez de los materiales. Por otro lado, el porcentaje de mejora logrado al añadir nanopartículas de sílice es considerablemente superior para los materiales fabricados utilizando azodicarbonamida. El análisis de las propiedades mecánicas relativas revela que la disolución de gas en un molde genera estructuras celulares más efectivas, (celda cerrada).

Materiales Celulares con Base Polipropileno

- Se ha puesto a punto un sistema para producir materiales celulares mediante disolución de CO_2 en un autoclave mediante el cual es posible controlar de forma precisa la densidad de muestras moldeadas. Utilizando dicho sistema se ha fabricado una batería de probetas con grados de expansión que varían entre 1.6 y 4, y se ha comparado la microestructura y la respuesta mecánica de dichos materiales con aquellos producidos mediante la ruta ICM.
- El análisis de la densidad de ambos tipos de probetas determina que ambos procesos son adecuados para producir muestras moldeadas con un elevado control de la densidad final de la pieza.
- La expansión restringida del polímero debido al crecimiento del material dentro de un molde en el proceso de disolución de gas, genera estructuras celulares altamente anisotrópicas en los materiales con menores densidades. De este modo, se amplía el rango de estructuras celulares que es posible generar dentro del rango de densidades medias para materiales celulares con base polipropileno.
- En ambos procesos el tamaño de celda y la densidad celular dependen tanto de la densidad como de la cantidad de agente espumante, si bien en el proceso de disolución de CO_2 estos dos conceptos van asociados, ya que al disminuir la densidad es necesario aumentar la cantidad de agente espumante. La ruta ICM presenta aquí una gran ventaja por tanto, ya que permite controlar la estructura celular y la densidad de forma independiente. Por otro lado, el contenido de celda abierta es casi nulo en los materiales producidos por disolución de gas mientras que depende tanto de la densidad como de la cantidad de azodicarbonamida en los producidos mediante la ruta ICM.

- La respuesta mecánica de los materiales depende tanto de la composición química como del proceso de fabricación. A altas densidades los materiales fabricados mediante moldeo por compresión mejorado utilizando bajos porcentajes de agente espumante, (1%) son más rígidos que los producidos por disolución de CO_2. A igualdad de densidad y de contenido de celda abierta, la distribución de tamaño de celdas más homogenea obtenida mediante la ruta ICM genera respuestas mecánicas superiores. A bajas densidades por el contrario, las estructuras altamente orientadas generadas durante el espumado mediante disolución de gas en un molde hace que dichas muestras sean superiores. En términos de resistencia la respuesta es más similar aunque es ligeramente superior la de las probetas producidas utilizando un agente espumante físico. Respecto a la absorción de energía, la presencia de residuos en la matriz polimérica procedentes de la descomposición de la azodicarbonamida influye negativamente en la respuesta de los materiales así producidos.

Proceso de Recuperado de Materiales Celulares de baja Densidad Entrecruzados

- Se ha optimizado un proceso de recuperación de residuos de materiales celulares con base LDPE entrecruzado producidos mediante un proceso de moldeo por compresión en dos etapas. La ventaja principal de este proceso respecto a los ya existentes es permite que producir materiales celulares recuperados manteniendo el valor de la densidad de los mismos dentro del rango que presentan productos comerciales producidos de la misma forma que los materiales de partida.
- La microestructura de los materiales se ve afectada por el proceso de recuperado debido a una reducción del tamaño de celda, la aparición de estructuras altamente orientadas y la presencia de las uniones entre las virutas de espuma. También se genera un mayor porcentaje de celda abierta debido al proceso de compresión de las virutas en caliente.
- Los efectos a nivel microestructural se ven reflejados en las propiedades térmicas, mecánicas y acústicas de los materiales recuperados. La conductividad térmica de los materiales recuperados es ligeramente superior cuando se incluye piel entre las virutas de residuo, (aumenta la densidad y tiene una capa de material sólido). Las propiedades mecánicas son ligeramente inferiores a las que presentan materiales comerciales con

densidades similares. El aumento del porcentaje de celdas abiertas conlleva una mejora de la respuesta como absorbedores acústicos de los materiales recuperados.

- El proceso es sencillo, rápido, económico y fácil de implantar a nivel industrial. En algunos casos las propiedades de los materiales recuperados son inferiores a las que presentan materiales comerciales con densidades similares, aún así, esas ligeras diferencias no son un impedimento para utilizar los materiales recuperados en aplicaciones similares a las de los materiales de partida.

9.2.- LÍNEAS FUTURAS DE INVESTIGACIÓN

Los resultados obtenidos en este trabajo despliegan un amplio abanico de posibilidades para el futuro, unas directamente relacionados con los materiales analizados y otras que se pueden comenzar utilizando otros tipos de nanopartículas o matrices poliméricas. Quizá algunas de las más interesantes serían las siguientes:

- Ampliar el rango de densidades bajo estudio para los materiales con base LDPE/SiO_2. Dado que los dos procesos de producción utilizados permiten un buen control de la densidad, sería interesante comprobar si los efectos de las nanopartículas se conservan al reducir la densidad de los materiales.
- También respecto a los materiales con base LDPE/SiO_2 sería útil producir probetas mediante la ruta ICM. Aquí existen dos posibilidades, por un lado utilizar un porcentaje de espumante menor para producir materiales cono celda cerrada y de este modo lograr un estudio comparativo más adecuado y por otro, fabricar mediante esta ruta materiales sin compatibilizante con el fin de analizar que como afecta en el caso de utilizar un agente espumante químico la compatibilización polímero-partícula.
- Analizar la respuesta como absorbedores acústicos de las probetas de polipropileno sería útil para completar la caracterización que se ha hecho de las mismas.
- Respecto a los materiales con base PP, sería interesante ver los efectos de la modificación de la reología del polímero, bien por adición de cargas o

bien por la mezcla del polímero utilizado con uno de alta resistencia en fundido. Utilizando dichas variaciones en la composición química en cualquiera de las dos rutas de producción permitirían ahondar aún más en la relación estructura-propiedades de dichos materiales.

- Utilizar el proceso de producción de espumas mediante disolución de CO_2 en un molde con otro tipo de matrices poliméricas, bien sean amorfas o semicristalinas. Existen multitud de trabajos relacionados con la producción de espumas mediante técnicas de disolución de gas y la mayoría de ellos se limitan a la caracterización microestructural de los materiales. Aplicar la metodología descrita en este trabajo nos permitiría generar conocimiento en la relación estructura-propiedades de multitud de sistemas.
- Por otro lado, la metodología desarrollada para cuantificar el grado de dispersión de las nanopartículas puede ser útil para relacionar el efecto de la dispersión de las cargas en los nanocompuestos sólidos con los que producen en los materiales celulares.